Analysis and Design of Prestressed Concrete Bridges to Eurocodes

Jennifer L. Dietrich, BSc

Dissertation submitted in total fulfillment of the requirements of the degree of Master of Science in Advanced Structural Engineering

School of Engineering and the Built Environment
Edinburgh Napier University

August 2011

AUTHORSHIP DECLARATION

I, Jennifer Dietrich, confirm that this dissertation and the work presented in it are my own achievement.

Where I have consulted the published work of others this is always clearly attributed.

Where I have quoted from the work of others the source is always given. With the exception of such quotations this dissertation is entirely my own work.

I have acknowledged all main sources of help.

If my research follows on from previous work or is part of a larger collaborative research project I have made clear exactly what was done by others and what I have contributed myself.

I have read and understand the penalties associated with plagiarism.

Jennifer Dietrich Matriculation No. 10014255

ACKNOWLEDGEMENTS

I would like to express my gratitude to the all of the people who have helped me throughout my studies at Edinburgh Napier University. In particular, I would like to thank my supervisor, Dr. Ben Zhang, who has provided guidance and encouragement, not only in the development of this dissertation, but throughout my studies this year.

I would also like to express many thanks to my parents, Robert and Laura, who have encouraged and supported me throughout my education and my career.

ABSTRACT

This paper examines the design of prestressed concrete bridges in accordance with Eurocodes. The design of these bridges is complex and challenging for a number of reasons and the difficulty increases with the Eurocode requirements, which have only been implemented in the last year. This study provides guidance on the principles and procedures for design and explains how they are applied with the Eurocodes. Following a discussion of the basic design principles, two design procedures are developed; the first for the application of traffic loads on a bridge and the second for the design of both single and continuous composite prestressed concrete beams. These procedures outline the basic design process for a prestressed concrete bridge that may be followed by engineers. With clarification of the steps in each procedure and calculations for two bridges, the design is better understood. While this dissertation cannot replace the value of engineering experience, conclusions regarding application of these procedures may help to streamline the process for future investigations.

TABLE OF CONTENTS

Authorship Declaration 2
Acknowledgements 3
Abstract 4
Table of Contents 5
List of Tables 11
List of Figures 14

1 INTRODUCTION 19
1.1 HISTORY AND BACKGROUND 19
1.2 AIMS AND OBJECTIVES 24
1.2.1 Structure of the Dissertation 26
2 DESIGN PRINCIPLES 29
2.1 BASIC CONCEPT OF PRESTRESSING 29
2.2 COMPOSITE CONSTRUCTION 31
2.3 TECHNOLOGY OF PRESTRESSING 33
2.3.1 Pre-tensioning 33
2.3.2 Post-tensioning 35
3 MATERIAL PROPERTIES 37
3.1 CONCRETE 37
3.1.1 Strength of Concrete 37
3.1.2 Modulus of Elasticity, Creep, and Shrinkage 39
3.1.3 Concrete Properties for the Design Examples 41
3.2 REINFORCEMENT 41
3.3 PRESTRESSING STEEL 42
3.3.1 Cold-Drawn Wire 42
3.3.2 Prestressing Strands 43
3.3.3 Hot-Rolled Bars 44
3.3.4 Prestressing Properties for the Design Examples 44
3.4 POST-TENSIONING DUCTS 45
3.5 POST-TENSIONING ANCHORAGES AND JACKS 46
3.5.1 Wedge Anchorages 47

3.5.2 Buttonhead Anchorages 48
3.5.3 Threaded Bar Anchorages 48
4 TRAFFIC LOADING ON A BRIDGE 49
4.1 APPLICATION OF THE LOAD MODELS 49
4.2 DIVISION OF THE CARRIAGEWAY INTO NOTIONAL LANES 50
4.3 VERTICAL LOAD MODELS 51
4.3.1 Load Model 1 – Normal Traffic 51
4.3.2 Load Model 2 – Single Axle 53
4.3.3 Load Model 3 – Special Vehicles 53
4.3.4 Load Model 4 – Crowd Loading 58
4.4 POSITION OF THE WHEELS 58
4.4.1 Resultant Axle Weight for Load Model 1 60
4.4.2 Resultant Axle Weight for Load Model 2 61
4.4.3 Resultant Axle Weight for Load Model 3 61
4.5 HORIZONTAL FORCES 62
4.5.1 Braking and Acceleration Forces 62
4.5.2 Centrifugal Forces 63
4.6 FOOTPATH LOADING 64
4.7 GROUPS OF TRAFFIC LOADS 65
4.8 APPLICATION OF THE GROUPS OF TRAFFIC LOADS 68
4.8.1 Minimum and Maximum Moments Due to Load Group gr1a 68
4.8.2 Minimum and Maximum Moments Due to Load Group gr1b 72
4.8.3 Minimum and Maximum Moments Due to Load Group gr4 74
4.8.4 Minimum and Maximum Moments Due to Load Group gr5 75
4.9 MINIMUM AND MAXIMUM MOMENTS DUE TO TRAFFIC 79
5 DESIGN PROCEDURES 81
5.1 PRELIMINARY DESIGN DATA 84
5.2 DURABILITY AND FIRE RESISTANCE 85
5.2.1 Minimum Cover Due to Bond Requirements 86
5.2.2 Minimum Cover Due to Environmental Conditions 87
5.2.3 Nominal Cover 87
5.3 ACTIONS ON THE STRUCTURE 88
5.3.1 Self-Weight 88

5.3.2 Snow Loads 90
5.3.3 Wind Actions 90
5.3.4 Thermal Actions 91
5.3.5 Actions During Execution 92
5.3.6 Accidental Actions 92
5.3.7 Traffic Loads 93
5.4 COMBINATIONS OF ACTIONS 93
5.4.1 Combinations for Serviceability Limit States 94
5.4.2 Combinations for Ultimate Limit States 95
5.4.3 Summary of the Results 96
5.5 INITIAL DESIGN OF THE BEAM 96
5.5.1 Initial Selection of Beam Size and Prestress Loss 97
5.5.2 Concrete Stress Limits for the Beam 97
5.5.3 Basic Inequalities for the Concrete Stresses 98
5.5.4 Required Elastic Section Moduli 100
5.5.5 The Magnel Diagram and Selection of Prestressing Steel 100
5.5.6 Secondary Moments and Effective Eccentricity 102
5.5.7 Verification of Concrete Stresses with Selected Prestress Force 104
5.5.8 Confirmation of Tendon Profile and Eccentricity 104
5.5.9 Prestress Loss Calculations 105
5.6 DESIGN OF THE COMPOSITE SECTION 106
5.6.1 Concrete Stress Limits for the Beam and Slab 106
5.6.2 Verification of Concrete Stresses in the Composite Section 106
5.7 DEFLECTION 107
5.7.1 Deflection Limits 107
5.7.2 Deflection Calculations 108
5.8 END BLOCK DESIGN 109
5.8.1 Bearing Stress Under the Anchor 109
5.8.2 Required Reinforcement 110
5.8.3 Compressive Stress in the Concrete Struts 111
5.9 BENDING MOMENT AT THE ULTIMATE LIMIT STATE 111
5.9.1 Stress-Strain Relationship for the Prestressing Strands 112
5.9.2 Calculation of the Ultimate Bending Moment Resistance 113

5.10 SHEAR AT THE ULTIMATE LIMIT STATE 115
5.10.1 Shear Forces on the Beam 115
5.10.2 Shear Resistance of the Concrete 116
5.10.3 Required Shear Reinforcement 117
6 CONCLUSION 119
6.1 FUTURE WORKS 122
REFERENCES 124
APPENDIX A APPLICATION OF TRAFFIC LOADING 128
A.1 LOAD MODELS 128
A.1.1 Load Model 1 – Normal Traffic 128
A.1.2 Load Model 2 – Single Axle 130
A.1.3 Load Model 3 – Special Vehicles 130
A.1.4 Load Model 4 – Crowd Loading 132
A.2 TRANSVERSE INFLUENCE LINES 132
A.2.1 Degree of Indeterminacy and Redundants 133
A.2.2 Compatibility Equations 133
A.2.3 Deflections of the Primary Beam 134
A.2.4 Solutions for the Redundants 137
A.3 POSITION OF THE NOTIONAL LANES AND WHEELS 141
A.3.1 Application of Wheel Loads for Load Model 1 141
A.3.2 Application of Wheel Loads for Load Model 2 144
A.3.3 Application of Wheel Loads for Load Model 3 146
A.4 APPLICATION OF THE LOADS TO THE BEAM 148
A.4.1 Maximum Moment Due to Load Group gr1a (Load Model 1) 149
A.4.2 Maximum Moment Due to Load Group gr1b (Load Model 2) 159
A.4.3 Maximum Moments Due to Load Group gr4 (Load Model 4) 164
A.4.4 Maximum Moments Due to Load Group gr5 (Load Model 3) 167
A.5 SUMMARY OF RESULTS FOR THE TRAFFIC LOADING 175
A.5.1 Maximum Moments for the Single span 176
A.5.2 Maximum and Minimum Moments for the Continuous Span 177
APPENDIX B SINGLE SPAN DESIGN 178
B.1 DESIGN DATA 179
B.1.1 Material Properties 179

B.2 DURABILITY REQUIREMENTS 180
B.2.1 Determination of Nominal Cover 180
B.3 ACTIONS ON THE STRUCTURE 181
B.3.1 Permanent Actions 181
B.3.2 Variable Actions – Traffic Loads 182
B.4 COMBINATIONS OF ACTIONS 182
B.4.1 Serviceability Limit State 182
B.4.2 Ultimate Limit State 183
B.5 INITIAL DESIGN OF THE PRESTRESSED BEAMS 184
B.5.1 Beam Properties and Initial Prestress Loss Assumptions 184
B.5.2 Stress Limits 184
B.5.3 Basic Inequalities for Concrete Stresses 185
B.5.4 Required Elastic Moduli 185
B.5.5 Determination of Prestress and Eccentricity 186
B.5.6 Summary of Selected Prestress – 15.2mm φ Y1820S7G Strands 188
B.5.7 Verification of the Basic Inequalities 189
B.5.8 Confirmation of Selected Tendon Profile 189
B.6 DESIGN OF THE COMPOSITE SECTION 191
B.6.1 Stress Limits 191
B.6.2 Verification of the Inequalities for Final Stresses 192
B.7 DEFLECTION CHECKS 194
B.8 ULTIMATE BENDING MOMENT RESISTANCE 195
B.8.1 Stress-Strain Relationship for the Prestressing Strands 195
B.8.2 Stress and Strain Distribution for the Beam and Slab 196
B.8.3 Calculation of the Ultimate Bending Moment Resistance 197
B.9 SHEAR DESIGN AT ULTIMATE LIMIT STATE 199
B.9.1 Shear Forces Acting on the Beam 199
B.9.2 Shear Resistance of the Concrete 200
B.9.3 Shear Reinforcement 201
B.10 DESIGN SUMMARY 204
APPENDIX C CONTINUOUS SPAN DESIGN 205
C.1 DESIGN DATA 206
C.1.1 Material Properties 206

C.1.2 Beam Properties 207
C.2 DURABILITY REQUIREMENTS 208
C.2.1 Determination of Nominal Cover 208
C.3 ACTIONS ON THE STRUCTURE 209
C.3.1 Permanent Actions 209
C.3.2 Variable Actions – Traffic Loads 210
C.4 COMBINATIONS OF ACTIONS 211
C.4.1 Serviceability Limit State 211
C.4.2 Ultimate Limit State 212
C.5 INITIAL DESIGN OF THE PRESTRESSED BEAMS 213
C.5.1 Beam Properties and Initial Prestress Loss Assumptions 213
C.5.2 Stress Limits 213
C.5.3 Basic Inequalities for Concrete Stresses 213
C.5.4 Required Elastic Moduli 214
C.5.5 Initial Determination of Prestress and Eccentricity 215
C.5.6 Equivalent Loading and Secondary Moments Due to Prestress 218
C.5.7 Verification of the Basic Inequalities with Effective Eccentricity 224
C.5.8 Confirmation of Selected Tendon Profile 225
C.6 DESIGN OF THE COMPOSITE SECTION 225
C.6.1 Stress Limits 226
C.6.2 Verification of the Inequalities for the Final Stresses 226
C.7 DEFLECTION CHECKS 228
C.8 END BLOCK DESIGN 230
C.8.1 Bearing Stress Under the Anchor 230
C.8.2 Required Reinforcement 230
C.8.3 Compressive Stress in the Struts 231
C.9 ULTIMATE BENDING MOMENT RESISTANCE 231
C.9.1 Stress-Strain Relationship for the Prestressing Strands 232
C.9.2 Stress and Strain Distribution for the Beam and Slab 232
C.9.3 Calculation of the Ultimate Bending Moment Resistance 234
C.10 DESIGN SUMMARY 238

LIST OF TABLES

Table 1.1 – Eurocodes and standards for prestressed concrete bridge design 25
Table 3.1 – Concrete Properties (BS EN 1992-1-1, Table 3.1) 38
Table 3.2 – Properties of concrete for both designs 41
Table 3.3 – Properties of strands for both designs (Part 3 of prEN 10138, Table 2). 45
Table 4.1 – Load Model 1 - Characteristic values and adjustment factors (BS EN 1991-2, Cl. 4.3.2 and NA to BS EN 1991-2, Table NA.1) 52
Table 4.2 – Characteristic values and factors for SV models (NA to BS EN 1991-2, Figure NA.1 and Table NA.2) 56
Table 4.3 – Maximum resultant axle load for LM1 60
Table 4.4 – Maximum resultant axle load for LM2 61
Table 4.5 – Maximum resultant axle load for LM3 62
Table 4.6 – Centrifugal forces for LM1 (BS EN 1991-2, Cl. 4.4.2) 64
Table 4.7 – Groups of traffic loads (NA to BS EN 1991-2, Table NA.3) 65
Table 4.8 – Groups of traffic loads for frequent combination (BS EN 1991-2, Table 4.4b) 67
Table 4.9 – Summary of M_{gr1a} for the single span 70
Table 4.10 – Summary of M_{pgr1a} and M_{ngr1a} for the continuous spans 71
Table 4.11 – Summary of M_{gr1b} for the single span 72
Table 4.12 – Summary of M_{pgr1b} and M_{ngr1b} for the continuous spans 73
Table 4.13 – Summary of M_{gr4} for the single span 74
Table 4.14 – Summary of M_{pgr4} and M_{ngr4} for the continuous spans 75
Table 4.15 – Summary of M_{gr5} for the single span 77
Table 4.16 – Summary of maximum and minimum moments due to Load Group gr5 for the continuous spans 78
Table 4.17 – Summary of maximum and minimum moments due to traffic 79
Table 5.1 – Nominal concrete cover requirements for design examples 88
Table 5.2 – Nominal densities for self-weight of design examples 89
Table 5.3 – Final self-weight for each element in the design examples 89
Table 5.4 – Summary of maximum and minimum moments due to traffic 93
Table 5.5 – ψ factors for road bridges (NA to BS EN 1990 Table NA.A2.1) 95

Table 5.6 – Partial factors for design values of actions (NA to BS EN 1990 Table NA.A2.4(B); NA to BS EN 1992-1-1 Cl. 2.4.2.2) 96
Table 5.7 – Combinations of actions for the design examples 96
Table A.1 – Deflections for applied unit load at Cy (2) and Iy (5)..... 138
Table A.2 – Deflections for applied unit load at E_y (3) and G_y (4)..... 139
Table A.3 – Influence line ordinates for E_y (3)..... 140
Table A.4 – Resultant axle loading on Beam 3 for LM1 TS 143
Table A.5 – Resultant axle loading on Beam 3 for LM2 145
Table A.6 – Resultant axle loadings on Beam 3 for LM3 147
Table A.7 – Groups of traffic loads (NA to BS EN 1991-2 Table NA.3) 148
Table A.8 – Groups of traffic loads: frequent (BS EN 1991-2 Table 4.4b)..... 148
Table A.9 – Summary of M_{gr1a} for the single span 152
Table A.10 – Moment distribution method for LM1 at X_R = 17.8m 154
Table A.11 – Moment distribution method for LM1 at X_R = 23.1m 157
Table A.12 – Summary of M_{pgr1a} and M_{ngr1a} for the continuous spans..... 159
Table A.13 – Summary of M_{gr1b} for the single span 160
Table A.14 – Summary of M_{pgr1b} and M_{ngr1b} for the continuous spans..... 163
Table A.15 – Summary of M_{gr4} for the single span 165
Table A.16 – Summary of M_{pgr4} and M_{ngr4} for the continuous spans 167
Table A.17 – Summary M_{gr5} for the single span..... 171
Table A.18 – Summary of M_{pgr5} and M_{ngr5} for the continuous spans 175
Table A.19 – Summary of moments due to traffic 176
Table A.20 – Maximum moments for each load group 176
Table A.21 – Maximum positive moments for each load group..... 177
Table B.1 – Combination factors (ψ) for traffic loads 182
Table B.2 – Partial factors for design values of actions..... 183
Table B.3 – Limits of eccentricity for the prestressed beam..... 190
Table B.4 – Imposed loading every 2.5m 193
Table B.5 – Verification of concrete stresses in the beam..... 193
Table B.6 – Summary of shear forces acting on the beam..... 199
Table C.1 – Combination factors (ψ) for traffic loads 211
Table C.2 – Partial factors for design values of actions..... 212
Table C.3 – Eccentricities 218
Table C.4 – Segments for curvature calculations..... 218

Table C.5 – Fixed End Moment calculations 221
Table C.6 – Moment distribution method 221
Table C.7 – Reactions due to each segment 222
Table C.8 – Effective Eccentricities 223
Table C.9 – Concrete stresses at transfer and service every 5m 225
Table C.10 – Imposed loading every 5.0m 227
Table C.11 – Verification of concrete stresses in the beam 228

LIST OF FIGURES

Figure 1.1 – Eugène Freyssinet (Burgoyne, 2005) 20
Figure 1.2 – Boutiron Bridge (Burgoyne, 2005)..... 21
Figure 1.3 – Walnut Lane Memorial Bridge (Nasser, 2008) 23
Figure 1.4 – Gustav Magnel (Burgoyne, 2005) 24
Figure 1.5 – Cross section for the single span design example 26
Figure 1.6 – Cross section for the two-span continuous design example 26
Figure 2.1 – Wooden cart wheel compressed by contracting tyre 29
Figure 2.2 – Stress distributions for a simply supported prestressed beam 31
Figure 2.3 – Stress distributions for a composite prestressed beam 32
Figure 2.4 – Method for pre-tensioning 34
Figure 2.5 – Method for post-tensioning 35
Figure 3.1 – Indentations for cold-drawn wires (Part 2 of prEN 10138, Figure 1) ... 43
Figure 3.2 – 7-wire strand (CCL, 2011)..... 43
Figure 3.3 – Hot-rolled bar (Freyssinet, 2010b) 44
Figure 3.4 – Steel and plastic ducts (CCL, 2011) 46
Figure 3.5 – Wedge anchorage (Freyssinet, 2010a)..... 47
Figure 3.6 – Hydraulic jacking of wedge anchorage (Freyssinet, 2010a) 48
Figure 3.7 – Threaded bar anchorage (Freyssinet, 2010b)..... 48
Figure 4.1 – Procedure for application of traffic loads to the beam 50
Figure 4.2 – Notional Lanes..... 51
Figure 4.3 – Application of LM1 (BS EN 1991-2, Cl. 4.3.2) 52
Figure 4.4 – Longitudinal configuration for the SV80 model (NA to BS EN 1991-2, Figure NA.1) 54
Figure 4.5 – Longitudinal configuration for the SV100 model (NA to BS EN 1991-2, Figure NA.1) 54
Figure 4.6 – Longitudinal configuration for the SV196 model (NA to BS EN 1991-2, Figure NA.1) 55
Figure 4.7 – Lateral arrangement of wheel loads for SOV models (NA to BS EN 1991-2, Figure NA.3)..... 56
Figure 4.8 – Axle weights and configuration for SOV models (NA to BS EN 1991-2, Figure NA.2) 57

Figure 4.9 – Bridge cross section for both design examples..... 58
Figure 4.10 – Influence line for Beam 3 59
Figure 4.11 – Application of LM1 for the maximum resultant axle load..... 60
Figure 4.12 – Application of LM2 for the maximum resultant axle load..... 61
Figure 4.13 – Application of LM3 for the maximum resultant axle load..... 62
Figure 4.14 – Application of Load Group gr5 with the SV or SOV vehicle applied fully within a notional lane (NA to BS EN 1991-2, Figure NA.4)..... 66
Figure 4.15 – Application of Load Group gr5 with the SV or SOV vehicle applied between two adjacent lanes (NA to BS EN 1991-2, Figure NA.5) 67
Figure 4.16 – Application of Load Group gr1a on the single span..... 69
Figure 4.17 – Envelope of moments for Load Group gr1a on the single span 69
Figure 4.18 – Application of Load Group gr1a for the maximum and minimum moments on the continuous spans..... 70
Figure 4.19 – Envelope of moments for Load Group gr1a on continuous spans..... 71
Figure 4.20 – Application of Load Group gr1b 72
Figure 4.21 – Envelope of moments for Load Group gr1b on the..... 73
continuous spans 73
Figure 4.22 – Application of Load Group gr4 74
Figure 4.23 – Application of Load Group gr5 75
Figure 4.24 – Envelope of moments for Load Group gr5 on the single span..... 76
Figure 4.25 – Envelope of moments for Load Group gr5 (LM3+freq. LM1) on the continuous spans..... 78
Figure 4.26 – Summary of maximum moments on the single span..... 80
Figure 4.27 – Summary of maximum moments on the continuous span..... 80
Figure 5.1 – Design procedure for prestressed concrete..... 83
Figure 5.2 – Bridge cross section for both design examples..... 85
Figure 5.3 – Stress distributions for transfer and service stage..... 98
Figure 5.4 – Magnel Diagram for the single span design 101
Figure 5.5 – Primary, secondary and final moments due to prestress..... 103
Figure 5.6 – Curved tendon profile for a continuous beam 103
Figure 5.7 – Strut and tie model for end block 110
Figure 5.8 – Stress-strain relationship for prestressing steel..... 112
Figure 5.9 – Stress and strain diagrams for the composite section..... 113
Figure A.1 – Bridge cross section..... 128

Figure A.2 – Load Model 1 129
Figure A.3 – Load Model 2 130
Figure A.4 – Load Model 3 – SV196 vehicle 131
Figure A.5 – Load Model 4 132
Figure A.6 – Indeterminate deck 133
Figure A.7 – Primary element subjected to unit load 133
Figure A.8 – Conjugate beam for unit load at C 135
Figure A.9 – Primary beam subjected to redundant C_y 135
Figure A.10 – Conjugate beam for unit load at E 136
Figure A.11 – Primary beam subjected to redundant E_y 136
Figure A.12 – Primary beam subject to unit load 137
Figure A.13 – Influence line for reaction at Beam 3 (E_y) 141
Figure A.14 – Lane placement for Load Model 1 142
Figure A.15 – Resultant axle loads for LM1 - Q_{ik} 142
Figure A.16 – Resultant axle loads for LM2 - Q_{ak} 144
Figure A.17 – Load placement for Load Model 2 144
Figure A.18 – Resultant axle loads for LM3 – Q_{196ak}, Q_{196bk}, and Q_{196ck} 146
Figure A.19 – Load placement for Load Model 3 146
Figure A.20 – Application of Load Group gr5 (NA to BS EN 1991-2 Figure NA.5) 149
Figure A.21 – Application of Load Group gr1a 149
Figure A.22 – Maximum moments due to Load Group gr1a (LM1) 150
Figure A.23 – Maximum moments due to Load Group gr1a (LM1) 150
Figure A.24 – Shear and moment diagram for axles applied at X_R = 12.1m 151
Figure A.25 – Envelope of moments due to gr1a (LM1) on the single span 152
Figure A.26 – Application of Load Group gr1a (LM1) for the maximum positive moment and minimum negative moment on the continuous spans 153
Figure A.27 – Maximum moments due to Load Group gr1a (LM1) 153
Figure A.28 – Shear and moment diagrams for the overall maximum moment 155
Figure A.29 – Minimum moments due to Load Group gr1a (LM1) 156
Figure A.30 – Shear and moment diagrams for the overall minimum moment 157
Figure A.31 – Envelope of moments due to Load Group gr1a (LM1) on the continuous spans 158
Figure A.32 – Application of load group gr1b 159

Figure A.33 – Shear and moment diagrams for the overall maximum moment..... 160
Figure A.34 – Maximum moments due to Load Group gr1b (LM2)..... 161
Figure A.35 – Minimum moments due to Load Group gr1b (LM2) 162
Figure A.36 – Envelope of moments for Load Group gr1b for continuous spans... 163
Figure A.37 – Application of Load Group gr4 164
Figure A.38 – Shear and moment diagram for distributed load, w_{gr4} 164
Figure A.39 – Shear and moment diagram for w_{gr4} on one span 166
Figure A.40 – Shear and moment diagrams for w_{gr4} on both spans..... 166
Figure A.41 – Application of Load Group gr5 168
Figure A.42 – Maximum moments due to Load Group gr5 169
Figure A.43 – Shear and moment diagram for SV196 applied at X_R = 15.7m..... 169
Figure A.44 – Envelope of moments due to Load Group gr5 (LM3+freq. LM1) on the single span..... 170
Figure A.45 – Maximum moments due to Load Group gr5 171
Figure A.46 – Shear and moment diagrams for the overall maximum moment..... 172
Figure A.47 – Negative moment results from Positive moment calculations for Load Group gr5..... 173
Figure A.48 – Shear and moment diagrams for the overall minimum moment 174
Figure A.49 – Envelope of moments due to Load Group gr5 (LM3+freq. LM1) on the continuous spans 175
Figure A.50 – Maximum moments for each load group on the single span 176
Figure A.51 – Maximum and minimum moments for each load group 177
Figure B.1 – Bridge cross section 178
Figure B.2 – Magnel Diagram 186
Figure B.3 – Beam cross section for U12 Beam..... 187
Figure B.4 – Profile of eccentricity limits for the prestressed beam..... 190
Figure B.5 – Stress-strain relationship for the prestressing steel 196
Figure B.6 – Strain and stress diagrams..... 197
Figure B.7 – Plot of shear forces and shear resistance for the beam 203
Figure B.8 – Bridge cross section 204
Figure C.1 – Bridge cross section 205
Figure C.2 – Magnel Diagram 216
Figure C.3 – Strand Profile 218
Figure C.4 – Profile of segment 1 219

Figure C.5 – Profile of Segment 2 219
Figure C.6 – Profile of Segment 3 220
Figure C.7 – Beam with partial loading 221
Figure C.8 – Equivalent loads on Span 1 (AB) 221
Figure C.9 – Secondary moments induced by reactions 222
Figure C.10 – Primary, secondary and total moments due to prestress 223
Figure C.11 – Stress-strain relationship for the prestressing steel 232
Figure C.12 – Strain and stress diagrams 233
Figure C.13 – Bridge cross section 238

1 INTRODUCTION

The basic design philosophy behind prestressing is to prepare a structure for loading by applying a pre-emptive force which will counteract the load. While this definition of prestressing is very wide, in bridge design it is primarily applied to concrete members with steel cables in tension. This type of design increases the structures capacity for heavy loads, as well as resistance to the effects of shortening due to creep, shrinkage, and temperature changes (Benaim, 2008).

Prestressed concrete is the most recent form of major construction to be introduced to structural engineering. In a relatively short time period, it has become a well-established and common method of construction. For bridge engineers, the development has allowed the design of longer spans in concrete bridges, and more economical solutions for smaller bridges (Hurst, 1998). As a result, the use of prestressed concrete for bridge design has become very common worldwide.

The concept of prestressed concrete has a relatively recent history when compared to that for the use of concrete as a construction material. However, knowledge and understanding of this structure type has grown extensively over the last century, and continues to be developed today.

1.1 HISTORY AND BACKGROUND

Some sources suggest that the first use of concrete dates back to 7000 B.C. in Israel, where a concrete floor was constructed. Since then production and use of concrete has come a long way. It was developed over many centuries by the Egyptians, the Greeks, the Romans, and many others for structures in compression. However, it was not until the 19th and 20th centuries that reinforced concrete and then prestressed concrete were developed and put into use. It was then that concrete was finally given strength in tension, first with the use of steel or iron, and then with the use of high tensile prestressing steel. This discovery expanded the use and versatility of concrete tremendously (Benaim, 2008).

The history of prestressed concrete, in particular, begins just before the Second World War, when Eugène Freyssinet, a French structural and civil engineer, first made a discovery that allowed the idea to be put into practice. The idea of adding tension to the steel in concrete had been around almost as long as reinforced concrete; however, all early attempts at prestressing failed, and the structures ended up acting as though they were only reinforced. Then, in the late 1920s, the discovery of creep in concrete was made. There is some debate as to who should receive credit for this discovery; however, there is no doubt that Freyssinet was the first to apply the knowledge to the application of prestressed concrete (Burgoyne, 2005).

Figure 1.1 – Eugène Freyssinet
(Burgoyne, 2005)

Creep is the increase of strain in concrete over time due to sustained loads. In other words, the concrete shortens over time (Neville, 1995). It was Freyssinet who recognized that the steel was losing the prestress as a result of these strains. He reasoned from this that the steel used must be high tensile steel so that some prestress will remain after creep has occurred. He also reasoned that high strength concrete should be used, to minimize the amount of creep (Burgoyne, 2005).

Leading up to his discovery, Freyssinet was in charge of the construction of three bridges across the River Allier in France, for which he proposed three reinforced concrete arch bridges. Of these three structures, the Boutiron Bridge, shown in Figure 1.2, was the only one to survive World War II (Grote and Marrey, 2003).

Figure 1.2 – Boutiron Bridge

(Burgoyne, 2005)

Freyssinet monitored the structures closely, and found that dangerous deformations occurred after construction was completed which, according to theories held at the time, were impossible. Then, in 1928, the existence of creep and shrinkage in concrete became known. He was able to apply this knowledge to his observations and make important discoveries regarding prestressing steel and concrete. From this point, he developed a system for the manufacture of prestressed concrete and eventually applied for a patent (Grote and Marrey, 2003).

Initially, Freyssinet's system did not attract much attention, as it was not believed to be profitable. Then in 1933, Freyssinet took on an assignment to rehabilitate the Transatlantic Quay in Le Havre, France. He successfully prevented collapse of the structure by installing three large prestressed concrete girders underneath it with underpinning. Supposedly, these girders are still in place today, below the new terminal that was built in 1954. The success of this rehabilitation created a breakthrough for Freyssinet and the development of prestressed concrete as a whole (Grote and Marrey, 2003).

A few years later, the first prestressed concrete bridge was erected in Algeria by the construction firm Campenon Bernard with Freyssinet's design. Around this time, many attempts were made by leading engineers to develop different versions of prestressed concrete design that would not conflict with Freyssinet's patent. Rather than come up with their own version, in 1934 the German company Wayss and Freytag entered into a license agreement with Freyssinet, which held throughout the World War II and during the post-war years (Grote and Marrey, 2003).

The Germans became interested in prestressed concrete because they were trying to save steel for use in the war. In the years before the war broke out, a series of precast prestressed concrete girders were produced for the construction of factory halls that were important to the war effort. During the war years, the prestressed concrete system was applied almost exclusively for the construction of bowstring roof girders over bunkers built for the German navy (Grote and Marrey, 2003).

Unfortunately there are not many records regarding the developments in prestress concrete during this time, due to the fact that the technique was developed largely in relation to preparations for war, so everything was considered top secret. Much of the information that is known was provided orally by a number of people who lived during that time and later shared their stories (Grote and Marrey, 2003).

However, a few documents did make it out of Germany in 1939. Initially, the chief negotiator who obtained the license agreement with Freyssinet for Wayss and Freytag was Professor Karl W. Mautner. The Professor was a Jew by birth and therefore was eventually removed from his office and sent to a concentration camp in November of 1938. Through the help of a London firm, Mautner managed to escape from the concentration camp in the summer of 1939 with his family and came to Britain. With him he brought records of prestressing trials that had been carried out in France and Germany through his Company. With these records, the technology of prestressed concrete quickly advanced in Britain, where it was also used almost exclusively for the construction of bunkers or temporary bridge construction in preparation for war (Grote and Marrey, 2003).

During the war, Freyssinet took advantage of opportunities to test some of his new theories on post-tensioning systems and curved tendons. At the same time that Freyssinet was developing his own new ideas, engineers around the world began to add to and improve upon his initial system and patent for prestressed straight tendons. In Brussels between 1943 and 1944, Gustave Magnel built the first railway bridge in prestressed concrete, testing a new idea of curved, multi-wire tendons in flexible rectangular ducts. Also, Robert Shama of Egypt applied Freyssinet’s new curved tendons in the construction of a military aircraft hanger located north of Delhi between 1940 and 1941. In Germany, Ewald Hoyer developed a system for the

manufacture of small pre-tensioned beams with thin hard-drawn wires that could be cut to any length required. It was found that the wires would expand elastically at the cut and re-anchor themselves instead of losing tension (Grote and Marrey, 2003).

Following the end of World War II, much of the infrastructure in Europe was heavily damaged, and steel was in short supply. Therefore, the application of prestressed concrete for the construction of bridges became preferable, and many new bridges were constructed with the new innovative technology. The use of this technology began to spread around the world as well. In 1949 it was introduced to bridge designers in the United States with the construction of the Walnut Lane Memorial Bridge in Philadelphia, Pennsylvania which is shown below (Nasser, 2008).

Figure 1.3 – Walnut Lane Memorial Bridge
(Nasser, 2008)

This bridge was the first major prestressed concrete structure in the United States and its construction was a profound event, especially considering that American engineers had very little experience with prestressed concrete at the time (Precast/Prestressed Concrete Institute, 1997). It was designed by Gustav Magnel, shown in Figure 1.4, who developed a reputation as one of the world's leading authorities on prestressed concrete. He was from Belgium, although was fluent in English and French and therefore was able to pass on his knowledge of prestressed concrete to engineers in other countries (Nasser, 2008).

Figure 1.4 – Gustav Magnel

(Burgoyne, 2005)

Following the construction of Walnut Lane Memorial Bridge, the industry for prestressed concrete in the United States took off. As a result, over 70% of the bridges constructed in the United States today are constructed with prestressed concrete (Nasser, 2008). This result has been mirrored around the world, as for most developed countries, prestressed concrete is now a very common choice in design.

Despite the extensive growth in the application of prestressed concrete, it is still a relatively new technology. Therefore, advancements continue to be made today, covering a number of aspects in the design, such as types of steel tendons, post-tensioning ducts, anchorages, and fabrication and construction methods, just to name a few (Precast/Prestressed Concrete Institute, 1997).

1.2 AIMS AND OBJECTIVES

As the knowledge of prestressed concrete has developed over the past century, so has the complexity of prestressed concrete designs. The aim of this dissertation is to provide some basic guidance and understanding of these complex designs for the purpose of bridge construction. This includes consideration of external loads, material properties, and limit state design.

To accomplish this, a simplified design procedure covering composite prestressed concrete bridge design for single and continuous spans is provided. All discussions are in accordance with the requirements set by Eurocodes, which have only become mandatory in the past year. The Eurocodes which must be applied for this design are summarized in Table 1.1.

Table 1.1 – Eurocodes and standards for prestressed concrete bridge design

Eurocode	Part	Title and/or scope
BS EN 1990 Eurocode – Basis of Structural Design	**Main text**	**Structural safety, serviceability and durability, partial factor design**
	Annex A2	**Application for bridges (combinations of actions)**
BS EN 1991 Eurocode 1 – Actions on structures	**Part 1-1**	**Densities, self-weight and imposed loads**
	Part 1-3	Snow loads
	Part 1-4	Wind actions
	Part 1-5	Thermal actions
	Part 1-6	Actions during execution
	Part 1-7	Accidental actions due to impact and explosions
	Part 2	**Traffic loads on bridges (road bridges, footbridges, railway bridges)**
BS EN 1992 Eurocode 2 – Design of Concrete Structures	**Part 1-1**	**General rules and rules for buildings**
	Part 2	**Reinforced and prestressed concrete bridges**
BS EN 1997 Eurocode 7 – Geotechnical design	Part 1	Geotechnical design
BS EN 1998 Eurocode 8 – Design of structures for earthquake resistance	Part 1	General rules, seismic actions and rules for buildings
	Part 2	Bridges

The Eurocodes that are considered in this report have been highlighted in the table. EN 10080, prEN10138, and BS 8500-1 are also applied as per guidance from the Eurocodes. These cover steel properties and durability requirements.

1.2.1 Structure of the Dissertation

This study focuses on two main design procedures; the first for the application of traffic loading, and the second for the design of a prestressed concrete beam. Due to its complexity, the traffic loading for a bridge has been analysed separately, and the results are then incorporated into the prestressed concrete design.

To illustrate the discussions provided in each chapter, two simplified design examples have been developed. The first is for a single span prestressed concrete bridge consisting of pre-tensioned U12 Beams and spanning 25.0 metres. The cross section of the structure is shown in Figure 1.5.

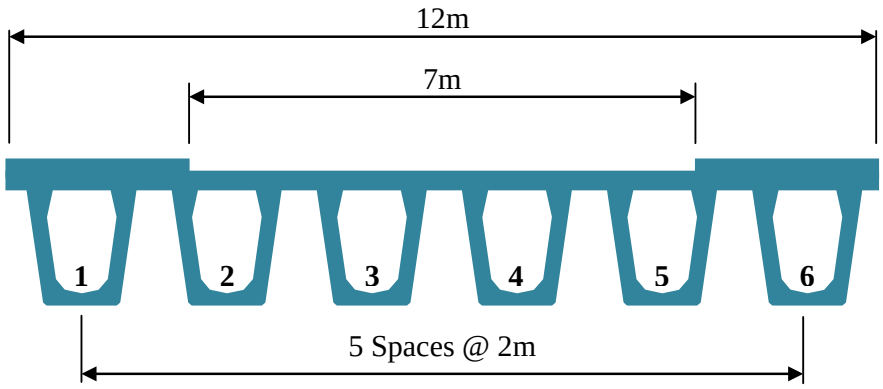

Figure 1.5 – Cross section for the single span design example

The second is for a two-span continuous prestressed concrete bridge consisting of post-tensioned I Beams with two equal spans of 40.0 metres. The cross section assumed for this structure is shown in Figure 1.6.

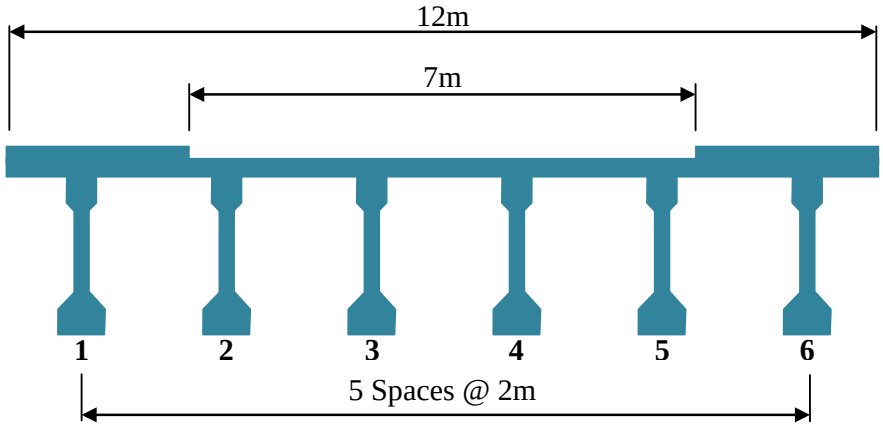

Figure 1.6 – Cross section for the two-span continuous design example

The purpose of this study is to provide a simplified procedure for the analysis and design of a prestressed concrete bridge deck. It does not cover the full design of a structure. Reference is made throughout the report to aspects of the design that, due to time constraints must be left for future investigations.

Chapter 2 of this study introduces the main design principles that must be applied for prestressed concrete. This includes discussion of the basic concept of prestressing illustrated by concrete stress distributions, the benefits of composite construction and its effect on the stress distributions, and the technology of prestressing with a comparison between pre-tensioned and post-tensioned concrete. Understanding of these basic concepts is required in the design of a prestressed concrete bridge.

With the basic concepts defined, Chapter 3 begins discussion of the design process with information regarding the material properties. In this chapter, the strength, modulus of elasticity, creep, and shrinkage of concrete are covered. The properties of reinforcement and three types of prestressing steel are also investigated.

Chapter 4 covers the analysis of traffic loading on a bridge. This topic is very extensive, and therefore requires a separate chapter from the overall design procedures. Vertical load models, horizontal forces, and footpath loading defined by BS EN 1991-2 are covered, with discussion on the final groups of loads for application in design.

Chapter 5 provides a design procedure for the design of concrete bridges, with discussion of each step in the process. This chapter covers collection of preliminary design data, determination of durability, calculation of actions on the structure, initial design of the beam, design of the composite section, deflection checks, end block design, and ultimate limit state checks for bending moment and shear.

Chapter 6 provides conclusions drawn from the information presented in this dissertation. Due to the complexity of prestressed concrete design, it is not possible to cover every aspect of the design in this dissertation. Therefore, discussion on necessary future works is also provided.

Appendix A of this dissertation provides full calculations for the traffic loading that has been discussed in Chapter 4, covering the determination of influence lines, positioning of wheel loads, and calculation of maximum moments. Calculations are provided for two design examples, the first a 25.0 metre single span, and the second a continuous span design with both span lengths equal to 40.0 metres.

Appendix B consists of design calculations for a 25.0 metre single span prestressed concrete bridge. The calculations follow the design procedure described in Chapter 5.

Appendix C provides a design for a two span continuous prestressed concrete bridge. Both spans are 40 metres in length. The design follows the design procedure described in Chapter 5, similar to the design in Appendix B. This design also considers elements of the design applied for continuous beams such as secondary moments and additional checks on concrete stresses.

2 DESIGN PRINCIPLES

In order to fully understand the design procedures described in this report, it is important to be aware of a few basic design concepts and methods, which are applied in the design of prestressed concrete. This chapter discusses the basic concept of prestressing, the benefits of composite construction, and the methods of prestressing.

2.1 BASIC CONCEPT OF PRESTRESSING

In a broad definition, prestressing is described as the application of forces to neutralize stresses caused by external loads (Bhatt, 2011). This concept was around long before its application in concrete. A common example of this is the creation of wooden cart wheels. The wheels are prestressed by placing a heated iron tyre around the wooden rim. As the iron cools, the tyre contracts around the rim, strengthening the joints by placing them all in compression (Hurst, 1998). This example is illustrated in Figure 2.1. The compression in the joints allows them to support higher tensile stresses caused by external loads before failure occurs.

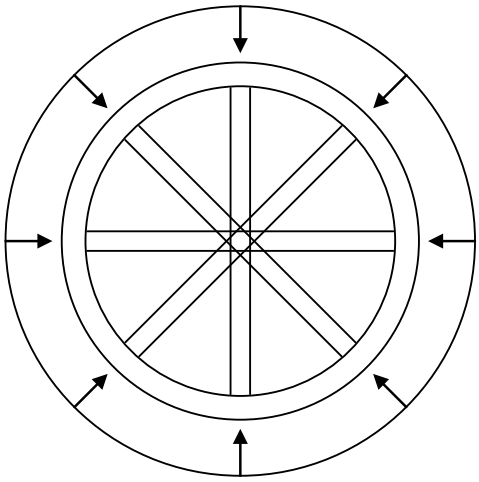

Figure 2.1 – Wooden cart wheel compressed by contracting tyre

As mentioned in the introduction, at the beginning of the 20th century engineers began applying this concept to concrete construction. It is commonly known that concrete is very weak in tension while steel is very strong. Therefore, to increase tensile strength of concrete, steel reinforcement is placed in the locations where tensile stresses are caused by external loads (Collins and Mitchell, 1987). This allows the concrete to carry tensile loads; however it does not solve all of the problems.

In reinforced concrete, vertical and inclined cracks tend to develop as a result of tensile and shear stresses in the concrete, even under working loads. This leads to a number of disadvantages, only a few of which are mentioned here. One disadvantage is that the cracked portion of the concrete no longer provides structural capacity and only adds to the dead load the structure must support. The structure also has a tendency to deflect more under load once cracks have occurred. Furthermore, cracking makes the reinforcement more prone to corrosion, reducing the ability of the concrete to resist shear stresses (Bhatt, 2011).

To overcome this problem, engineers began designing prestressed concrete. In the construction of prestressed concrete the steel is tensioned before application of external loads, causing large compressive stresses in the concrete which allow the concrete to resist higher tensile forces prior to cracking, similar to the construction of the wooden cartwheel. The application of the prestressing force essentially creates a self-equilibrating system of stresses in the concrete. The high tensile stresses in the prestressing steel are counterbalanced by equal and opposite compressive stresses in the concrete (Collins and Mitchell, 1987). The benefits of prestressed concrete are best explained based on the distribution of stresses, illustrated for a simply supported beam in Figure 2.2.

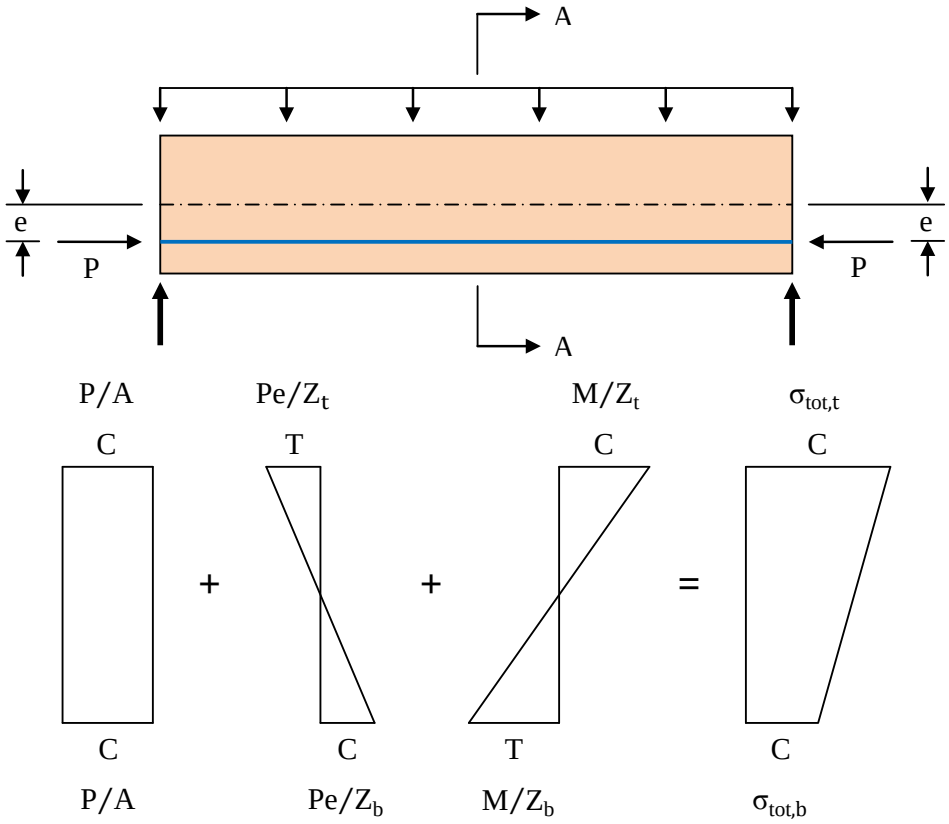

Figure 2.2 – Stress distributions for a simply supported prestressed beam

As shown in Figure 2.2, the higher compressive force in the bottom fibre due to the prestressing force, P, counteracts the tensile force caused by external loading, M. The main goal in prestressing an element is to transfer all of the tension in the cross section to the steel strands and keep the concrete in compression throughout, since this is when the material is at its strongest (Bungey, Hulse and Mosley 2007). Due to these stress distributions, a prestressed beam is generally free of cracks under working loads, and is therefore much stiffer than a reinforced beam. As a result, the design of more slender members is possible. This reduces the overall dead weight of the structure allowing the design of structures with longer spans (Bhatt, 2011).

2.2 COMPOSITE CONSTRUCTION

Often, prestressed concrete bridge beams are designed to act in combination with a cast in-situ reinforced concrete slab. To create the composite section, adequate reinforcement is provided between the beam and slab, creating a horizontal shear connection. Often, the top of the beam is deliberately roughened, increasing the

resistance to slip and facilitating the transfer of horizontal shear through the reinforcement. The connection between the two elements creates a stiffer and stronger bridge deck. It also provides lateral stability for the girders (Gilbert and Mickleborough, 1990). A composite section is beneficial in the design of the prestressed beam as well, since the slab acts as a compression flange, allowing the design of a more slender beam (Hurst, 1998). The benefits of this type of construction are further explained based on the resulting concrete stress distributions illustrated in Figure 2.3.

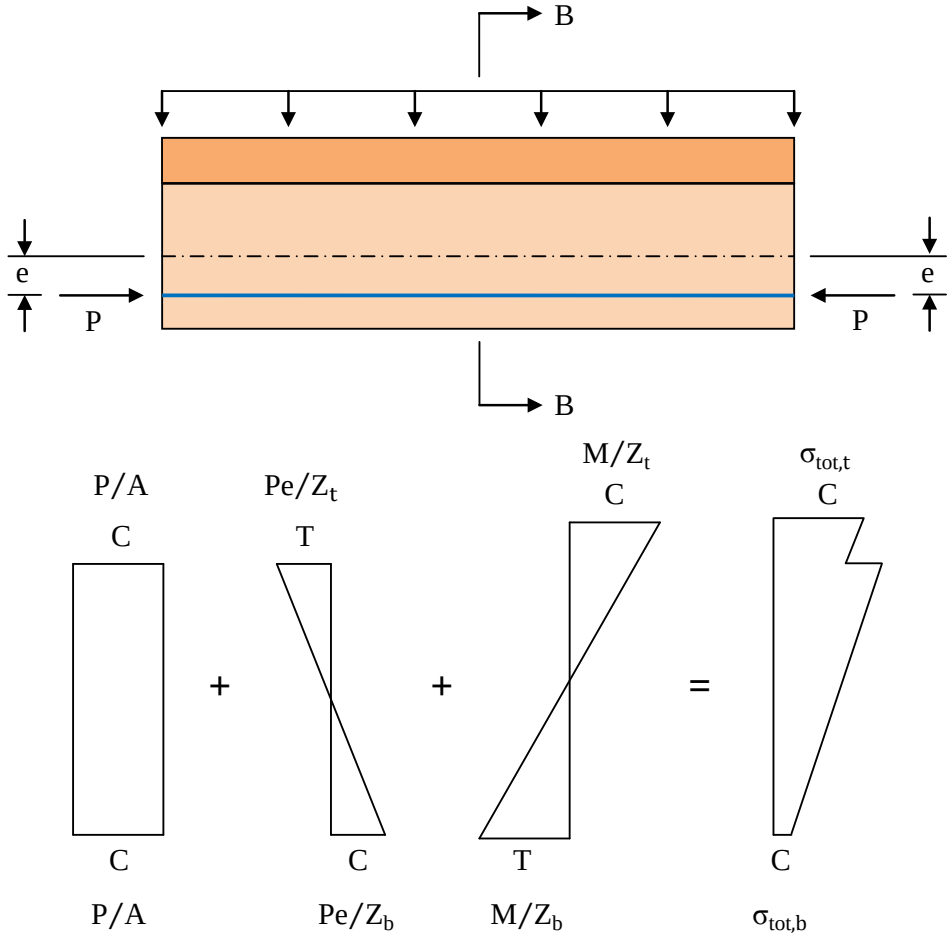

Figure 2.3 – Stress distributions for a composite prestressed beam

As illustrated by Figure 2.3, the maximum compressive stress occurs in the upper fibre of the beam, but the stress is much lower than that which the same loading would create on a non-composite beam. The discontinuity in the final stress diagram accounts for the fact that the slab only takes stresses induced by the composite section (Hurst, 1998). Typically, the prestressing is applied to the beam prior to

placement of the slab (Gilbert and Mickleborough, 1990). Consequently, the beams have an initial stress distribution before the section becomes composite. For this reason, the prestressed beam is initially designed based on the self-weight of the beam and the weight of the beam and slab. The application of the imposed loads and composite section then becomes a separate step in the design.

While composite construction has clear benefits, it does require some initial considerations in design. A composite section consists of two concrete elements which have different concrete strengths, elastic moduli, and creep and shrinkage properties. Even if the same concrete strength is chosen for both elements, the fabrication of precast elements is typically of higher quality than cast in-situ concrete. Restraining actions will develop over time in the structure, as a result of the differential creep and shrinkage. These effects must be considered and accounted for in the design of the structure (Gilbert and Mickleborough, 1990).

2.3 TECHNOLOGY OF PRESTRESSING

For the application of prestressing, the two most common methods are pre-tensioning and post-tensioning. In bridge design pre-tensioned concrete is typically used for relatively short bridge decks with standard bridge beams (Benaim, 2008). Post-tensioned concrete is more applicable to longer bridge decks and continuous spans (Bhatt, 2011).

2.3.1 Pre-tensioning

For the fabrication of pre-tensioned concrete, the steel tendons are first tensioned to the desired stress and anchored to fixed supports. The formwork for the concrete is then built around the steel and the concrete is cast. Once the concrete hardens to an appropriate strength the tension in the steel is released, typically by flame cutting or sawing (Bhatt, 2011). This process is illustrated in Figure 2.4.

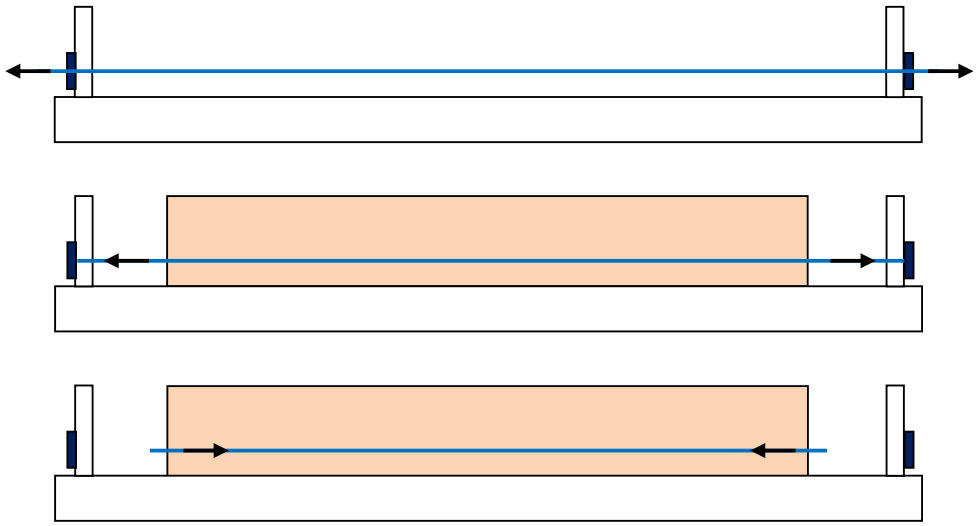

Figure 2.4 – Method for pre-tensioning

With this method of prestressing, the tension is transferred to the structural member through the bond between the steel and concrete. Often it is determined in design to provide debonding at the end of some of the steel tendons. To accomplish this, the tendons are wrapped in plastic tubing at the ends, preventing a bond from forming between the steel and concrete. This technique allows the variation of prestress force across the section and prevents cracking at the top face of the member, which may occur if all of the strands are tensioned to the same stress (Bhatt, 2011).

Due to the necessity for large anchorages to accommodate the large number of steel tendons typically required, this method is ideally suited for precast members, which are produced in a fabrication plant and delivered to the construction site. One advantage is that it allows for casting of several members along the same tendons, reducing the time required for manufacture (Hurst, 1998).

Typically, with the help of accelerated curing techniques, the prestressing force can be transferred to the concrete after only three days (Martin and Purkiss, 2006). A disadvantage of stressing the concrete at this early age is that elastic shortening can occur, along with high creep strains, which can result in a significant reduction in the tensile strain of the steel and a relatively high loss of prestress force (Gilbert and Mickleborough, 1990). This loss should be accounted for during the design process.

2.3.2 Post-tensioning

For the fabrication of post-tensioned concrete, post-tensioning ducts are placed at the desired profile with un-tensioned steel tendons inside and the concrete is cast around them. Or in some cases, the steel tendons may be threaded into the ducts after the concrete is cast. Once the concrete hardens to the appropriate strength, the tendons are tensioned and the force is transferred to the concrete through special built-in anchorages. Usually after tensioning, the space left in the ducts is filled with cement grout. The grout protects the tendons from corrosion and also adds to the ultimate strength capacity (Hurst, 1998). This process is illustrated in Figure 2.5.

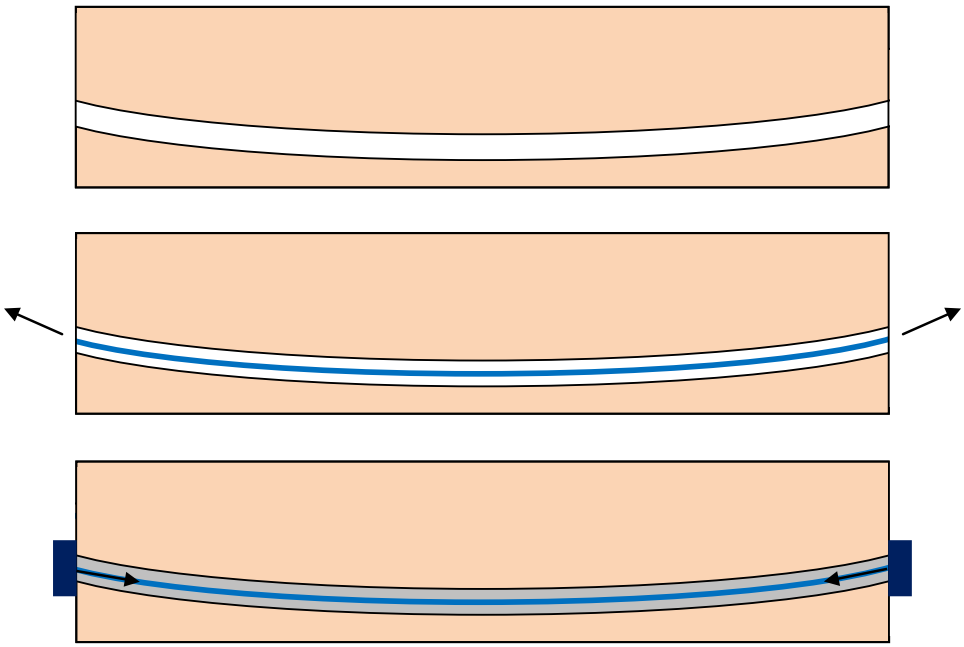

Figure 2.5 – Method for post-tensioning

With this method, additional reinforcing is required around the anchorage to prevent the concrete from splitting at the ends (Hurst, 1998). This is referred to as the end block, and will be discussed further in the design procedures.

An advantage of post-tensioning is that the tensioning can be carried out in stages, which can be useful in situations where the load must be applied in well-defined stages (Hurst, 1998). Also, the ducts can be fixed to any desired profile for the strands, allowing for the reduction of eccentricity at the beam ends and also for resistance against negative moments that occur in continuous beams. In this case,

consideration must be made in design for the transverse forces these curved tendons will apply to the beam (Gilbert and Mickleborough, 1990). Another advantage of this method is that there is less urgency in construction since the shuttering can be removed within a few days and the concrete can then be allowed to mature before the prestressing force is applied (Martin and Purkiss, 2006). This reduces the effects of elastic shortening and creep that can occur in the pre-tensioned beams.

Discussion on the choice of post-tensioning ducts and anchorages is provided in Sections 3.4 and 3.5 of the next chapter.

3 MATERIAL PROPERTIES

Before a design can be started, the materials must be selected. This is an important aspect, because the quality of materials chosen can significantly affect the performance of the structure. Here, the properties of concrete, reinforcement, and prestressing steel are discussed, as well as the ducts, anchorages, and jacking systems required for post-tensioned concrete.

3.1 CONCRETE

Concrete is sometimes defined as an artificial stone. It has very high strength in compression; however it is weak and brittle in tension. The ratio of tensile strength to compressive strength is quite small, and as the compressive strength increases, the tensile strength does so at a decreasing rate, causing the ratio to become even smaller (Neville, 1995). Once cracks occur in the concrete, which can sometimes happen before loading due to internal stresses, the tensile strength reduces even more. To account for this effect, the concrete tensile strength is usually ignored when calculating the bending strength of the beam (Benaim, 2008). If the structural member must resist forces in tension, steel reinforcement or, in the case of prestressed concrete, tensioned steel strands must be used to provide tensile strength. The properties of the steel will be discussed later in this chapter.

3.1.1 Strength of Concrete

For the purpose of bridge design, the strength of concrete is its most valuable property. This is determined by measuring the forces required to crush standard samples of concrete. In the United Kingdom, as well as the rest of Europe, the standard samples consist of 150 millimetre cubes while in the United States 150 millimetre diameter by 300 millimetre high cylinders is used. Typically the strength is measured after 28 days of curing, however in most cases it will continue to gain strength after those first four weeks (Neville, 1995).

Concrete bridges are usually built with a cube strength between 40 and 60 MPa, but in special cases strengths up to 100 MPa have been used (Benaim, 2008). Table 3.1 presents properties of some typical concrete strength classes. BS EN 1992-1-1 provides a wide range of strength classes; however for bridge design, Clause 3.1.2(102)P of BS EN 1992-2 recommends limiting the range to between C30/37 and C70/85. The UK National Annex then limits the range for shear strength even further, to C50/60, unless there is evidence of satisfactory past performance for the mix.

Table 3.1 – Concrete Properties (BS EN 1992-1-1, Table 3.1)

	C30/37	C35/45	C40/50	C45/55	C50/60
f_{ck} (MPa)	30	35	40	45	50
$f_{ck,cube}$ (MPa)	37	45	50	55	60
f_{cm} (MPa)	38	43	48	53	58
f_{ctm} (MPa)	2.9	3.2	3.5	3.8	4.1
E_{cm} (GPa)	33	34	35	36	37

In the table above, f_{ck} represents the cylinder and cube strengths, f_{cm} represents the mean compressive strength, f_{ctm} is the mean axial tensile strength, and E_{cm} is the mean value of the modulus of elasticity. The strength of concrete is influenced by a number of factors including, but not inclusive of, the water-cement ratio, the properties of aggregate, the porosity of the concrete, and admixtures. Durability and permeability of concrete are also important factors. These can be controlled with the mix design (Neville, 1995).

In addition to the properties given in Table 3.1, BS EN 1992-1-1 also provides guidance on the estimation of the compressive strength with time, which is required for the calculation of concrete stresses at multiple stages of construction. Typically, the strength is estimated at 7 days, when the tension in the prestressing strands is transferred to the beam and at 28 days, when the slab and eventually all imposed loading are applied to the beam. For these estimations, a mean temperature of 20°C and curing in accordance with EN 12390 are assumed. First, the mean compressive strength at time t is defined by the following equation from Clause 3.1.2(6).

$$f_{cm}(t) = \beta_{cc}(t) f_{cm} \quad (3.1)$$

with: $\beta_{cc}(t) = e^{s\left[1 - (28/t)^{0.5}\right]}$

In the expression above t represents the age of concrete in days and s is a coefficient that depends on the cement type. With the result, the characteristic concrete strength at time t is estimated by applying the following equations from Clause 3.1.2(5).

$$f_{ck}(t) = f_{cm}(t) - 8 \qquad \text{for } 3 < t < 28 \text{ days} \quad (3.2)$$

$$f_{ck}(t) = f_{ck} \qquad \text{for } t \geq 28 \text{ days} \quad (3.3)$$

In addition to analyzing the concrete stresses at different stages in construction, Equations (3.1), (3.2), and (3.3) can be used to estimate the time required to achieve a particular strength in concrete, such as the required strength for application of the prestress force or striking of formwork.

3.1.2 Modulus of Elasticity, Creep, and Shrinkage

Other properties must also be defined for consideration in design including the modulus of elasticity, creep, and shrinkage. The modulus of elasticity, E_{cm}, which provides a measurement of the elastic deformation, is important in the design of concrete since it not only effects deflections in the concrete, but also some of the prestress losses that occur. It is very difficult to predict the value of E_{cm} for concrete and the effects creep has on it. Therefore, in most normal bridge design applications it is satisfactory to use the mean value given in Table 3.1 of BS EN 1992-1-1, which is defined by the following equation (Hendy and Smith, 2007).

$$E_{cm} = 22\left[(f_{ck}+8)/10\right]^{0.3} \quad (3.4)$$

An estimate for variance with time is also provided by Clause 3.1.3(3).

$$E_{cm}(t) = 22[f_{cm}(t)/f_{cm}]^{0.3} E_{cm} \quad (3.5)$$

The estimation of creep is very important in the design of prestressed concrete as well, since it can lead to a reduction of the prestressing force in the steel tendons.

The creep of concrete causes deformations under sustained loading to grow over time (Hendy and Smith, 2007). Clause 3.1.4(1)P states that creep is dependent on the ambient humidity, dimensions of the element, and composition of the concrete. It is also influenced by the age of the concrete at first loading and the magnitude and duration of the loading. Deformation due to creep is related to the modulus of elasticity with the application of a creep factor, $\varphi(\infty,t_0)$, which is derived from Figure 3.1 of BS EN 1992-1-1. In design, creep effects the calculations for deflection as well as prestress losses.

If the compressive stress of the concrete at the time of first loading, t_0, is greater than 0.45 $f_{ck}(t_0)$, nonlinear creep may give rise to greater creep deformations. This often occurs in precast pre-tensioned beams, since they are stressed at an early age with only a small dead load initially (Hendy and Smith, 2007). Clause 3.1.4(4) of BS EN 1992-1-1 provides a revised creep factor for this situation, referred to as the non-linear notional creep coefficient, shown below.

$$\varphi_{nl}(\infty,t_0) = \varphi(\infty,t_0)\, e^{1.5(k_\sigma - 0.45)} \qquad (3.6)$$

where: $k_\sigma = \sigma_c / f_{ck}(t_0)$ (stress-strength ratio)

The consideration of shrinkage in concrete is split into two components. The first is autogenous shrinkage, which occurs during hydration and hardening of concrete. The majority of this shrinkage occurs relatively quickly and is substantially complete within only a few months. The second component is drying shrinkage, which is associated with the movement of water through and out of the concrete. Drying shrinkage depends on composition of the concrete, relative humidity, and effective section thickness. It typically takes much longer and is not substantially complete until the concrete has aged a few years (Hendy and Smith, 2007). Both components are defined by Clause 3.1.4(6) of BS EN 1992-1-1 and the total shrinkage is taken as the sum of these two.

In design, both creep and shrinkage of concrete are especially important, since the shortening causes a reduction in the prestress force, usually between 150 and 350 MPa (Gilbert and Mickleborough, 1990). For composite sections, shrinkage becomes

significant, since the differential shrinkage between parts of the cross section can cause secondary moments and forces due to restraint on the free deflections (Hurst, 1998). Due to time constraints, these effects are not considered in this dissertation, however a brief discussion on prestress losses is provided in Chapter 5.

3.1.3 Concrete Properties for the Design Examples

For both designs in this dissertation, it has been decided to use C50/60 concrete for the beams and C40/50 concrete for the deck. Table 3.2 provides a summary of the properties determined for these classes, based on the information provided in this section. It should be noted that the calculation of compressive strengths with time is only performed for the C50/60 concrete in the beam, since the deck only requires consideration of stresses at the final loading condition. In these calculations, time t of 7 days is applied and CEM 42.5R Cement is assumed with a value of 0.20 for the coefficient s, as defined in Clause 3.1.2(6) of BS EN 1992-1-1. For detailed calculations, refer to Section B.1 and C.1 of the Appendices.

Table 3.2 – Properties of concrete for both designs

Concrete Properties	C40/50	C50/60
f_{ck} (MPa)	40	50
$f_{ck,cube}$ (MPa)	50	60
f_{cm} (MPa)	48	58
f_{ctm} (MPa)	3.5	4.1
E_{cm} (GPa)	35	37
$\beta_{cc}(t = 7)$	-	0.819
$f_{cm}(t = 7)$ (MPa)	-	47.486
$f_{ck}(t = 7)$ (MPa)	-	39.486
$E_{cm}(t = 7)$ (MPa)	-	34.845

3.2 REINFORCEMENT

While the primary steel in a prestressed concrete beam is of course the prestressing strands, there are requirements for additional reinforcement in the beams, as well as reinforcement in the deck. For the selection of reinforcement, BS EN 1992-1-1 relies on EN 10080. In accordance with this standard, each bar is specified by its yield strength and ductility class. For example, a bar with 500 MPa yield strength noted as

B500 and a ductility class B is specified as “B500B”. There are three classes for ductility, A, B, and C. For bridges, Clause 3.2.4(101)P in the National Annex to BS EN 1992-2 recommends that classes B and C be used. The ductility classes are based on the strain at maximum force and the ratio of tensile strength to the yield stress.

The important property of reinforcement from the designer’s perspective is the characteristic yield strength, f_{yk}, which is obtained by dividing the characteristic yield load by the nominal cross-sectional area of the bar (Hendy and Smith, 2007). The yield strength typically lies between 400 and 500 MPa. Steel with a higher strength tends to cause cracking in the concrete and therefore cannot be used effectively. The elastic modulus is also defined, usually between 190 and 210 GPa (Benaim, 2008). Other properties which characterize reinforcement include tensile strength, bendability, bond characteristics, and fatigue strength (Hendy and Smith, 2007).

It has been decided to use B500B reinforcement for the designs in this dissertation with a characteristic yield strength of 500 MPa. The sizes are determined later in the design procedure.

3.3 PRESTRESSING STEEL

It is no surprise that the selection of prestressing steel is a very important factor in the design of a prestressed concrete bridge. For the prestressing steel, often referred to as prestressing tendons, the use of wires, bars, or strands is allowed by BS EN 1992-1-1. For specifications the designer is referred to provisions provided in prEN 10138. As indicated by the name, prEN 10138 is in draft form. Therefore, future investigations should verify the information provided here with the final published document.

3.3.1 Cold-Drawn Wire

For the prestressing wires, Part 2 of prEN 10138 provides specifications for stress relieved high tensile steel wires ranging in diameter from 3.0 to 10.0 millimetres. These include dimensions and properties of the wires as well as testing methods that should be applied. It should be noted that the nominal modulus of elasticity may be taken as 205 GPa in accordance with Table 2 in Part 2 of prEN 10138.

The cold-drawn wires are more commonly used in pre-tensioned concrete, in which the prestressing force is transferred to the concrete by the bond between steel and concrete (Hurst, 1998). While it is not required, the wires often have deformations or as shown in Figure 3.1, which help to strengthen this bond.

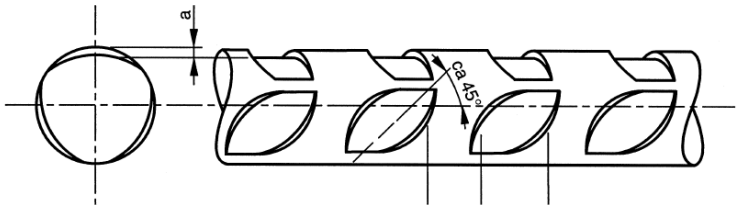

Figure 3.1 – Indentations for cold-drawn wires
(Part 2 of prEN 10138, Figure 1)

3.3.2 Prestressing Strands

Part 3 of prEN 10138 provides specifications for high tensile steel wire strands that have undergone stress relieving heat treatment. It covers five strand types including 3-wire strands, indented 3-wire strands, 7-wire strands, indented 7-wire strands, and 7-wire compacted strands. Dimensions and properties for all strand types with diameters ranging from 5.2 to 18.0 millimetres are provided as well as guidance on testing methods for the strands. It should be noted that the nominal modulus of elasticity for strands may be taken as 195 GPa in accordance with Table 2 in Part 3 of prEN 10138.

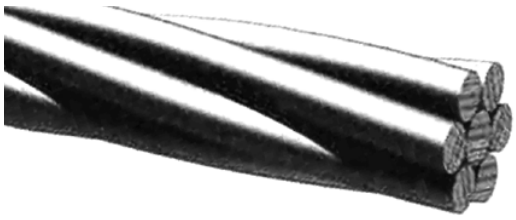

Figure 3.2 – 7-wire strand (CCL, 2011)

The 7-wire strands like that shown in Figure 3.2 are produced by spinning six individual wires around a core wire. They may be created as simply wound, or may be compacted after winding of the wires, creating a “drawn” strand (Hurst, 1998). Strands are applied in both pre-tensioned and post-tensioned structures.

3.3.3 Hot-Rolled Bars

Specifications for preferred sizes of round straight steel bars are provided by Part 4 of prEN 10138. The bars may be plain or ribbed. Dimensions and properties as well as testing methods are provided for diameters ranging from 15.0 to 40.0 millimetres. It should be noted that the nominal modulus of elasticity may be taken as 205 GPa in accordance with Table 2 in Part 4 of prEN 10138.

Figure 3.3 – Hot-rolled bar
(Freyssinet, 2010b)

The hot-rolled steel bars are stretched after they have cooled to improve the mechanical properties. Typically, they are either ribbed throughout the entire length, providing a continuous thread, or they are smooth with threading at each end for connection to the anchorages (Hurst, 1998). Prestressing bars are only applied in post-tensioned concrete where straight tendons are required.

3.3.4 Prestressing Properties for the Design Examples

It has been decided to use high tensile 7-wire strands for both design examples in this dissertation. Drawn strands with a 15.2 millimetre diameter, designated as "Y1820S7G" are selected for the single span and drawn strands with a 12.7 millimetre diameter, designated as "Y1860S7G" are selected for the continuous spans. Table 3.3 provides a summary of the properties for these strands.

Table 3.3 – Properties of strands for both designs
(Part 3 of prEN 10138, Table 2)

	Y1820S7G	Y1860S7G
φ_p (mm)	15.2	12.7
A (mm^2)	165	112
f_{pk} (MPa)	1820	1860
$f_{p0.1k}$ (MPa)	1565.2	1610
P_u (kN)	300	208
P_i (kN)	219	153

3.4 POST-TENSIONING DUCTS

For pre-tensioned beams, the concrete is cast around the steel and the strands are held in tension by the bond between steel and concrete. For post-tensioned beams, the strands are not tensioned until after the concrete has hardened. Therefore, ducts must be provided to allow tensioning of the steel and anchors are installed to hold tension in the steel and transfer the forces to the beam.

For the post-tensioning ducts, a wide range of options are available, all varying in shape, size, and material. In some cases with straight tendons, forms have been applied and then removed, creating an unlined duct for the strands. Lined ducts are typically formed using welded or spirally wound steel tubes. The spirally wound tubes can be advantageous in that they are flexible and easy to bend for curved profiles. In more recent designs, non-metallic ducts made of high-density polyethylene (HDPE), also known as PE80 or polypropylene, have been applied. These ducts are advantageous in that they provide corrosion resistance and better sealing against ingress. It should be noted, however, that the development of non-metallic ducts is still at a relatively early stage, and further investigation into the performance is required (The Concrete Society, 2010).

Figure 3.4 – Steel and plastic ducts (CCL, 2011)

The diameter of the ducts depends on the size and number of tendons inside. The duct must be large enough to allow threading of the tendons as well as grouting after the tendons have been stressed. Typically, a maximum tendon-to-duct area ratio of 0.40 to 0.45 is used (The Concrete Society, 2010). BS EN 1992-1-1 does not provide much guidance in regards to ducts, or as they are referred to in the code, sheaths. The only requirement, stated in Clause 3.3.7, is that tendons are adequately protected against corrosion. Decisions regarding size, type, and material are left to the designer.

3.5 POST-TENSIONING ANCHORAGES AND JACKS

The choice of which anchorage and corresponding jacking system to use should be given consideration early in the design process, since the spacing of the anchorages is affected by the jacking system that must be used. The choice of which anchorage will also affect the distribution of the prestressing strands in the beam (Hurst, 1998).

It should be noted that the location and positioning of anchorages in design is very important. It has been found that the ingress of contaminants occurs most often at the anchorages, causing corrosion in the tendons just behind the anchors. The design of the beam ends must be such that prevents access of water to the ducts (The Concrete Society, 2010).

The variability in anchorage systems makes it difficult to provide detailed specifications here. BS EN 1992-1-1 provides some guidance in Section 3.4.1 related to ensuring sufficient strength, elongation, and fatigue characteristics in the anchors

(Hendy and Smith, 2007). The code stipulates that each anchor must be in accordance with relevant European Technical Approval. For each design, further specifics on the anchorages and post-tensioning system should be obtained from the manufacturer.

An overview of the systems is provided here to give some understanding to how post-tensioning is applied in the field. Generally, the post-tensioning anchorages fall into three main categories: wedge anchorages, buttonhead anchorages, and threaded bar anchorages. For the continuous span design example, a wedge anchorage, discussed below, is chosen for the post-tensioned beam. Further details are provided in Appendix C.

3.5.1 Wedge Anchorages

Wedge anchorages may be used with tensioned steel wires or strands. The tensioning force is held by steel wedges which are locked into tapered holes in the anchor. It is most common for multiple strands or wires to be anchored in one anchorage system (Hurst, 1998). Figure 3.5 gives an example of a typical wedge anchorage.

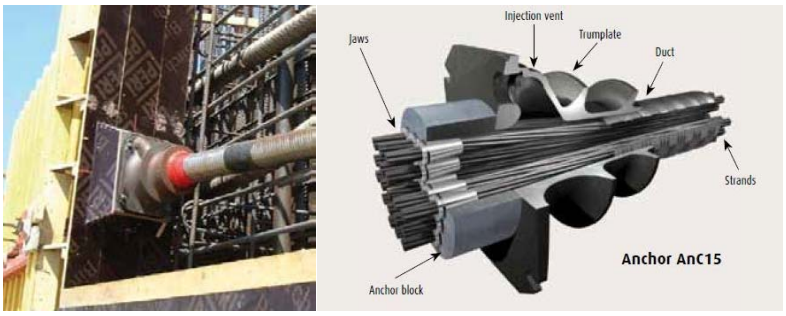

Figure 3.5 – Wedge anchorage (Freyssinet, 2010a)

Tensioning with wedge anchorages is usually carried out with single-strand or multi-strand hydraulic jacks of appropriate size, such as that shown in Figure 3.6. The tendons are gripped by the jack and pulled to the required extension and pressure. When the strands are released, the draw-in locks the steel wedges into the tapered holes (Hurst, 1998).

Figure 3.6 – Hydraulic jacking of wedge anchorage (Freyssinet, 2010a)

3.5.2 Buttonhead Anchorages

For prestressing wires, an alternative to the steel wedge is to form a "buttonhead" at the end of the wires, which is shaped to bear against a steel plate. In this case, multiple wires are threaded into one buttonhead and bear against an anchor plate. For this system, the wires are tensioned simultaneously by a jack and when the required pressure is achieved a steel shim is inserted between the anchor block and the bearing plate. Typically, these systems are more suitable for shorter members. Measurements in required length of the wires must be very precise (Hurst, 1998).

3.5.3 Threaded Bar Anchorages

The third category is a single threaded bar anchorage. The threaded bars are locked in with a nut bearing against a steel plate at the beam end. Often the full length of the bar is threaded, providing better bond once the grout is injected into the duct (Hurst, 1998). An example of this is given in Figure 3.4. To tension the prestressed bars, a hydraulic jack can be used to apply the required pressure, at which stage the nut is tightened firmly before the release of the jack (Hurst, 1998).

Figure 3.7 – Threaded bar anchorage (Freyssinet, 2010b)

4 TRAFFIC LOADING ON A BRIDGE

One of the most challenging aspects to the design of a bridge is the application of traffic loading. In most cases, traffic will be the leading variable action in the combinations of actions. Therefore, detailed and careful analysis of this loading is important. BS EN 1991-2 provides guidance for traffic actions on road bridges, pedestrian bridges, and railway bridges. This chapter will explain the application for road bridges in particular. To provide an illustration of the procedure, the traffic loading for both design examples is analyzed.

BS EN 1991-2 defines four vertical load models that must be considered on road bridges for serviceability and ultimate limit state verifications. Horizontal forces associated with two of these models due to braking, acceleration, and centrifugal forces are also defined. These loads are then combined in groups of traffic loads and the worst case is included in the load combinations defined by BS EN 1990. Guidance is also provided on fatigue load models and actions for accidental design situations; however the analysis of these is beyond the scope of this study.

4.1 APPLICATION OF THE LOAD MODELS

One of the most common methods for determining the maximum loading due to traffic on a bridge is to develop a grillage analysis using structural analysis software. Due to the complexity and high number of variations in the loading, using a software program will likely produce more accurate results in much less time if it is done correctly. This is especially true for multi-span structures, where the number of possible combinations for loading can become quite high.

While these programs may produce faster, more precise results, an understanding of how the program is calculating the loading on the structure is important so that the accuracy of the model can be verified. To provide a basic understanding of the load paths and applications, the traffic loadings considered in this dissertation are all determined by hand using the procedure outlined in Figure 4.1.

1	• Define the notional lanes and load models that must be applied.
2	• Determine the influence lines of the deck for the reaction of the beam.
3	• Calculate the greatest resultant axle load from the wheel loads.
4	• Calculate additional loading due to horizontal forces and/or footpath.
5	• Define the groups of traffic loads to be applied to the beam.
6	• Apply each group of traffic loads and determine maximum moments.
7	• Create an envelope of moments for all positions of the load model.
8	• Determine the minimum and maximum moments acting at each section.

Figure 4.1 – Procedure for application of traffic loads to the beam

4.2 DIVISION OF THE CARRIAGEWAY INTO NOTIONAL LANES

For the application of various load models, the number and location of notional lanes on the structure must be defined. In accordance with Table 4.1 of BS EN 1991-2, any carriageway width above 6.0 metres is divided into an integer number of 3.0 meter wide lanes with any excess width referred to as the "remaining area". For carriageway widths less than 6.0 metres, smaller notional lane widths may be used. The lanes are not required to follow the guidelines set for traffic on the bridge. Instead, they should be positioned so they will have the most adverse effect on the element of the structure under consideration.

The lanes must be numbered such that the lane producing the most unfavourable effect is identified as Lane No. 1, the lane producing the second most unfavourable effect is identified as Lane No. 2, and so on. It is generally understood that for limit states other than fatigue, this numbering is based on the characteristic values of the vertical load models, and should not be changed when those loads are applied with other representative values (Calgaro, Gulvanessian and Tschumi, 2010). Figure 4.2 presents the notional lanes that are defined for the design examples included in this dissertation. The positioning and numbering for the worst case are discussed in Section 4.4.

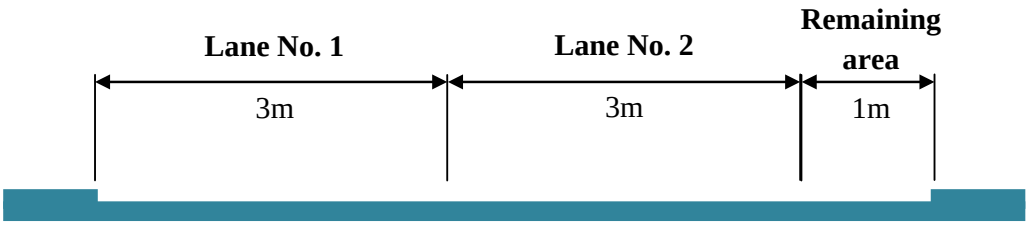

Figure 4.2 – Notional Lanes

4.3 VERTICAL LOAD MODELS

The vertical load models are to be applied for all limit state verifications except fatigue. These models are applicable for spans lengths of 200 metres or less, due to how the loads have been calibrated. It is possible to use these models for longer lengths; however, caution should be exercised, as the results may become unreliable beyond a certain point (Calgaro, Gulvanessian and Tschumi, 2010). For structures in the United Kingdom, the National Annex to BS EN 1991-2 allows Load Model 1 to be applied on loaded lengths up to 1500 metres.

4.3.1 Load Model 1 – Normal Traffic

The first load model, referred to as Load Model 1 (LM1), represents conditions for normal traffic and is applicable to all bridges (Jackson et al. 2010). The model is considered to be the main characteristic model. It does not define an actual vehicle but has been developed through traffic studies and theoretical investigations to account for the most common effects of traffic on a bridge (Calgaro, Gulvanessian and Tschumi, 2010). As noted in BS EN 1991-2, the load model is intended to cover flowing, congested, and traffic jam situations with a high percentage of lorries.

The model consists of a tandem system (TS) and uniformly distributed load (UDL) in each lane with a maximum of three notional lanes, as defined in Clause 4.3.2 of BS EN 1991-2. For each tandem system, the two axles are 1.2 metres apart with the wheels spaced at 2.0 metres as shown in Figure 4.3. The axles should be centred in the lanes and the lanes should be positioned to produce the most severe effect. The position of the UDL and TS longitudinally along the lanes should also be such that is most unfavourable. To this effect, it is not required to apply the UDL to the full width or span of a lane (Calgaro, Gulvanessian and Tschumi, 2010).

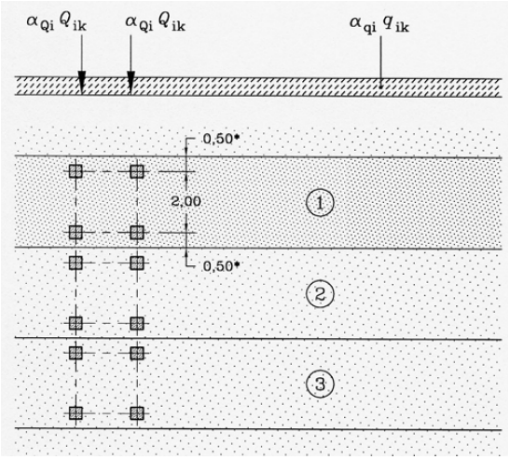

Figure 4.3 – Application of LM1
(BS EN 1991-2, Cl. 4.3.2)

Table 4.1 presents the values from BS EN 1991-2 for the axle loads and uniformly distributed loads (UDL) in each lane. For the design examples in this report, only two lanes are considered, with values of 300 kN and 200 kN on the respective tandem axles.

Table 4.1 – Load Model 1 - Characteristic values and adjustment factors
(BS EN 1991-2, Cl. 4.3.2 and NA to BS EN 1991-2, Table NA.1)

	Tandem System			UDL		
	Q_{ik} (kN)	α_{Qi}	$Q_{ik}\,\alpha_{Qi}$ (kN)	q_{ik} (kN/m^2)	α_{qi}	$q_{ik}\,\alpha_{qi}$ (kN/m^2)
Lane 1	300	1.00	300	9	0.61	5.5
Lane 2	200	1.00	200	2.5	2.20	5.5
Lane 3	100	1.00	100	2.5	2.20	5.5
Other Lanes	0	-	-	2.5	2.20	5.5
Remaining Area	0	-	-	2.5	2.20	5.5

All of the loads are multiplied by nationally determined adjustment factors, α_{Qi} and α_{qi}, which are defined in Table NA.1 of the UK National Annex to BS EN 1991-2. The axle loads for the tandem system are to be distributed evenly to each of the two wheels. For the purpose of local verifications the National Annex to BS EN 1991-2 defines the contact area of the wheels to be a 0.40 meter square.

4.3.2 Load Model 2 – Single Axle

Load Model 2 (LM2) is also a characteristic model, which may be considered as a complimentary model to LM1. This model is applied for verifications of local effects on short structural members such as orthotropic slabs that are not necessarily covered by the main characteristic model (Calgaro, Gulvanessian and Tschumi, 2010). Typically, for members of 7.0 metres or less, this model may cause more severe effects than LM1; however, it will most likely not control in the global analysis of the structure (Jackson et al. 2010).

The model consists of a single axle with a weight of 400 kN that is evenly distributed between two wheels spaced at 2.0 metres, as defined by Clause 4.3.3 of BS EN 1991-2. It is not combined with any other traffic loading. The adjustment factor, β_Q, is defined to be equal to α_{Qi} of LM1 with a value of 1.0 set by the National Annex to BS EN 1991-2 and the contact surface for the wheel loads is defined to be a 0.40 meter square as well. The axle can be applied to any location on the roadway, and the effects of only a single wheel load may be considered if relevant.

4.3.3 Load Model 3 – Special Vehicles

Load Model 3 (LM3) is intended to cover the effects of special convoys crossing the structure (Calgaro, Gulvanessian and Tschumi, 2010). A series of special vehicle (SV) load models are defined by Clause NA.2.16 in the National Annex for BS EN 1991-2 which represent the effect of vehicles that are compliant with the Special Types General Order (STGO) and Special Order (SO) Regulations. These models do not describe actual vehicles, but have been calibrated to represent the maximum effects that may be induced by the actual STGO or SO compliant vehicles.

To represent the STGO compliant vehicles, the National Annex defines three load models including SV80, SV100, and SV196. Details for each of these models are described below. Only one special vehicle is applied to the carriageway at a time. This vehicle can be placed anywhere in the roadway to create the most adverse effect, and does not have to follow the guidelines of the notional lanes. It should be noted that the wheel spacing for all three of these models is slightly wider than that of LM1 and LM2 with a distance of 2.65 metres. Figures 4.4 through 4.6 show the axle spacing for each model, which varies along the length of the vehicle.

SV80 Vehicle:

SV80 models the effects of STGO Category 2 vehicles that have a maximum gross weight of 80 tonnes and a maximum basic axle load of 12.5 tonnes.

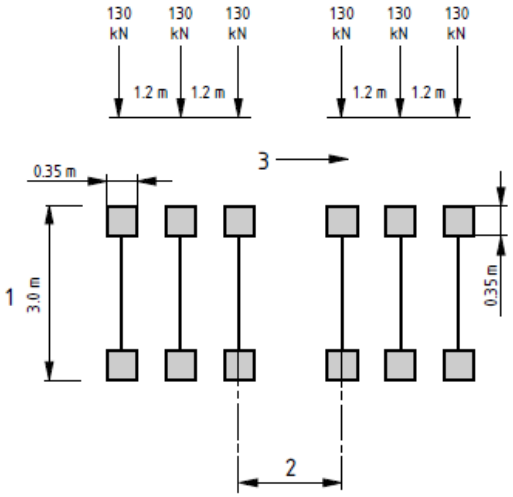

Figure 4.4 – Longitudinal configuration for the SV80 model (NA to BS EN 1991-2, Figure NA.1)

SV100 Vehicle:

SV100 models the effects of STGO Category 3 vehicles that have a maximum gross weight of 100 tonnes and a maximum basic axle load of 16.5 tonnes.

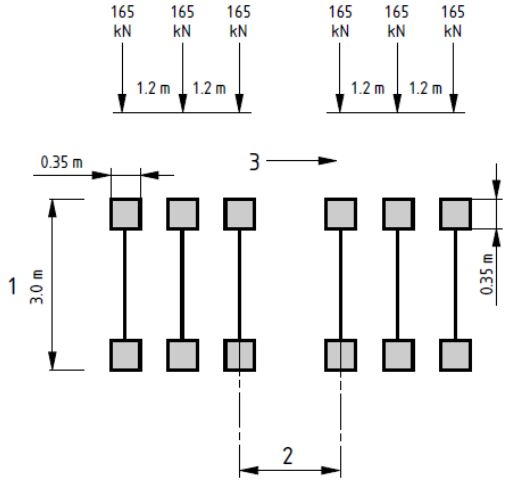

Figure 4.5 – Longitudinal configuration for the SV100 model (NA to BS EN 1991-2, Figure NA.1)

SV196 Vehicle:

SV196 models the effects of a single locomotive pulling an STGO Category 3 vehicle with a maximum gross weight of 150 tonnes and a maximum basic axle load of 16.5 tonnes. The gross weight of the train must not exceed 196 tonnes.

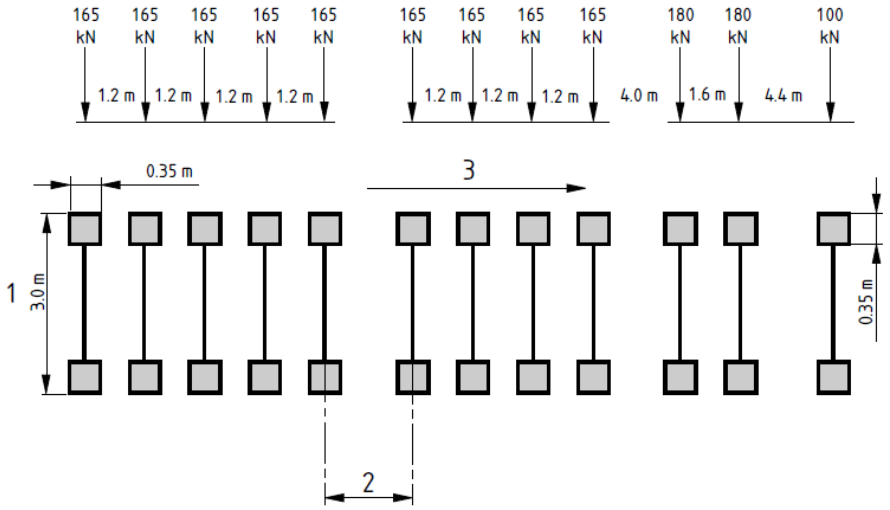

Figure 4.6 – Longitudinal configuration for the SV196 model (NA to BS EN 1991-2, Figure NA.1)

In Figures 4.4 through 4.6, 1 identifies the overall vehicle width, 2 is equal to the critical of 1.2m, 5.0m, or 9.0m, and 3 represents the direction of travel.

The values for the axle loads on each model are summarized in Table 4.2. The axle weights are multiplied by a dynamic amplification factor (DAF) that is defined based on the axle weight in the National Annex to BS EN 1991-2, Table NA.2. Each axle weight is distributed evenly to the two wheels. For local verifications, the wheel load is to be distributed over a 0.35 meter square as shown in Figures 4.4 through 4.6.

Table 4.2 – Characteristic values and factors for SV models (NA to BS EN 1991-2, Figure NA.1 and Table NA.2)

Vehicle	Q_k (kN)	DAF	Q_k DAF (kN)
SV80	130	1.16	150.8
SV100	165	1.12	184.8
SV196	100	1.20	120.0
	180	1.10	198.0
	165	1.12	184.8

The National Annex to BS EN 1991-2 also defines four models to simulate the effects of Special Order Vehicles (SOV), compliant with SO regulations, with gross weights above 150 tonnes (Jackson et al. 2010). The models represent maximum total weights of 250 tonnes, 350 tonnes, 450 tonnes, and 600 tonnes. Each model consists of a trailer with two bogies and two tractors, one pushing and one pulling. On each axle the loads are distributed to four wheels, as shown in Figure 4.7. Similar to the STGO vehicles, these load models can be applied to any position on the carriageway, without restrictions from the notional lanes. Figure 4.8 summarizes axle weights and configurations of the four load models.

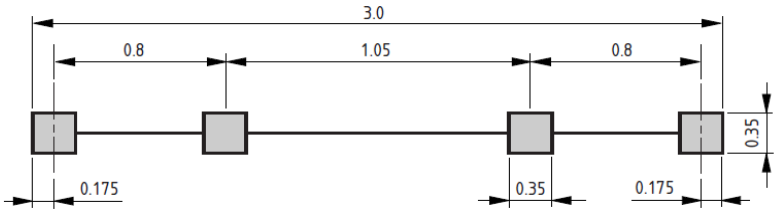

Figure 4.7 – Lateral arrangement of wheel loads for SOV models (NA to BS EN 1991-2, Figure NA.3)

(a) ***SOV-250*** **Vehicle**

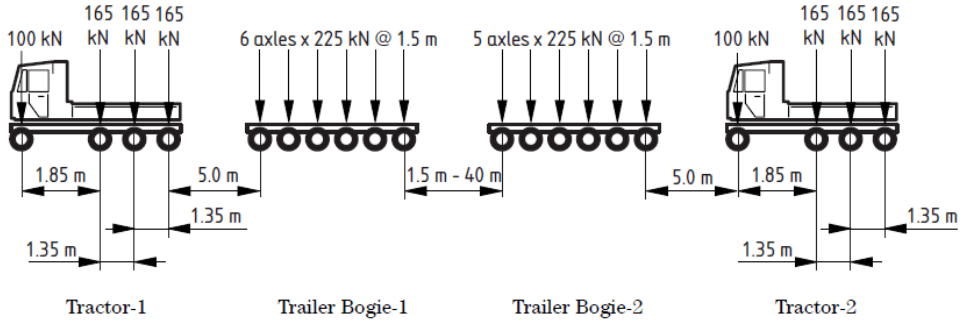

(b) ***SOV-350*** **Vehicle**

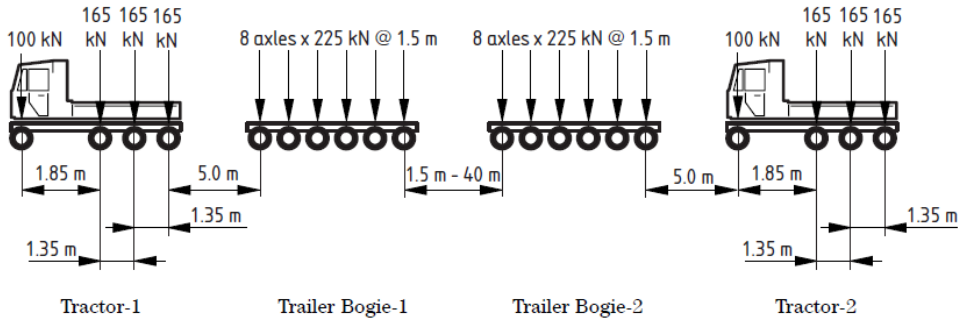

(c) ***SOV-450*** **Vehicle**

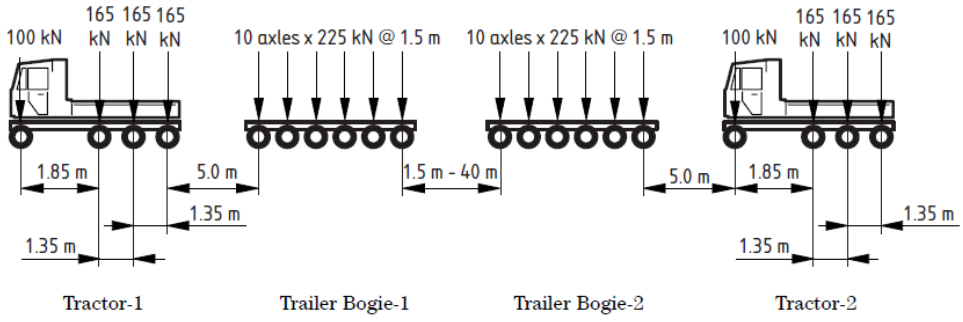

(d) ***SOV-600*** **Vehicle**

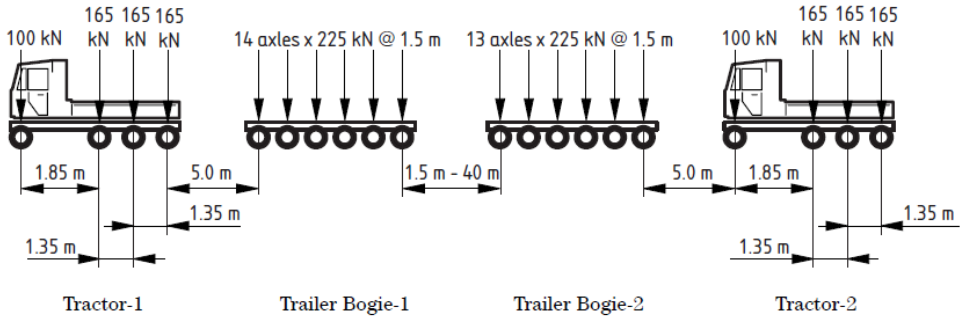

NOTE For simplicity, 6-axle trailer bogies are shown. The actual number of axles of trailer bogie should be that stated above the figure.

Figure 4.8 – Axle weights and configuration for SOV models

(NA to BS EN 1991-2, Figure NA.2)

The occurrence of special order vehicles in traffic is not as common and only needs to be taken into account on certain routes (Jackson et al. 2010). The decision on which of the SV or SOV models to apply for design should be made for each individual project based on the type of traffic the structure will have to carry. It is left to the client and/or designer to determine the appropriate model to use (Calgaro, Gulvanessian and Tschumi, 2010). To illustrate the application of special vehicles, SV196 will be considered for the design examples in this dissertation.

4.3.4 Load Model 4 – Crowd Loading

Load Model 4 (LM4) corresponds to the physical maximum load from human beings. It is intended for use in urban areas where crowds may form on the structure due to cultural or sporting events (Calgaro, Gulvanessian and Tschumi, 2010). The model consists of a uniformly distributed load of 5.0 kN/m^2 applied to the whole deck, including both the carriageway and the footway, as defined in Clause 4.3.5 of BS EN 1991-2. This loading already includes the dynamic amplification. It need only be considered when expressly demanded for (Jackson et al. 2010). Explanation and calculations for the loading are included in this report. However, the loading will not control in the global analysis of the structure.

4.4 POSITION OF THE WHEELS

Now that the individual load models are defined, the resultant axle weights acting on the beam due to the applied wheel loads must be determined. For clarity, the discussions in this section are based on the bridge cross section in Figure 4.9 which applies to both design examples.

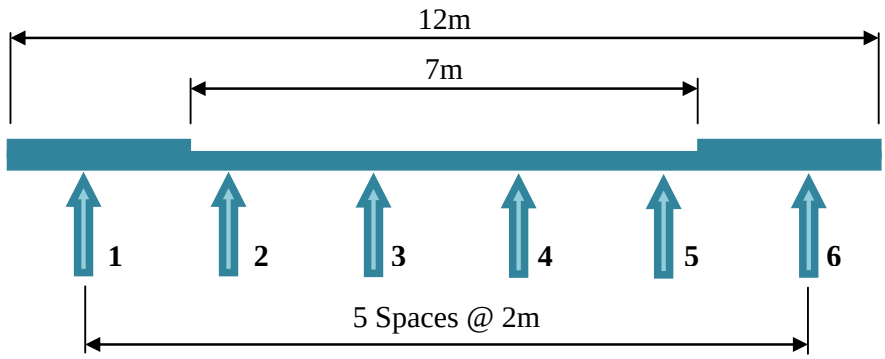

Figure 4.9 – Bridge cross section for both design examples

Before the wheel loads are applied, the influence lines of the deck for the reaction of the beam under consideration must be determined. The procedure for this is outlined in Section A.1 of Appendix A. Further explanation can also be found in many structural analysis books. Figure 4.10 presents the resulting influence line for Beam 3, at 4.0 metres, which is the critical beam in both design examples.

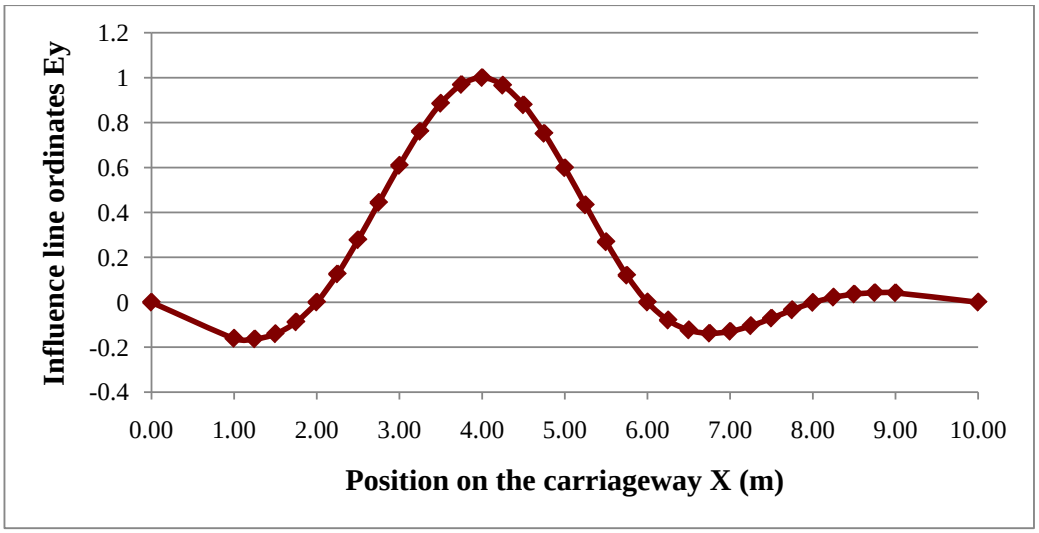

Figure 4.10 – Influence line for Beam 3

It should be noted that the influence line ordinates have been calculated at 0.25 meter intervals. For more accurate results in determining the position of the maximum loading, additional ordinates may be determined; however, there is less than 1% error between these results and those from 0.05 metres intervals. Therefore, the results from these ordinates are accurate enough for the calculation of resultant axle loads.

Once the influence line for Beam 3 is known, the wheel loads for each load model defined in the previous section are applied and the resultant axle loads are calculated by multiplying each wheel load by the influence line ordinate at the location of that wheel, and summing the results. The wheel loads are applied at a number of positions on the carriageway to determine that which will create the greatest resultant axle load. The results of these calculations are included in the following sections for Load Models 1, 2, and 3. Load Model 4 is not considered in this section since there are no wheel loads in the model.

4.4.1 Resultant Axle Weight for Load Model 1

As mentioned previously, Load Model 1 is applied within notional lanes. Based on the carriageway width, two tandem systems should be applied to the structure in the design examples. From the axle weights determined in Section 4.3.1 it is determined that the wheel loads are 150 kN each in Lane No. 1 and 100 kN each in Lane No. 2.

It is found that the maximum resultant axle loading for this load model occurs when the wheels in Lane No. 1 are directly over Beams 2 and 3, as shown in Figure 4.11. Table 4.3 presents a summary of the calculations at this location for the maximum resultant load. Further details are provided in Section A.3.1 of Appendix A.

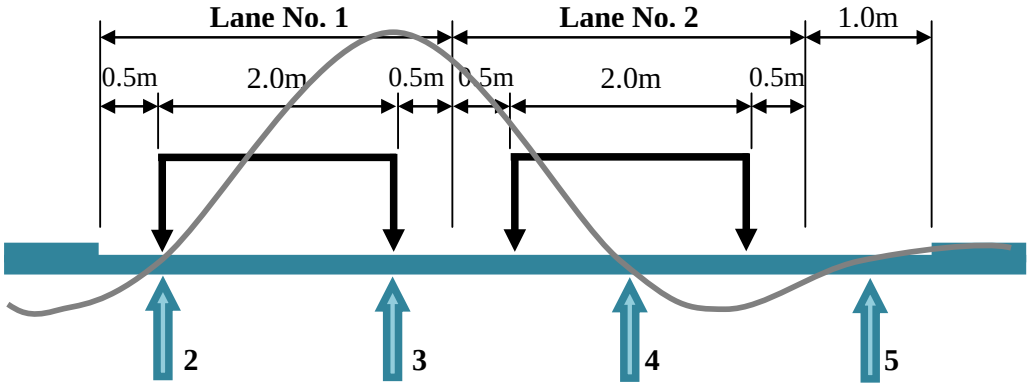

Figure 4.11 – Application of LM1 for the maximum resultant axle load

Table 4.3 – Maximum resultant axle load for LM1

X (m)	E_y	Q_w (kN)	P_{LM1} (kN)
2.00	0.0003	150	0.0430
4.00	1.0000	150	150.0000
5.00	0.5983	100	59.8305
7.00	-0.1297	100	-12.9675
		$Q_{LM1} = \Sigma P_{LM1} =$	197

In addition to the tandem system, LM1 includes a uniformly distributed load which has been defined in Table 4.1. For the application of this loading the UDL is simply multiplied by the spacing of the beams to find a distributed load along the length of the beam. In this case, with a beam spacing of 2.0 metres, a load of 11.0 kN/m will be distributed on the beam.

4.4.2 Resultant Axle Weight for Load Model 2

Load Model 2 consists of only a single axle with a total weight of 400 kN. Therefore, 200 kN is applied for each wheel load. For this load model, the worst case occurs when the centre of the axle is placed directly over Beam 3, as shown in Figure 4.12. Table 4.4 presents a summary of the calculations at this location for the maximum resultant axle weight. For further explanation of these results, refer to Section A.3.2 of Appendix A.

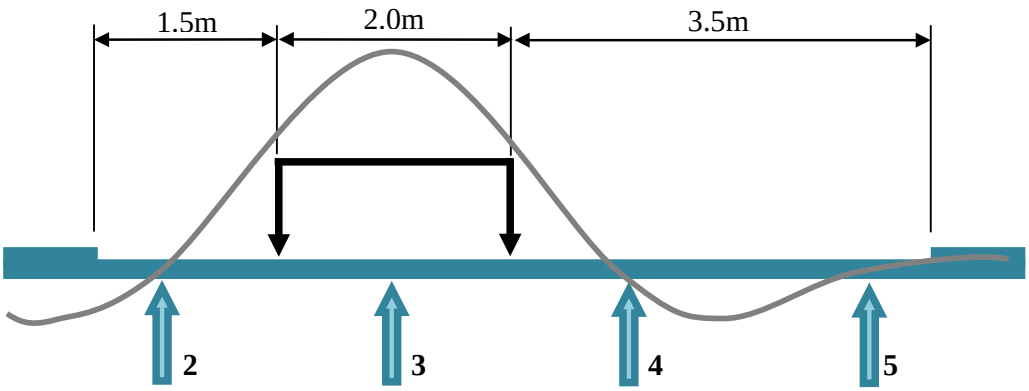

Figure 4.12 – Application of LM2 for the maximum resultant axle load

Table 4.4 – Maximum resultant axle load for LM2

X (m)	E_y	Q_w (kN)	P_{LM2} (kN)
3.00	0.6088	200	121.7676
5.00	0.5983	200	119.6610
		$Q_{LM2} = \Sigma P_{LM2} =$	242

4.4.3 Resultant Axle Weight for Load Model 3

For Load Model 3, it has been decided to apply the SV196 vehicle, which will have the most adverse effect of the three STGO models described in Section 4.3.3. For this model, there are three different axle weights to be applied; however, the calculations are the same for each since they all have the same wheel spacing. The wheel loads for each axle will be 60 kN, 99 kN, and 92.4 kN. Refer to Section A.3.3 of Appendix A for a summary of all the resultant axle loads. The worst case occurs when the first wheel is 2.40 metres from the edge of the carriageway, or 0.10 metres to the left of Beam 3, as shown in Figure 4.13. Table 4.5 presents a summary of the calculations at this location.

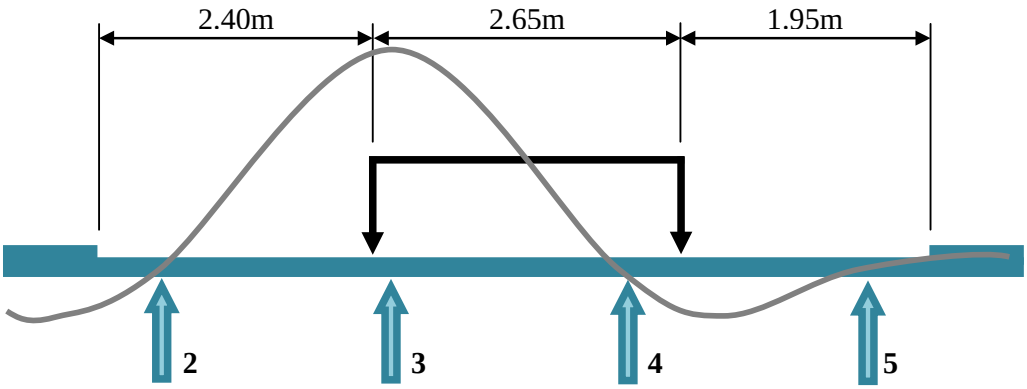

Figure 4.13 – Application of LM3 for the maximum resultant axle load

Table 4.5 – Maximum resultant axle load for LM3

X (m)	E_y	Q_w (kN)	P_{LM3} (kN)
3.90	0.9943	60	59.6581
6.55	-0.1288	60	-7.7276
		$Q_{aLM3} = \Sigma P_{aLM3}$ =	52
3.90	0.9943	99	98.4358
6.55	-0.1288	99	-12.7505
		$Q_{bLM3} = \Sigma P_{bLM3}$ =	86
3.90	0.9943	92.4	91.8734
6.55	-0.1288	92.4	-11.9005
		$Q_{cLM3} = \Sigma P_{cLM3}$ =	80

4.5 HORIZONTAL FORCES

For Load Model 1 and Load Model 3, BS EN 1991-2 and the National Annex define horizontal forces that may occur due to braking and acceleration or centrifugal forces.

4.5.1 Braking and Acceleration Forces

The longitudinal braking and acceleration forces are represented with a force, Q_{lk}, acting at the surface of the carriageway. This force has a characteristic value limited to 900 kN for the total width of the bridge. For LM1, it is calculated as a fraction of the total maximum vertical loads applied to Lane No. 1. Clause 4.4.1 of BS EN 1991-2 defines the following expression for the characteristic value of Q_{lk}.

$$Q_{lk} = 0.6\alpha_{Q1}(2Q_{1k}) + 0.10\alpha_{q1}q_{1k}w_1L \quad (4.1)$$

for: $180\alpha_{Q1}\ (kN) \leq Q_{lk} \leq 900\ (kN)$

In this equation, L represents the length of the deck or the part that is under consideration and w_1 represents the width of the lane considered. All other values have been defined for LM1 in Table 4.1.

For LM3, the National Annex defines separate longitudinal forces for braking and acceleration, and specifies that the more severe of the two should be applied. The acceleration force is defined by Clause NA.2.18.1 to be 10% of the gross weight of the SV or SOV vehicle, and distributed between the axles and wheels in the same proportion as the vertical loads. The braking force is calculated based on the following equation, which represents the braking force on the individual axles.

$$Q_{lk,S} = \delta\omega \quad (4.2)$$

In this equation, δ represents the deceleration factor and ω is the basic axle load, Q_{ik}, that has been defined in Table 4.2. The deceleration factor is defined in Clause NA.2.18.1 for each SV and SOV vehicle.

For the design examples in this dissertation, the braking and acceleration forces will not be included due to time restraints. Typically, these forces are small enough to be ignored for the design of a bridge deck. However they should be considered for any future investigations into the design of supports for the structure such as the abutment foundations (Jackson et al. 2010).

4.5.2 Centrifugal Forces

If the carriageway has a curved centreline, a centrifugal force should also be applied. This force is represented by a transverse force, Q_{tk}, which is applied at the surface of the carriageway, perpendicular to its axis. Calculation of the force is based on the horizontal radius, r, of the carriageway for both load models. Table 4.6 defines the transverse force for LM1 from Clause 4.4.2 of BS EN 1991-2.

Table 4.6 – Centrifugal forces for LM1

(BS EN 1991-2, Cl. 4.4.2)

$Q_{tk} = 0.2Q_v$ (kN)	if r < 200 m
$Q_{tk} = 40Q_v/r$ (kN)	if 200 ≤ r ≤ 1500 m
$Q_{tk} = 0$	if r > 1500 m

where: $Q_v = \sum \alpha_{Qi}(2Q_{ik})$

For LM3, the transverse force is defined based on the speed limit, V_{limit}, as well as the horizontal radius, r. Clause NA.2.18.2 of the National Annex gives the following expression for the characteristic value of Q_{tk}.

$$Q_{rk,S} = \frac{W \times V^2}{g \times r} \tag{4.3}$$

where: $V = \rho \left(\text{greater of 30 or } \sqrt{\frac{100 \times g \times r}{r+150}} \right) \leq V_{limit}$

For Equation (4.3), V represents the velocity of the vehicle, W represents the weight of the vehicle, and g represents the acceleration due to gravity (9.8 m/sec^2). Values for ρ are given for each SV or SOV vehicle in the code. Similar to the braking and acceleration forces, the centrifugal force should be distributed between the wheels in the same proportion as the vertical loads. For the design examples in this report, these forces need not be considered, as there is no curvature in the carriageway.

4.6 FOOTPATH LOADING

For bridges that carry a footway in addition to the carriageway, variable loading on the footpath due to pedestrians must also be considered. Clause NA.2.36 of the National Annex to BS EN 1991-2 gives the following expression for the calculation of the uniformly distributed load, q_{fk}, to be applied to the footway.

$$q_{fk} = 2.0 + \frac{120}{L + 10} \quad \text{kN/m}^2 \tag{4.4}$$

for: $2.5 \text{ kN/m}^2 \leq q_{fk} \leq 5.0 \text{ kN/m}^2$

The uniformly distributed load should be applied to the width of the footpath and distributed appropriately to the beams. In Equation (4.4), L represents the loaded length of the footway. The application of the load should be such that will create the most severe effect. In other words, the loaded length does not necessarily have to be the full length of the structure. Clause NA.2.36 also specifies that if the structure is located in a location where there is risk of continuous dense crowds, q_{fk} should be taken as 5.0 kN/m^2. For the design examples, only the critical beam is analyzed, which is Beam 3. Therefore, the footpath loading will not be considered, since the footpath is not supported by this beam.

4.7 GROUPS OF TRAFFIC LOADS

To determine the final traffic action that is to be included in the combinations of actions with other non-traffic loads, BS EN 1991-2 defines groups of traffic loads. These groups may be thought of as sub-combinations which define global actions for traffic (Calgaro, Gulvanessian and Tschumi, 2010). Table 4.7 presents the six load groups for traffic that are defined by the National Annex. The resulting actions from these groups are considered to be characteristic values of multi-component action.

Table 4.7 – Groups of traffic loads (NA to BS EN 1991-2, Table NA.3)

	Carriageway					Footways
	Vertical forces				Horizontal forces	
Groups of Loads	LM1	LM2	LM3	LM4	Braking & centrifugal	UDL
gr1a	Char.					0.6*Char.
gr1b		Char.				
gr2	Frequent				Char.	
gr3						Char.
gr4				Char.		Char.
gr5	Frequent		Char.			
gr6			Char.		Char.	
NOTES: Char. = Characteristic (1) gr3 is irrelevant if gr4 is considered. (2) the ψ_1 factors for frequent values are taken from NA to BS EN 1990						

As explained in Sections 4.5 and 4.6, the footway and horizontal forces will not be considered for the design examples in this dissertation. Therefore, only load groups gr1a, gr1b, gr4, and gr5 need to be considered. Further explanation of Load Group gr5 in particular is required, with the combination of Load Model 3 and frequent values of Load Model 1.

For the simultaneous application of these two load models, Clause NA.2.16.4 of the National Annex to BS EN 1991-2 provides detailed guidance. The code stipulates that one SV or SOV vehicle for LM3 should be placed at the most unfavourable position on the carriageway. The frequent values of LM1 should then be applied within the notional lanes that were defined for the application of LM1 and Load Group gr1a, but should not be applied within 5.0 metres of the centre of the outermost axles (front and rear). Further explanation of these guidelines is provided in Figures 4.14 and 4.15.

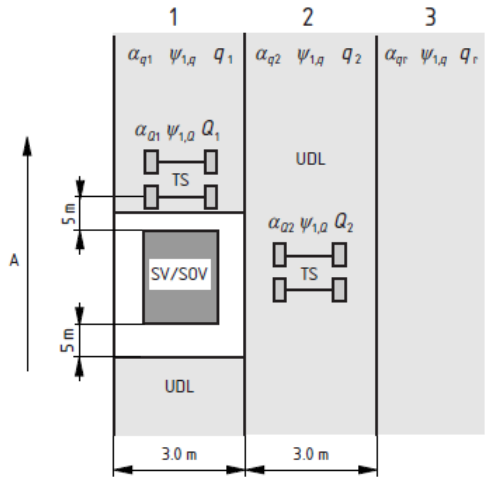

Key
A = Direction of travel 1 = Lane 1 2 = Lane 2 3 = Remaining area

Figure 4.14 – Application of Load Group gr5 with the SV or SOV vehicle applied fully within a notional lane (NA to BS EN 1991-2, Figure NA.4)

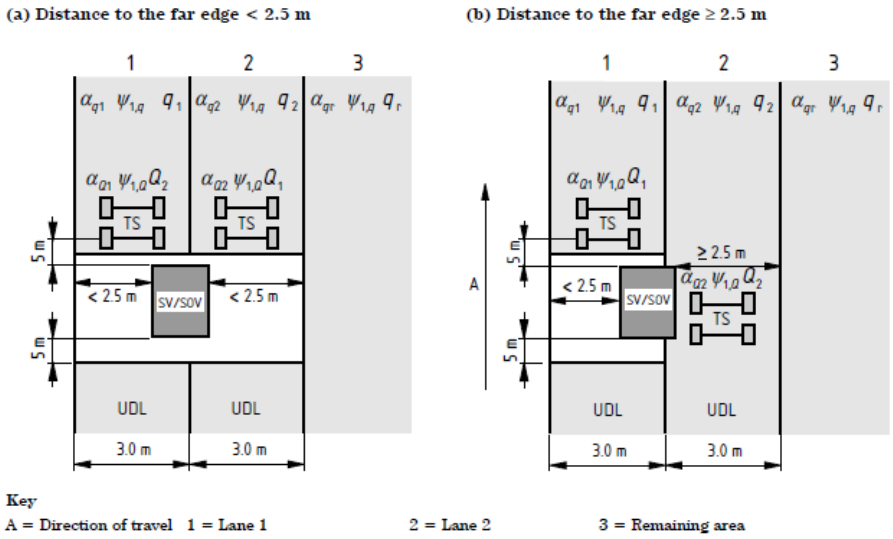

Figure 4.15 – Application of Load Group gr5 with the SV or SOV vehicle applied between two adjacent lanes (NA to BS EN 1991-2, Figure NA.5)

Based on the position of the SV196 vehicle established in Section 4.4.3 and represented in Figure 4.13, the application of Load Group gr5 for the design examples will be in accordance with Figure 4.15(a). The distance to the edge of the carriageway on either side is less than 2.5 metres. Therefore, the frequent values of LM1 will only be applied before and after the SV vehicle.

In addition to the characteristic groups of traffic loads, Table 4.4b of BS EN 1991-2 also defines a series of load groups for frequent values of multi-component action. Table 4.8 presents the three load groups. The worse case of these three groups should be applied in the calculation of the frequent combination of actions. For the frequent values, ψ_1 factors defined in the National Annex to BS EN 1990 are applied.

Table 4.8 – Groups of traffic loads for frequent combination (BS EN 1991-2, Table 4.4b)

	Carriageway		Footways
	Vertical forces		
Groups of Loads	LM1	LM2	UDL
gr1a	Frequent		
gr1b		Frequent	
gr3			Frequent

4.8 APPLICATION OF THE GROUPS OF TRAFFIC LOADS

Now that the groups of traffic loads have been defined, each one must be applied to the structure, as described in the procedure outlined in Figure 4.1. For prestressed concrete, the beams are generally designed for flexure. Therefore, the maximum moment acting on the beam is determined. In the design example for the single span, this has been accomplished through the basic application of force equilibrium and shear and moment diagrams with the tandem axle at a number of positions on the beam. From the series of maximum moments calculated, the position of the axles in the load model which will cause the greatest moment is determined.

For the two-span continuous design example, the same method is applied with some variation. First, this structure is an indeterminate structure, and therefore the calculation of support reactions for the shear and moment diagrams requires the application of the moment distribution method. This method has been outlined in Section A.4 of Appendix A. Another difference is that in addition to calculating the maximum moment, the minimum moment must also be determined. These beams experience negative moments around the supports that must be designed for.

In the design of prestressed concrete, the balance of stresses must be checked along the entire length of the beam, not just at the location of maximum moments. Therefore, the maximum moments acting at a number of sections on the beam must be determined in addition to the overall maximum moment. To accomplish this, an envelope of moments is established. For the single span, the moments are established at 2.5 metre intervals and for the continuous spans they are established at 5.0 metre intervals. To account for any missing values in the envelopes, trend lines are applied. The envelope of moments and summary of maximum moments are provided here for each load group. Refer to Section A.4 of Appendix A for full calculations.

4.8.1 Minimum and Maximum Moments Due to Load Group gr1a

As defined in the last section, Load Group gr1a for the design examples in this report consists of Load Model 1. For this model, the axle weights, Q_{LM1}, for the tandem system are found to be 197 kN each, and the distributed load, w_{UDL}, is 11 kN/m.

The single span design example:

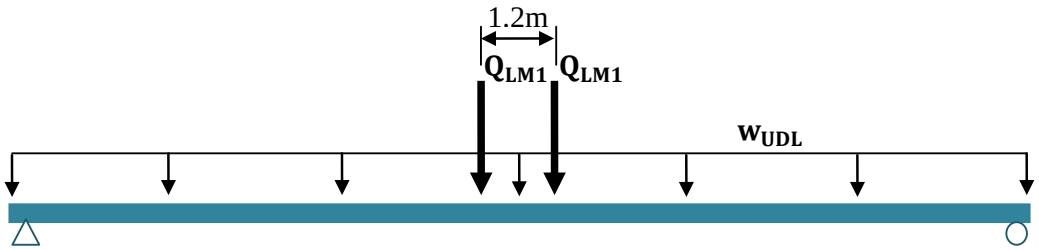

Figure 4.16 – Application of Load Group gr1a on the single span

On the 25.0 meter span, a maximum moment of 3205 kNm is found to occur when the resultant of the two axles is placed 12.1 metres from the support and 12.9 metres from the support, on either side of midspan. When comparing the results at these two locations to the moment resulting from the axle weights applied at midspan, an error of only 0.03% was found. Therefore, in future investigations, it is satisfactory to assume that the maximum moment due to LM1 will occur with the axles placed at midspan on single spans.

Figure 4.17 presents the envelope of moments produced for Load Group gr1a. From this, the results summarized in Table 4.9 are found. For further details and explanation of the results, refer to Section A.4.1 of Appendix A.

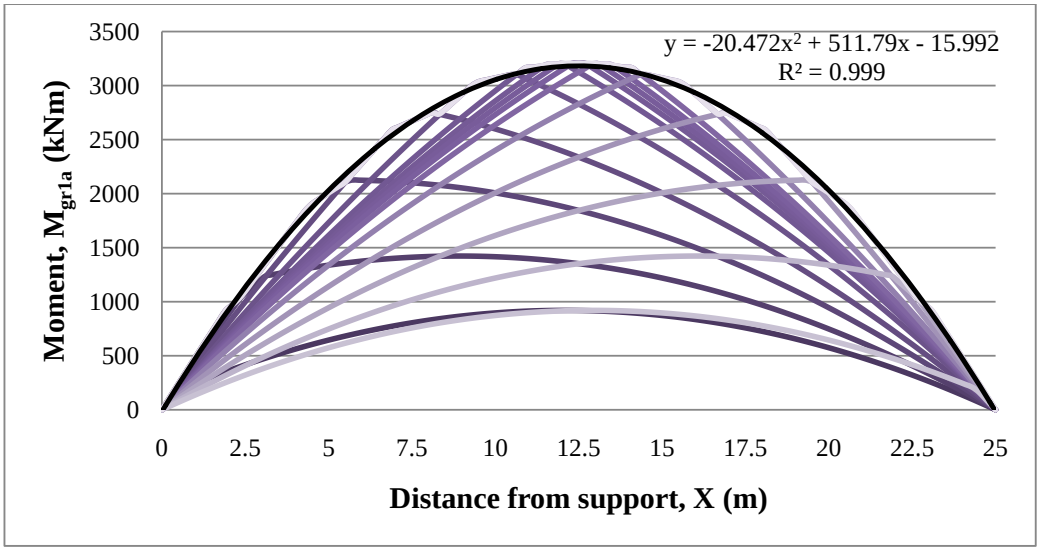

Figure 4.17 – Envelope of moments for Load Group gr1a on the single span

Table 4.9 – Summary of M_{gr1a} for the single span

Position (m)	M_{gr1a} (kNm)
0	0
2.5	1136
5	2031
7.5	2672
10	3071
12.5	3205
15	3071
17.5	2672
20	2031
22.5	1135
25	0

The two-span continuous design example:

As previously mentioned, for the continuous spans the minimum moment must be determined in addition to the maximum moment so that the negative moment acting around the supports can be designed for. Before applying the tandem system, preliminary calculations were performed based solely on the distributed load. From these calculations, it is determined that the maximum positive moment occurs when the UDL is only applied to one span, and the minimum negative moment occurs when the UDL is applied fully to both spans. Figure 4.18 illustrates the applications of Load Groupgr1a for both situations.

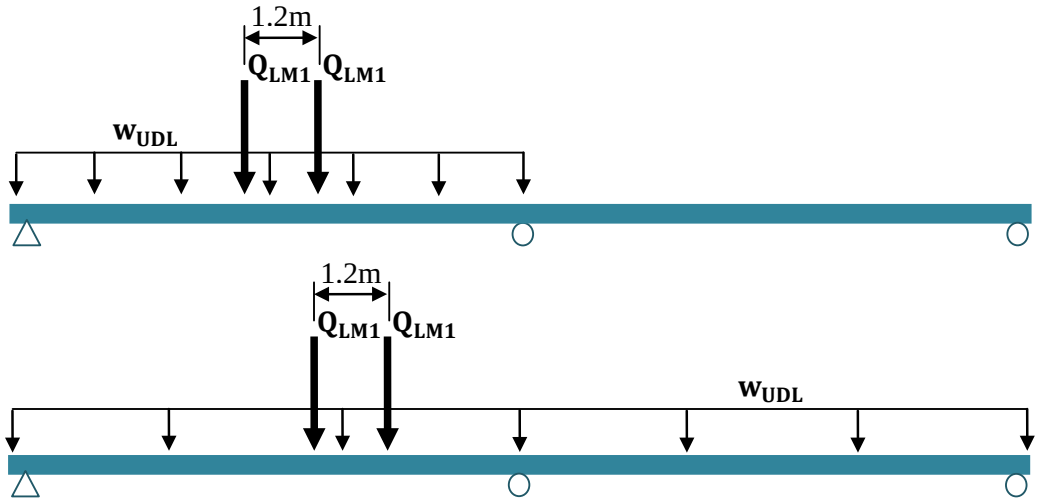

Figure 4.18 – Application of Load Group gr1a for the maximum and minimum moments on the continuous spans

On the continuous spans, each 40 metres in length, it is found that the maximum positive moment of 4841 kNm occurs when the resultant of the tandem axles is placed at 17.8 metres and 62.2 metres from the first support with the uniformly distributed load applied to the corresponding span. The minimum negative moment of -3715 kNm is found to occur when the resultant of the tandem axles is placed at 23.1 metres and 56.9 metres from the first support with the uniformly distributed load applied to both spans. Figure 4.19 presents the envelope of moments produced for Load Group gr1a. From this, the results summarized in Table 4.10 are determined. Further details are provided in Section A.4.1 of Appendix A.

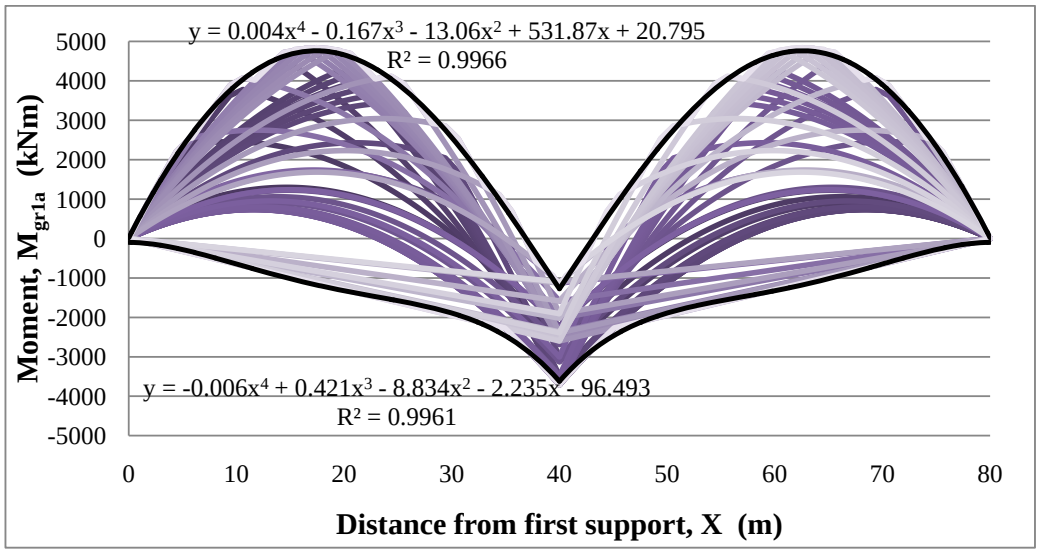

Figure 4.19 – Envelope of moments for Load Group gr1a on continuous spans

Table 4.10 – Summary of M_{pgr1a} and M_{ngr1a} for the continuous spans

Position (m)	M_{pgr1a} (kNm)	M_{ngr1a} (kNm)	Position (m)	M_{pgr1a} (kNm)	M_{ngr1a} (kNm)
0	0	0	45	901	-2421
5	2370	-325	50	2694	-1949
10	3981	-650	55	4014	-1624
15	4750	-1017	60	4734	-1319
20	4734	-1319	65	4750	-1017
25	4014	-1624	70	3981	-650
30	2694	-1949	75	2370	-325
35	901	-2421	80	0	0
40	-1130	-3715			
NOTE: M_{pgr1a} = maximum positive moment, M_{ngr1a} = minimum negative moment.					

4.8.2 Minimum and Maximum Moments Due to Load Group gr1b

As defined in the last section, Load Group gr1b for the design examples in this report consists of Load Model 2. For this model the axle weight, Q_{LM2}, on the single axle is determined to be 242 kN. Refer to Section A.4.2 of Appendix A for full calculations.

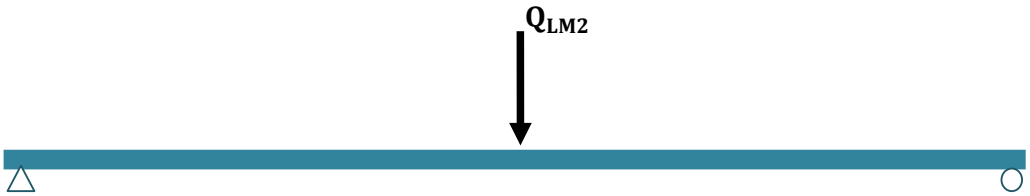

Figure 4.20 – Application of Load Group gr1b

The single span design example:

On the 25.0 metre span, an envelope of moments is not required for this load group. Due to the fact that only a single axle is applied, it is known that the maximum moment at each section occurs when the axle is placed directly over that section. An overall maximum moment of 1513 kNm is determined at midspan. Table 4.11 summarizes the results for each section.

Table 4.11 – Summary of M_{gr1b} for the single span

Position (m)	M_{gr1b} (kNm)
0	0
2.5	545
5	968
7.5	1271
10	1452
12.5	1513
15	1452
17.5	1271
20	968
22.5	545
25	0

The two-span continuous design example:

The maximum moments for the continuous spans are calculated with beam formulas since, like the single span, the maximum effect for each section occurs when the axle load is applied at that section. On the contrary, the minimum negative moment

always occurs at the centre support. Therefore, the envelope of moments has been developed to determine the minimum moments at each section.

For this load group, a maximum positive moment of 2008 kNm occurs when the axle is placed at 17.3 metres and 62.7 metres from the first support. And a minimum negative moment of -932 kNm occurs when the axle is placed at 23.1 metres and 56.9 metres from the first support. Figure 4.21 presents the envelope of moments, and the results for each section are summarized in Table 4.12.

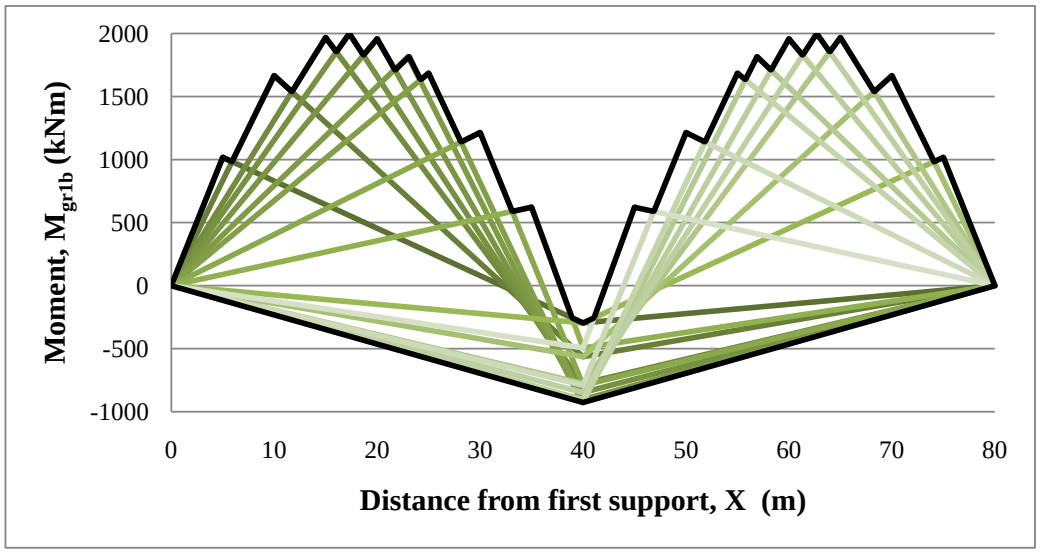

Figure 4.21 – Envelope of moments for Load Group gr1b on the continuous spans

Table 4.12 – Summary of M_{pgr1b} and M_{ngr1b} for the continuous spans

Position (m)	M_{pgr1b} (kNm)	M_{ngr1b} (kNm)	Position (m)	M_{pgr1b} (kNm)	M_{ngr1b} (kNm)
0	0	0	45	622	-803
5	1017	-115	50	1214	-688
10	1666	-229	55	1686	-574
15	1968	-344	60	1958	-459
20	1958	-459	65	1968	-344
25	1686	-574	70	1666	-229
30	1214	-688	75	1017	-115
35	622	-803	80	0	0
40	-297	-918			
NOTE: M_{pgr1b} represents the maximum positive moment, and M_{ngr1b} represents the minimum negative moment.					

4.8.3 Minimum and Maximum Moments Due to Load Group gr4

As previously defined, Load Group gr4 consists of Load Model 4, which has a UDL of 5.0 kN/m^2. For application to the beam, the load is multiplied by the spacing of the beams, resulting in a distributed load, w_{gr4}, of 10 kN/m^2. An envelope of moments is not required for either the single or continuous spans. Basic beam formulas for the calculation of the minimum and maximum moments are applied along with the shear and moment diagrams to determine the minimum and maximum moments. Details of the calculations can be found in A.4.3 of Appendix A.

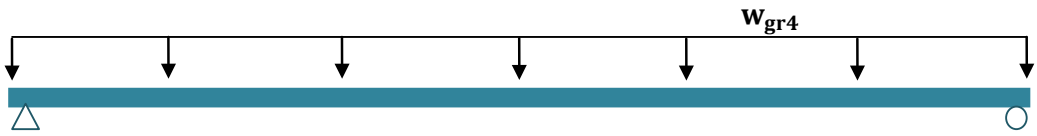

Figure 4.22 – Application of Load Group gr4

The single span design example:

On the 25.0 metre span, a maximum moment of 782 kNm is found at the midspan. Table 4.13 summarizes the results for each section.

Table 4.13 – Summary of M_{gr4} for the single span

Position (m)	Mgr4 (kNm)
0	0.00
2.5	281.25
5.0	500.00
7.5	656.25
10.0	750.00
12.5	781.25
15.0	750.00
17.5	656.25
20.0	500.00
22.5	281.25
25.0	0.00

The two-span continuous design example:

For the two 40 metre continuous spans, a maximum moment of 1532 kNm occurs at 17.5 metres and 62.5 metres from the first support due to the application of the distributed load to only one span. And a minimum moment of -2000 kNm occurs at

the centre support due to the application of the distributed load to both spans. The results for both loading conditions are then compared at each section and minimum and maximum moments in Table 4.14 are determined.

Table 4.14 – Summary of M_{pgr4} and M_{ngr4} for the continuous spans

Position (m)	M_{pgr4} (kNm)	M_{ngr4} (kNm)	Position (m)	M_{pgr4} (kNm)	M_{ngr4} (kNm)
0	0	0	45	0	-875
5	750	-125	50	750	-750
10	1250	-250	55	1250	-625
15	1500	-375	60	1500	-500
20	1500	-500	65	1500	-375
25	1250	-625	70	1250	-250
30	750	-750	75	750	-125
35	0	-875	80	0	0
40	-1000	-2000			

NOTE: M_{pgr1b} represents the maximum positive moment, and M_{ngr1b} represents the minimum negative moment.

4.8.4 Minimum and Maximum Moments Due to Load Group gr5

Load Group gr5 for the design examples in this report consists of Load Model 3 plus frequent values of Load Model 1. The resultant axle loads for LM3 have been determined to be 52 kN, 86 kN, and 80 kN. And the frequent LM1 values are 147.75 kN for the tandem system and 8.25 kN/m for the distributed load. As defined in Section 4.7, LM1 cannot be placed within 5.0 metres of the front and rear axles of the special vehicle.

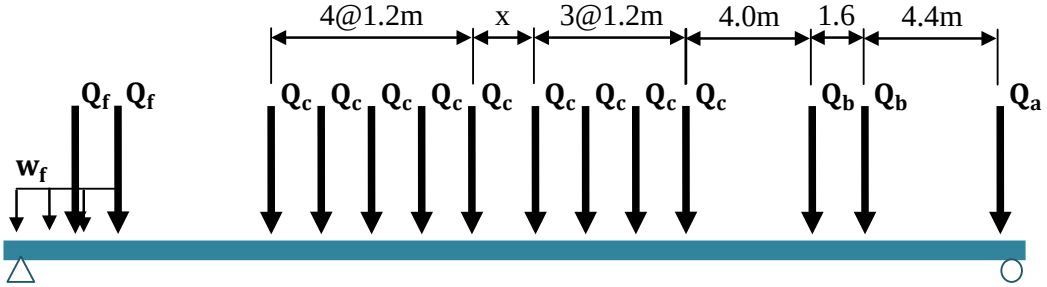

Figure 4.23 – Application of Load Group gr5

Determining the minimum and maximum moments for this load group is rather complicated, as there are a number of variances to consider in the model. First, for the special vehicle defined by LM3, there are three possibilities for the axle spacing, x, shown in Figure 4.23. In accordance with Clause NA.2.16.1.3, the spacing of the axle should be the most unfavourable of 1.2 metres, 5.0 metres, and 9.0 metres. For both design examples, it is found that a spacing of 1.2 metres is most unfavourable.

Second, the application of frequent LM1 in combination with LM3 significantly increases the number of possible combinations to consider, since LM1 can be placed anywhere in relation to LM3, to create the most unfavourable effect. A number of scenarios are considered for the determination of maximum and minimum moments. Further explanation is provided in Section A.4.4 of Appendix A.

The single span design example:

On the 25.0 metre span, a maximum moment of 4159 kNm is calculated. It is found that the maximum moment occurs when the resultant of the axles on the special vehicle is placed 15.7 metres from the support with the frequent LM1 applied 5.0 metres behind the vehicle. By symmetry, the same moment will occur at 9.3 metres from the support, with the vehicle facing the opposite direction. Figure 4.24 presents the envelope of moments produced for Load Group gr5 on the single span. From this, the results summarized in Table 4.15 are found.

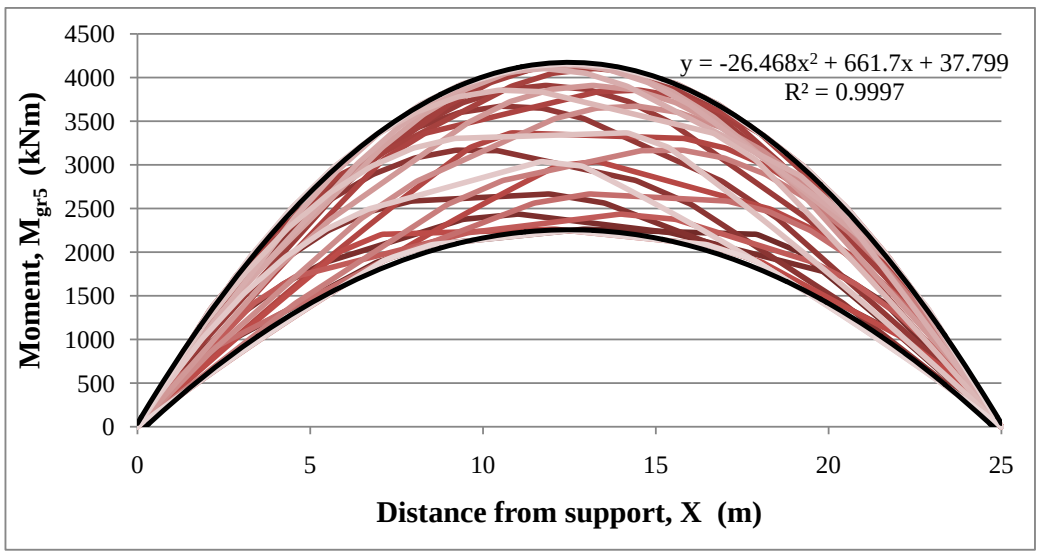

Figure 4.24 – Envelope of moments for Load Group gr5 on the single span

Table 4.15 – Summary of M_{gr5} for the single span

Position (m)	M_{gr5} (kNm)
0.0	0
2.5	1535
5.0	2710
7.5	3512
10.0	4008
12.5	4159
15.0	4008
17.5	3512
20.0	2710
22.5	1535
25.0	0

The two-span continuous design example:

As with previous load groups, the minimum moment must also be determined for the continuous spans. Based on the findings for the application of Load Group gr1a to the continuous spans, it is determined that the maximum positive moment occurs when the distributed load and axles are only applied to one span, and the minimum negative moment occurs when the distributed load is applied to both spans, with LM3 applied in one span, and the tandem system for LM1 applied in the other.

It is found that a maximum positive moment of 7015 kNm when the resultant of the special vehicle is placed at 64.5 metres from the first support, with the frequent values of LM1 applied in the same span, 5.0 metres behind the vehicle. By symmetry, the same moment occurs at 15.5m from the first support, with the vehicle facing the opposite direction. The minimum negative moment of -6172 kNm is found to occur when the resultant axle of the special vehicle is placed 25.0 metres from the first support with the uniformly distributed load applied to both spans and the tandem system applied at 56.9 metres from the first support, in the second span. It should be noted that the tandem system is placed at the same location that was determined for the minimum negative moment in Load Model 1. Figure 4.25 presents the envelope of moments produced for Load Group gr5 on the continuous spans. From this, the results summarized in Table 4.16 are found.

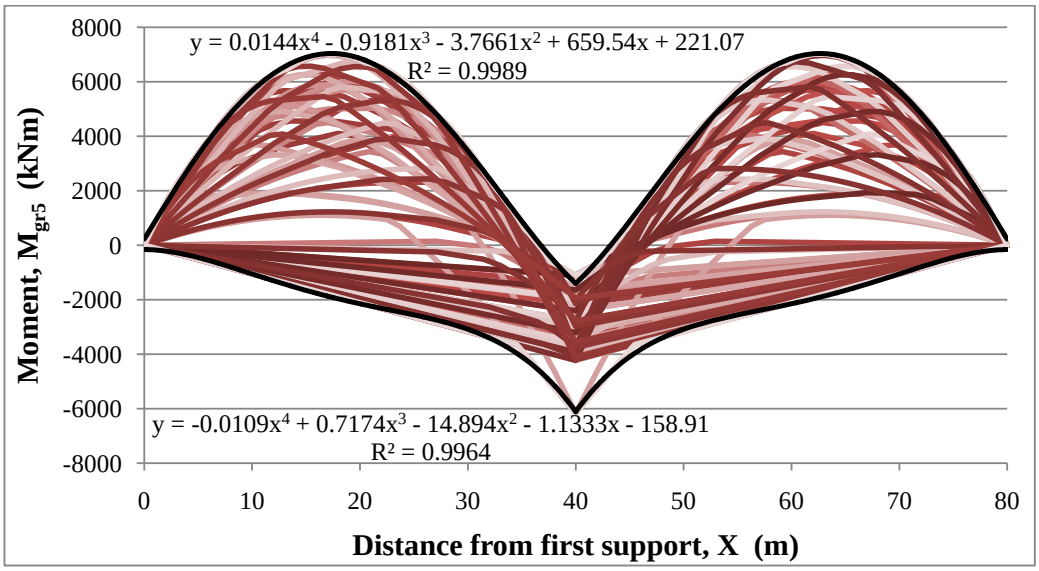

Figure 4.25 – Envelope of moments for Load Group gr5 (LM3+freq. LM1) on the continuous spans

Table 4.16 – Summary of maximum and minimum moments due to Load Group gr5 for the continuous spans

Position (m)	M_{pgr5} (kNm)	M_{ngr5} (kNm)	Position (m)	M_{pgr5} (kNm)	M_{ngr5} (kNm)
0	0	0	45	937	-4042
5	3355	-528	50	3541	-3170
10	5708	-1057	55	5723	-2642
15	6897	-1658	60	6865	-2144
20	6865	-2144	65	6897	-1658
25	5723	-2642	70	5708	-1057
30	3541	-3170	75	3355	-528
35	937	-4042	80	0	0
40	-1102	-6172			

NOTE: M_{pgr1b} represents the maximum positive moment, and M_{ngr1b} represents the minimum negative moment.

4.9 MINIMUM AND MAXIMUM MOMENTS DUE TO TRAFFIC

Once all of the maximum and minimum moments due to vertical load models are determined, they are applied to the design of the bridge beam. These loads will be applied in combination with other actions, such as permanent loads, wind loads, etc. which are discussed in Chapter 6. Table 4.17 provides a summary of the maximum and minimum moments that have been determined in this section.

Table 4.17 – Summary of maximum and minimum moments due to traffic

Load Group	Maximum Moment (kNm)	Minimum Moment (kNm)
Single Span		
gr1a	3205	-
gr1b	1513	-
gr4	782	-
gr5	4159	-
Continuous Spans		
gr1a	4841	-3715
gr1b	2008	-932
gr4	1532	-2000
gr5	7015	-6172

From this table, it becomes clear that Load Group gr5 controls for the maximum and minimum design loads, and will be included in the combinations of actions. Also, for the frequent load combination, Load Group gr5 is not considered, and therefore, Load Group gr1a controls. For the frequent load group, the moments determined here are simply multiplied by the ψ_1 factor defined to be 0.75 in Table NA.A2.1 of the NA to BS EN 1990. Figures 4.26 and 4.27 present plots of the minimum and maximum moments along the length of the beam for each load group. From these graphs, it is confirmed that Load Group gr5 and Load Group gr1a will control for every section on the beam.

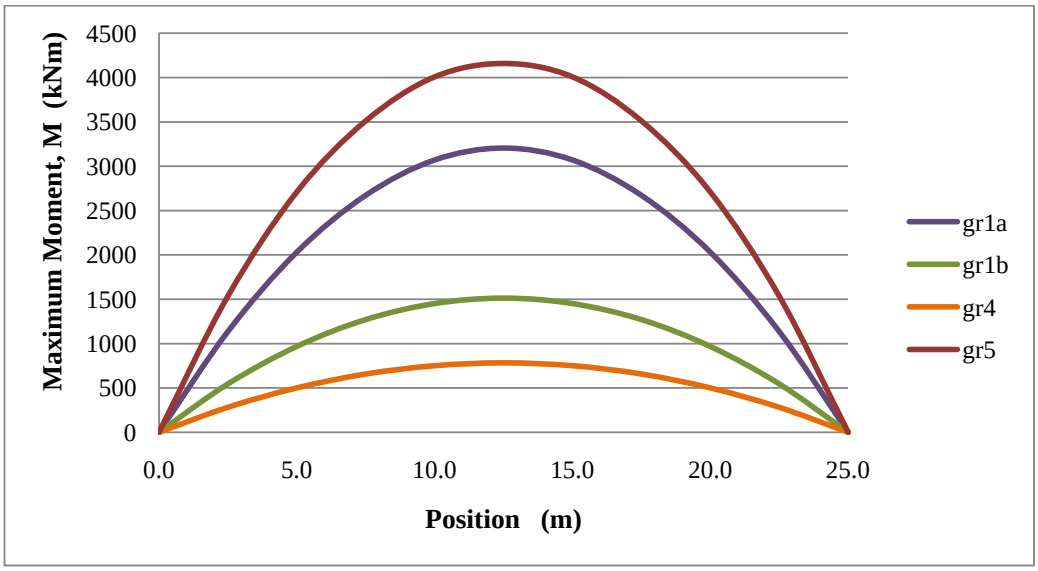

Figure 4.26 – Summary of maximum moments on the single span

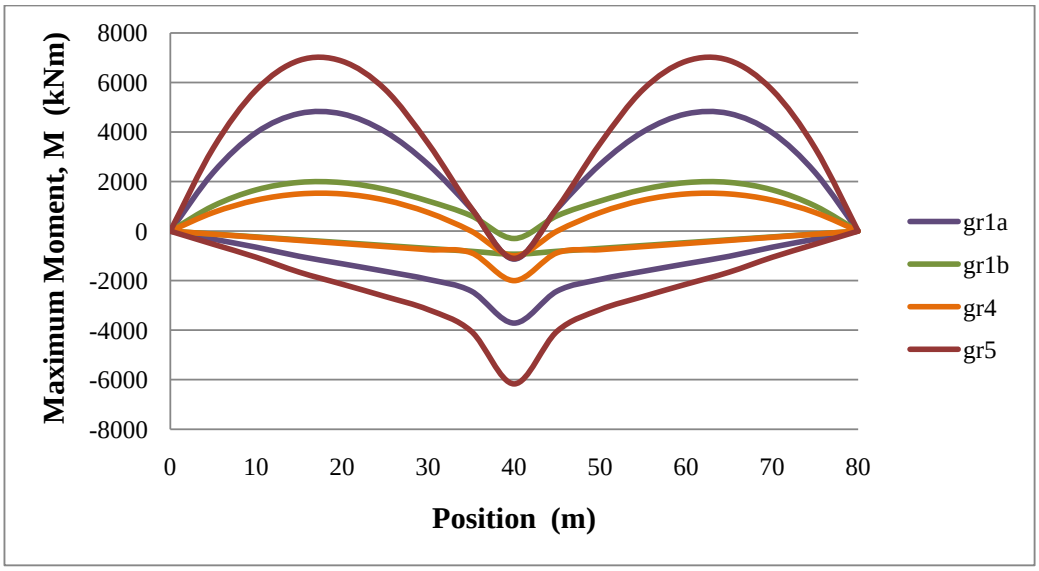

Figure 4.27 – Summary of maximum moments on the continuous span

5 DESIGN PROCEDURES

The design of prestressed concrete is a complicated, iterative process. The structure is required to simultaneously satisfy a number of different design requirements defined by the Eurocodes. Each of these requirements must be designed for separately, and satisfaction of one does not necessarily guarantee satisfaction of another (Gilbert and Mickleborough, 1990). The Eurocodes separate these requirements into two categories; the serviceability limit states and the ultimate limit states. The serviceability limit states cover stress limitations, crack control, and deflections while the ultimate limit states cover bending moment resistance, shear resistance, and fatigue verifications. Typically, the design is based on the requirements for the serviceability limit states first, as these account the working conditions of the structure. Then the ultimate limit state criteria are considered (Bungey, Hulse and Mosley 2007).

Throughout the design process, many of the Eurocodes must be applied. Of these, the most heavily applied for prestressed concrete bridge design are BS EN 1992-1-1 which covers the general rules and rules for buildings in the design of concrete structures and BS EN 1992-2 which covers concrete bridge design.

Due to the complicated stress distributions that occur in prestressed concrete, the design of a composite prestressed concrete beam must be considered at three stages encompassing the full range of loading the member will encounter during its life (Bungey, Hulse and Mosley 2007).

The first stage, referred to as the transfer stage, occurs when the tension in the steel strands is transferred to the beam. For pre-tensioned beams, this occurs in the manufacturing plant, when the strands are cut. For post-tensioned beams, transfer occurs in the field, when the strands are tensioned and anchored at each end of the beam. At this stage, only the self-weight of the prestressed beam is considered.

The second stage, referred to as a service stage, occurs at the placement of the concrete slab on the beam before it has hardened. At this point the slab is applied as dead weight on the structure, and does not provide any structural capacity. The only loads considered are the weight of the beam and wet slab. And the third stage, also a service stage, occurs after the concrete slab has hardened and is contributing to the capacity of the structure. At this stage, all imposed loading is applied (Hurst, 1998).

Each of these stages must be considered under the serviceability limit states. The ultimate limit states only take into account conditions in the third stage, at which point the structure is complete with the maximum capacity. If the beam is not composite only the first and third stage must be considered.

Generally, a procedure is adopted and followed for the design which encompasses all required checks for the serviceability and ultimate limit states along with the basic principles of prestress design. The designer can adjust the sequence of the steps in this process based on his or her preferences, as long as every step is covered. For this dissertation, the sequence of steps illustrated in Figure 5.1 has been adopted. It should be noted that this sequence of steps is not meant to cover every aspect of bridge design. There are several facets in the design which, due to time constraints have been omitted. However, the sequence of steps provides a simplified design procedure which is sufficient for gaining an understanding of the overall design of prestressed concrete bridges.

In order to begin the design of a prestressed concrete bridge, some initial decisions and assumptions must be made by the designer. These are discussed further in the first section. As the design is completed, it may be required to change some or all of these initial assumptions, requiring the designer to repeat some or all of the steps in the procedure that have been completed thus far. For a designer with experience, this process can become more streamline, as the designer is able to make informed decisions at the beginning of the process based on previous work. This aspect of the design also highlights the benefits of applying computer software to complete the design, allowing any changes to be made with ease.

1 DETERMINE PRELIMINARY DESIGN DATA

2 CONSIDER DURABILITY AND FIRE RESISTANCE

3 DETERMINE ACTIONS ON THE STRUCTURE

4 ESTABLISH THE COMBINATIONS OF ACTIONS

5 INITIAL DESIGN OF THE BEAM

- 5.1 Select initial section properties and prestress losses
- 5.2 Calculate stress limits for the beam
- 5.3 Determine basic inequalities for the concrete stresses
- 5.4 Check required elastic moduli against section properties
- 5.5 Develop the Magnel Diagram - select prestressing and eccentricity
- 5.6 Calculate secondary moments (continuous spans only)
- 5.7 Check stresses in the concrete with selected prestressing forces
- 5.8 Verify selected eccentricity and tendon profile
- 5.9 Calculate losses in the prestressing steel

6 DESIGN OF THE COMPOSITE STRUCTURE

- 6.1 Calculate stress limits for the beam and slab
- 6.2 Check the final stresses for the composite section

7 CHECK DEFLECTIONS FOR EACH STAGE

8 DESIGN THE END BLOCK REINFORCEMENT (post-tensioned only)

- 8.1 Check the bearing stress under the anchor
- 8.2 Determine required reinforcement
- 8.3 Check compressive stresses in concrete struts

9 CHECK THE ULIMATE MOMENT OF RESISTANCE

- 9.1 Determine the stress-strain curve for prestressing steel
- 9.2 Calculate the ultimate bending moment resistance

10 DESIGN THE SHEAR REINFORCEMENT

- 10.1 Determine shear forces acting on the beam
- 10.2 Determine shear resistance of the concrete
- 10.3 Calculate required shear reinforcement

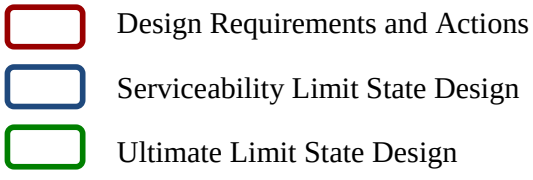

Figure 5.1 – Design procedure for prestressed concrete

5.1 PRELIMINARY DESIGN DATA

The first step in any design process is to determine the requirements for the design and how they can be met in a cost effective manner. This is often done by developing a preliminary plan consisting of the collection and analysis of site information, establishment of policies and practices, and consideration of alternatives with cost evaluations. It should also incorporate any requirements set by the client. The preliminary plan essentially lays the groundwork for the final design (Precast/Prestressed Concrete Institute, 1997).

With the bridge site data, a preliminary plan is developed for the bridge, incorporating initial geometric design data for the structure such as the number of spans, span lengths, deck width, beam type, and beam layout, as well as size and type of the foundations and hydraulic analysis. In a true design process, this plan is reported with cost estimates, evaluation of alternatives, drawings, established design methods and limits, and initial design loads. Approval is then sought before beginning the final design (Precast/Prestressed Concrete Institute, 1997).

In this dissertation, the design examples are hypothetical bridge sites spanning a river, and therefore, a number of assumptions have been made for the preliminary design data. In both designs, the limits and requirements are set in accordance with the Eurocodes. Details of these limits will be provided in the sections that follow.

In regards to the geometric design data, most has already been defined in Chapter 5 for the calculation of traffic loads; however, it is reviewed here for clarity. The span length for the single span is assumed to be 25.0 metres, and the continuous spans are assumed to be two equal spans of 40.0 metres each. Both spans are assumed to be straight, with no skew or curvature. As shown in Figure 5.2, the deck width on both is assumed to be 12.0 metres, with a carriageway width of 7.0 metres and a footpath on each side of the structure. Also, the beams are spaced at 2.0 metres, with a 1.0 metre overhang on either side.

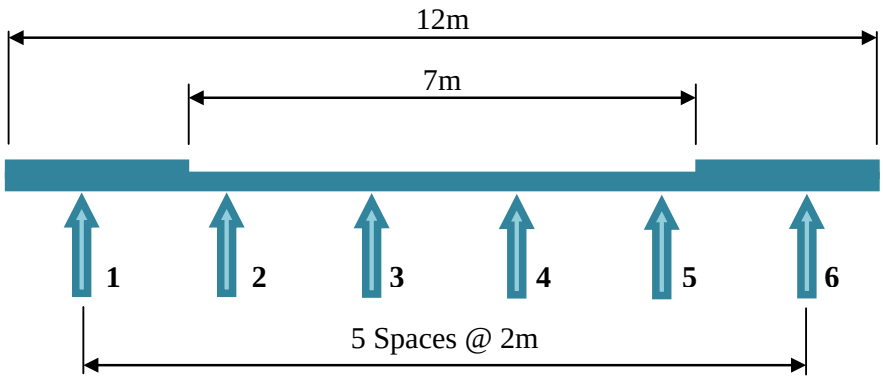

Figure 5.2 – Bridge cross section for both design examples

On the single span, six pre-tensioned U beams are selected for the beam type, and on the continuous spans, six post-tensioned SY beams are selected. In regards to material properties, C50/60 concrete is chosen for the beams and C40/50 concrete for the deck slabs. The foundation data and hydraulic data are not within the scope of this dissertation, and are therefore not included here.

5.2 DURABILITY AND FIRE RESISTANCE

Two of the design requirements set by the Eurocodes are appropriate durability and suitable resistance to fire. Specifications for fire resistance are in place to make sure that the concrete member is capable of withstanding fire for a specified period of time. This ensures that occupants can evacuate the structure safely and the fire can be fought without excessive danger to the fire fighters. Generally, in the design of bridges, fire resistance can be ignored since the risk of fire is very low (Martin and Purkiss, 2006). Therefore, restrictions for fire resistance are not considered here.

In relation to the durability requirements, Clause 2.4(1)P of BS EN 1990 states the following.

> "The structure shall be designed such that deterioration over its design working life does not impair the performance of the structure below that intended, having due regard to its environment and the anticipated level of maintenance" (BS EN 1990, 2010).

To accomplish this, BS EN 1992-1-1 provides extensive guidance on the durability of concrete structures, promoting the consideration of a low whole-life cost design. In order to ensure durability, a nominal concrete cover to reinforcement is determined based on a number of factors including design life, material properties, and environmental conditions (Hendy and Smith, 2007). Clauses 4.4.1.1 and 4.4.1.2 of BS EN 1992-1-1 provide the following equations for the calculation of required nominal cover.

Nominal cover:

$$c_{nom}=c_{min}+\Delta c_{dev} \quad (5.1)$$

Minimum cover:

$$c_{min}=\max[c_{min.b};c_{min,dur}+\Delta c_{dur,\gamma}-\Delta c_{dur,st}-\Delta c_{dur,add};10mm] \quad (5.2)$$

where:

Δc_{dev} = allowance in design for deviation

$c_{min,b}$ = minimum cover due to bond requirement

$c_{min,dur}$ = minimum cover due to environmental conditions

$\Delta c_{dur,\gamma}$ = additive safety element

$\Delta c_{dur,st}$ = reduction of minimum cover for use of stainless steel

$\Delta c_{dur,add}$ = reduction of minimum cover for use of additional protection

5.2.1 Minimum Cover Due to Bond Requirements

One of the durability requirements is sufficient concrete cover for the transmission of bond forces between the steel and concrete. Clause 4.4.1.2(3) defines the minimum cover due to bond requirements, $c_{min,b}$, to be the diameter of the bar for reinforcement, 2.5 times the diameter of the tendons for pre-tensioned concrete, or the diameter of the duct for post-tensioned concrete.

For both design examples, a maximum reinforcement diameter of 25 millimetres is assumed, requiring a minimum cover of 25 millimetres. For the single span design, pre-tensioned strands with a diameter of 15.2 millimetres are selected, requiring a cover of 38 millimetres. And for the continuous spans, a cover of 60 millimetres is required for the post-tensioned duct.

5.2.2 Minimum Cover Due to Environmental Conditions

The second durability requirement is adequate concrete cover for protection against the environment, preventing corrosion of the reinforcement and prestressing steel. In order to calculate the minimum cover due to environmental conditions, $c_{min,dur}$, the design life and exposure class of the bridge must first be determined.

In accordance with Table NA.2.1 of the UK National Annex to BS EN 1990, the design working life for a bridge is 120 years. The exposure class is determined from both Table 4.1 in BS EN 1992-1-1 and recommendations from Section 4.2 in BS EN 1992-2. These exposure classes refer to the level of exposure the structure is likely to have to unfavourable environmental conditions such as saturation, humidity, sulphate attack, acid attack, chloride ingress, etc. Both design examples are assumed to span a fresh water river and are protected by waterproofing. Therefore, the exposure class is determined to be XC3 for moderate humidity on all surfaces of the bridge.

In accordance with the National Annex to BS EN 1992-1-1, the minimum cover due to environmental conditions, $c_{min,dur}$, is taken from Tables A.5 and A.11 of BS 8500-1:2006. With a design life of 120 years, C50/60 concrete for the beams, C40/50 concrete for the deck, and an exposure class of XC3, the minimum cover for both design examples is determined from Table A.5 to be 30 millimetres. Also, Table NA.1 of the National Annex defines the additive safety factor and reduction factors to be equal to zero.

5.2.3 Nominal Cover

The nominal cover is the sum of the minimum cover and an allowance for deviations in fabrication. The minimum cover, c_{min}, is the most unfavourable of those determined in the last two sections and 10 millimetres. The allowance for deviation, Δc_{dev}, is recommended by Table NA.1 of the National Annex to be 10 millimetres. This allowance may be reduced by up to 5 millimetres if the fabrication of the beams is subjected to quality assurance or up to 10 millimetres if it can be assured that an accurate measuring device is used for monitoring and that non-conforming members are refused. Table 5.1 summarizes the nominal concrete cover requirements for the three strand types used in the design examples. Refer to Section B.2 of Appendix B and Section C.2 of Appendix C for full calculations.

Table 5.1 – Nominal concrete cover requirements for design examples

	Diameter, (mm)	c_{min} (mm)	Δc_{dev} (mm)	c_{nom} (mm)
Single span				
Reinforcement	25	30	10	40
Pre-tensioned tendons	15.2	38	10	48
Continuous Spans				
Reinforcement	25	30	10	40
Post-tensioned ducts	50	50	10	60

5.3 ACTIONS ON THE STRUCTURE

Before a prestressed concrete bridge can be designed, the actions on it must be determined. This includes both the permanent actions and the variable actions. The detailed calculation of all applied loads to the structure is a complicated process in itself, requiring a full study that due to time constraints is beyond the scope of this report. Here all loading types are briefly discussed; however, detailed analysis is only given to the self-weight and traffic loads on the structure. These loads will have the most adverse affect on the structure, and will provide enough loading to give an accurate representation of a prestressed concrete bridge design.

5.3.1 Self-Weight

Clause 5.1(2) of BS EN 1991-1-1 defines the self-weight of a structure to include the structure as well as any non-structural elements. For a bridge, non-structural elements include any fixed services and bridge furniture, as well as the weight of any earth or ballast. Fixed services may consist of cables, pipes, or service ducts which are sometimes located within the deck structure. Bridge furniture may include waterproofing, surfacing, traffic restraint systems, and acoustic or anti-wind screens attached to the structure (Calgaro, Gulvanessian and Tschumi, 2010).

Tables A.1 through A.12 of BS EN 1991-1-1 provide nominal densities of typical construction materials that can be used with the nominal dimensions to determine the weight of each component of the bridge. For the design examples in this report, the densities in Table 6.2 are applied.

Table 5.2 – Nominal densities for self-weight of design examples

Material	Density, γ (kN/m^3)	BS EN 1991-1-1
Reinforced/Prestressed Concrete	25	Table A.1
Wet Concrete	26	Table A.1
Hot-rolled asphalt	23	Table A.6

For surfacing, waterproofing, and coatings on the bridge as well as any of fixed services previously mentioned, there is a high probability of variation in the weight which must be accounted for. Clause 5.2.3(3) and (4) in the National Annex of BS EN 1991-1-1 specify deviations that should be considered in the calculation of self-weight. For the designs in this report, the nominal thickness for surfacing will be increased by 55% to account for this variation.

In the final load combinations, the self-weight of the structure is represented by a single characteristic value in accordance with clause 4.1.2(5) of BS EN 1990. To begin a design the self-weight is initially estimated, and once final design is completed the calculations are adjusted with the actual weight of the beam.

For the design examples in Appendices B and C, the self-weight includes six beams, the concrete slab, 60 millimetres of surfacing on the carriageway, and a footway and parapet on each side of the structure. Both designs focus on Beam 3, since this beam represents the critical case. Therefore, only the weight of the beam, slab, and surfacing are considered. A summary of the final self weights for each example is provided in Table 5.3. Refer to the Appendices for full calculations.

Table 5.3 – Final self-weight for each element in the design examples

	Depth, d (mm)	Variation Factor	Area, A (mm^2)	Density, γ (kN/m^3)	Weight, w (kN/m)
Single span					
Beam	-	-	745153	25	18.63
Slab	200	-	400000	25	10.00
Surfacing	60	1.55	120000	23	4.28
Continuous Spans					
Beam	-	-	735475	25	18.39
Slab	300	-	600000	25	15.00
Surfacing	60	1.55	120000	23	4.28

5.3.2 Snow Loads

There are currently no specifications in BS EN 1991-1-3 for snow loads acting on a bridge. This does not necessarily mean they should be excluded, however, in normal climatic zones significant snow loads cannot act simultaneously with traffic loads on a bridge deck, and the effects of the characteristics values for snow loads are far less important than those for traffic loads. It should be noted that in some Nordic countries, the snow load may be the leading action on the deck for footbridges (Calgaro, Gulvanessian and Tschumi, 2010).

For roofed bridges, a combination of the loads can be defined and should be determined on a national level or specifically for the individual project. The characteristic value for the weight of snow on the roof can be determined using the same methods as those defined for a building roof (Calgaro, Gulvanessian and Tschumi, 2010).

5.3.3 Wind Actions

Section 8 of BS EN 1991-1-4 provides guidance for determination of the quasi-static effects of wind actions on bridge decks and piers with spans up to two hundred metres. In general, the most significant wind loading will be that due to wind pressures acting parallel to the deck width and perpendicular to the direction of travel. The wind loads acting vertically on the structure should also be considered, as they may cause uplift on the bridge deck (Calgaro, Gulvanessian and Tschumi, 2010).

The design wind forces acting on a structure are determined based on the wind pressures applied to the deck, piers, and equipment such as barriers or acoustic screens, as well as the wind pressure applied to the traffic vehicles crossing the structure. BS EN 1991-1-4 provides guidance on the determination of these areas. In addition, the height of the deck above the lowest ground level must be determined so that the appropriate pressures can be applied.

BS EN 1991-1-4 defines a number of expressions for the calculation of wind forces on the structure. First, the structure must be assessed to establish whether or not a dynamic response procedure is needed. This is determined by the National Annex.

With this information, the choice of which expression to apply can be made. Due to time constraints, further consideration of wind loading is not included in this dissertation. However, the consideration of these forces is important in the design of a bridge deck, and the calculations should be included in future investigations.

5.3.4 Thermal Actions

Thermal actions on a bridge can cause stresses in the structure resulting from contraction and expansion of the materials due to temperature differentials. To determine these stresses BS EN 1991-1-5 should be applied. The effect can be divided into three components including the uniform temperature component, the temperature difference component, and the non-linear temperature difference component (Jackson et al. 2010).

The uniform temperature component causes expansion and contraction of the deck, which results in stresses applied to the deck. If the movements are relatively small, the force required to create them will be negligible and does not need to be considered in the analysis. It should, however, be included for the design of foundations (Jackson et al. 2010). It can also be used to design the expansion joints and bearings (Calgaro, Gulvanessian and Tschumi, 2010).

In addition to the overall expansion and contraction of the deck, variations in temperature along the depth of the bridge deck must also be considered. This is assessed with the temperature difference component. These variations in temperature have a tendency to cause curvature in the deck. If the structure is simply supported, as in the first example, the curvature can occur freely, and will not cause any stress in the structure. However, for continuous spans, stresses will occur due to resistance from the restraints at the abutments and pier. These stresses should be included in the global model of the bridge (Jackson et al. 2010).

The non-linear temperature component also causes local stresses within the structure, but these stresses are in equilibrium and do not cause changes in length or curvature of the bridge. Therefore, the stresses do not need to be included in the global analysis, although the component should still be considered for some local verifications (Jackson et al. 2010). Due to the complicated analysis required for the

thermal actions, consideration of the effects is beyond the scope of this report and is left for future investigations.

5.3.5 Actions During Execution

BS EN 1991-1-6 provides guidance on the determination of loading applied to structural members during construction. While the execution of a bridge is a transient situation, accidental actions or situations may occur such as the failure of a stabilizing device, or the loss of equilibrium due to the fall of a member. Therefore, the designer should take into account appropriate transient design situations. BS EN 1991-1-6 provides a series of simplified rules for the determination of actions which may occur in these situations. The actions from execution are then combined into combinations of actions for the serviceability and ultimate limit states, which must be considered in design (Calgaro, Gulvanessian and Tschumi, 2010). Further consideration of this loading is left to future investigations.

5.3.6 Accidental Actions

While accidental actions due to vehicles on the structure are considered in BS EN 1991-2, a few design situations are covered by BS EN 1991-1-7. More specifically, BS EN 1991-1-7 covers the impact of ships, trains, or vehicles travelling under the structure (Calgaro, Gulvanessian and Tschumi, 2010).

Consideration of these actions is separated into two categories: strategies based on identified accidental actions, and strategies for limiting localized failure due to unidentified actions. A few examples of identified accidental actions are scour effects around bridge piers and abutments, overloading due to heavy unauthorized vehicles, and impact from vehicles on the piers and/or decks. Unidentified accidental actions may occur as a result of vandalism or the development of exceptional conditions which are unexpected and cannot be planned for. At the design stage, the designer should establish a set of accidental design situations for the individual project, including both identified and unidentified actions. Based on these actions, protective measures should be taken for the design of the structure (Calgaro, Gulvanessian and Tschumi, 2010). Due to time constraints, consideration of these effects is also left for future investigations.

5.3.7 Traffic Loads

Chapter 4 of BS EN 1991-2 and the corresponding National Annex provide extensive guidance on the application of traffic loads. Consideration is given to vertical load models and corresponding horizontal forces, fatigue load models, and actions for accidental design situations. Due to the complexity of this loading, the explanation has been separated and the full discussion can be found in Chapter 5 of this dissertation. The load models have been combined into groups of traffic loads, which define the global actions of traffic loads that are then included in the combinations of actions. Only four of the groups are considered in the design examples for this dissertation. Table 5.4 summarizes the results found in Chapter 5 for each design.

Table 5.4 – Summary of maximum and minimum moments due to traffic

Load Group	Maximum Moment (kNm)	Minimum Moment (kNm)
Single Span		
gr1a	3205	-
gr1b	1513	-
gr4	782	-
gr5	4159	-
Continuous Spans		
gr1a	4841	-3715
gr1b	2008	-932
gr4	1532	-2000
gr5	7015	-6172

5.4 COMBINATIONS OF ACTIONS

Once all of the permanent and variable actions are defined, they must be combined into design values for the verification of structural reliability under the serviceability and ultimate limit states. This is accomplished with the combinations of actions defined by BS EN 1990. The following simplified rules may be adopted for determination of the combinations of actions for most cases. Although, there are special cases when more accurate combinations of actions are required (Calgaro, Gulvanessian and Tschumi, 2010).

- Snow loads are never combined with traffic loads unless the structure has a roof.
- The combination of wind and thermal actions is not taken into account.
- Wind actions only need to be combined with Load Group gr1a.
- No other variable actions are taken into account simultaneously with Load Group gr1b.
- The combination of non-traffic actions with Load Group gr5 is determined in the National Annex.

5.4.1 Combinations for Serviceability Limit States

For the serviceability limit states, three combinations of actions are considered: characteristic, frequent, and quasi-permanent. The characteristic combination, associated with irreversible serviceability limit state criteria, represents the most severe load the structure should be subjected to. The frequent combination, used to evaluate reversible criteria, is considered to be the most severe load case that the structure will be subjected to on a regular basis. And the quasi-permanent combination is the loading which the structure is subjected to most of the time. This combination is used to evaluate long term effects and concerns with aesthetics and durability (Jackson et al. 2010). Equations (5.3) to (5.5) describe each combination of actions.

Characteristic Combination:

$$E_d = E(\sum G_{k,j} + P + Q_{k.1} + \sum \psi_{0,i} Q_{k,i}) \quad (5.3)$$

Frequent Combination:

$$E_d = E(\sum G_{k,j} + P + \psi_{1,1} Q_{k,1} + \sum \psi_{2,i} Q_{k,i}) \quad (5.4)$$

Quasi-permanent Combination:

$$E_d = E(\sum G_{k,j} + P + \sum \psi_{2,i} Q_{k,i}) \quad (5.5)$$

where:

G_k = characteristic permanent actions

P = prestress actions

Q_k = the characteristic variable actions

ψ_0 = the combination factor

ψ_1 = the frequent factor

ψ_2 = the quasi-permanent factor

In the case of road bridges, as well as footbridges or railway bridges, each group of loads defined in BS EN 1991-2 should be considered as a unique variable action (Calgaro, Gulvanessian and Tschumi, 2010). The ψ factors are defined in Table NA.A2.1 of the National Annex to BS EN 1990 for road bridges. Table 5.5 presents the factors that are applicable to the design examples in this report.

Table 5.5 – ψ factors for road bridges
(NA to BS EN 1990 Table NA.A2.1)

		ψ_0	ψ_1	ψ_2
gr1a	Tandem System	0.75	0.75	0
	UDL	0.75	0.75	0
	Pedestrian loads	0.40	0.40	0
gr3	Pedestrian loads	0	0.40	0
gr5	Special Vehicles	0	0	0

5.4.2 Combinations for Ultimate Limit States

For the ultimate limit states, four categories are considered: equilibrium (EQU), structural member resistance (STR), geotechnical limit states (GEO), and fatigue verifications (FAT). These limit states correspond to the idealization of structural failures that must be avoided. The FAT limit state is defined by the individual material codes (BS EN 1992-1-1) rather than BS EN 1990 (Calgaro, Gulvanessian and Tschumi, 2010). Due to time constraints, fatigue verifications are not considered in this study but are left for future investigations.

In the design of a bridge deck, the STR limit state is typically the main concern. Clause NA.2.3.7.1 of the National Annex specifies that for bridges, Eq. (6.10) in BS EN 1990, shown below, should be applied for the combination of actions.

$$E_d = E(\sum \gamma_{G,j} G_{k,j} + \gamma_P P + \gamma_{Q,1} Q_{k,1} + \sum \gamma_{Q,i} \psi_{0,i} Q_{k,i}) \quad (5.6)$$

For this limit state, partial factors of safety are also included in the combination, defining design values for each action. For the permanent actions, both a favourable and unfavourable partial factor are provided. In the case of variable actions, only the unfavourable factor is provided since the variable actions are only applied for

unfavourable results. The National Annex to BS EN 1990 defines the partial factors for each limit state in Tables NA.A2.4(A), (B), and (C). And Clause 2.4.2.2 in the National Annex to BS EN 1992-1-1 defines favourable and unfavourable partial factors for the prestress force. For the designs in this dissertation, the STR limit state is applied with the equation above, and the partial factors are defined by Table NA.A2.4(B). Table 5.6 provides a summary of the factors applied in the examples.

Table 5.6 – Partial factors for design values of actions (NA to BS EN 1990 Table NA.A2.4(B); NA to BS EN 1992-1-1 Cl. 2.4.2.2)

	γ_{unfav} (unfavourable)	γ_{fav} (favourable)	ψ_0
Self weight	1.35	0.95	-
Super-imposed DL	1.20	0.95	-
Prestress	1.10	0.90	-
Traffic	1.35	0	N/A

5.4.3 Summary of the Results

Table 5.7 provides a summary of the maximum moments determined for both design examples. For detailed calculations refer to Section B.3 and Section C.3 of the Appendices.

Table 5.7 – Combinations of actions for the design examples

	Combination	Maximum Moment (kNm)	Minimum Moment (kNm)
Single span	Characteristic (SLS)	6730	-
	Frequent (SLS)	4975	-
	Quasi-permanent (SLS)	2571	-
	STR (ULS)	9036	-
Continuous Spans	Characteristic (SLS)	10790	-12574
	Frequent (SLS)	7406	-9188
	Quasi-permanent (SLS)	3775	-6402
	STR (ULS)	14468	-16846

5.5 INITIAL DESIGN OF THE BEAM

For composite construction, the design of a beam is separated into two phases. The initial design of the beam takes into account the loading at the transfer stage, when

the tension is transferred to the beam, and the service stage when the slab has been placed but has not hardened. At this point, only the capacity of the beam is considered. The imposed loading on the structure is not considered, as it will not be applied until the section becomes composite.

It should be noted that the initial design of the beam is an iterative process. Initial selections are made regarding beam sizes, prestressing force, eccentricity, and prestress loss. More often than not some or all of these initial selections require adjustment, at which point the process must be repeated. For full calculations of the following steps, refer to Section B.5 and C.5 of the Appendices.

5.5.1 Initial Selection of Beam Size and Prestress Loss

First, a selection of the beam size and section properties must be made, as well as assumptions on initial and long-term prestress loss. For experienced engineers, an appropriate selection can often be made based on the loading and geometric requirements determined in the first few steps. While this selection is not critical, an informed choice can save time and reduce the work load for the designer.

5.5.2 Concrete Stress Limits for the Beam

Before a member can be designed, the limits on the design must be determined. For design at the serviceability limit state, BS EN 1992-1-1 defines concrete stress limits based on an acceptable degree of flexural cracking as well as prevention of excessive creep. These limits also prevent the occurrence of longitudinal and micro cracking, which can result from excessive compression (Bungey, Hulse and Mosley 2007).

Clause 5.10.2.2(5) in BS EN 1992-1-1 defines the limit for compressive stress to be 0.6 $f_{ck}(t)$. This limit is applied at transfer, typically 7 days after casting, and again at service with a time t of 28 days assumed. The compressive strength of concrete, f_{ck}, must be determined based on the age of the concrete at each stage. Details for this calculation are provided in Section 3.1.1 of Chapter 3. It should be noted that for pre-tensioned members, the National Annex allows the limit to be raised to 0.7 $f_{ck}(t)$ if it can be justified that longitudinal cracking is prevented. Conservatively, the limit will be kept at 0.6 $f_{ck}(t)$ for the pre-tensioned design in Appendix B of this report.

The Eurocodes do not provide specific guidance on the tensile stress limits for concrete. In practice, the limit for tensile stress at this phase of design is typically taken as 1.0 MPa at transfer and 0 MPa at service for sections that are not designed to be in tension during service (Bungey, Hulse and Mosley 2007).

5.5.3 Basic Inequalities for the Concrete Stresses

The design of prestressed concrete is based on the stress distributions throughout the concrete member, as discussed in Chapter 2. The goal of design is to maintain these concrete stresses within specified limits at all stages in the life of the member. For the initial design of the beam, the first set of inequalities considers the prestressing force and self-weight of the beam and the second set considers the prestressing force and weight of the beam and slab. If the designer is not designing a composite beam, then at this point the service stage would include the application of imposed loads as well. Figure 5.3 illustrates the variance between the stress distributions for each of these stages.

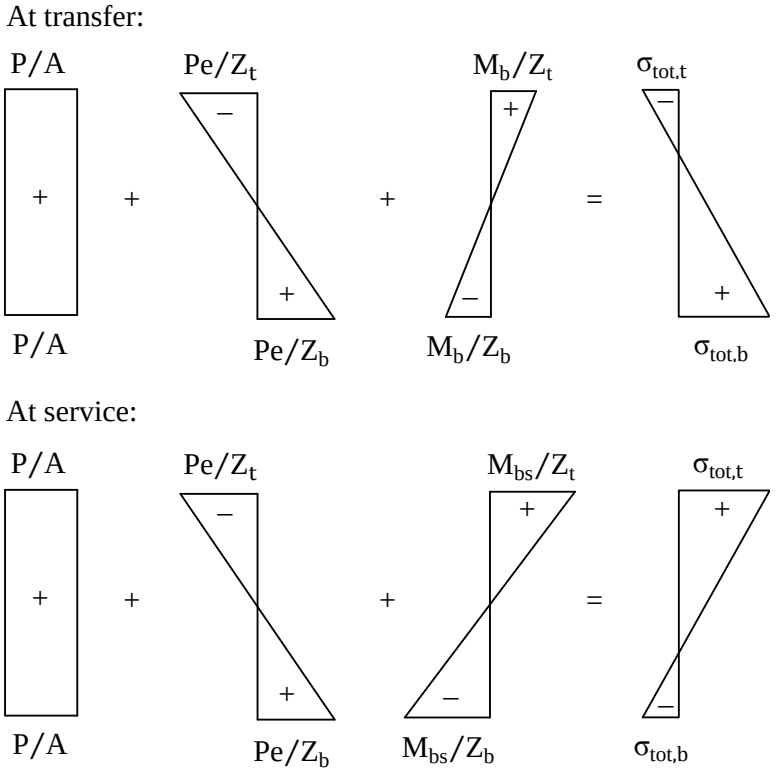

Figure 5.3 – Stress distributions for transfer and service stage

From these stress distributions, the reason for checking the concrete stresses at all stages in the life of the member becomes apparent. At the beginning of its life, the concrete member must resist high compressive forces in the bottom fibre induced by the prestressing force, while at later stages when the loading is applied the top fibre must resist compressive forces. Four inequalities are defined below based on these stress distributions and the concrete stress limits defined above (Bungey, Hulse and Mosley 2007). The following steps in the design are based off of these inequalities, ensuring that the stresses are balanced at all stages.

At transfer:

For the top fibre $$\frac{\alpha P_i}{A_b} - \frac{\alpha P_i e_b}{Z_{tbm}} + \frac{M_b}{Z_{tbm}} \geq f_{trmin} \quad (5.8a)$$

For the bottom fibre $$\frac{\alpha P_i}{A_b} + \frac{\alpha P_i e_b}{Z_{bbm}} - \frac{M_b}{Z_{bbm}} \leq f_{trmax} \quad (5.8b)$$

At service:

For the top fibre $$\frac{\beta P_i}{A_b} - \frac{\beta P_i e_b}{Z_{tbm}} + \frac{M_{bs}}{Z_{tbm}} \leq f_{max} \quad (5.8c)$$

For the bottom fibre $$\frac{\beta P_i}{A_b} + \frac{\beta P_i e_b}{Z_{bbm}} - \frac{M_{bs}}{Z_{bbm}} \geq f_{min} \quad (5.8d)$$

where:

α = short-term prestress loss factor

β = long-term prestress loss factor

A_b = area of the beam

e = eccentricity of the prestressing strands

f_{max} = the maximum allowable stress at service

f_{min} = the minimum allowable stress at service

f_{trmax} = the maximum allowable stress at transfer

f_{trmin} = the minimum allowable stress at transfer

M_b = moment due to self-weight of the beam

M_{bs} = moment due to self-weight of the beam and slab

P_i = initial prestressing force

For any sections with negative moments, due to a continuous span, the inequalities hold true with the reversal of signs on the moments.

5.5.4 Required Elastic Section Moduli

By combining and rearranging the inequalities from Section 5.5.1, expressions for the required section modulus on the top and bottom fibre of the beam are derived. The final equations are shown here.

For the top fibre $$Z_{tbm} \geq \frac{\alpha M_{bs} - \beta M_b}{\alpha f_{max} - \beta f_{trmin}} \quad (5.9a)$$

For the bottom fibre $$Z_{bbm} \geq \frac{\alpha M_{bs} - \beta M_b}{\beta f_{trmax} - \alpha f_{min}} \quad (5.9b)$$

These equations provide the first of several verifications required for the section properties of the selected beam. It should be noted that in the rearrangement, the prestressing force and eccentricity cancel out. Therefore, the required elastic modulus of a beam is based on the applied moments and concrete stress limits.

5.5.5 The Magnel Diagram and Selection of Prestressing Steel

Equations (5.8a) to (5.8d) may once again be rearranged to determine the requirements and limits for the initial prestressing force, as shown here.

$$\frac{1}{P_i} \leq \frac{\alpha(Z_{tbm}/A_b - e_b)}{Z_{tbm} f_{trmin} - M_b} \quad (5.10a)$$

$$\frac{1}{P_i} \geq \frac{\alpha(Z_{bbm}/A_b + e_b)}{Z_{bbm} f_{trmax} + M_b} \quad (5.10b)$$

$$\frac{1}{P_i} \geq \frac{\beta(Z_{tbm}/A_b - e_b)}{Z_{tbm} f_{max} - M_{bs}} \quad (5.10c)$$

$$\frac{1}{P_i} \leq \frac{\beta(Z_{bbm}/A_b + e_b)}{Z_{bbm} f_{min} + M_{bs}} \quad (5.10d)$$

When these equations are plotted together, they enclose an area from which feasible values for the initial prestress force and corresponding eccentricities can be determined. The diagram is referred to as the Magnel diagram, named for Gustav Magnel who first introduced it. Figure 5.4 presents the Magnel diagram for the single span design in this dissertation, providing an illustration of the concept.

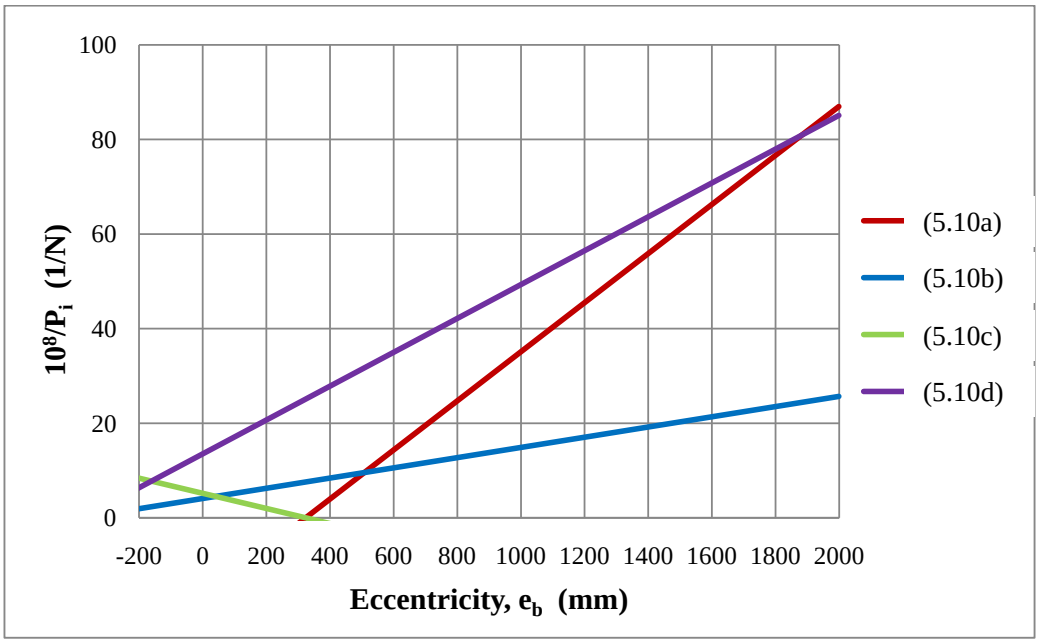

Figure 5.4 – Magnel Diagram for the single span design

From the diagram, the maximum and minimum allowable eccentricities may be determined. It should be noted that restrictions due to required nominal cover also provide a limit in the selection of eccentricity. With the selected eccentricity, the minimum and maximum allowable initial prestressing forces are determined based on the upper and lower boundaries of the diagram, and a prestressing force is selected. With the diagram, it is easy to simultaneously adjust the initial prestressing force and eccentricity to find an appropriate balance.

When making these selections, it is recommended that a point on the graph closer to the upper boundary for $1/P_i$ (or $10^8/P_i$) be selected, as this will reduce the prestressing force and create a more economical design. Also, points on the diagram near a vertex should be avoided, since they will not allow much flexibility when it comes to position of the strands in the beam (Bhatt, 2011).

In addition to the boundaries provided by the Magnel Diagram, Clause 5.10.3(2) in BS EN 1992-1-1 also limits stress of the strands based on an allowance for losses. This limit is put in place to avoid stresses in tendons under the serviceability conditions that could lead to inelastic deformation. The code defines this limiting stress to be the minimum of $0.75\,f_{pk}$ and $0.85\,f_{p0.1k}$. The limit is accounted for in

design by ensuring that the characteristic value of the prestressing force is greater than a required prestressing force equal to the minimum initial prestressing force divided by a factor of 0.75.

For the continuous spans, the selection of prestressing force will most likely need adjusted due to secondary moments. The initial selection is typically based on the hogging moment at the centre support, requiring a few slight alterations in the inequalities to account for the negative moment.

5.5.6 Secondary Moments and Effective Eccentricity

This step in the design procedure is only applied to the design of continuous spans. Up until this point in the design, the same procedure can be followed for both single and continuous spans, with only a few small adjustments. The secondary moments that occur in continuous prestressed beams are the first main difference between the designs.

In the case of statically determinate structures, the application of prestressing forces does not create any reactive forces at the supports, because the beam is allowed to deflect with the prestressing force freely. Therefore, the moment due to prestressing is determined simply by multiplying the prestressing force by the eccentricity of the strands. On the contrary, for indeterminate structures the application of prestressing forces causes additional moments on the beam due to the reactive forces at the centre support. These are referred to as “secondary” or “parasitic” moments (Hurst, 1998). While these moments require additional work in the analysis and design of the structure, they are often beneficial to the design.

In the calculation of secondary moments, the primary moment refers to the moment calculated based on the prestress force and eccentricity neglecting the effects of the centre support. The secondary moments are based solely on the reactions caused by the prestressing force, and therefore the moment diagrams vary linearly between the supports. The final bending moment due to prestress is then the sum of the primary and secondary moments (Bhatt, 2011). From this final bending moment, the effective eccentricity can be determined by simply dividing the moment by the prestressing force. These concepts are illustrated for a simplified beam in Figure 5.5.

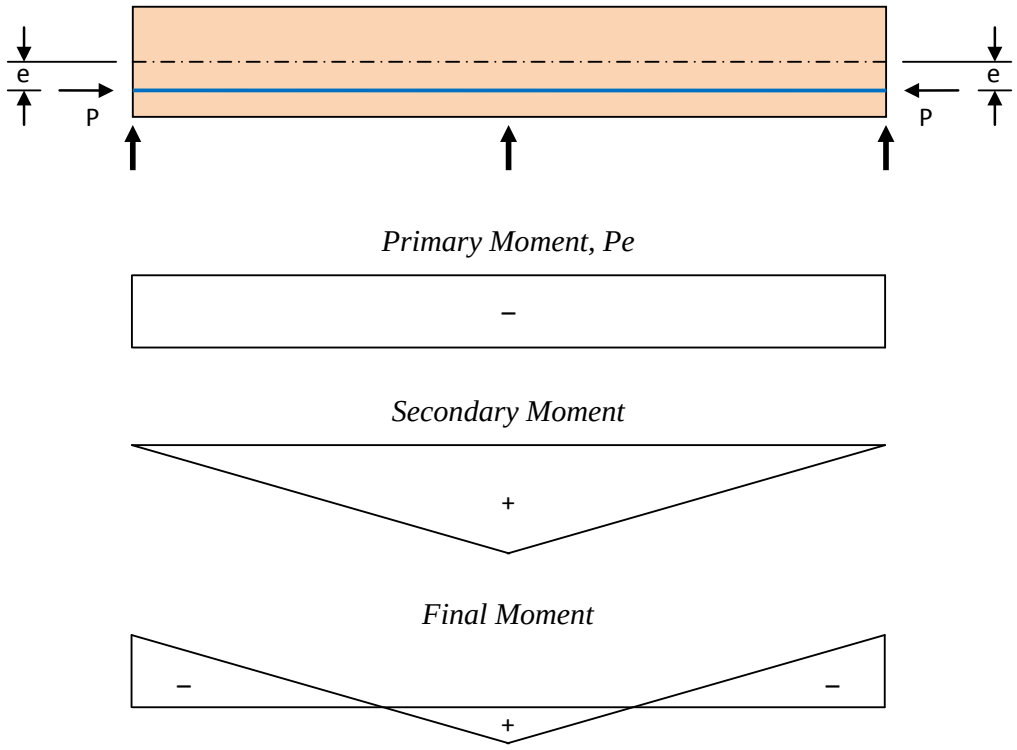

Figure 5.5 – Primary, secondary and final moments due to prestress

For most continuous prestressed beams, the profile of strands is not as simple as that shown in Figure 5.5. Due to the hogging moments at the support, prestressing must be provided in the top fibres of the beam as well as the bottom. Typically this is accomplished by using a curved tendon profile, similar to that shown in Figure 5.6.

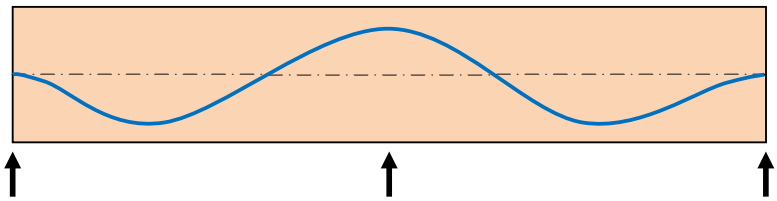

Figure 5.6 – Curved tendon profile for a continuous beam

There are a number of methods which can be applied to determine the secondary moments due to curved profiles. One of the most common methods is to determine equivalent loads on the beam due to the prestressing force. Then, through structural analysis, the reactions due to these loads are determined and the secondary moments calculated. Bhatt (2011) provides detailed instructions for this method, which have been applied in this dissertation. Refer to Section C.5.8 of Appendix C for details.

With the resulting final moment, the effective eccentricities are determined. In the design procedure, these values should replace the selected eccentricities in all calculations, accounting for the effect of secondary moments throughout the design.

5.5.7 Verification of Concrete Stresses with Selected Prestress Force

The next step in the design process is to verify that the stresses in the concrete at the critical section with the selected prestressing force and eccentricity fall within the concrete stress limits. This is done with the inequalities defined by Equations (5.8a) to (5.8d) in Section 5.5.2. For a single span, the critical section occurs at midspan. For continuous spans, two critical sections are checked, the first at the location of the maximum positive moment, and the second at the centre support where the minimum negative moment occurs. Also, for the continuous spans the effective eccentricity is applied in place of the selected eccentricity.

5.5.8 Confirmation of Tendon Profile and Eccentricity

After confirmation of the stresses at critical sections, the distribution of stresses should also be checked at a number of sections along the beam, due to variation in loading across the structure. For the single span design, this is accomplished by rearranging the inequalities once again to define limits for the eccentricity. The resulting inequalities are shown below.

$$e_b \leq \frac{Z_{tbm}}{A_b} + \frac{1}{\alpha P_i}(M_b - Z_{tbm} f_{trmin}) \qquad (5.11a)$$

$$e_b \leq -\frac{Z_{bbm}}{A_b} + \frac{1}{\alpha P_i}(M_b + Z_{bbm} f_{trmax}) \qquad (5.11b)$$

$$e_b \geq \frac{Z_{tbm}}{A_b} + \frac{1}{\beta P_i}(M_{bs} - Z_{tbm} f_{max}) \qquad (5.11c)$$

$$e_b \geq -\frac{Z_{bbm}}{A_b} + \frac{1}{\beta P_i}(M_{bs} - Z_{bbm} f_{min}) \qquad (5.11d)$$

As long as the selected eccentricity falls within the limits created by these equations, the stress limits are satisfied. In the case of post-tensioned beams, these inequalities may also be used to determine a profile for the tendons that satisfies the requirements.

For the continuous design, a profile was previously selected for the calculations of secondary moments, and therefore the stresses are simply verified for each section by applying Equations (5.8a) to (5.8d).

5.5.9 Prestress Loss Calculations

The concept of prestressed concrete was first thought of not long after the invention of reinforced concrete, and the construction of it was attempted many times, but each time the steel lost its tension and the beams acted only as reinforced beams. Engineers of the time did not yet know about the properties of steel and concrete that caused the loss in tension. It was not until the discovery of creep early in the 20th century that Freyssinet was finally able to understand the problem and develop a solution for prestressed concrete construction.

Today a great deal is known about the effects of concrete and steel properties on a structure, and they must be accounted for in design. These effects are considered with the calculation of prestress losses. In design, consideration is given to both short-term losses and long-term losses.

Short-term losses occur at the transfer stage as a result of elastic shortening for both pre-tensioned and post-tensioned concrete, and as a result of friction between the duct and cables and slip in the anchors for post-tensioned concrete. These losses typically come to around 10% of the jacking force (Bhatt, 2011). Long-term losses of around 25% occur over a period of time due to the effects of creep and shrinkage in concrete and relaxation of the prestressing steel (Bhatt, 2011).

Calculations for losses due to each of these effects must be considered in design, with guidance provided by Section 5.10 of BS EN 1992-1-1. Once the actual prestress losses are known, the design must be verified with these values since the initial design was performed based on initial assumptions. The calculations for these losses are rather extensive, and due to time constraints are beyond the scope of this report. Consideration of these effects should be made in future investigations and designs.

5.6 DESIGN OF THE COMPOSITE SECTION

With the initial design of the beam completed and verified, the next consideration is the design of the composite section. At this stage the slab has hardened and the slab and beam are assumed to act as one. This type of construction increases the capacity of the structure and allows the design of more slender members and/or longer span lengths (Hurst, 1998). For further discussion on composite construction refer to Section 2.2 in Chapter 2. For full calculations of this stage in the design process refer to Sections B.6 and C.6 of the Appendices.

First the section properties must be adjusted for the combined capacity of the beam and slab. With the addition of the concrete slab to the section, properties such as the moment of inertia increase, which affect the capacity of the structure.

5.6.1 Concrete Stress Limits for the Beam and Slab

As for the calculations in Section 5.5.2, the compressive stress limits are calculated based on Clause 5.10.2.2(5) in BS EN 1992-1-1. At this stage, the stress limits are calculated based on 28 day strengths for both the beam and the slab. Also, the tensile stress limits are taken as $-f_{ctm}(t)$, which is found in Table 3.1 of BS EN 1992-1-1.

5.6.2 Verification of Concrete Stresses in the Composite Section

The stresses must first be checked at the critical section. The stress distributions for the composite section include the application of all imposed loading on the structure, as well as the capacity of the slab. The following equations are applied to determine the stress distributions. These expressions consist of the stress distributions determined in Section 5.5.3 with the addition of a fourth stress resulting from the imposed loading on the composite section.

In the beam:

For the top fibre

$$\frac{\beta P_i}{A_b} - \frac{\beta P_i e_b}{Z_{tbm}} + \frac{M_{bs}}{Z_{tbm}} + \frac{M_{imp} y_{tbm}}{I_c} \leq f_{max} \qquad (5.12a)$$

For the bottom fibre

$$\frac{\beta P_i}{A_b} + \frac{\beta P_i e_b}{Z_{bbm}} - \frac{M_{bs}}{Z_{bbm}} - \frac{M_{imp} y_{bbm}}{I_c} \geq f_{min} \qquad (5.12b)$$

In the slab:

For the top fibre $$\frac{M_{imp}y_{tsb}}{I_c} \leq f_{smax} \quad (5.12c)$$

For the bottom fibre $$\frac{M_{imp}y_{bsb}}{I_c} \geq f_{smin} \quad (5.12d)$$

where:

M_{imp} = moment due to the imposed loading on the structure

I_c = moment of inertia for the composite section

y_t and y_b are based on the composite section

f_{min} and f_{max} = stress limits for the beam

f_{smin} and f_{smax} = stress limits for the slab

Once the stresses are verified for the critical sections, the designer should also consider the stresses at a number of sections along the beam. This is required due to the variation in loading across the structure. The designer must ensure that the stresses are always balanced within the required limits.

5.7 DEFLECTION

5.7.1 Deflection Limits

For bridge design, there is not much guidance on deflection checks in the Eurocodes. Clause 7.4.1 of BS EN 1992-2 specifies that the deflection limits provided for buildings in BS EN 1992-1-1 do not apply to bridges, but it fails to give any other limits. While deflection for prestress concrete typically does not control the design, the deflections should still be calculated. Therefore, the limits must be set on a case by case basis.

In accordance with Clause 7.4.1(1)P of BS EN 1992-1-1, the deformation of the bridge beam should not be such that will adversely affect its function or appearance. While excessive deflection on a bridge may not directly affect the capacity of the structure, it can cause problems with drainage paths and can also damage surfacing or waterproofing systems. The comfort of passengers must also be taken into account (Hendy and Smith, 2007).

To find a reasonable assumption for the deflection limits in the design examples, the requirements applied in the United States are considered. In accordance with Clause 8.9.3.1 of the AASHTO LFD Specifications, live load deflections should be limited to L/800 for ordinary bridges, and L/1000 for bridges in urban areas which are subject to pedestrian use. The AASHTO LRFD Specifications, to which most structures are designed to currently in the United States, also incorporate these limits through optional serviceability criteria. It should be noted that these limits are based on live load only, and do not include the affects of dead load acting on the structure. Conservatively, a limit of L/1000 is applied to both design examples in this report, for which the deflection calculations include dead load. As this limit is met with these conservative assumptions, it is determined that the deflection requirements are met in accordance with the Eurocodes.

5.7.2 Deflection Calculations

The deflections in prestressed concrete must be checked at three stages: at transfer, at service before application of finishes, and long-term with imposed loading. For the transfer and service stage, only the weight of the beam and composite section are considered (Bungey, Hulse and Mosley 2007). At the service stage, in accordance with BS EN 1991-1-1, additional loading of 1.0 kN/m^3 for the wet concrete may be considered as well as 1.0 kN/m^3 for construction equipment during placement of the slab. For long-term deflections on road bridges, Clause A2.4.2(3) of BS EN 1990 recommends application of the frequent combination of actions.

Deflections due to the prestressing force are calculated with the double integration of the equation (5.13). From this, equations (5.14) and (5.15) for deflection are derived, incorporating the distributed load, w, on the structure as well.

$$M_x = Pe_x = EI\frac{d^2y}{dx^2} \tag{5.13}$$

For straight tendons:

$$\delta = \frac{5}{384}\frac{wL^4}{EI} - \frac{1}{8}\frac{P_i e_b L^2}{EI} \tag{5.14}$$

For parabolic tendons:

$$\delta = \frac{5}{384}\frac{wL^4}{EI} - \frac{5}{48}\frac{P_i e_{max} L^2}{EI} \tag{5.15}$$

For each of the three stages, adjustments should be made for prestress losses. Consideration must also be given to the age of the concrete by determining the effective modulus of elasticity. Further explanation is given for this in Section 3.1.2 of Chapter 3. Also, for the continuous spans, the deflections are calculated based on the maximum positive moment and effective eccentricity. An effective span length equal to 85% of the span is applied as well, in accordance with Figure 5.2 of BS EN 1992-1-1. In both design examples, the deflections are well within the limit of L/1000, so designs are satisfactory with respect to deflections. For calculations, refer to Sections B.7 and C.7 of the Appendices.

5.8 END BLOCK DESIGN

For pre-tensioned members, the force from the prestressing steel is transferred to the concrete gradually through the bond between the steel and concrete. For post-tensioned members this is not the case, and some additional forces need to be accounted for in the design. In these members, the force is transmitted to the beam through an anchor. As a result, the force is concentrated over a small area at each end, which can lead to high-tensile forces, also known as bursting forces, acting perpendicular to the direction of the compression force. This area is referred to as the end block (Bungey, Hulse and Mosley 2007).

The tensile forces tend to cause the concrete to split apart. This effect is similar to that of driving a nail into the end of a timber joist (Hurst, 1998). To avoid bursting or spalling of the concrete due to these tensile forces, the end block must be heavily reinforced by steel. This reinforcement generally consists of closed links (Bungey, Hulse and Mosley 2007).

5.8.1 Bearing Stress Under the Anchor

The first step in designing the end block is to verify that the bearing stress under the anchor does not exceed the allowable stress. Clause 8.10.3(3) of BS EN 1992-1-1 specifies that this should be checked in accordance with relevant European Technical Approval (ETA), but gives no further guidance. Bungey, Hulse, and Mosley (2007) provide the following equations for the calculations of these stresses.

For the actual bearing stress:

$$\sigma_c = \frac{\gamma_{punfav} \times \text{Prestressing Force}}{A_o} \quad (5.16)$$

For the allowable bearing stress:

$$f_{Rdu} = 0.67 f_{ck} \sqrt{\frac{A_{c1}}{A_o}} \leq 2.2 f_{ck} \quad (5.17)$$

where: γ_{punfav} = partial factor for local effects (BS EN 1992-1-1 Cl. 2.4.2.2(3))

A_o = loaded area under the anchorage

A_{c1} = maximum area with same shape as A_o

f_{ck} = concrete compressive strength

Clause J.104.2(102) in BS EN 1992-2 also recommends that minimum spacings and edge distances be observed in accordance with the relevant ETA (Hendy and Smith, 2007). Due to the fact that the design examples in this report are hypothetical, consideration of these requirements is not given here, however it should be included in future designs.

5.8.2 Required Reinforcement

The next step is to determine the required reinforcement for resisting the lateral tensile bursting forces. To accomplish this, first the bursting forces are determined based on the pattern or "flow lines" of compressive forces in the end block, which differ depending on the type of anchorage used (Bungey, Hulse and Mosley 2007). Clauses 8.10.3(4) and (5) of BS EN 1992-1-1 recommend the application of a strut and tie model, illustrated in Figure 5.7, for this calculation with a dispersion angle, β, of 33.7°. In addition, Clause 8.10.3(104) of BS EN 1992-2 stipulates that for bridges, if the stress in the reinforcement is limited to 250 MPa, a check of crack widths is not required.

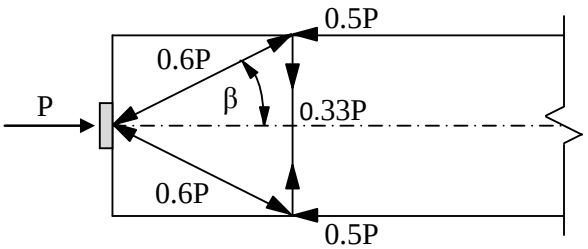

Figure 5.7 – Strut and tie model for end block

From the strut and tie model illustrated in Figure 5.7, the tensile bursting force is determined to be 33% of the prestressing force. It should be noted that the prestressing force should include the unfavourable partial factor, γ_{punfav}. With this force, the required area of steel is determined, based on the stress limit of 250 MPa. With the required area, the size and number of closed links is selected. These should then be distributed over a length of the end block equal to the largest dimension of the anchorage block considered (Bungey, Hulse and Mosley 2007). The required reinforcement may be determined for each individual anchorage and also for all of the anchorages as a whole (Hurst, 1998).

Clause J.104.2 of Annex J in BS EN 1992-2 also provides a method for determining the required reinforcement that is meant to account for situations in which two or more anchorages are applied. This method has many shortcomings. Therefore, as Annex J is only informative, it is recommended to base the design on the strut and tie model (Hendy and Smith, 2007).

5.8.3 Compressive Stress in the Concrete Struts

The last step for end block design is to check the compressive stress in the concrete struts. This step is performed for each individual anchor. The allowable compressive stress may be taken as $0.4\, f_{ck}$ and the actual stress in the strut is determined by dividing the force by the cross sectional area (Hurst, 1998). The force in the strut is determined to be 60% of the prestressing force from the strut and tie model. And the cross sectional area is based on the dispersion angle, β, of 33.7^{o}. Refer to Section C.8 of Appendix C for the end block design performed in the post-tensioned design example.

5.9 BENDING MOMENT AT THE ULTIMATE LIMIT STATE

After ensuring that all of the serviceability limit state requirements are met, the section must be analyzed to ensure that the ultimate limit state requirements are met. While the serviceability limit state typically controls the design, satisfaction of those requirements does not necessarily guarantee the satisfaction of requirements for the ultimate limit state.

When the loads in a prestressed member increase above the working loads, the concrete cracks and the prestressing steel starts to behave as conventional reinforcement. Therefore, the behaviour of a prestressed member at the ultimate limit state is the same as that for a reinforced member, with the additional consideration of initial strain due to prestress in the steel (Bungey, Hulse and Mosley 2007).

The first of the ultimate limit state requirements to be checked is the ultimate bending moment. The ultimate bending moment resistance must be determined to ensure that it exceeds the applied moments for the ultimate limit state, discussed in Section 5.4.2. Partial factors of safety on steel and concrete are included in this stage of the design, as well as a partial factor of safety on the prestress force for the favourable effect. These factors are defined in Clause 2.4.2.2 of the National Annex for BS EN 1992-1-1 and Clause 2.4.2.4 of BS EN 1992-1-1. For concrete, a partial factor, γ_C, of 1.50 is applied and for reinforcing steel a partial factor, γ_S, of 1.15 is applied. For the prestressing steel, the favourable partial factor, γ_P, is 0.90.

5.9.1 Stress-Strain Relationship for the Prestressing Strands

The first step in the calculation of the ultimate bending moment resistance is the determination of the stress-strain relationship for the prestressing strands. This relationship is used to calculate tension forces for each layer of strands in the member (Bungey, Hulse and Mosley 2007). Figure 5.8 presents the stress-strain relationship developed for the single span design example.

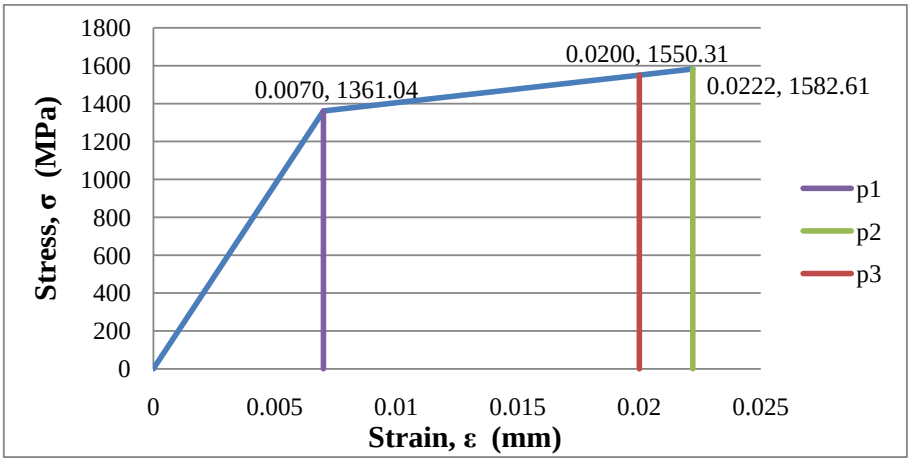

Figure 5.8 – Stress-strain relationship for prestressing steel

This curve is developed with the calculation of three points: the first is for the yield point of the steel, the second is for the maximum design, and the third is the failure point of the steel. The following equations are applied to calculate these points.

$$\sigma_{p1} = f_{p0.1k}/\gamma_s \quad (5.18)$$

$$\varepsilon_{p1} = \sigma_{p1}/E_s \quad (5.19)$$

$$\sigma_{p3} = f_{pk}/\gamma_s \quad (5.20)$$

$$\varepsilon_{p3} = \varepsilon_{ud}/0.9 \quad (5.21)$$

$$\varepsilon_{p2} = \varepsilon_{ud} \quad (5.22)$$

$$\sigma_{p2} = \sigma_{p1} + (\sigma_{p3} - \sigma_{p1}) \times (\varepsilon_{p2} - \varepsilon_{p1})/(\varepsilon_{p3} - \varepsilon_{p1}) \quad (5.23)$$

where:

$f_{p0.1k}$ = the 0.1% proof stress

E_s = the elastic modulus of elasticity, taken as 195 GPa for strands

f_{pk} = the characteristic tensile strength

ε_{ud} = strain limit defined by Cl. 3.3.6(7), BS EN 1992-1-1 as 0.02

5.9.2 Calculation of the Ultimate Bending Moment Resistance

For the calculation of bending moment resistance, the stress and strain diagrams such as those illustrated in Figure 5.9 are applied (Bungey, Hulse and Mosley 2007).

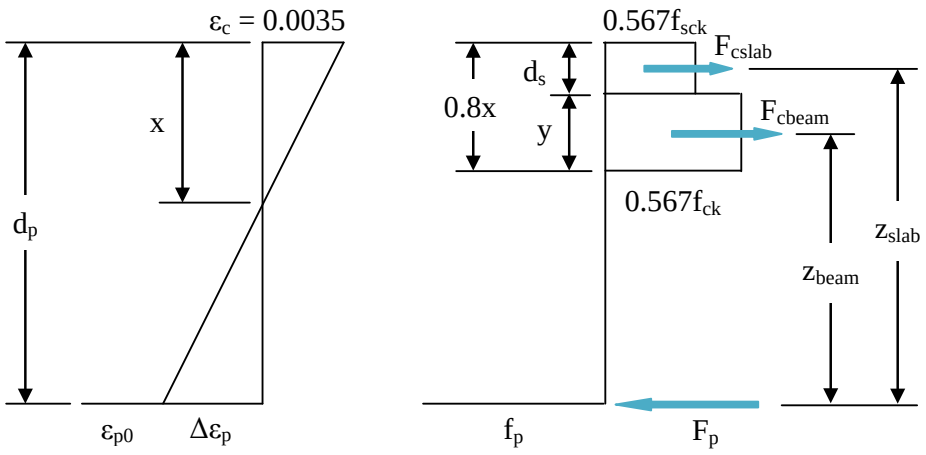

Figure 5.9 – Stress and strain diagrams for the composite section

Some guidance on the development of these diagrams is provided in Section 3.1 of BS EN 1992-1-1. It should be noted that the prestressing force in this diagram is represented as a resultant force for all of the strands and is placed at the CGS of the strands. For more accurate results, calculations should be performed for each layer of strands.

To determine the bending moment resistance, the depth of the neutral axis, x, for which the compressive force in the top fibres equals the tensile force in the bottom fibres must be determined through trial and error. The ultimate bending moment resistance is then determined by multiplying the compressive or tensile force by the lever arm, z, between the two resultants. The tensile and compressive forces are calculated with the following equations, which are derived from Figure 5.10.

Steel tensile force:

$$F_p = f_p A_p = \min\left(\varepsilon_p E_s; f_{pd}\right) A_p = \min\left[\left(\Delta\varepsilon_p + \gamma_{p,fav}\varepsilon_{p0}\right) E_s; f_{pd}\right] A_p \qquad (5.24)$$

where:

$\Delta\varepsilon_p = \varepsilon_c\left(d_p - x\right)/x$

ε_c = ultimate compressive strain for concrete (Table 3.1, EC2)

$\varepsilon_{p0} = \left(P_{istr}/A_{pstr}\right)/E_s$

$\gamma_{p,fav}$ = favourable partial factor for prestress

$f_{pd} = \sigma_{p1}$

A_p = area of prestressing strands

Concrete compressive force:

$$F_c = F_{c,slab} + F_{c,beam} = s_{bm} d_s (0.567 f_{sck}) + b_{bm}(0.8x - d_s)(0.567 f_{ck}) \qquad (5.25)$$

where:

s_{bm} = spacing of the beams

d_s = depth of the slab

f_{sck} = concrete strength for the slab

b_{bm} = width of the beam

f_{ck} = concrete strength for the beam

Ultimate bending moment resistance:

$$M_{Rd} = F_p z = F_c z \quad (5.26)$$

The designer must verify that the bending moment resistance is greater than the ultimate bending moment applied to the structure, the calculation of which is discussed in Section 5.4.2. In addition to checking the bending moments, the strain should be checked against the strain limit, $\varepsilon_{ud} = 0.0200$, recommended by Clause 3.3.6(7) of BS EN 1992-1-1.

In the case of continuous spans, there are a couple of differences in the design which must be considered. First, the secondary moments discussed in Section 5.5.6 should be added to the applied ultimate bending moment for final verification (Bhatt, 2011). Also, the ultimate bending moment must be checked at two locations, the first at the location of the maximum positive moment and the second at the support with the minimum negative moment. If the bending moment resistance exceeds the applied bending moment for both of these locations, it can be assumed that it will exceed the applied bending moment at all sections in the beam. For further details and calculations on both single spans and continuous spans refer to Sections B.8.2 and C.9.2 of the Appendices.

5.10 SHEAR AT THE ULTIMATE LIMIT STATE

In addition to the prestressing steel, shear reinforcement must also be provided to support high shear forces that occur near the supports. For prestressed concrete, the members resist shear forces in the same way as reinforced members except for some additional effects of the compression due to the prestressing force in the beam. This compression increases the shear resistance considerably on the beam (Bungey, Hulse and Mosley 2007).

5.10.1 Shear Forces on the Beam

The first step for shear design is to determine the design shear forces applied to the beam. The forces should be determined at a number of sections on the beam since the reinforcement will vary in spacing along the span. For the design examples in this

report, the determination of these forces is easily accomplished with the shear diagrams created in calculating the maximum moment. Also, for members with curved tendon profiles, the axial forces of inclined tendons may be included in the calculation of the design shear force (Bungey, Hulse and Mosley 2007).

5.10.2 Shear Resistance of the Concrete

Before designing the shear reinforcement, the shear resistance of the concrete must be determined. Often, regions where shear forces are small do not require shear reinforcement. Although minimal links are typically still provided in these regions. Clause 6.2.2(101) in BS EN 1992-2 provides the following equation for concrete shear resistance in bridges.

$$V_{Rd,c} = \left[C_{Rd,c} k \left(100\rho_1 f_{ck}\right)^{1/3} + k_1 \sigma_{cp}\right] b_w d \qquad (5.27)$$

with a minimum of:

$$V_{Rd,c} = \left(v_{min} + k_1 \sigma_{cp}\right) b_w d$$

where:

$C_{Rdc} = \frac{0.18}{\gamma_c}$ (NA to BS EN 1992-2, Cl.6.2.2(101))

$\gamma_c = 1.50$ (BS EN 1992-1-1, Cl. 2.4.2.4)

$k = 1 + \sqrt{\frac{200}{d_p}} \leq 2.0$ with d in mm

d_p = distance from top of slab to CGS of strands

$\rho_1 = \frac{A_p}{b_w d_p} \leq 0.02$

b_w = smallest width of the cross section

A_p = total area of the prestressing strands

f_{ck} = concrete strength in MPa

$k_1 = 0.15$ (NA to BS EN 1992-2, Cl. 6.2.2(101))

$\sigma_{cp} = \frac{\gamma_{pfav} P}{A_c} \geq 0.2 f_{ctd}$

$\gamma_{pfav} = 0.9$ (NA to BS EN 1992-1-1, Cl. 2.4.2.2)

P = prestressing force

A_c = area of the section

$f_{cd} = \frac{\alpha_{cc} f_{ck}}{\gamma_c}$ (BS EN 1992-2, Cl. 3.1.6(101)P)

$\alpha_{cc} = 1.0$

d = depth of the section

$\nu_{min} = 0.035\ k^{3/2}\ f_{ck}^{1/2}$ (NA to BS EN 1992-2, Cl. 6.2.2(101))

In this equation, the $k_1\sigma_{cp}$ factor accounts for the compression due to prestress. With the factor k_1 equal to 0.15, as per the National Annex to BS EN 1992-2, the shear capacity of the section is enhanced by 15% of the longitudinal stress due to prestressing. With the results from this expression, the regions of the beam which require shear reinforcement are determined.

5.10.3 Required Shear Reinforcement

For regions in which reinforcement is required, the shear links are designed assuming the entire shear force is resisted by them. The resistance of the concrete section is not included in these calculations, in accordance with BS EN 1992-2. However, the design shear force must not exceed the crushing strength, $V_{Rd,max}$, of the concrete diagonal strut. If it is found that the shear force does exceed the crushing strength, the section must be redesigned (Bhatt, 2011). Therefore, before determining the steel required in each section, the crushing strength of the concrete struts is checked against the maximum design shear force. The crushing strength is determined with the following expression, provided by Clause 6.2.3(103) of BS EN 1992-2.

$$V_{Rd,max} = \frac{\alpha_{cw} b_w\ z\ \nu_1 f_{cd}}{\cot\theta + \tan\theta} \tag{5.28}$$

where:

for α_{cw}: (NA to BS EN 1992-2, Cl. 6.2.3(103))

$\alpha_{cw} = 1 + \sigma_{cp}/ f_{cd}$ for $0 < \sigma_{cp} \leq 0.25\ f_{cd}$

$\alpha_{cw} = 1.25$ for $0.25\ f_{cd} < \sigma_{cp} \leq 0.5\ f_{cd}$

$\alpha_{cw} = 2.5\ (1 - \sigma_{cp}/ f_{cd})$ for $0.5\ f_{cd} < \sigma_{cp} \leq 1.0\ f_{cd}$

b_w = smallest width of the section

z = lever arm

$\nu_1 = \nu = 0.6\ (1 - fck/250)$ (BS EN 1992-1-1, Eq. (6.6N))

$$f_{cd} = \frac{\alpha_{cc} f_{ck}}{\gamma_c} \quad \text{(BS EN 1992-2, Cl. 3.1.6(101)P)}$$

$\gamma_c = 1.50$ (BS EN 1992-1-1, Cl. 2.4.2.4)

$\alpha_{cc} = 1.0$

θ = angle of the strut

Once the crushing strength is verified, the vertical shear reinforcement is designed by rearranging the following expression, provided by Clause 6.2.3(103) in BS EN 1992-2. For these calculations an initial selection of shear links should be made, and applied to determine the minimum spacing based on the design shear force.

$$V_{Rd,s} = \frac{A_{sw}}{s} z \, (0.8 f_{ywd}) \cot \theta \qquad (5.29)$$

where:

A_{sw} = cross-sectional area of the reinforcement

s = spacing of the reinforcement

z = lever arm

f_{ywd} = design yield strength of the shear reinforcement

θ = angle of the strut

By applying this expression to a number of sections along the beam, an arrangement of shear links is developed, ensuring that the maximum spacing requirements are met for each region. In the areas where reinforcement is not required, shear links should be provided at a maximum spacing of 0.75 d.

6 CONCLUSION

Considered as a whole, this dissertation clearly illustrates the complexity and difficulty of designing a prestressed concrete bridge. Not only in the design of the prestressed concrete itself, but also in the determination of loading on the structure.

The calculation of loading becomes quite complicated due to the fact that its application is very open ended. The designer must consider and account for a wide range of possibilities, and each design has its own unique requirements. The Eurocodes cover a range of possible actions on the structure by defining a series of load models for the designer to apply, which are calibrated to represent the effects of traffic. However, even with the load models defined; there is often difficulty in determining what combination of loads will have the most adverse effect on the structure.

The calculations required to determine the greatest loading on a bridge can become very extensive, especially with continuous multi-span structures for which both the maximum and minimum loadings must be determined. As a result, the probability of errors in hand calculations becomes quite high. It is therefore concluded that for accurate and timely results, structural analysis software should be applied in the design. That being said, if the designer wishes to perform hand calculations, or check the results from a structural analysis program, a few conclusions based on this study may help to speed the process.

Of the four load groups considered, perhaps the two most difficult to apply are Load Group gr1a and Load Group gr5. For the application of Load Group gr1a, on a single span the designer may assume that the maximum moment will occur with the resultant of the tandem system from Load Model 1 located directly at midspan. Technically, this is not the exact location for maximum moment, as in design it was determined that the maximum moment occurred when the resultant was placed 0.4 metres to the right or left of midspan; however, the difference in results is found to be negligible. Also, for continuous spans it was found that the maximum moment

occurs when the resultant is placed at 17.2 metres from the first support, which is just past midspan of the effective length of 34.0 metres (0.85 L). Therefore, the designer may assume the maximum positive moment will occur when the resultant of the axles is placed somewhere around the centre of the effective span length. It is more difficult to define a location of the resultant which will create the minimum moment; however, it is known that the minimum moment will occur when the resultant is closer to the centre support.

The application of Load Group gr5 is especially difficult, since the special vehicle defined for Load Model 3 must be combined with frequent values of Load Model 1. Given that the frequent loads from Load Model 1 may be placed anywhere within the span that is not within 5.0 metres the special vehicle, it is not possible to define a specific location for the resultant of the axles that will have the most adverse effect on every bridge. However, some general conclusions may be drawn. For the single span, it was found that the more axles on the span, and the closer they all were to the centre span, the higher the loading. And for two span continuous bridges, it was determined through the development of the envelope of moments that maximum moment will occur when all of the loading is applied to only one span, while the minimum moment will occur when the tandem system is applied in a separate span from the special vehicle.

While the application of these two load groups is the most difficult, they typically create the most adverse effects on the structure, and therefore must be calculated for design. This is confirmed in Section 4.9 of this dissertation, where it is determined that the maximum characteristic moment acting on the structure is due to Load Group gr5 for both design examples, and the maximum frequent moment acting on the structure is due to Load Group gr1a.

In contrast to the loading calculations, the design of prestressed concrete becomes difficult because it has boundaries on all sides, so to speak. A successful prestressed concrete design depends on the balance of stresses throughout the section at all stages in its life. Therefore, prestressed concrete must satisfy the requirements at the transfer stage with minimal loading, as well as the requirements at service stage with maximum loading. This ensures that the force from the prestressing steel does not

cause damage to the structure before imposed loading is applied. Adding to the complexity, a number of different factors affect the balance of stresses, including material properties for both concrete and steel, beam properties, strand configuration and eccentricity, prestress losses, etc. It can become quite a challenge to find the right combination of factors for a design solution. As a result, it is difficult to provide a straight forward solution for these designs.

For instance, in the initial design of a prestressed beam, the amount of prestressing force must be selected. While the selection of a high prestressing force will obviously resist higher loads, consideration must be given to the stages before loading is applied as well. Too much prestress may cause damage in the beam before construction is complete. The design must find a unique balance of material properties, beam size, strand selection, number or strands and slab depth (for composite structures). This balance is further complicated by the influence of prestress loss and secondary moments in continuous spans.

Overall, it is concluded that the ability to create an efficient and cost effective design depends largely on the experience level of the designer. The design process for prestressed concrete is an iterative one, in which many initial assumptions must be made regarding the factors listed above. If the design does not work with one or more of these initial assumptions, the designer must go back and adjust all calculations that have been completed thus far. With more experience, a designer is able to make informed choices throughout the process, allowing him or her to find a successful design solution in a timelier manner.

Another benefit of experience is that the engineer gains more understanding of the properties of prestressed concrete and how it reacts to stress. As a result, the designer is able to create more cost effective and durable designs. Even so, with all of the information available today on prestressed concrete, it is still a relatively new form of construction, and more is discovered regarding its properties and strengths every day. The study of prestressed concrete illustrates why engineers must commit themselves to a lifelong learning process.

While the design does become rather complicated, the results of this study clearly demonstrate the benefits of prestressed concrete design. First, with the application of the prestressing force in the beam, fewer cracks occur in the concrete, creating a more durable structure. Also, as was illustrated with the stress-strain diagrams, the effects of prestress significantly increase the capacity of the structure, allowing it to resist higher loads before cracking occurs. Clearly, the design of prestressed concrete is worthwhile and significant, and the study of it is important for engineers, as it has become a well-established and common form of construction in a relatively short time period.

6.1 FUTURE WORKS

As previously mentioned, the design of prestressed concrete can become very complex. There are a number of aspects to consider and it is not possible to cover all of them within this dissertation. The omission of these does not mean they are any less important to the design process and many of them, mentioned here, should be considered in future investigations.

Despite the extensive discussion provided for loading on a bridge, there are many actions which have not been considered in full. These include, but are not limited to, wind actions, fatigue and accidental load models for traffic, actions during execution of the structure, and thermal actions. While the vertical load models discussed in Chapter 4 typically provide the most severe loading, consideration of other actions is still necessary in the design of a bridge.

One of the most important aspects of prestressed concrete design is the determination of prestress loss. As briefly mentioned in Chapter 5, a significant amount of loss in the tension of the strands can occur due to elastic shortening of the concrete, friction between the ducts and strands, creep and shrinkage of the concrete and relaxation in the steel. In the design examples for this report, initial assumptions are made regarding the losses that will occur, however the calculation of actual prestress loss has not been covered. This loss has a significant effect on the strength of the structure, and should be investigated fully in the future.

It is also recommended that future studies investigate the design of the composite section further, specifically with the determination of section properties. With the application of two different concrete strengths, an effective area should be determined for either the slab or the beam, based on the difference between the moduli of elasticity.

In the ultimate bending moment design, further analysis is required for the determination of the bending moment resistance. For the design examples in this report, a resultant force for the prestressing strands was applied at the centre of gravity of the strands. This method provides a sufficient estimation for the calculation of bending moment resistance; however, it is not entirely accurate. It does not allow for variation in the prestressing force across the member and it does not account for the possibility that some strands may fall inside the compressive zone, which often occurs in pre-tensioned concrete. It is recommended that future studies perform a detailed calculation by considering the effects for each row of strands.

This report includes a simplified design procedure which provides a good starting point for the study and design of a composite prestressed concrete bridge. However, due to the complexity of these structures, there is clearly much left for future investigations to consider.

REFERENCES

American Association of State Highway and Transportation Officials (1996) *Load Factor Design: Bridge Design Specifications* 16th Edition. Washington D.C.: AASHTO.

American Wood Council (2007) *Beam Formulas with Shear and Moment Diagrams*. Available from: http://www.awc.org/pdf/DA6-BeamFormulas.pdf [accessed 16th July, 2011].

Benaim R. (2008) *The Design of Prestressed Concrete Bridges: Concepts and Principles.* Oxon: Taylor & Francis.

Bhatt P. (2011) *Prestressed Concrete Design to Eurocodes*. Oxon: Routledge.

British Standard Institution (2006) *BS 8500-1:2006 Concrete – Complimentary British Standard to BS EN 206-1 – Part 1: Method of specifying and guidance for the specifier*. London: BSI.

British Standard Institution (2010) *BS EN 1990:2002+A1:2005 Eurocode – Basis of structural design.* London: BSI.

British Standard Institution (2009) *NA to BS EN 1990:2002+A1:2005 UK National Annex for Eurocode – Basis of structural design.* London: BSI.

British Standard Institution (2010) *BS EN 1991-1-1:2002 Eurocode 1: Actions on structures – Part 1-1: General actions – Densities, self-weight, imposed loads for buildings*. London: BSI.

British Standard Institution (2010) *BS EN 1991-2:2003 Eurocode 1: Actions on structures – Part 2: Traffic loads on bridges*. London: BSI.

British Standard Institution (2008) *NA to BS EN 1991-2:2003 UK National Annex to Eurocode 1: Actions on structures – Part 2: Traffic loads on bridges*. London: BSI.

British Standard Institution (2008) *BS EN 1992-1-1:2004 Eurocode 2: Design of concrete structures – Part 1-1: General rules and rules for buildings*. London: BSI.

British Standard Institution (2009) *NA to BS EN 1992-1-1:2004 UK National Annex to Eurocode 2: Design of concrete structures – Part 1-1: General rules and rules for buildings*. London: BSI.

British Standard Institution (2010) *BS EN 1992-2:2005 Eurocode 2: Design of concrete structures – Part 2: Concrete bridges – Design and detailing rules*. London: BSI.

British Standard Institution (2007) *NA to BS EN 1992-2:2005 UK National Annex to Eurocode 2: Design of concrete structures – Part 2: Concrete bridges – Design and detailing rules*. London: BSI.

Bungey J., Hulse R. and Mosley B. (2007) *Reinforced Concrete Design to Eurocode 2* 6th Edition. Hampshire: Palgrave Macmillan.

Burgoyne C. (2005) *Analysis of Continuous Prestressed Concrete Beams*. Available from: http://www-civ.eng.cam.ac.uk/cjb/papers/cp71.pdf [accessed 26th June 2011].

Calgaro J.-A., Tschumi M. and Gulvanessian H. (2010) *Designers' guide to Eurocode 1: Actions on bridges, EN 1991-2, EN 1991-1-1, -1-3, to -1-7 and EN 1990 Annex A2*. London: Thomas Telford Limited.

CCL (2011) *Post-tensioning Systems, Civil Engineering Construction.* Available from: http://www.cclint.com/what-we-do/post-tensioned-concrete/ccl-civil-structures /download-brochure.html [accessed 2nd August 2011].

Collins M.P. and Mitchell D. (1987) *Prestressed Concrete Basics.* Ontario: The Canadian Prestressed Concrete Institute.

The Concrete Society (2010) *Durable post-tensioned concrete structures*. Camberley: The Concrete Society [Technical Report No. 72].

European Committee for Standardization (2000) *DRAFT prEN 10138-2 Prestressing Steels – Part 2: Wire*. Brussels: CEN.

European Committee for Standardization (2000) *DRAFT prEN 10138-3 Prestressing Steels – Part 3: Strand*. Brussels: CEN.

European Committee for Standardization (2000) *DRAFT prEN 10138-4 Prestressing Steels – Part 4: Bars.* Brussels: CEN.

Freyssinet (2010a) *Freyssinet Prestressing: The System of the Inventor of Prestressed Concrete.* Available from: http://www.freyssinet.co.uk/pdfs/freyssinet_prestressing.pdf [accessed 2nd August 2011].

Freyssinet (2010b) *Freyssibar: The Prestressing Bar for Civil Works.* Available from: http://www.freyssinet.co.th/Commercial%20Brochures/NEW/FREYSSIBAR%2012P%20GB%20V26.pdf [accessed 2nd August 2011].

Gilbert R.I. and Mickleborough N.C. (1990) *Design of Prestressed Concrete.* London: Unwin Hyman Ltd.

Grote J. and Marrey B. (2003) The story of prestressed concrete from 1930 to 1945: A step towards the European Union. In: *Proceedings of the First International Congress on Construction History*. Madrid.

Hendy C.R. and Smith D.A. (2007) *Designers' Guide to EN 1992-2, Eurocode 2: Design of concrete structures, Part 2: Concrete bridges*. London: Thomas Telford Limited.

Hurst M.K. (1998) *Prestressed Concrete Design* 2nd Edition. Oxon: Taylor & Francis.

Jackson P., Salim S., Takács P.F. and Walker G.M. (2010) *Integral Concrete Bridges to Eurocode 2, Commentary and a worked example of a two span bridge, Technical Guide No. 13*. Surrey: The Concrete Society.

Kassimali A. (2005) *Structural Analysis* 3rd Edition. Toronto: Thompson.

Kumar A. (1988) *Composite Concrete Bridge Superstructures*. Slough: British Cement Association.

Martin L.H. and Purkiss J.A. (2006) *Concrete Design to EN 1992* 2nd Edition. London: Butterworth-Heinemann.

Nasser G.D. (2008) The Legacy of the Walnut Lane Memorial Bridge. *STRUCTURE magazine.* [Online] (October) pp. 27-31, Available from: http://www.structuremag.org/Archives/2008-10/F-WalnutLane-Nasser-Oct08.pdf [accessed 8th August 2011].

Neville A.M. (1995) *Properties of Concrete* 4th Edition. Essex: Pearson Education Limited.

Precast/Prestressed Concrete Institute (1997) PCI Bridge Design Manual. Chicago: PCI. Available from: http://www.pci.org/publications/bridge/index.cfm [accessed 25th July 2011].

Tarmac (2010?) *Prestressed concrete beams: technical documents*. Lincolnshire: Tarmac Precast Concrete Limited.

APPENDIX A APPLICATION OF TRAFFIC LOADING

BS EN 1991-2 describes a set of four load models that must be considered in the design of a bridge to determine to the most adverse loading on the structure. This appendix demonstrates the application of these load models for the design examples that are considered in Appendix B and C. Figure A.1 presents the bridge cross section that is to be used for both designs.

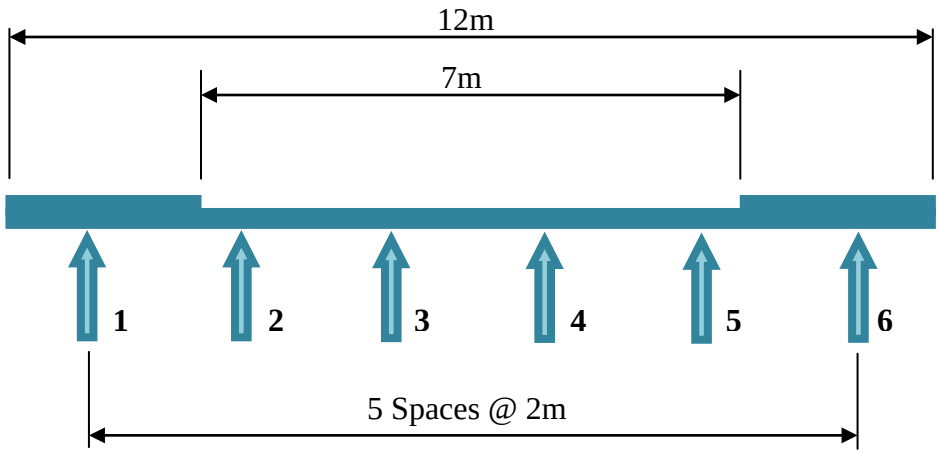

Figure A.1 – Bridge cross section

A.1 LOAD MODELS

The following provides a summary of the four vertical load models which are defined in BS EN 1991-2 and the corresponding national annex.

A.1.1 Load Model 1 – Normal Traffic

This load model consists of a tandem system and a uniformly distributed load, as shown in Figure A.2. The loads are applied within the notional lanes defined here.

Notional lanes:		**BS EN 1991-2**
Carriageway width	$w = 7.0$ m	Cl. 4.2.3 &
Width of notional lanes	$w_l = 3.0$ m	Table 4.1
Number of notional lanes	$n_l = 2$	
Width of remaining area	$w_r = 1.0$ m	

Tandem System (TS):

BS EN 1991-2

$Q_{1k} = 300\ kN \qquad \alpha_{Q1} = 1.0 \qquad \alpha_{Q1}Q_{1k} = 300\ kN$ — Cl. 4.3.2

$Q_{2k} = 200\ kN \qquad \alpha_{Q2} = 1.0 \qquad \alpha_{Q2}Q_{2k} = 200\ kN$ — Table 4.2

(α = adjustment factor defined in the National Annex) — Table NA.1

Axle spacing: $s_a = 1.2\ m$

Wheel spacing: $s_w = 2.0\ m$

Wheel loads: $Q_{1w} = \frac{\alpha_{Q1}Q_{1k}}{2} = 150\ kN$

$Q_{2w} = \frac{\alpha_{Q2}Q_{2k}}{2} = 100\ kN$

Uniformly Distributed Load (UDL):

$q_{1k} = 9.0\ kN/m^2 \qquad \alpha_{q1} = 0.61 \qquad \alpha_{q1}q_{1k} = 5.5\ kN/m^2$ — Table 4.2

$q_{2k} = 2.5\ kN/m^2 \qquad \alpha_{q2} = 2.20 \qquad \alpha_{q2}q_{2k} = 5.5\ kN/m^2$ — Table NA.1

$q_{rk} = 2.5\ kN/m^2 \qquad \alpha_{qr} = 2.20 \qquad \alpha_{qr}q_{rk} = 5.5\ kN/m^2$

Beam spacing: $s_b = 2.0\ m$

Load on the beam: $w_{UDL} = \alpha_q q_k s_b = 11.0\ kN/m$

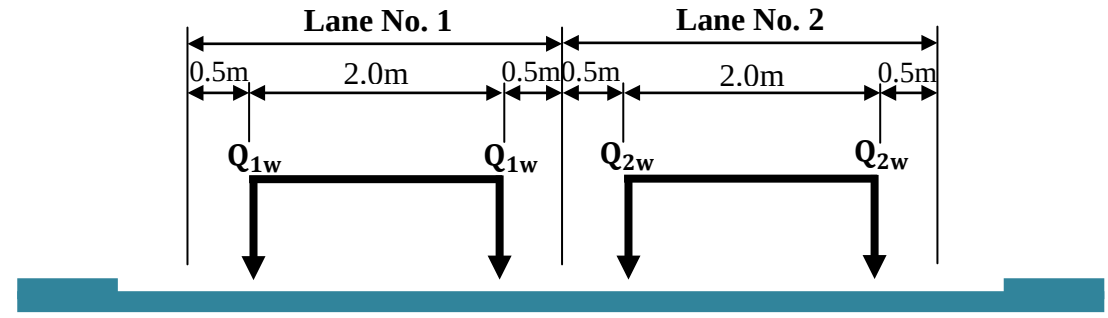

Application in the transverse direction

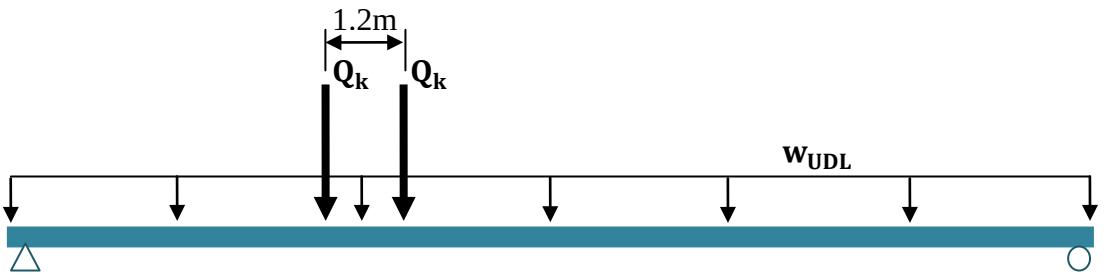

Application in longitudinal direction

Figure A.2 – Load Model 1

A.1.2 Load Model 2 – Single Axle

For this load model a single axle is applied to the structure as shown in Figure A.3.

Single Axle: **BS EN 1991-2**

$Q_{ak} = 400\ kN \quad \beta_Q = \alpha_{Q1} = 1.0 \quad \beta_Q Q_{ak} = 400\ kN$ Cl. 4.3.3

(β = adjustment factor defined in the National Annex) NA.2.14

Wheel spacing: $s_w = 2.0\ m$

Wheel loads: $Q_{aw} = \frac{\beta_Q Q_{ak}}{2} = 200\ kN$

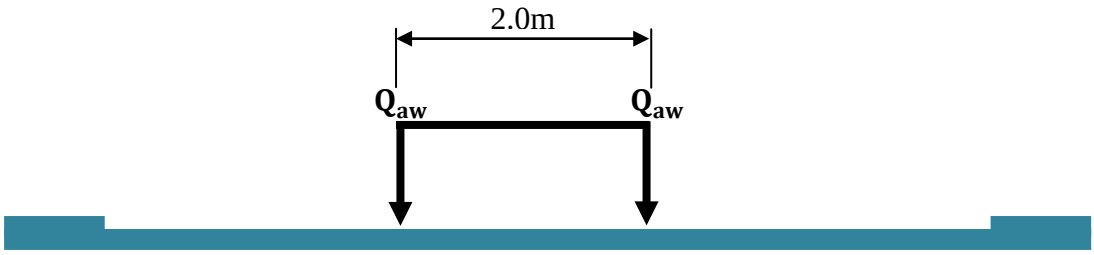

Application in transverse direction

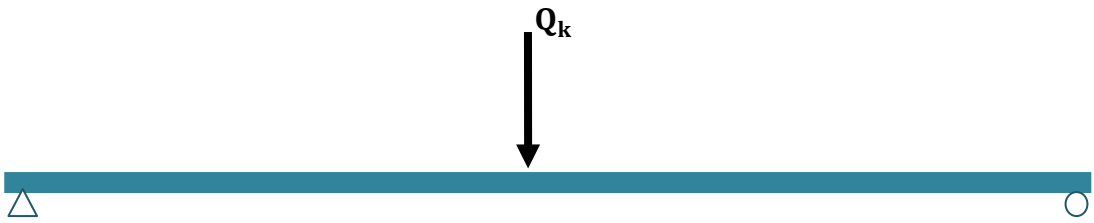

Application in longitudinal direction

Figure A.3 – Load Model 2

A.1.3 Load Model 3 – Special Vehicles

This model consists of a standardized special vehicle intended to cover the effects of special convoys. The national annex to BS EN 1991-2 defines a number of models for the standardized special vehicle, which are discussed in Section 4.3.3, Chapter 4. As per Clause NA.2.16 of the national annex to BS EN 1991-2, the choice of which vehicle to apply is determined by the designer for each individual project. In this case it is decided to apply SV196.

Special Vehicle SV196: **BS EN 1991-2**

Single locomotive pulling a maximum gross weight of 150 tonnes, STGO Category 3 — Cl. 4.3.4, Cl. NA.2.16

12 axles, each which a wheel spacing of 2.65m — Table NA.2

$Q_{196ak} = 100\ kN \quad DAF_{100} = 1.20 \quad DAF_{100}Q_{196ak} = 120.0\ kN$

$Q_{196bk} = 180\ kN \quad DAF_{180} = 1.10 \quad DAF_{180}Q_{196bk} = 198.0\ kN$

$Q_{196ck} = 165\ kN \quad DAF_{165} = 1.12 \quad DAF_{165}Q_{196ck} = 184.8\ kN$

DAF = Dynamic Amplification Factor

Wheel loads:

$$Q_{aw} = \frac{DAF_{100}Q_{196ak}}{2} = 60\ kN$$

$$Q_{bw} = \frac{DAF_{180}Q_{196bk}}{2} = 99\ kN$$

$$Q_{cw} = \frac{DAF_{165}Q_{196ck}}{2} = 92.4\ kN$$

Application in transverse direction

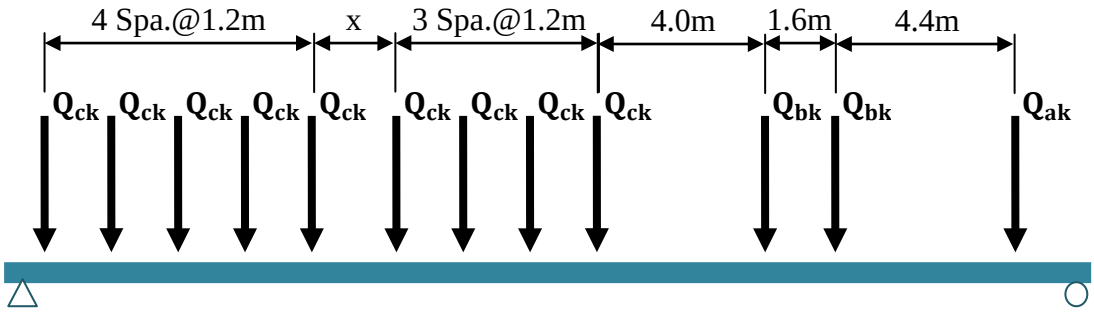

Application in longitudinal direction

(x = the critical of 1.2m, 5.0m, or 9.0m)

Figure A.4 – Load Model 3 – SV196 vehicle

A.1.4 Load Model 4 – Crowd Loading

This model consists of a uniformly distributed load, applicable to the whole deck.

$q_{ck} = 5.0\ kN/m^2$ (which includes dynamic amplification) **BS EN 1991-2**

Beam spacing: $s_b = 2.0\ m$ Cl. 4.3.5

Load on the beam: $w_c = q_{ck} s_b = 10.0\ kN/m$

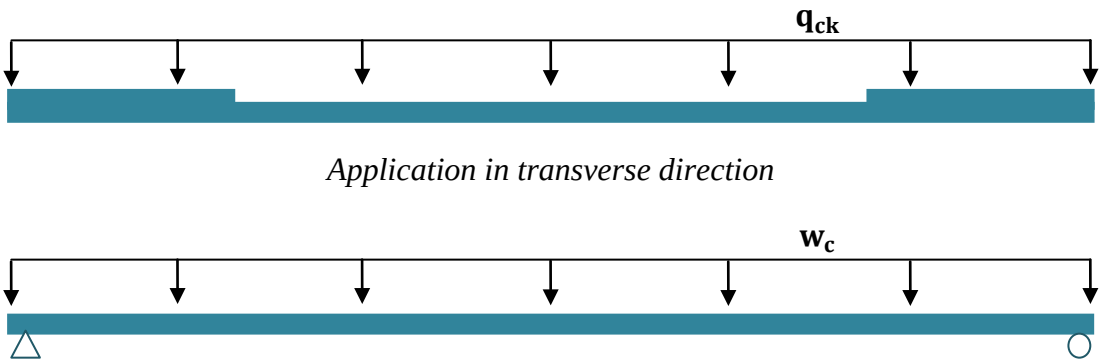

Figure A.5 – Load Model 4

A.2 TRANSVERSE INFLUENCE LINES

The following applies to both design examples. The calculations focus on Beam 3, which is the critical case. Kassimali (2005) provides instruction for the methods applied here, although any structural analysis book may be used.

Now that the load models are defined, the distribution of the wheel loads to the beams must be determined so that the wheels can be positioned to have the most adverse effect. This distribution can be established with the application of influence lines for the deck. Once the influence lines are developed the maximum resultant axle loads for each load model are determined in Section A.3, and applied longitudinally to calculate the maximum moment in Section A.4.

For development of the influence lines, the deck is considered as a continuous beam with each of the six beams acting as a support. To simplify calculations, the 1.0m overhang on each side is not considered, as it will not take traffic loading and its affect on the influence line for Beam 3 is minimal.

A.2.1 Degree of Indeterminacy and Redundants

The first step in the development of influence lines is to determine the degree of indeterminacy and select an equivalent number of redundants.

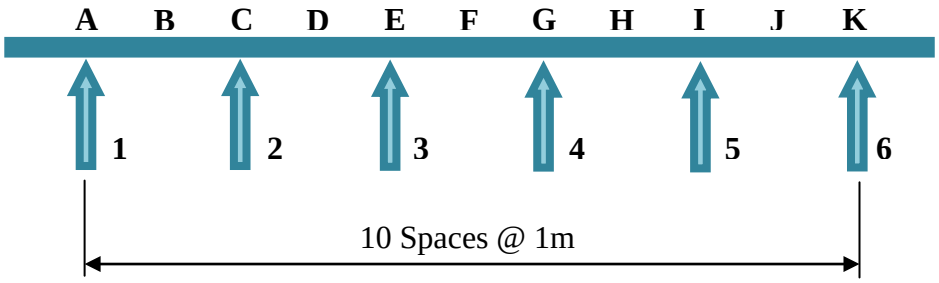

Figure A.6 – Indeterminate deck

The deck for both examples in this report is indeterminate to the fourth degree. It follows that four beams must be selected as redundants. For simplicity, beams 2 through 5 are chosen.

To provide clarity in the calculations, the deck has been divided into ten 1.0 meter sections, separated by points A through K.

A.2.2 Compatibility Equations

The next step is to determine the compatibility equations for each redundant. First the redundants are removed, creating a fictional structure referred to as the primary beam. This beam is illustrated in Figure A.7. The equations are then derived from the primary beam considering the compatibility condition that the combined effect of a unit load and the unknown redundants must be equal to zero.

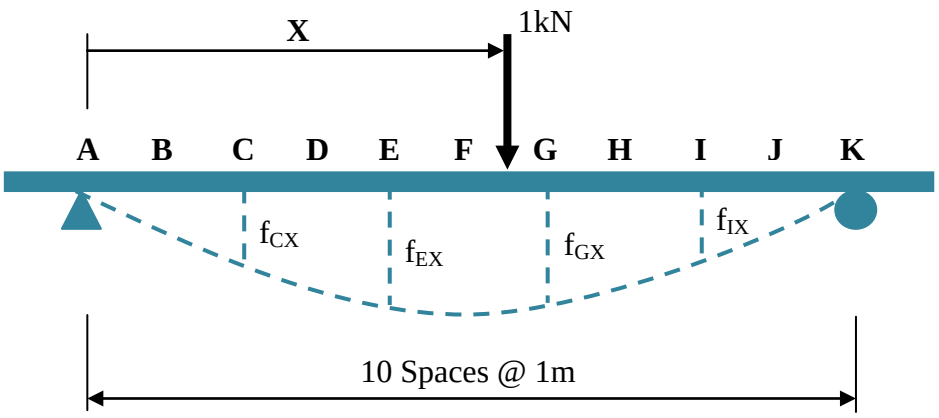

Figure A.7 – Primary element subjected to unit load

The following compatibility equations are determined:

$$f_{XC} + f_{CC}C_y + f_{EC}E_y + f_{GC}G_y + f_{IC}I_y = 0$$

$$f_{XE} + f_{CE}C_y + f_{EE}E_y + f_{GE}G_y + f_{IE}I_y = 0$$

$$f_{XG} + f_{CG}C_y + f_{EG}E_y + f_{GG}G_y + f_{IG}I_y = 0$$

$$f_{XI} + f_{CI}C_y + f_{EI}E_y + f_{GI}G_y + f_{II}I_y = 0$$

A.2.3 Deflections of the Primary Beam

The third step is to calculate the deflections due to an applied unit load. In this case, the deflections are determined via the conjugate beam method.

For this method, the M/EI diagram of the primary beam is first constructed for a unit load acting downwards at the location of the redundant under consideration. This diagram is then applied to the conjugate beam as shown in Figure A.8. In this case, the conjugate beam is identical to the primary beam. From the conjugate beam, the deflections are calculated as shown. This process must be repeated for each redundant.

Once the deflections are known, the upward deflections due to a unit load at the location of the redundant are also known, as they are equal and opposite to those calculated for each redundant location.

Due to the symmetry of the structure, the deflections calculated for the unit load at C are the same as those calculated for the unit load at I. Similarly, the deflections for the unit load at E are the same as those for the unit load at G.

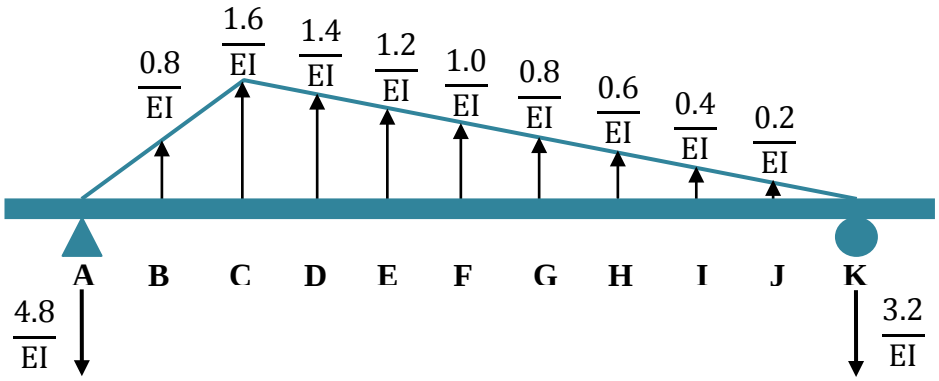

Figure A.8 – Conjugate beam for unit load at C

Deflections at redundants due to applied unit load at C:

By symmetry:

$f_{AC} = 0$ $\qquad$ $f_{KI} = 0$

$f_{CC} = -\frac{1}{EI}\left(4.8 \times 2 - \frac{1}{2} \times 1.6 \times 2 \times \frac{2}{3}\right) = \frac{-8.533}{EI}$ $\qquad$ $f_{II} = \frac{-8.533}{EI}$

$f_{EC} = -\frac{1}{EI}\left(3.2 \times 6 - \frac{1}{2} \times 1.2 \times 6 \times \frac{6}{3}\right) = \frac{-12.00}{EI}$ $\qquad$ $f_{GI} = \frac{-12.00}{EI}$

$f_{GC} = -\frac{1}{EI}\left(3.2 \times 4 - \frac{1}{2} \times 0.8 \times 4 \times \frac{4}{3}\right) = \frac{-10.667}{EI}$ $\qquad$ $f_{EI} = \frac{-10.667}{EI}$

$f_{IC} = -\frac{1}{EI}\left(3.2 \times 2 - \frac{1}{2} \times 0.4 \times 2 \times \frac{2}{3}\right) = \frac{-6.133}{EI}$ $\qquad$ $f_{CI} = \frac{-6.133}{EI}$

$f_{KC} = 0$ $\qquad$ $f_{AI} = 0$

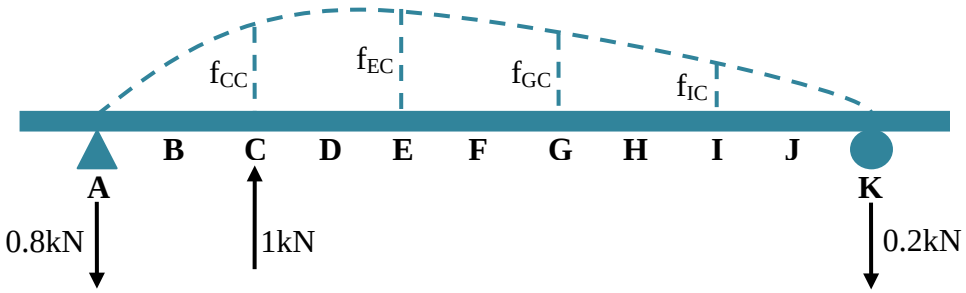

Figure A.9 – Primary beam subjected to redundant C_y

Upward deflections due to the unit values of redundants C_y and I_y (+):

$f_{CC} = \frac{8.533}{EI}$ $\qquad$ $f_{EC} = \frac{12.00}{EI}$ $\qquad$ $f_{GC} = \frac{10.667}{EI}$ $\qquad$ $f_{IC} = \frac{6.133}{EI}$

$f_{CI} = \frac{6.133}{EI}$ $\qquad$ $f_{EI} = \frac{10.667}{EI}$ $\qquad$ $f_{GI} = \frac{12.00}{EI}$ $\qquad$ $f_{II} = \frac{8.533}{EI}$

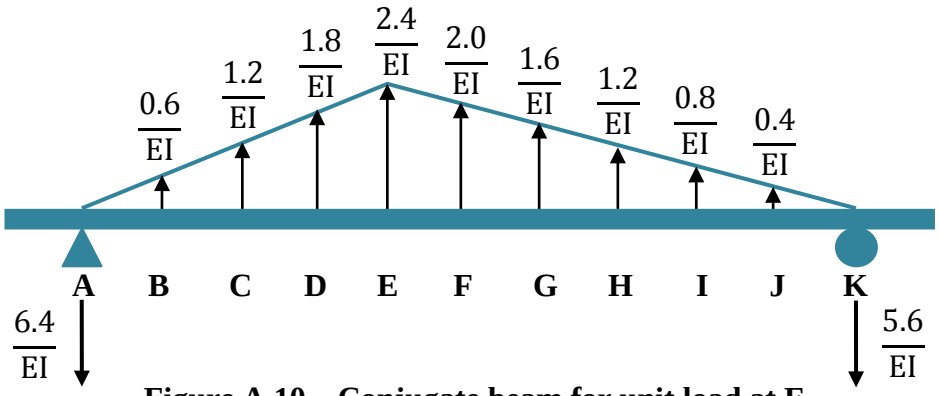

Figure A.10 – Conjugate beam for unit load at E

Deflections at redundants due to applied unit load at E:

By symmetry:

$f_{AE} = 0$ $\qquad$ $f_{KG} = 0$

$f_{CE} = -\frac{1}{EI}\left(6.4 \times 2 - \frac{1}{2} \times 1.2 \times 2 \times \frac{2}{3}\right) = \frac{-12.00}{EI}$ $\qquad$ $f_{IG} = \frac{-12.00}{EI}$

$f_{EE} = -\frac{1}{EI}\left(6.4 \times 4 - \frac{1}{2} \times 2.4 \times 4 \times \frac{4}{3}\right) = \frac{-19.20}{EI}$ $\qquad$ $f_{GG} = \frac{-19.20}{EI}$

$f_{GE} = -\frac{1}{EI}\left(5.6 \times 4 - \frac{1}{2} \times 1.6 \times 4 \times \frac{4}{3}\right) = \frac{-18.133}{EI}$ $\qquad$ $f_{EG} = \frac{-18.133}{EI}$

$f_{IE} = -\frac{1}{EI}\left(5.6 \times 2 - \frac{1}{2} \times 0.8 \times 2 \times \frac{2}{3}\right) = \frac{-10.667}{EI}$ $\qquad$ $f_{CG} = \frac{-10.667}{EI}$

$f_{KE} = 0$ $\qquad$ $f_{AG} = 0$

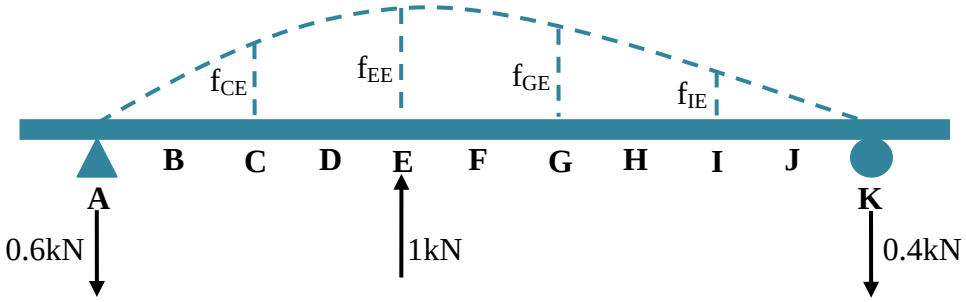

Figure A.11 – Primary beam subjected to redundant E_y

Upward deflections due to the unit values of redundants E_y and G_y (+):

$f_{CC} = \frac{12.00}{EI}$ $\qquad$ $f_{EC} = \frac{19.20}{EI}$ $\qquad$ $f_{GC} = \frac{18.133}{EI}$ $\qquad$ $f_{IC} = \frac{10.667}{EI}$

$f_{CI} = \frac{10.667}{EI}$ $\qquad$ $f_{EI} = \frac{18.133}{EI}$ $\qquad$ $f_{GI} = \frac{19.20}{EI}$ $\qquad$ $f_{II} = \frac{12.00}{EI}$

A.2.4 Solutions for the Redundants

The final step is to solve the compatibility equations for the redundants with the upward deflections. The downward deflections can then be substituted to obtain the influence line ordinates for each redundant.

By substituting upward deflections into the compatibility equations:

$$f_{XC} + \frac{8.533}{EI} C_y + \frac{12.00}{EI} E_y + \frac{10.667}{EI} G_y + \frac{6.133}{EI} I_y = 0$$

$$f_{XE} + \frac{12.00}{EI} C_y + \frac{19.20}{EI} E_y + \frac{18.133}{EI} G_y + \frac{10.667}{EI} I_y = 0$$

$$f_{XG} + \frac{10.667}{EI} C_y + \frac{18.133}{EI} E_y + \frac{19.20}{EI} G_y + \frac{12.00}{EI} I_y = 0$$

$$f_{XI} + \frac{6.133}{EI} C_y + \frac{10.667}{EI} E_y + \frac{12.00}{EI} G_y + \frac{8.533}{EI} I_y = 0$$

Solving for redundants by substitution:

$$C_y = -\frac{EI}{8.533}(10.5276 f_{XC} - 10.1201 f_{XE} + 4.3867 f_{XG} - 1.0840 f_{XI})$$

$$E_y = -\frac{EI}{2.3244}(-2.7562 f_{XC} + 4.0625 f_{XE} - 3.0523 f_{XG} + 1.1948 f_{XI})$$

$$G_y = -\frac{EI}{1.6451}(0.8447 f_{XC} - 2.1596 f_{XE} + 2.8754 f_{XG} - 1.9511 f_{XI})$$

$$I_y = -\frac{EI}{0.8105}(-0.1025 f_{XC} + 0.4163 f_{XE} - 0.9612 f_{XG} + f_{XI})$$

From this point forward only the equation for E_y (Beam 3) will be considered. Additional deflections are determined at 0.25m intervals. Tables A.1 and A.2 present a summary of these and Table A.3 presents the resulting influence line ordinates.

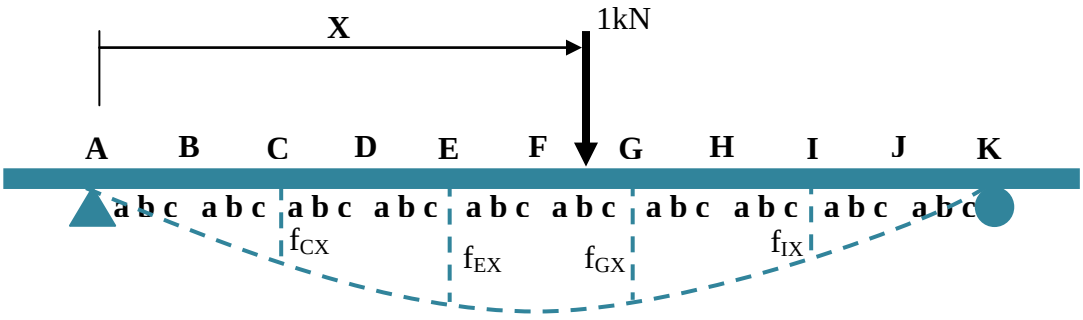

Figure A.12 – Primary beam subject to unit load

Table A.1 – Deflections for applied unit load at Cy (2) and Iy (5)

Location XX		[R]/EI	X (m)	[V]/EI	$[f_{XX}]/EI$
AC	KI	4.8	0	0	0
BC	JI	4.8	1.00	0.80	-4.6667
BaC	IcI	4.8	1.25	1.00	-5.7396
BbC	IbI	4.8	1.50	1.20	-6.7500
BcC	IaI	4.8	1.75	1.40	-7.6854
CC	II	4.8	2.00	1.60	-8.5333
CaC	HcI	3.2	7.75	1.55	-9.2839
CbC	HbI	3.2	7.50	1.50	-9.9375
CcC	HaI	3.2	7.25	1.45	-10.4974
DC	HI	3.2	7.00	1.40	-10.9667
DaC	GcI	3.2	6.75	1.35	-11.3484
DbC	GbI	3.2	6.50	1.30	-11.6458
DcC	GaI	3.2	6.25	1.25	-11.8620
EC	GI	3.2	6.00	1.20	-12.0000
EaC	FcI	3.2	5.75	1.15	-12.0630
EbC	FbI	3.2	5.50	1.10	-12.0542
EcC	FaI	3.2	5.25	1.05	-11.9766
FC	FI	3.2	5.00	1.00	-11.8333
FaC	EcI	3.2	4.75	0.95	-11.6276
FbC	EbI	3.2	4.50	0.90	-11.3625
FcC	EaI	3.2	4.25	0.85	-11.0411
GC	EI	3.2	4.00	0.80	-10.6667
GaC	DcI	3.2	3.75	0.75	-10.2422
GbC	DbI	3.2	3.50	0.70	-9.7708
GcC	DaI	3.2	3.25	0.65	-9.2557
HC	DI	3.2	3.00	0.60	-8.7000
HaC	CcI	3.2	2.75	0.55	-8.1068
HbC	CbI	3.2	2.50	0.50	-7.4792
HcC	CaI	3.2	2.25	0.45	-6.8203
IC	CI	3.2	2.00	0.40	-6.1333
IaC	BcI	3.2	1.75	0.35	-5.4214
IbC	BbI	3.2	1.50	0.30	-4.6875
IcC	BaI	3.2	1.25	0.25	-3.9349
JC	BI	3.2	1.00	0.20	-3.1667
KC	AI	3.2	0	0	0

R = support reaction from conjugate beam
X = distance from end support to unit load
V = shear at location of unit load from conjugate beam
(Refer to Figure A.8)

Table A.2 – Deflections for applied unit load at E_y (3) and G_y (4)

Location XX		[R]/EI	X (m)	[V]/EI	$[f_{XX}]/EI$
AE	KG	6.4	0	0	0
BE	JG	6.4	1.00	0.60	-6.3000
BaE	IcG	6.4	1.25	0.75	-7.8047
BbE	IbG	6.4	1.50	0.90	-9.2625
BcE	IaG	6.4	1.75	1.05	-10.6641
CE	IG	6.4	2.00	1.20	-12.0000
CaE	HcG	6.4	2.25	1.35	-13.2609
CbE	HbG	6.4	2.50	1.50	-14.4375
CcE	HaG	6.4	2.75	1.65	-15.5203
DE	HG	6.4	3.00	1.80	-16.5000
DaE	GcG	6.4	3.25	1.95	-17.3672
DbE	GbG	6.4	3.50	2.10	-18.1125
DcE	GaG	6.4	3.75	2.25	-18.7266
EE	GG	6.4	4.00	2.40	-19.2000
EaE	FcG	5.6	5.75	2.30	-19.5260
EbE	FbG	5.6	5.50	2.20	-19.7083
EcE	FaG	5.6	5.25	2.10	-19.7531
FE	FG	5.6	5.00	2.00	-19.6667
FaE	EcG	5.6	4.75	1.90	-19.4552
FbE	EbG	5.6	4.50	1.80	-19.1250
FcE	EaG	5.6	4.25	1.70	-18.6823
GE	EG	5.6	4.00	1.60	-18.1333
GaE	DcG	5.6	3.75	1.50	-17.4844
GbE	DbG	5.6	3.50	1.40	-16.7417
GcE	DaG	5.6	3.25	1.30	-15.9115
HE	DG	5.6	3.00	1.20	-15.0000
HaE	CcG	5.6	2.75	1.10	-14.0135
HbE	CbG	5.6	2.50	1.00	-12.9583
HcE	CaG	5.6	2.25	0.90	-11.8406
IE	CG	5.6	2.00	0.80	-10.6667
IaE	BcG	5.6	1.75	0.70	-9.4427
IbE	BbG	5.6	1.50	0.60	-8.1750
IcE	BaG	5.6	1.25	0.50	-6.8698
JE	BG	5.6	1.00	0.40	-5.5333
KE	AG	5.6	0	0	0

R = support reaction from conjugate beam
X = distance from end support to unit load
V = shear at location of unit load from conjugate beam (Figure A.10)
(Refer to Figure A.10)

$$E_y = -\frac{EI}{2.3244}(-2.7562f_{XC} + 4.0625f_{XE} - 3.0523f_{XG} + 1.1948f_{XI})$$

(EI cancels out)

Table A.3 – Influence line ordinates for E_y (3)

Location	X (m)	$[f_{XC}]/EI$	$[f_{XE}]/EI$	$[f_{XG}]/EI$	$[f_{XI}]/EI$	E_y
A	0.00	0	0	0	0	0
B	1.00	-4.6667	-6.3000	-5.5333	-3.1667	-0.1611
Ba	1.25	-5.7396	-7.8047	-6.8698	-3.9349	-0.1635
Bb	1.50	-6.7500	-9.2625	-8.1750	-4.6875	-0.1408
Bc	1.75	-7.6854	-10.6641	-9.4427	-5.4214	-0.0879
C	2.00	-8.5333	-12.0000	-10.6667	-6.1333	0.0003
Ca	2.25	-9.2839	-13.2609	-11.8406	-6.8203	0.1257
Cb	2.50	-9.9375	-14.4375	-12.9583	-7.4792	0.2779
Cc	2.75	-10.4974	-15.5203	-14.0135	-8.1068	0.4435
D	3.00	-10.9667	-16.5000	-15.0000	-8.7000	0.6088
Da	3.25	-11.3484	-17.3672	-15.9115	-9.2557	0.7606
Db	3.50	-11.6458	-18.1125	-16.7417	-9.7708	0.8851
Dc	3.75	-11.8620	-18.7266	-17.4844	-10.2422	0.9691
E	4.00	-12.0000	-19.2000	-18.1333	-10.6667	1.0000
Ea	4.25	-12.0630	-19.5260	-18.6823	-11.0411	0.9656
Eb	4.50	-12.0542	-19.7083	-19.1250	-11.3625	0.8785
Ec	4.75	-11.9766	-19.7531	-19.4552	-11.6276	0.7515
F	5.00	-11.8333	-19.6667	-19.6667	-11.8333	0.5983
Fa	5.25	-11.6276	-19.4552	-19.7531	-11.9766	0.4328
Fb	5.50	-11.3625	-19.1250	-19.7083	-12.0542	0.2687
Fc	5.75	-11.0411	-18.6823	-19.5260	-12.0630	0.1199
G	6.00	-10.6667	-18.1333	-19.2000	-12.0000	0.0003
Ga	6.25	-10.2422	-17.4844	-18.7266	-11.8620	-0.0799
Gb	6.50	-9.7708	-16.7417	-18.1125	-11.6458	-0.1238
Gc	6.75	-9.2557	-15.9115	-17.3672	-11.3484	-0.1381
H	7.00	-8.7000	-15.0000	-16.5000	-10.9667	-0.1297
Ha	7.25	-8.1068	-14.0135	-15.5203	-10.4974	-0.1051
Hb	7.50	-7.4792	-12.9583	-14.4375	-9.9375	-0.0710
Hc	7.75	-6.8203	-11.8406	-13.2609	-9.2839	-0.0343
I	8.00	-6.1333	-10.6667	-12.0000	-8.5333	-0.0014
Ia	8.25	-5.4214	-9.4427	-10.6641	-7.6854	0.0221
Ib	8.50	-4.6875	-8.1750	-9.2625	-6.7500	0.0362
Ic	8.75	-3.9349	-6.8698	-7.8047	-5.7396	0.0424
J	9.00	-3.1667	-5.5333	-6.3000	-4.6667	0.0419
K	10.00	0	0	0	0	0

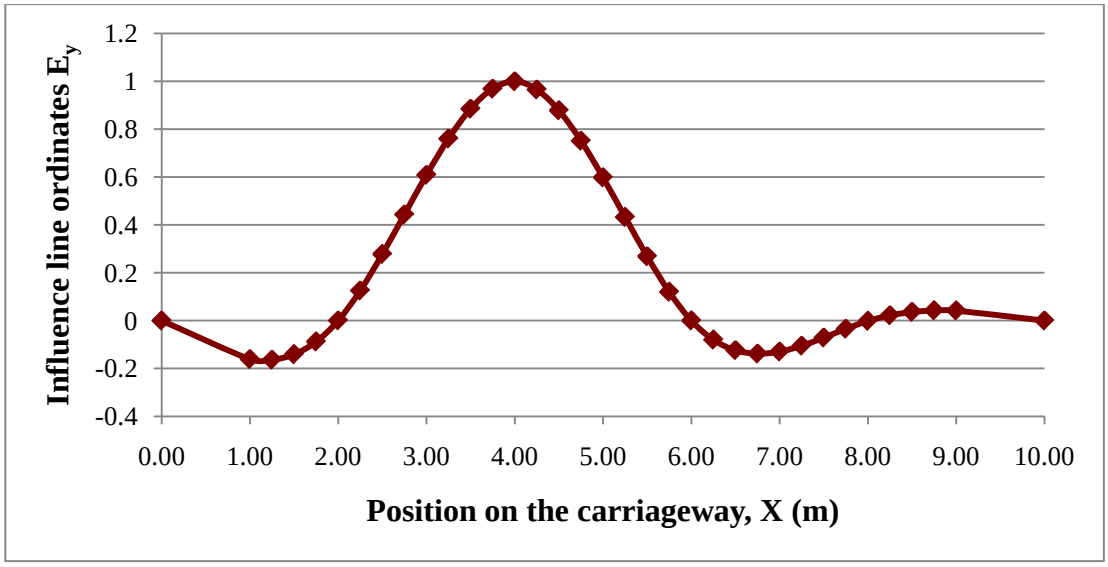

Figure A.13 – Influence line for reaction at Beam 3 (E_y)

A.3 POSITION OF THE NOTIONAL LANES AND WHEELS

Now that the transverse influence line is determined, the most adverse position of the notional lanes and respective wheel loads around Beam 3 is found. The following applies to both design examples. Application of the UDL for each load model is considered under Section A.4 and Load Model 4 is not included here, as it does not include wheel loads.

A.3.1 Application of Wheel Loads for Load Model 1

From Section A.1.1: Wheel loads $Q_{1w} = 150$ kN

$Q_{2w} = 100$ kN

Wheel spacing $s_w = 2.0$ m

To find the most adverse position, the series of axles illustrated in Figure A.14 is placed every 0.25m along the width of the carriageway and the resultant axle load to Beam 3 (E_y) is calculated with the influence line ordinates. This process is then repeated after switching the positions of Lane No. 1 and Lane No. 2. From these calculations, the maximum loading is determined.

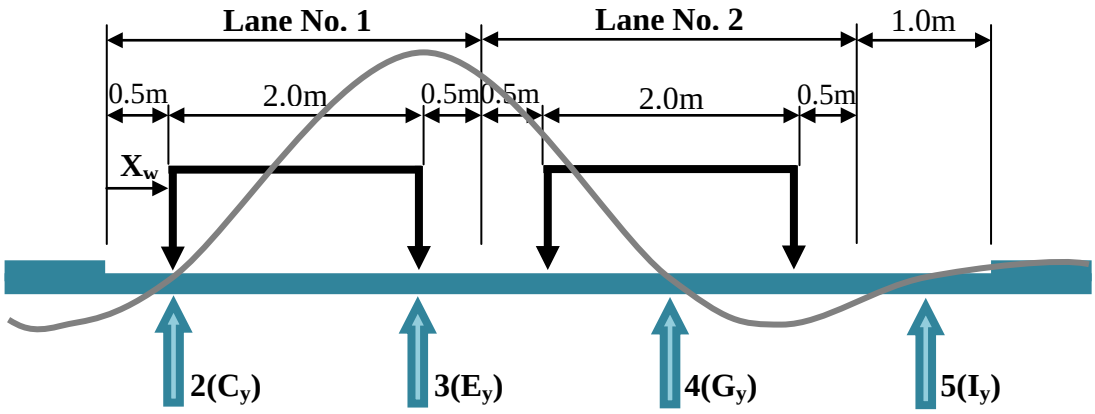

Figure A.14 – Lane placement for Load Model 1

Figures A.15 summarizes the resultant axle loads for each position.

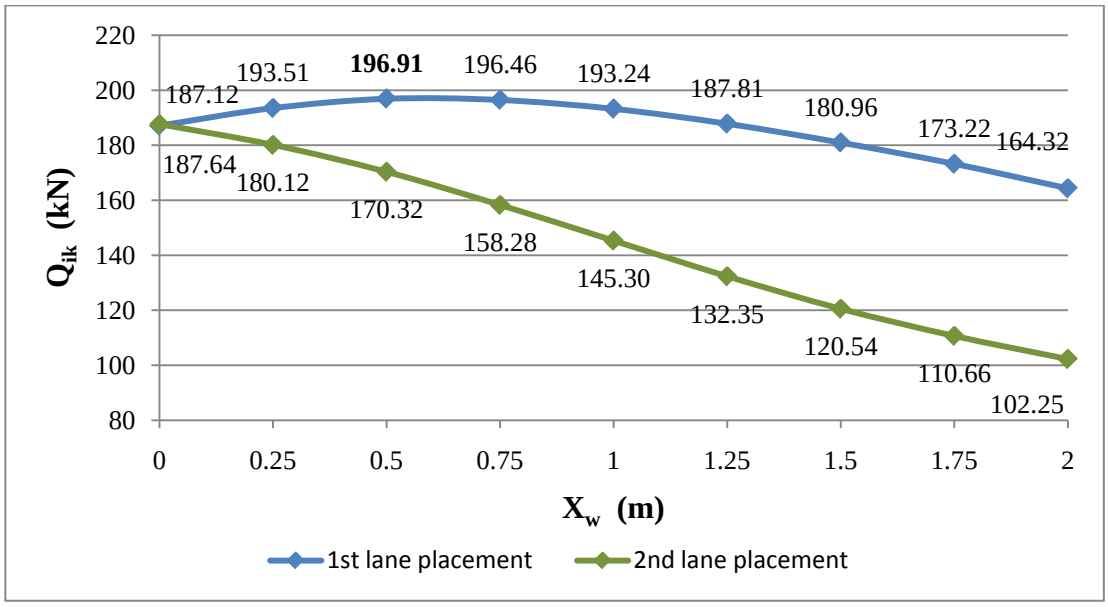

Figure A.15 – Resultant axle loads for LM1 - Q_{ik}

The results show that the maximum affect occurs with the first lane placement when the wheel loads from Lane No. 1 are positioned directly over Beams 2 (C_y) and 3 (E_y). Table A.4 presents the calculations for the resultant axle load at this location. In the table, X represents the position on the carriageway.

Table A.4 – Resultant axle loading on Beam 3 for LM1 TS

Beam	X (m)	E_y	Q_{iw} (kN)	P_{LM1} (kN)
BM 1 (A_y)	0.00	0.0000		
	1.00	-0.1611		
	1.25	-0.1635		
	1.50	-0.1408		
	1.75	-0.0879		
BM 2 (C_y)	2.00	0.0003	150	0.0430
	2.25	0.1257		
	2.50	0.2779		
	2.75	0.4435		
	3.00	0.6088		
	3.25	0.7606		
	3.50	0.8851		
	3.75	0.9691		
BM 3 (E_y)	4.00	1.0000	150	150.0000
	4.25	0.9656		
	4.50	0.8785		
	4.75	0.7515		
	5.00	0.5983	100	59.8305
	5.25	0.4328		
	5.50	0.2687		
	5.75	0.1199		
BM 4 (G_y)	6.00	0.0003		
	6.25	-0.0799		
	6.50	-0.1238		
	6.75	-0.1381		
	7.00	-0.1297	100	-12.9675
	7.25	-0.1051		
	7.50	-0.0710		
	7.75	-0.0343		
BM 5 (I_y)	8.00	-0.0014		
	8.25	0.0221		
	8.50	0.0362		
	8.75	0.0424		
	9.00	0.0419		
BM 6 (K_y)	10.00	0.0000		

$$\Sigma P_{TS} = 197 \text{ kN}$$

A.3.2 Application of Wheel Loads for Load Model 2

From Section A.1.2: Wheel loads $Q_{aw} = 200$ kN

Wheel spacing $s_w = 2.0$ m

Similar to Load Model 1, the single axle is applied every 0.25m along the width of the carriageway and the resultant axle load on Beam 3 (E_y) is calculated. Figure A.16 provides a summary of the resultant axle loadings.

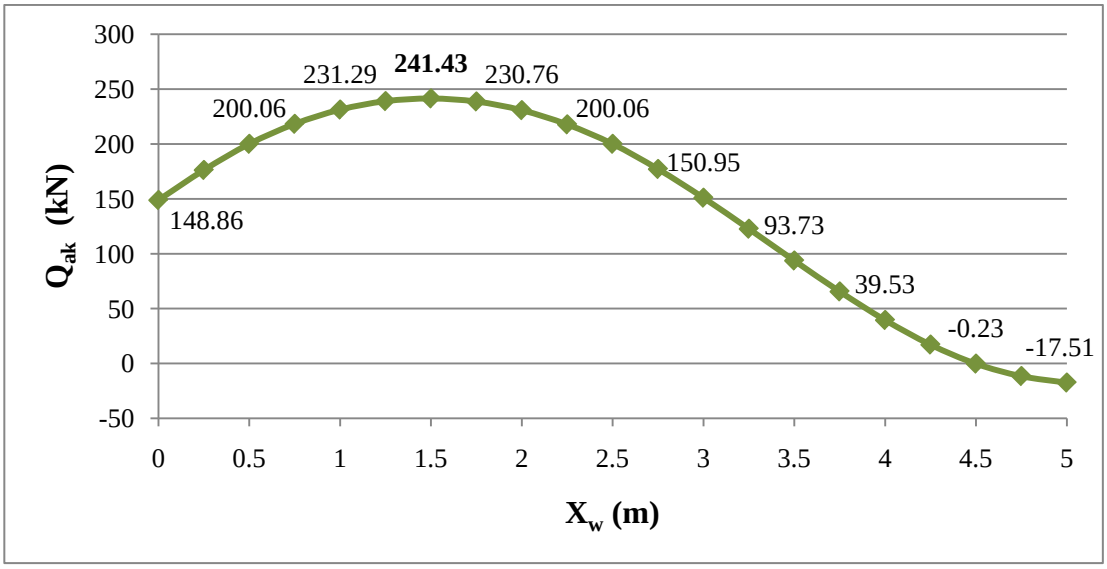

Figure A.16 – Resultant axle loads for LM2 - Q_{ak}

The results show that the maximum effect occurs when the first wheel load is positioned 1.5m from the left edge of the carriageway, straddling Beam 3, as shown in Figure A.17. Full calculations for this position are shown in Table A.5.

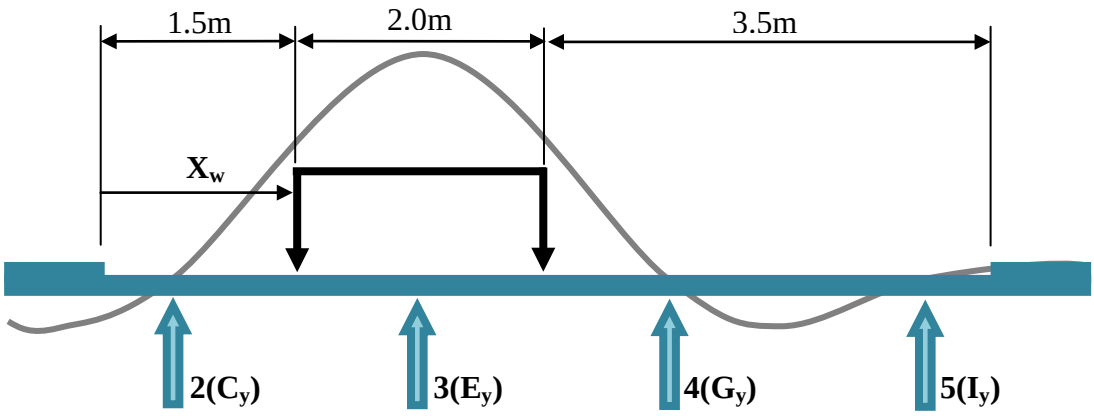

Figure A.17 – Load placement for Load Model 2

Table A.5 – Resultant axle loading on Beam 3 for LM2

Beam	X (m)	E_y	Q_{aw} (kN)	P_{LM2} (kN)
BM 1 (A_y)	0.00	0.0000		
	1.00	-0.1611		
	1.25	-0.1635		
	1.50	-0.1408		
	1.75	-0.0879		
BM 2 (C_y)	2.00	0.0003		
	2.25	0.1257		
	2.50	0.2779		
	2.75	0.4435		
	3.00	0.6088	200	121.7676
	3.25	0.7606		
	3.50	0.8851		
	3.75	0.9691		
BM 3 (E_y)	4.00	1.0000		
	4.25	0.9656		
	4.50	0.8785		
	4.75	0.7515		
	5.00	0.5983	200	119.6610
	5.25	0.4328		
	5.50	0.2687		
	5.75	0.1199		
BM 4 (G_y)	6.00	0.0003		
	6.25	-0.0799		
	6.50	-0.1238		
	6.75	-0.1381		
	7.00	-0.1297		
	7.25	-0.1051		
	7.50	-0.0710		
	7.75	-0.0343		
BM 5 (I_y)	8.00	-0.0014		
	8.25	0.0221		
	8.50	0.0362		
	8.75	0.0424		
	9.00	0.0419		
BM 6 (K_y)	10.00	0.0000		

$$\Sigma P_{LM2} = 242 \text{ kN}$$

A.3.3 Application of Wheel Loads for Load Model 3

From Section A.1.3: Wheel loads $Q_{aw} = 60$ kN

$Q_{bw} = 99$ kN

$Q_{cw} = 92.4$ kN

Wheel spacing $s_w = 2.65$ m

Through the same procedure as that described in Section A.3.2, the position of the wheel loads with the most adverse effect has been determined. Figure A.18 through summarizes the resultant axle loadings on Beam 3 (E_y) for each axle.

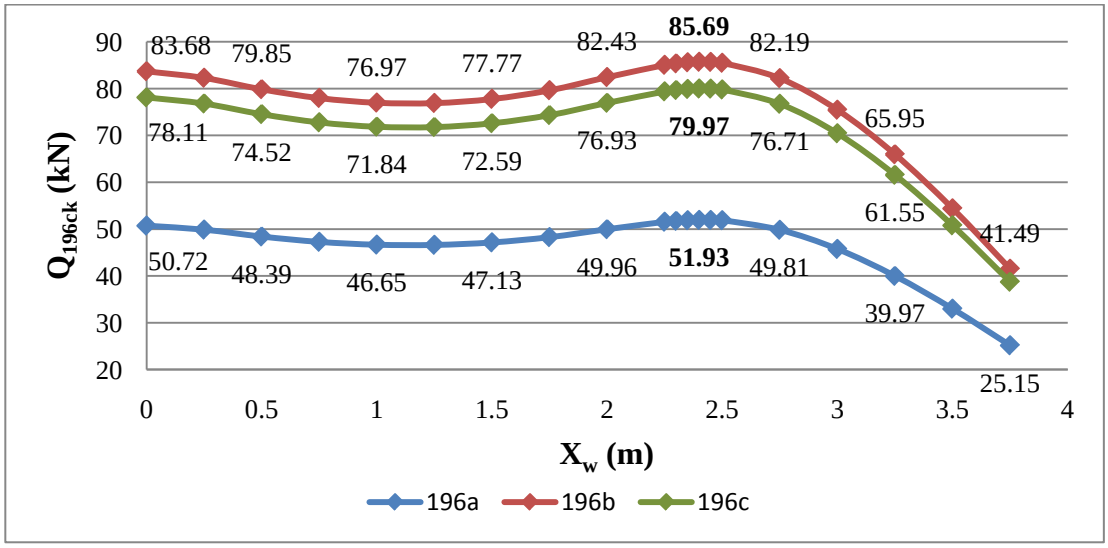

Figure A.18 – Resultant axle loads for LM3 – Q_{196ak}, Q_{196bk}, and Q_{196ck}

The results show that the maximum affect occurs when the first wheel load is positioned 2.40m from the edge of the carriageway (or 0.10m to the left of Beam 3) as shown in Figure A.19.

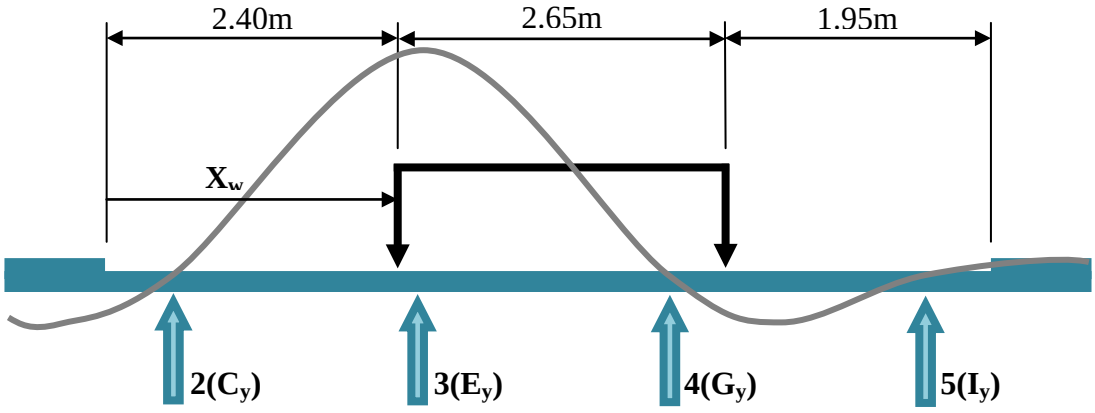

Figure A.19 – Load placement for Load Model 3

Due to the different wheel spacing for this load model, additional influence line ordinates at 0.05m intervals were calculated and added in the model. For simplicity, not all of the ordinance points are included in Table A.6.

Table A.6 – Resultant axle loadings on Beam 3 for LM3

Beam	X (m)	E_y	Q_{aw} (kN)	P_{196a} (kN)	Q_{bw} (kN)	P_{196b} (kN)	Q_{cw} (kN)	P_{196c} (kN)
2 (C_y)	2.00	0.0003						
	2.25	0.1257						
	2.50	0.2779						
	2.75	0.4435						
	3.00	0.6088						
	3.25	0.7606						
	3.50	0.8851						
	3.75	0.9691						
	3.80	0.9798						
	3.85	0.9882						
	3.90	0.9943	60	59.6581	99	98.4358	92.4	91.8734
	3.95	0.9979						
3 (E_y)	4.00	1.0000						
	4.25	0.9656						
	4.50	0.8785						
	4.75	0.7515						
	5.00	0.5983						
	5.25	0.4328						
	5.50	0.2687						
	5.75	0.1199						
4 (G_y)	6.00	0.0003						
	6.25	-0.0799						
	6.50	-0.1238						
	6.55	-0.1288	60	-7.7276	99	-12.7505	92.4	-11.9005
	6.60	-0.1327						
	6.65	-0.1355						
	6.70	-0.1373						
	6.75	-0.1381						
	7.00	-0.1297						
	7.25	-0.1051						
	7.50	-0.0710						
	7.75	-0.0343						
5 (I_y)	8.00	-0.0014						

$$\Sigma P_{196a} = 52 \text{ kN} \quad \Sigma P_{196b} = 86 \text{ kN} \quad \Sigma P_{196c} = 80 \text{ kN}$$

A.4 APPLICATION OF THE LOADS TO THE BEAM

Separate calculations are required for each design example. For all calculations on the continuous span design example, the centre support is defined as support B and the end supports are defined as supports A and C.

Now that the load models are defined and the resultant axle loads determined, the maximum moment acting on the beam due to traffic actions is calculated. Table NA.3 of the national annex to BS EN 1991-2 defines groups of traffic loads that should be applied to the beam simultaneously for calculations of these moments. Table A.7 presents the four traffic loads that are considered here.

Table A.7 – Groups of traffic loads (NA to BS EN 1991-2 Table NA.3)

	Carriageway			
	Vertical forces			
Groups of Loads	LM1	LM2	LM3	LM4
gr1a	Characteristic			
gr1b		Characteristic		
gr4				Characteristic
gr5	Frequent		Characteristic	

In addition to the characteristic groups of traffic loads, Table 4.4b of BS EN 1991-2 also defines a series of load groups for the frequent combination of actions. Table A.8 presents the two load groups that are considered here. For the frequent values, ψ_1 factors defined in the national annex to BS EN 1990 are applied.

Table A.8 – Groups of traffic loads: frequent (BS EN 1991-2 Table 4.4b)

	Carriageway	
	Vertical forces	
Groups of Loads	LM1	LM2
gr1a	Frequent	
gr1b		Frequent

For Load Group gr5 in Table A.7, LM3 is applied in combination with the frequent value of LM1. In accordance with Clause NA.2.16.4 of the NA to BS EN 1991-2, the frequent values of LM1 will be applied in front and in back of the SV196 vehicle as shown in Figure A.20.

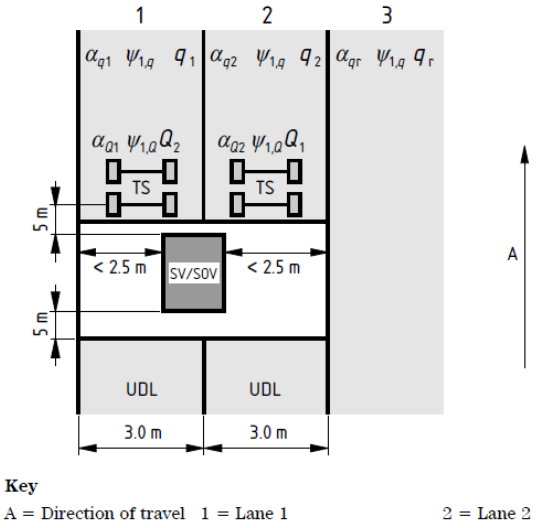

Key
A = Direction of travel 1 = Lane 1 2 = Lane 2

Figure A.20 – Application of Load Group gr5

(NA to BS EN 1991-2 Figure NA.5)

A.4.1 Maximum Moment Due to Load Group gr1a (Load Model 1)

For Load Model 1: $\Sigma P_{TS} = 197 \text{ kN}$

$s_a = 1.2 \text{ m}$

$w_{UDL} = 11.0 \text{ kN/m}$

For the Single span: $L_s = 25.0 \text{ m}$

To determine the overall maximum moment, the axles for the tandem system are placed at 2.5m intervals with the uniformly distributed load applied across the span.

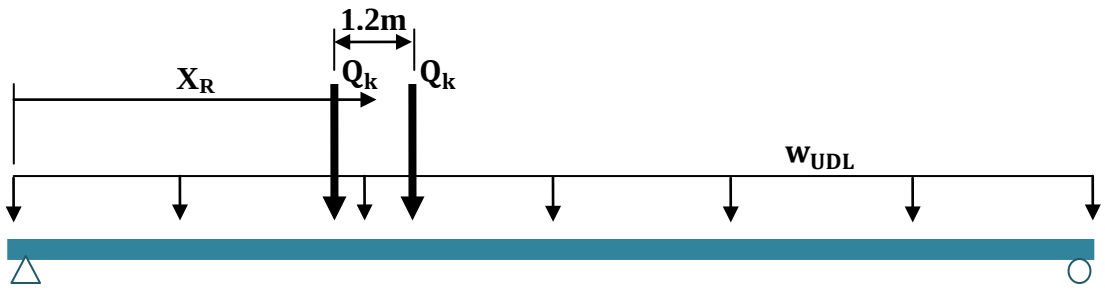

Figure A.21 – Application of Load Group gr1a

X_R represents the distance from the first support to the resultant of the two axles.

The maximum moments for each location are calculated via shear and moment diagrams. Figure A.22 presents a summary of the results.

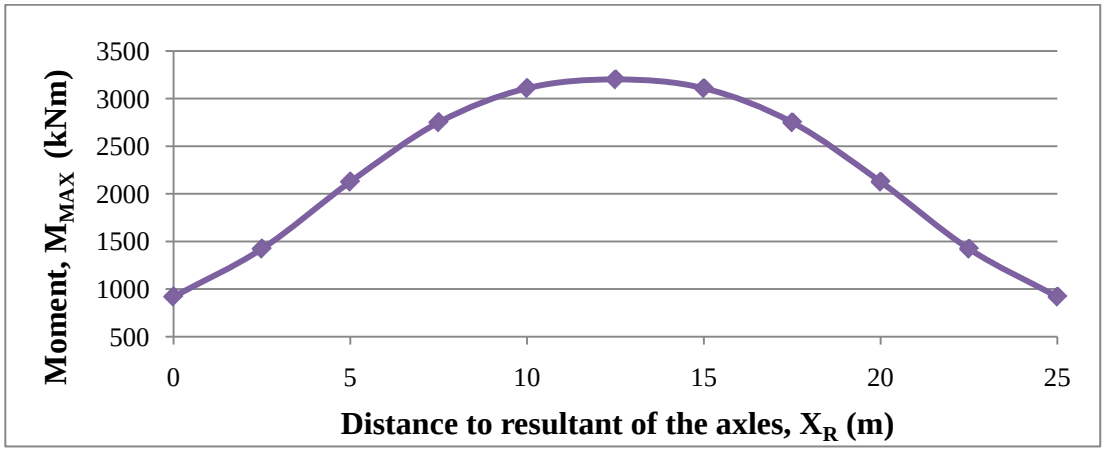

Figure A.22 – Maximum moments due to Load Group gr1a (LM1)

From these results it is determined that the greatest maximum moment will occur when the axles are applied around midspan. Further calculations at 0.1m intervals are completed at this location for more accurate results, as shown in Figure A.23.

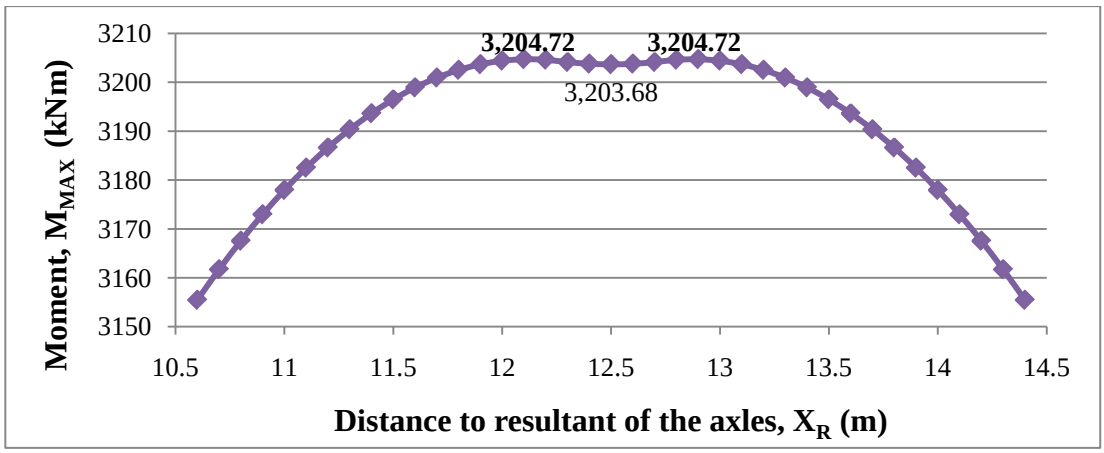

Figure A.23 – Maximum moments due to Load Group gr1a (LM1)

From Figure A.23 it is determined that the greatest maximum moment occurs when the resultant of the axles, X_R, is 12.1m or 12.9m from the support. When comparing the results of the maximum moment at these locations to the maximum moment for X_R equal to 12.5m (midspan), an error of only 0.03% is found. With such a small error, future applications of LM1 on a single span may assume the maximum moment will occur with the tandem system applied at the centre of the beam.

The calculations for the greatest of the maximum moments are provided here to show the procedure that has been applied. The support reactions for the shear diagram are determined by equilibrium.

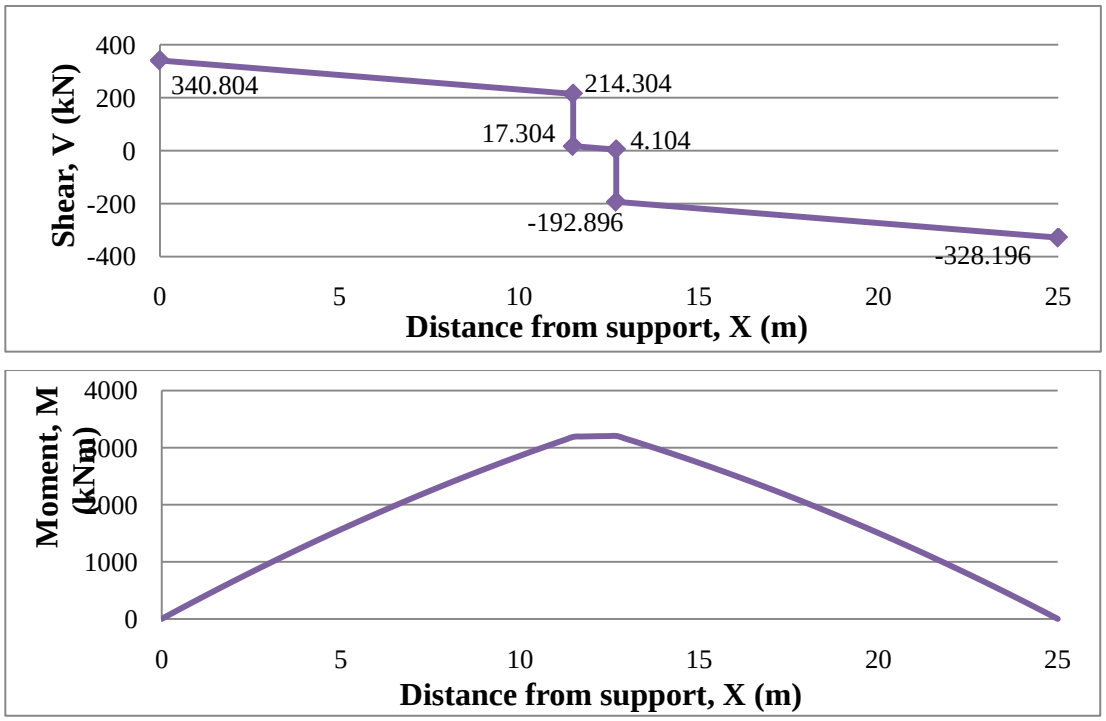

Figure A.24 – Shear and moment diagram for axles applied at X_R = 12.1m

The maximum moment is calculated based on the area under the shear diagram. The actual peak in the moment diagram occurs at 12.5m (midspan).

$$M_{MAX} = 0.5 \times (328.196 + 192.896) \times (25.0 - 11.5 - 1.2) = 3204.72 \text{ kN}$$

For design assume: $M_{gr1a} = M_{LM1} = 3205 \text{ kN}$

This moment is applied for the design of the prestressed beam in Appendix B. In addition to determining the overall maximum moment, the maximum moment occurring at each section must be found for design purposes. To calculate these moments, an envelope of moments for the beam is developed, by combining onto one graph all the moment diagrams due to the application of the axles at each location on the beam. Ideally, a moment diagram should be included for the application of the axles at every point along the beam. However, due to time constraints the envelope is created based on a series of 2.5m intervals. To provide an

estimate for the missing moment diagrams, a trend line is applied to the maximum points in the envelope. At each section, the maximum of the trend line results and the results from the moment diagrams in the envelope is assumed. Figure A.25 presents the envelope of moments and corresponding trend line. Table A.9 presents the moments determined from the envelope and trend line as well as the final moments for design. Results are symmetric about midspan (12.5m).

.

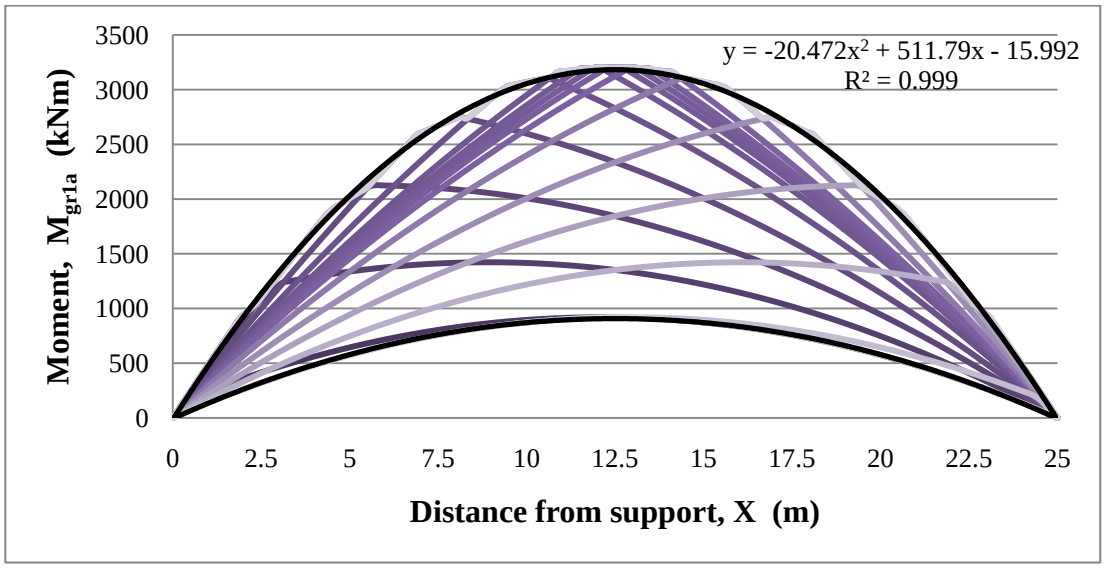

Figure A.25 – Envelope of moments due to gr1a (LM1) on the single span

Table A.9 – Summary of M_{gr1a} for the single span

Position (m)	M_{trend} (kNm)	M_{MAX} (kNm)	$M_{LM1} = M_{gr1a}$ (kNm)
0	-15.992	0	0
2.5	1135.533	1097.375	1136
5	2031.158	2007.745	2031
7.5	2670.883	2672.175	2672
10	3054.708	3070.745	3071
12.5	3182.633	3203.675	3205

For the continuous spans: $L_c = 40.0$ m

For continuous spans, the overall minimum negative moment which occur around the supports must be determined as well as the greatest maximum positive moment. Preliminary calculations found that the greatest maximum positive moment occurs when all the loading is applied to only one span, and the overall minimum negative moment occurs when the loading is applied to both spans, illustrated in Figure A.26.

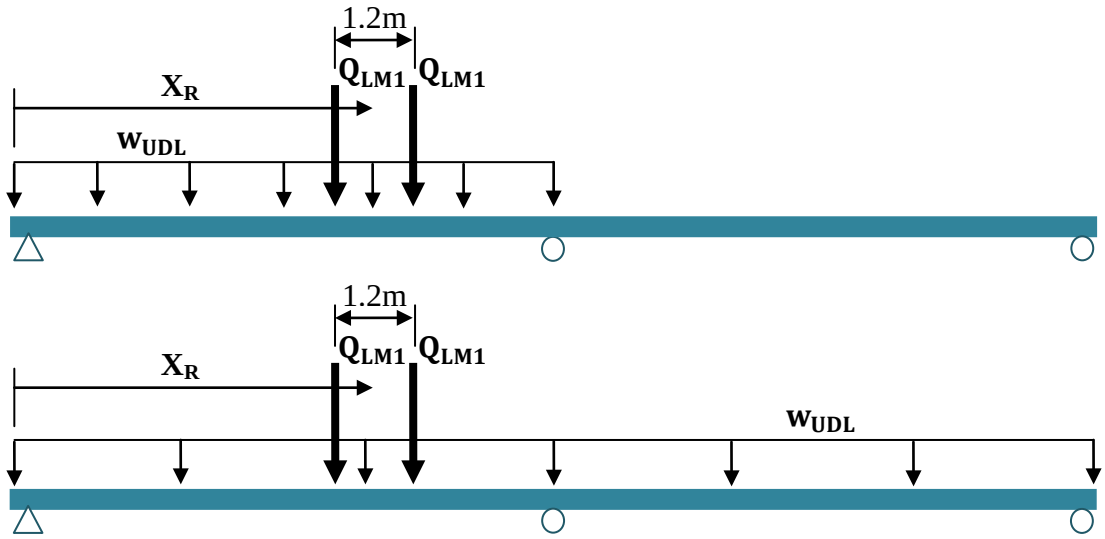

Figure A.26 – Application of Load Group gr1a (LM1) for the maximum positive moment and minimum negative moment on the continuous spans

X_R represents the distance from the first support to the resultant of the two axles.

First the maximum positive moment is considered. Figure A.27 presents a summary of the maximum moments calculated for each 5.0m interval, with the loading applied in only one span. These moments are calculated based on the shear and moment diagrams for the beam. It is initially determined that the overall maximum moment will occur between 15 and 20 metres. Further calculations are completed at this location for more accurate results, as shown. The results are symmetric about the centre support.

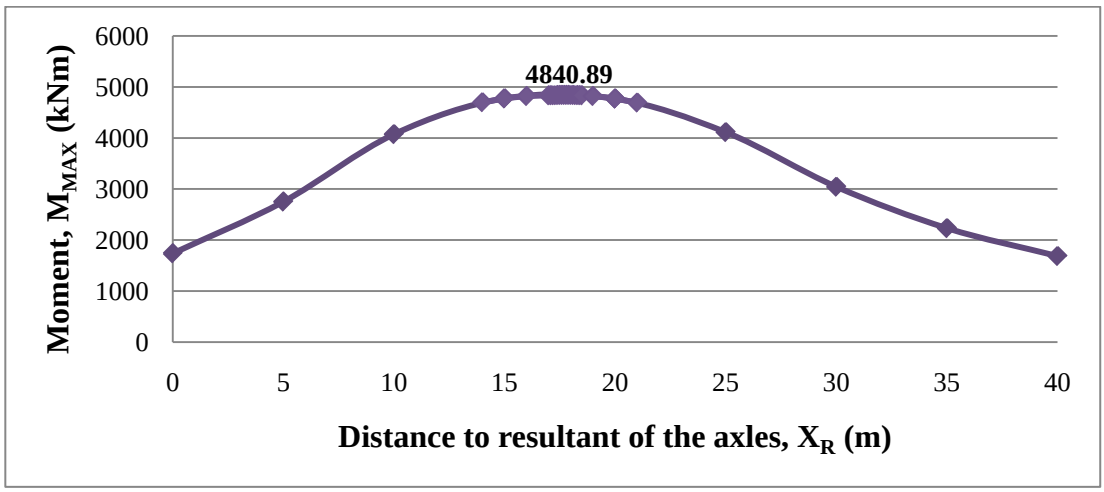

Figure A.27 – Maximum moments due to Load Group gr1a (LM1)

From Figure A.27, it is determined that the maximum moment occurs when the resultant of the axles is at 17.8m (or 62.2m) from the first support. The calculations for the resultant axle at 17.8m are provided here to show the procedure. Since the structure is indeterminate, the support reactions that are required for the development of the shear diagram are calculated by the moment distribution method. This method is illustrated in Table A.10 with explanation following.

Table A.10 – Moment distribution method for LM1 at X_R = 17.8m

X_R = 17.8 m				
w_{UDL} = 11 kN/m		L = 40 m		
Q_{LM1} = 197 kN		s_a = 1.2 m		
a_1 = 17.2 m		b_1 = 22.8 m		
a_2 = 18.4 m		b_2 = 21.6 m		
Support	**A**	**B**	**B**	**C**
DF	1	0.5	0.5	1
FEM	3624.55	-3197.56	0	0
Balance	-3624.55	1598.782	1598.782	0
Carry	799.391	-1812.27	0	799.391
Balance	-799.391	906.137	906.137	-799.391
Carry	453.069	-399.695	-399.695	453.069
Balance	-453.069	399.696	399.696	-453.069
Moment at the supports (kNm):	0	-2504.92	2504.919	0
Shear at the supports (kN):	376.047	457.953	62.623	-62.623

In Table A.10, the Distribution Factor (DF) at centre support B is determined by dividing the relative stiffness of the member by the sum of relative stiffness' for all members at the joint, as shown in the expression below.

$$DF_B = \frac{I/L}{I/L + I/L} = 0.50$$

The Fixed End Moments (FEM) are calculated for the distributed load and axles with the following equations which can be found in any structural analysis book. In these equations, a_i represents the distance from the first support to the axle, and b_i represents the distance from the axle to the second support.

$$FEM_A = \frac{w_{UDL}L_c^2}{12} + \frac{Pa_1b_1^2}{L_c^2} + \frac{Pa_2b_2^2}{L_c^2}$$

$$FEM_B = \frac{w_{UDL}L_c^2}{12} + \frac{Pa_1^2b_1}{L_c^2} + \frac{Pa_2^2b_2}{L_c^2}$$

The moments are then balanced by first distributing the negative of the unbalanced moments to the members connected at the joint, and carrying half of each distributed moment to the opposite end of the member. This process is repeated until the carryover and balance moments at each joint are equal, at which point the final moments for each end are determined by summing the FEM, distributed, and carryover moments. The shear forces at each member end are then determined by equilibrium of the members and the support reactions are calculated by equilibrium of the joints. From the shear at supports determined in Table A.8, the following support reactions are determined.

$$A_y = 376.047\ \text{kN} \qquad B_y = 520.576\ \text{kN} \qquad C_y = -62.623\ \text{kN}$$

With these reactions the shear and moment diagrams in Figure A.28 are developed.

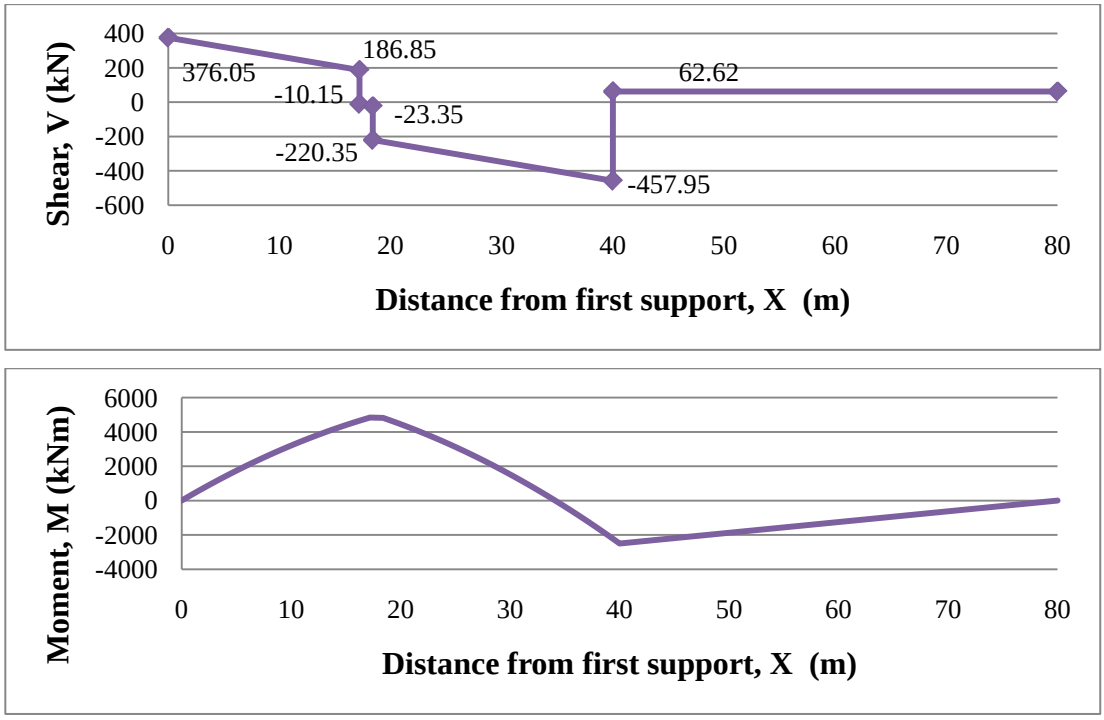

Figure A.28 – Shear and moment diagrams for the overall maximum moment

The maximum moment is then calculated based on the area under the shear diagram. The peak in the moment diagram occurs 17.2m from the first support.

$$M_{MAX} = 0.5 \times (376.05 + 186.85) \times (17.2) = 4840.9 \text{ kN}$$

For design assume: $M_{pgr1a} = M_{pLM1} = 4841 \text{ kN}$

This moment will be applied for the design of the prestressed beam in Appendix C.

The same procedure is used for calculation of the overall minimum negative moment. In calculating these moments, the uniformly distributed load is applied to both spans. Figure A.29 presents the summary of minimum moments calculated. Initially the moments were calculated at 5.0m intervals and from the results, it was determined that that the overall minimum moment occurs when the axles are placed between 20m and 25m. Further calculations were completed at this location for more accurate results as shown. Again, the results are symmetric about the centre support.

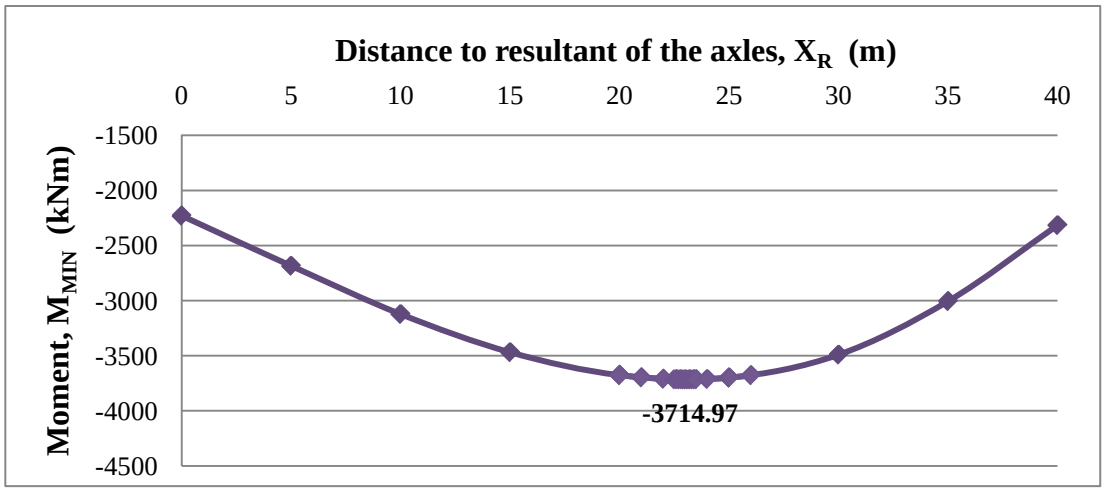

Figure A.29 – Minimum moments due to Load Group gr1a (LM1)

From Figure A.29, it is determined that the minimum moment occurs when the resultant of the axles is 23.1m (or 56.9m) from the first support. The calculations for the minimum moment follow the same procedure as that for the positive moments, illustrated in Table A.11 and Figure A.30.

Table A.11 – Moment distribution method for LM1 at X_R = 23.1m

X_R = 23.1 m	
w_{UDL} = 11 kN/m	L = 40 m
Q_{LM1} = 197 kN	s_a = 1.2 m
a_1 = 17.2 m	b_1 = 22.8 m
a_2 = 18.4 m	b_2 = 21.6 m

Support	A	B	B	C
DF	1	0.5	0.5	1
FEM	3090.375	-3684.75	1466.667	-1466.667
Balance	-3090.375	1109.044	1109.044	1466.667
Carry	554.522	-1545.190	733.333	554.522
Balance	-554.522	405.927	405.927	-554.522
Carry	202.964	-277.261	-277.261	202.964
Balance	-202.964	277.261	277.261	-202.964
Moment at the supports (kNm):	0	-3714.971	3714.971	0
Shear at the supports (kN):	293.591	540.409	312.874	127.126

From the shear at supports:

$$A_y = 293.591\ \text{kN} \qquad B_y = 853.284\ \text{kN} \qquad C_y = 127.126\ \text{kN}$$

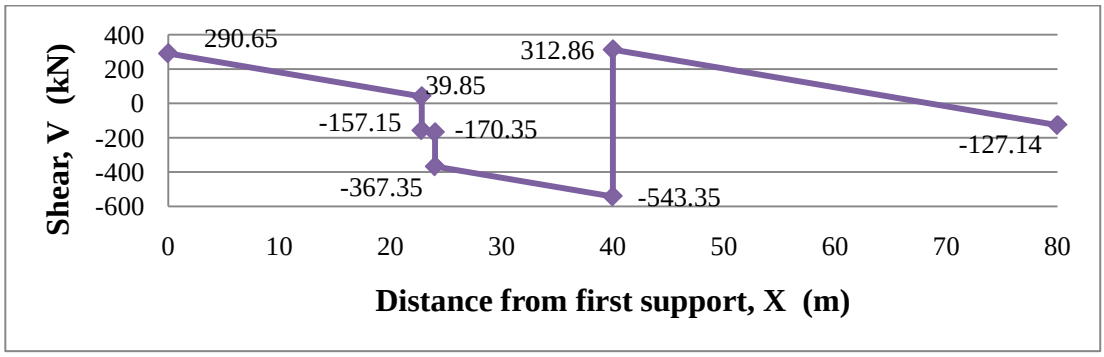

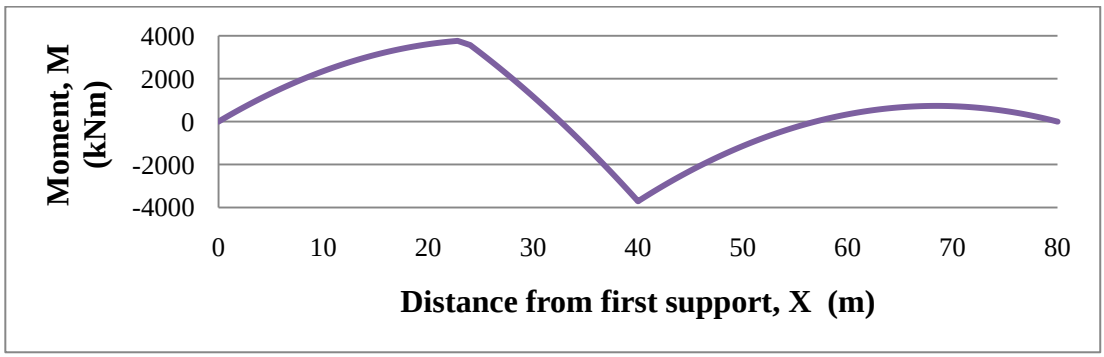

Figure A.30 – Shear and moment diagrams for the overall minimum moment

The minimum moment is then calculated based on the area under the shear diagram. The lowest point in the moment diagram occurs at the centre support.

$$M_{MIN} = -0.5 \times (312.86 - 127.14) \times (40) = -3714.97 \text{ kN}$$

For design assume: $M_{ngr1a} = M_{nLM1} = -3715 \text{ kN}$

This moment will be applied for the design of the prestressed beam in Appendix C. As with the single span, an envelope of moments is created so the moments at a number of sections along the beam can be found. For this envelope, the moment diagrams are created at 5.0m intervals. Figure A.31 presents the envelope of moments for both the minimum and maximum moments and the corresponding trend lines. For accuracy, the trend lines are created separately for each span. Table A.12 presents the moments determined from the envelope and trend line as well as the final moments for design. All results are symmetric around the centre support.

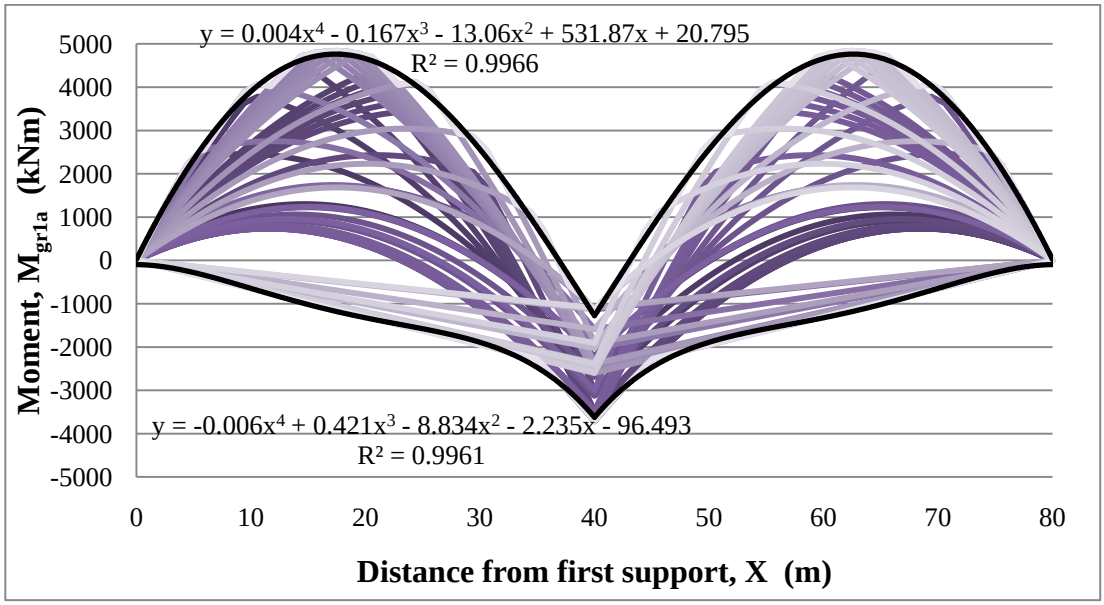

Figure A.31 – Envelope of moments due to Load Group gr1a (LM1) on the continuous spans

Table A.12 – Summary of M_{pgr1a} and M_{ngr1a} for the continuous spans

Position (m)	M_{ptrend} (kNm)	M_{MAX} (kNm)	M_{pgr1a} (kNm)	M_{ntrend} (kNm)	M_{MIN} (kNm)	M_{ngr1a} (kNm)
0	20.795	0	0	-96.493	0	0
5	2334.920	2369.991	2370	-279.883	-324.866	-325
10	3901.195	3981.107	3981	-644.702	-649.731	-650
15	4672.895	4749.777	4750	-1017.327	-974.596	-1017
20	4655.795	4733.715	4734	-1318.631	-1299.462	-1319
25	3908.170	4013.723	4014	-1563.991	-1624.327	-1624
30	2540.795	2693.687	2694	-1863.280	-1949.193	-1949
35	716.945	900.579	901	-2420.875	-2288.072	-2421
40	-1347.610	-1129.540	-1130	-3535.649	-3714.940	-3715

NOTE: M_{pgr1a} represents the maximum positive moment, and M_{ngr1a} represents the minimum negative moment. Results are symmetric about the centre support.

A.4.2 Maximum Moment Due to Load Group gr1b (Load Model 2)

For Load Model 2: $Q_{LM2} = \Sigma P_{LM2} = 242$ kN

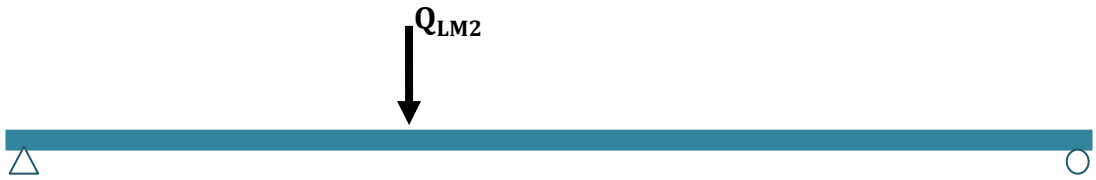

Figure A.32 – Application of load group gr1b

For the Single span: $L_s = 25.0$ m

Since this load group only has a single axle, the greatest moment for each section occurs when the axle is placed directly over that section. Therefore, an envelope of moments is not required on the single span. Calculations for the greatest moment are provided here. The support reactions for the shear diagram are determined by equilibrium. Table A.13 presents the maximum moment for each section. The results are symmetric about centre span.

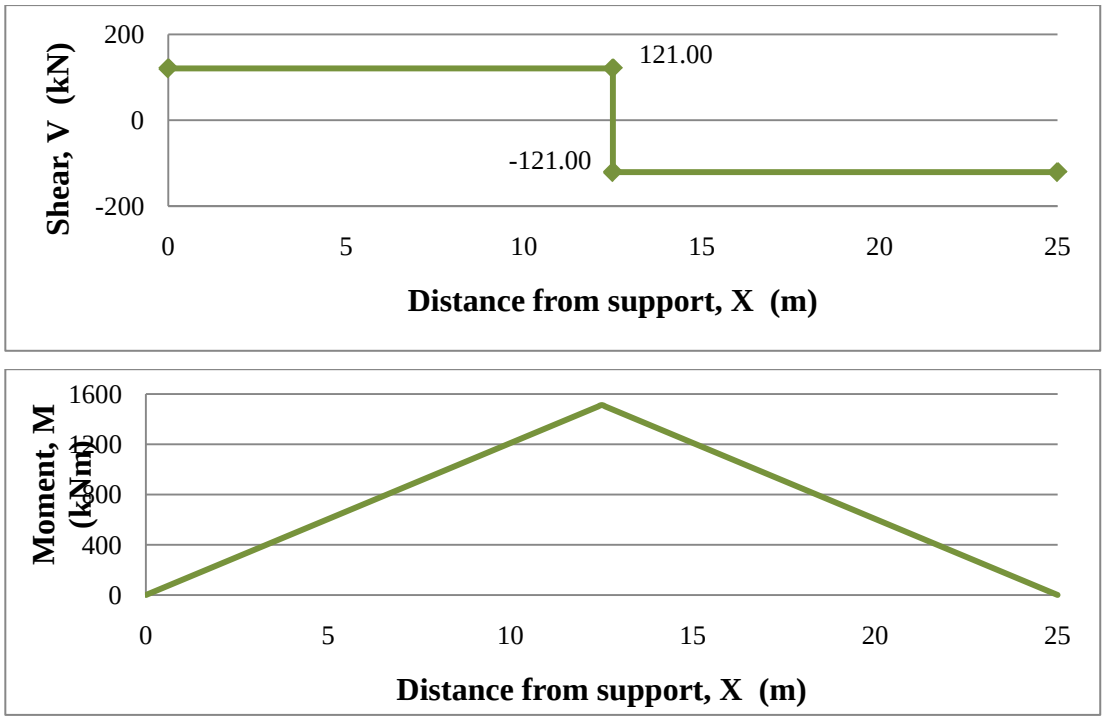

Figure A.33 – Shear and moment diagrams for the overall maximum moment

The maximum moment is then calculated based on the area under the shear diagram.

$$M_{MAX} = 121.0 \times 12.5 = 1512.5 \text{ kN}$$

For design assume: $M_{gr1b} = 1513$ kN

Table A.13 – Summary of M_{gr1b} for the single span

Position (m)	M_{gr1b} (kNm)
0.0	0
2.5	545
5.0	968
7.5	1271
10.0	1452
12.5	1513

For the continuous spans: $L_c = 40.0$ m

To determine the overall minimum and maximum moments due to the single axle, the axle load is placed at a number of locations and the maximum and minimum moments for each location are calculated based on the following beam formulas

(American Wood Council, 2007). Figures A.34 and A.35 summarize the results of these calculations. All results are symmetric about the centre support.

$$M_{MAX} = \frac{Pab}{4L^3}(4L^2 - a(L + a))$$

$$M_{MIN} = -\frac{Pab}{4L^2}(L + a)$$

where:

a = distance to the axle from the first support

b = distance to the axle from the second support

L = span length

P = resultant axle load, Q_{LM2}

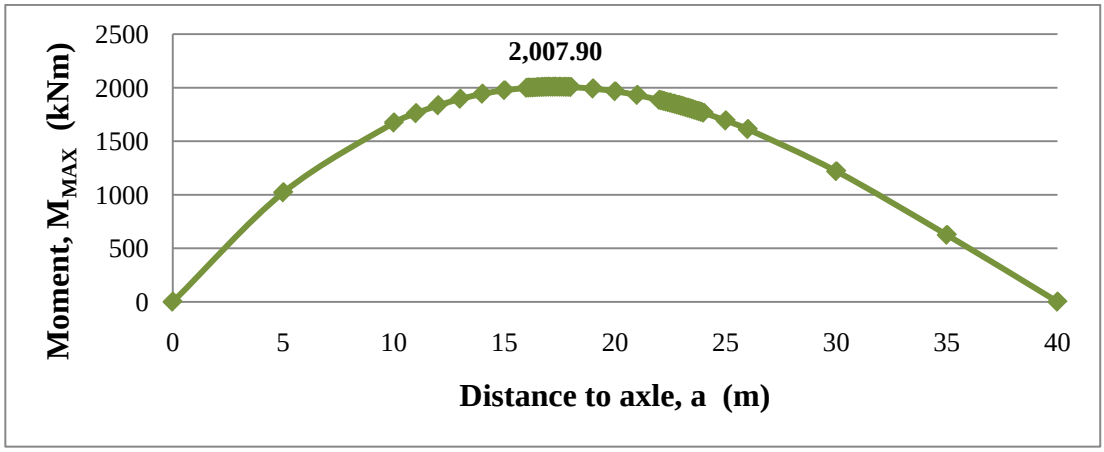

Figure A.34 – Maximum moments due to Load Group gr1b (LM2)

From Figure A.34, it is found that the greatest maximum moment occurs 17.3m from the first support. Calculations for this moment are shown here.

$$M_{MAX} = \frac{242 \times 17.3 \times 22.7}{4 \times 40^3}\left(4 \times 40^2 - 17.3(40 + 17.3)\right) = 2007.90 \text{ kNm}$$

For design assume:

$$M_{pgr1b} = 2008 \text{ kNm}$$

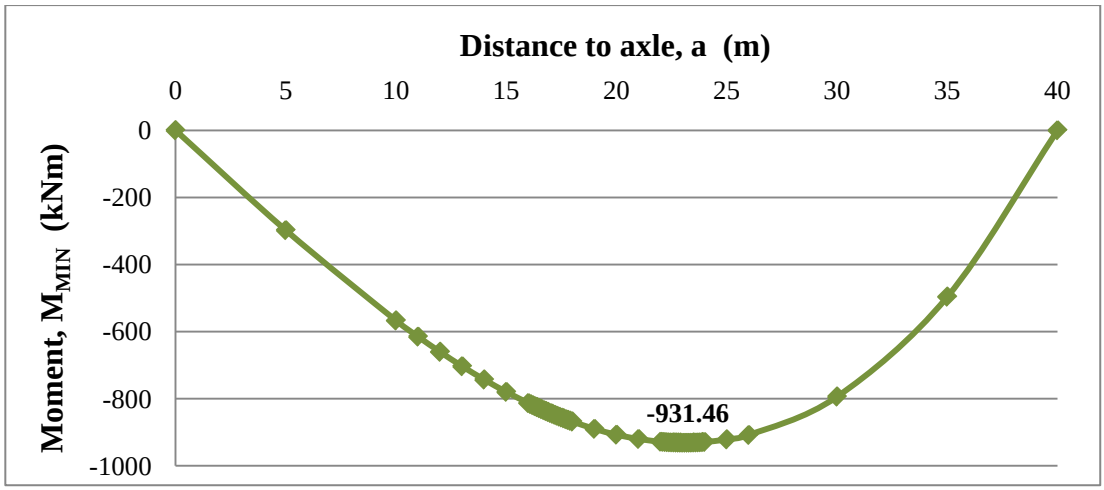

Figure A.35 – Minimum moments due to Load Group gr1b (LM2)

From Figure A.35, it is found that the overall minimum moment occurs when the axle is 23.1m from the first support. The lowest point in the moment diagram occurs at the centre support. Calculations for this moment are shown here.

$$\mathrm{M_{MIN}} = -\frac{242 \times 23.1 \times 16.9}{4 \times 40^2}(40 + 23.1) = -931.46 \text{ kNm}$$

For design assume:

$$\mathrm{M_{ngr1b}} = -932 \text{ kNm}$$

These moments will be considered for the design of the prestressed beam in Appendix C. As with the single span, the maximum positive moment for each section occurs when the axle load is placed directly over that section. To determine the minimum negative moment at each section, an envelope of moments is created.

For each shear and moment diagram, the support reactions are determined using the following formulas. These equations account for the application of the axle in the span between supports A and B. Figure A.36 presents the envelope of moments and Table A.14 presents the final moments for design determined from the envelope. The results are symmetric about the centre support.

$$R_A = \frac{Pb}{4L^3}\left(4L^2 - a(L+a)\right) \qquad R_B = \frac{Pa}{2L^3}(2L^2 - b(L+a)) \qquad R_C = -\frac{Pab}{4L^3}(L+a)$$

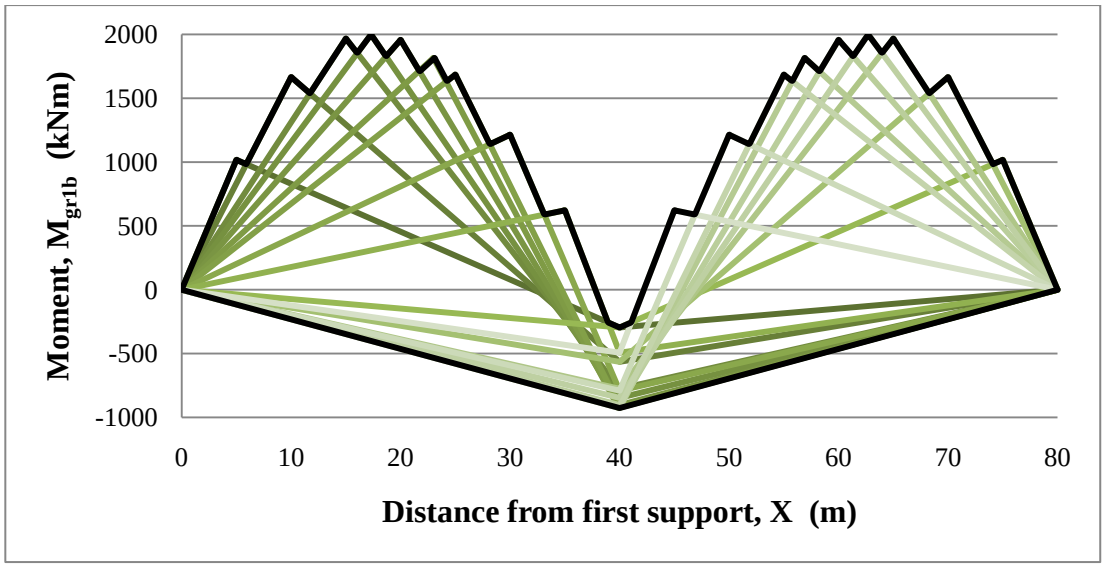

Figure A.36 – Envelope of moments for Load Group gr1b for continuous spans

Further analysis of the envelope reveals that, due to the linear variance of the negative moment between the supports, the minimum negative moment for each section occurs on the moment diagram for the overall minimum negative moment. Thus, future investigations need only consider this diagram for negative moments.

Table A.14 – Summary of M_{pgr1b} and M_{ngr1b} for the continuous spans

Position (m)	M_{pgr1b} (kNm)	M_{ngr1b} (kNm)
0	0	0
5	1017	-116
10	1666	-232
15	1968	-348
20	1958	-464
25	1686	-580
30	1214	-696
35	622	-812
40	-297	-928

NOTE: M_{pgr1b} is the maximum positive moment and M_{ngr1b} is the minimum negative moment. Results are symmetric about the centre support.

A.4.3 Maximum Moments Due to Load Group gr4 (Load Model 4)

For Load Model 4: $w_{gr4} = w_{LM4} = q_{ck} \times s_b = 10.0 \text{ kN/m}$

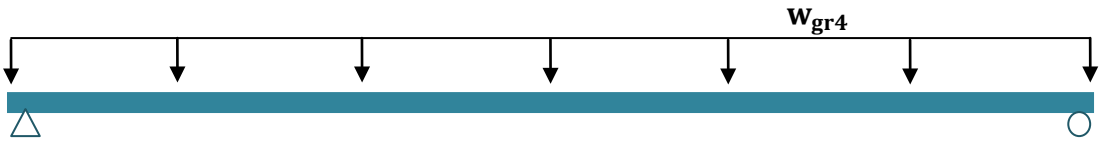

Figure A.37 – Application of Load Group gr4

For the Single span: $L_s = 25.0 \text{ m}$

Since this load group only has a distributed load, the greatest moment occurs at midspan and the maximum moment for each section occurs when the distributed load is applied to the entire span. The greatest maximum moment is calculated here.

$$M_{MAX} = \frac{w_{gr4} L_s^2}{8} = \frac{10 \times 25^2}{8} = 781.25 \text{ kNm}$$

For design assume:

$$M_{gr4} = M_{LM4} = 782 \text{ kN}$$

The shear and moment diagram, presented in Figure A.38, provide the maximum moment for each section. The support reactions are determined by equilibrium.

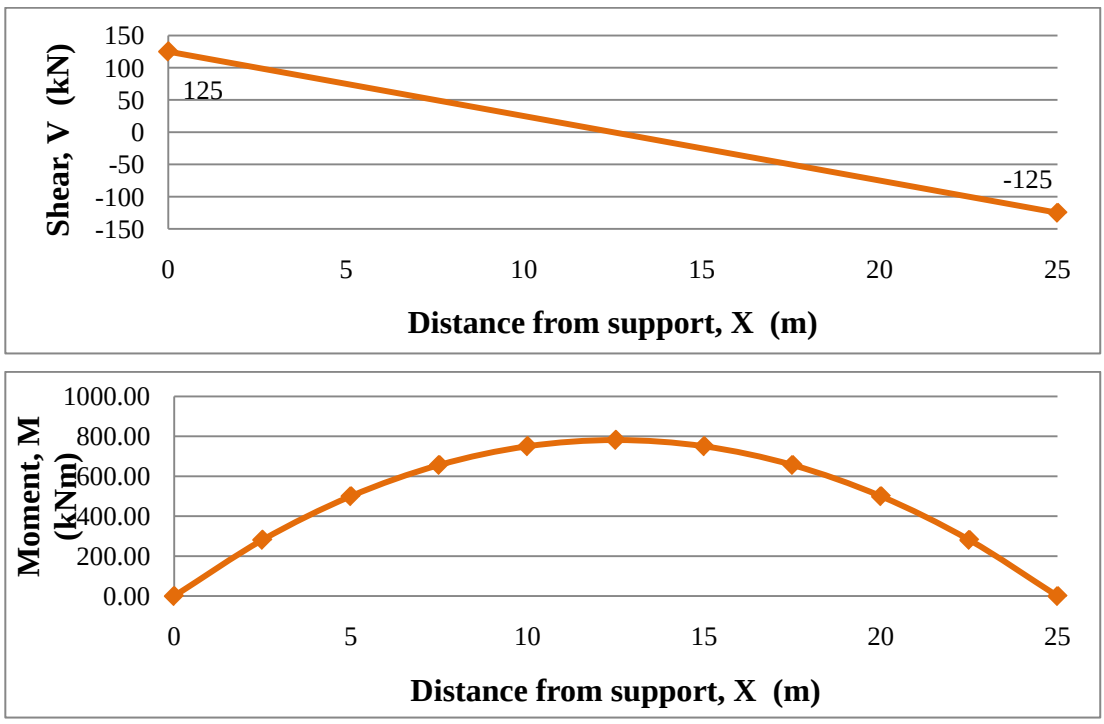

Figure A.38 – Shear and moment diagram for distributed load, w_{gr4}

Table A.15 presents the resulting maximum moments. The results are symmetric about midspan (12.5m).

Table A.15 – Summary of M_{gr4} for the single span

Position (m)	M_{gr4} (kNm)
0.0	0
2.5	281
5.0	500
7.5	656
10.0	750
12.5	782

For the continuous spans: $L_c = 40.0$ m

For the continuous spans, two sets of calculations must be performed. The first for the overall maximum positive moment, which occurs when only one span is loaded, and the second for the overall minimum negative moment, which occurs when both spans are loaded. It is found that the overall maximum moment occurs at 17.5m from the support and the minimum moment occurs at the centre support. The calculations for the overall maximum and minimum moments are shown here. Beam formulas have been applied which can be found in many structural design books.

$$M_{MAX} = \frac{49}{512} w_{gr4} L_c^2 = \frac{49}{512} \times 10 \times 40^2 = 1531.25 \text{ kNm} \quad \text{(one span loaded)}$$

$$M_{MIN} = -\frac{w_{gr4} L_c^2}{8} = -\frac{10 \times 40\text{^}2}{8} = -2000 \text{ kNm} \quad \text{(both spans loaded)}$$

For design assume:

$$M_{pgr4} = 1532 \text{ kN}$$

$$M_{ngr4} = -2000 \text{ kN}$$

The shear and moment diagrams for both loading conditions provide maximum and minimum moments at each section. For the condition in which only one span is loaded, the following equations are used for the support reactions. Figure A.39 presents the shear and moment diagram produced with these.

$$R_A = \frac{7}{16} w_{gr4} L_c \qquad R_B = \frac{5}{8} w_{gr4} L_c \qquad R_C = -\frac{1}{16} w_{gr4} L_c$$

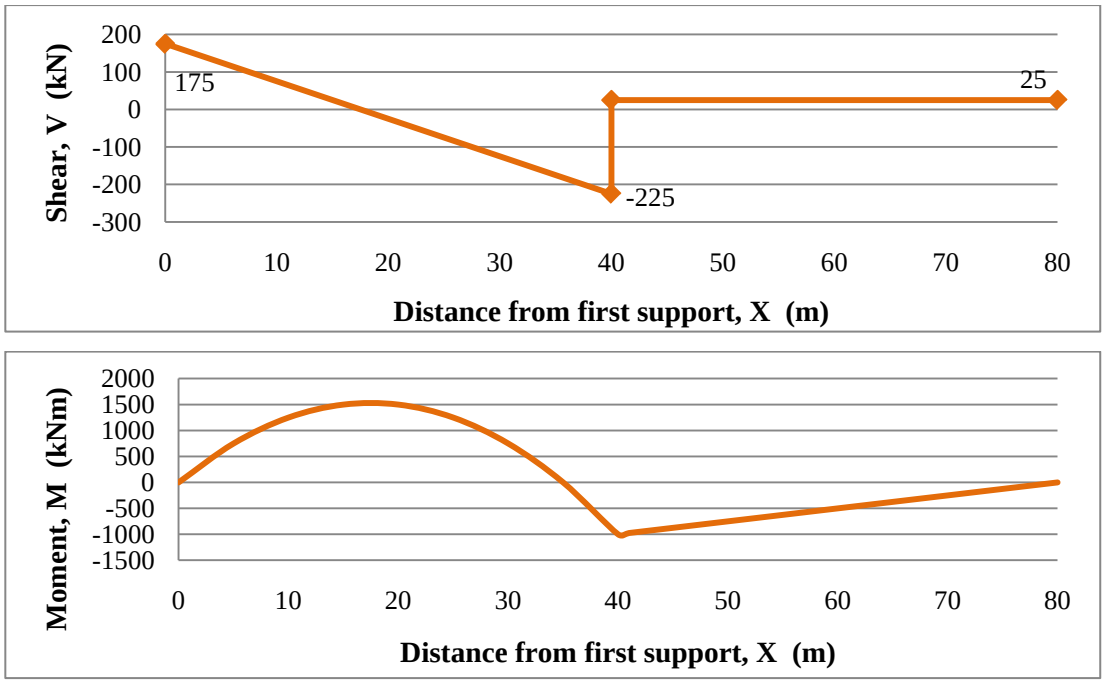

Figure A.39 – Shear and moment diagram for w_{gr4} on one span

And for both spans loaded, the following equations are applied for the support reactions. Figure A.40 presents the resulting shear and moment diagram.

$$R_A = R_C = \frac{3}{8} w_{gr4} L_c \qquad R_B = \frac{10}{8} w_{gr4} L_c$$

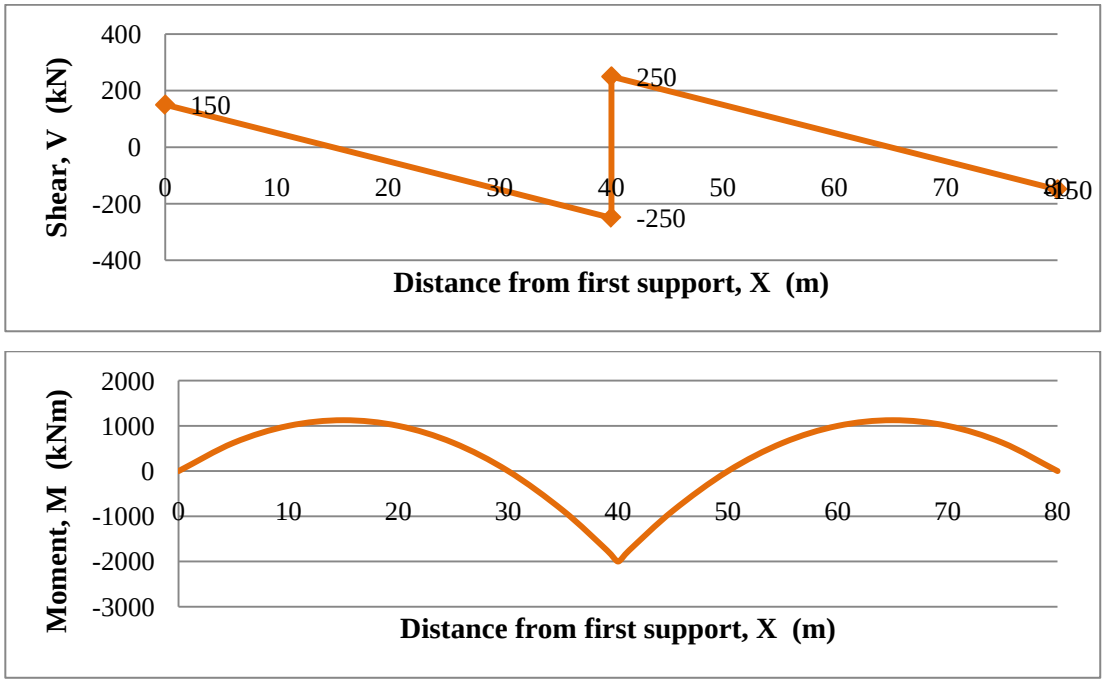

Figure A.40 – Shear and moment diagrams for w_{gr4} on both spans

Table A.16 – Summary of M_{pgr4} and M_{ngr4} for the continuous spans

Position (m)	M_{pgr4} (kNm)	M_{ngr4} (kNm)
0	0	0
5	750	-125
10	1250	-250
15	1500	-375
20	1500	-500
25	1250	-625
30	750	-750
35	0	-875
40	-1000	-2000
NOTE: M_{pgr4} is the maximum positive moment and M_{ngr4} is the minimum negative moment. Results are symmetric about the centre support.		

A.4.4 Maximum Moments Due to Load Group gr5 (Load Model 3)

From Load Model 3: $\Sigma P_{196a} = 52\ \text{kN}$

$\Sigma P_{196b} = 86\ \text{kN}$

$\Sigma P_{196c} = 80\ \text{kN}$

BS EN 1991-2

For frequent Load Model 1: $\Psi_1 = 0.75$

Cl. NA.16.4

$\Psi_1 \times \Sigma P_{TS} = 147.75\ \text{kN}$

BS EN 1990

$\Psi_1 \times w_{UDL} = 8.25\ \text{kN/m}$

Table NA.A2.1

There are a number of variances to consider in the model. First, in the special vehicle defined by LM3, there are three possibilities for the axle spacing x, shown in Figure A.45. In accordance with Clause NA.2.16.1.3, the spacing of the axle should be the most unfavourable of 1.2m, 5.0m, and 9.0m. Second, LM3 is applied in combination with frequent values of LM1, as illustrated in Figure A.41. The frequent values should be placed in the most unfavourable position on the span, but not within 5.0m of the special vehicle. Depending on the span lengths and arrangements, the most unfavourable placement may occur at any distance from the special vehicle.

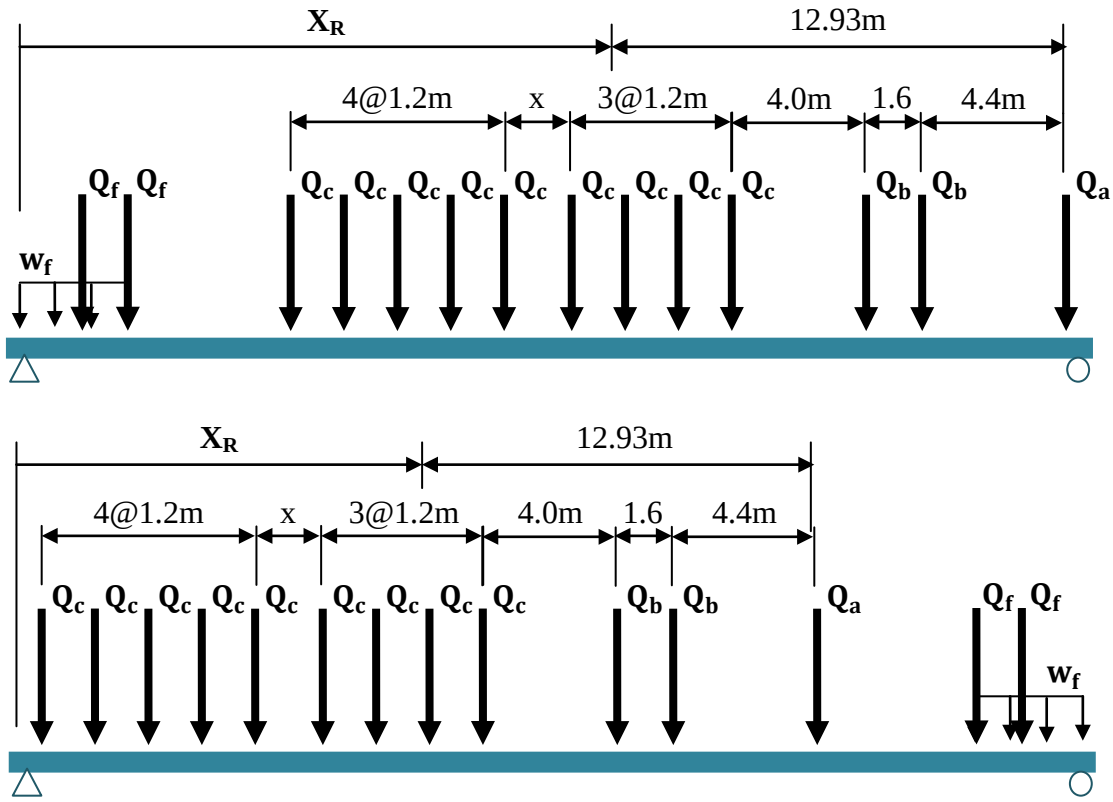

Figure A.41 – Application of Load Group gr5

X_R represents the distance from the first support to the resultant of the LM3 axles.

For the Single span: $L_s = 25.0$ m

The application of Load Group gr5 for the single span is fairly straight forward. The more axles on the span and the closer the resultant of the axles is to midspan, the greater the moment that occurs. Therefore, LM3 is applied with the axle spacing x equal to 1.2m, and the frequent values of LM1 are applied 5.0m from the front or rear axles of the special vehicle.

To determine the overall maximum moments, the same process as that described for LM1 has been applied. The loading is placed at 2.5m intervals and the maximum moment is calculated for each location via shear and moment diagrams. The application of frequent LM1 both in front and behind the special vehicle is included in these calculations. From the initial results it is determined that the greatest maximum moment occurs when the axles of SV196 are applied between 12.5m and 20.0m. Further calculations at 0.1m intervals are completed at this location for more accurate results. The results are summarized in Figure A.42.

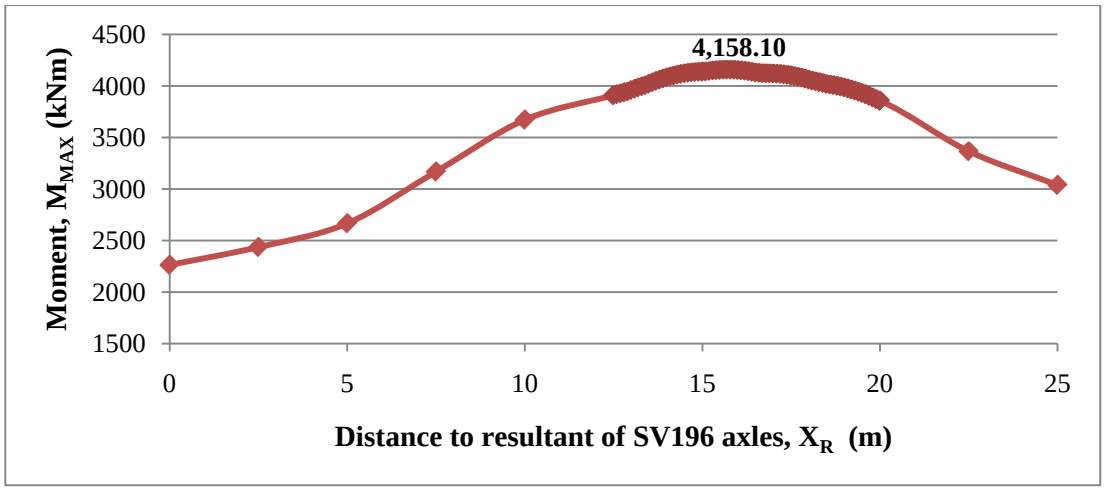

Figure A.42 – Maximum moments due to Load Group gr5

From Figure A.42 it is determined that the greatest maximum moment occurs when the resultant of the SV196 axles are applied at 15.7m from the first support, and the frequent LM1 is applied 5.0m *behind* the special vehicle. The calculations are provided here for the greatest of the maximum moments to show the procedure that has been applied.

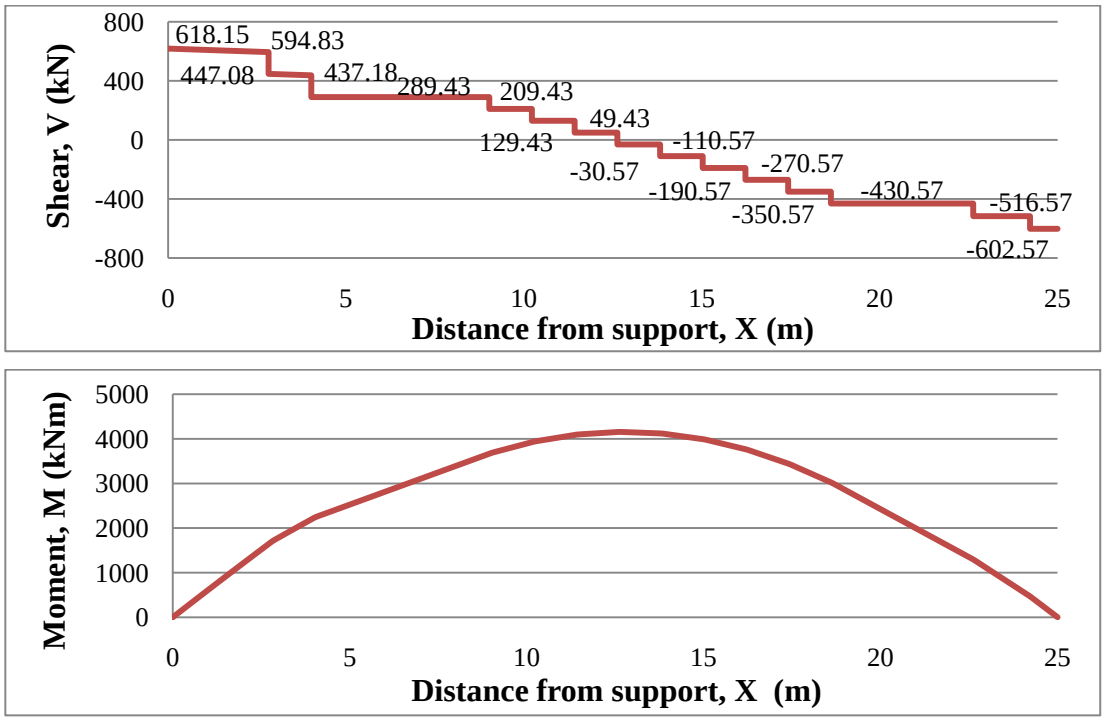

Figure A.43 – Shear and moment diagram for SV196 applied at X_R = 15.7m

The maximum moment is calculated based on the area under the shear diagram. The peak in the moment diagram occurs 12.6m from the first support.

$$M_{MAX} = 602.57 \times 0.77 + 516.57 \times 1.6 + 430.57 \times 4.0 + (350.57 + 270.57 + 190.57 + 110.57 + 30.57) \times 1.2 = 4158.10$$

For design assume:

$$M_{gr5} = 4159 \text{ kNm}$$

This moment is applied for the design of the prestressed beam in Appendix B. As was done for the last three load groups, the maximum moment at each section must be determined. To calculate these moments, an envelope of moments is developed based on the application of loads at 2.5m intervals and an estimate for the missing moment diagrams is provided by a trend line.

Figure A.44 presents the envelope of moments and corresponding trend line. It should be noted that this envelope encompasses the application of frequent LM1 in front and behind the special vehicle. Table A.18 presents the moments determined from the envelope and trend line as well as the final moments for design. Results are symmetric about midspan (12.5m).

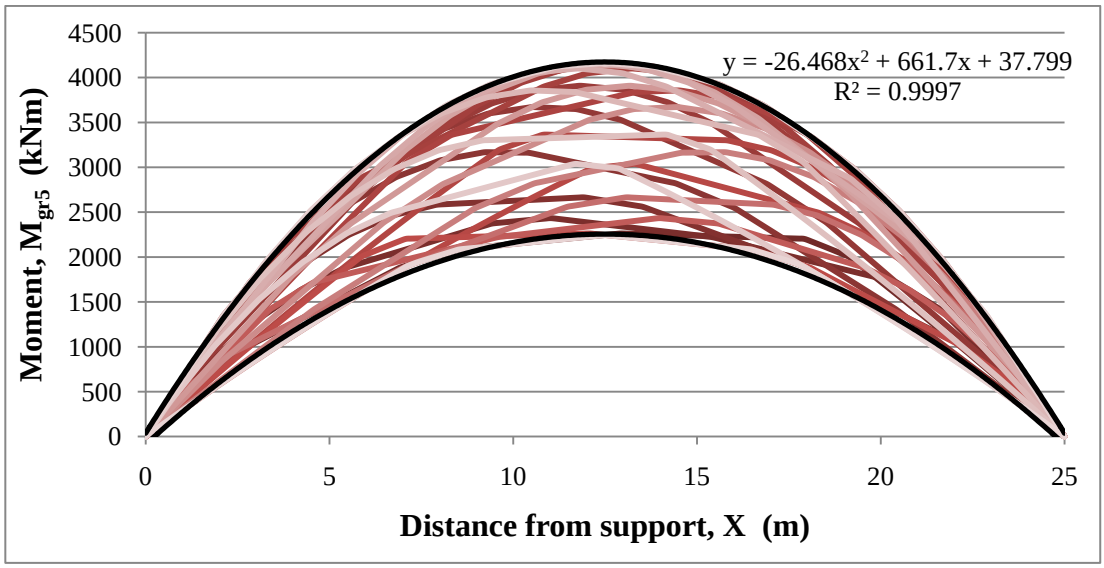

Figure A.44 – Envelope of moments due to Load Group gr5 (LM3+freq. LM1) on the single span

Table A.17 – Summary M_{gr5} for the single span

Position (m)	M_{trend} (kNm)	M_{MAX} (kNm)	M_{gr5} (kNm)
0.0	37.799	0	0
2.5	1526.624	1535.272	1535
5.0	2684.599	2709.682	2710
7.5	3511.724	3500.835	3512
10.0	4007.999	3993.203	4008
12.5	4173.424	4151.831	4159

For the continuous spans: $L_c = 40.0$ m

For the continuous spans, as with the previous load groups, the overall maximum and minimum moments must be determined. Preliminary calculations show that the overall maximum moment occurs with the loads applied to only one span, while the overall minimum moment occurs with the SV196 vehicle applied to one span and the frequent LM1 to the other.

First, the overall maximum positive moment is considered. The axles of the tandem system are placed at 5.0m intervals with the tandem system of frequent LM1 applied in front and then behind the special vehicle within the same span. From the initial results, shown in Figure A.45, it is determined that the overall maximum moment occurs when the resultant of the special vehicle axles is located around 65m from the first support with frequent LM1 behind the special vehicle. Further calculations are completed at this location for more accurate results.

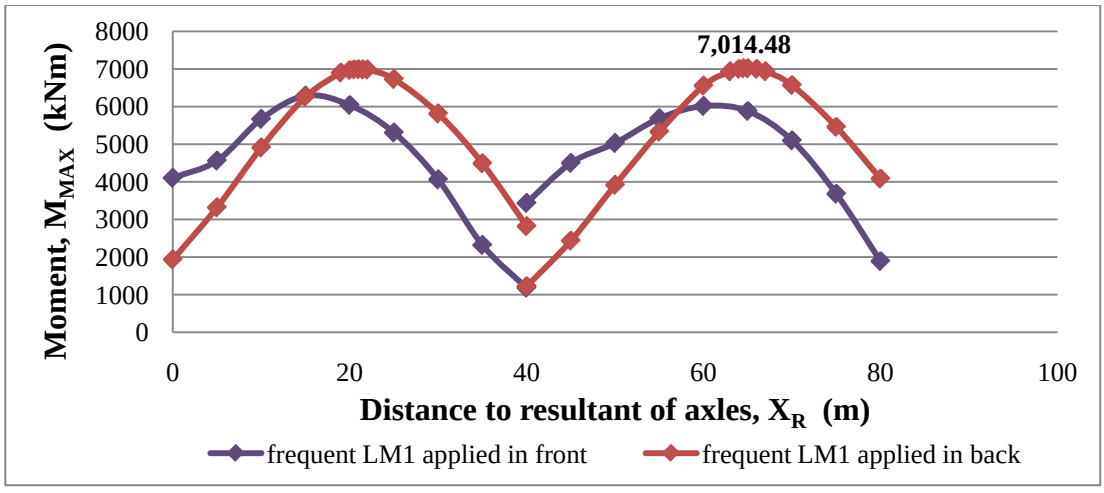

Figure A.45 – Maximum moments due to Load Group gr5

From Figure A.45, it is determined that the overall maximum moment occurs when the resultant of the axles on the special vehicle is located 64.5m from the first support, in the second span. Also, the frequent values of LM1 are applied only on the second span, with the tandem system applied 5.0m behind the special vehicle. By symmetry, the same results would occur for the first span, at 15.5m from the first support, with the vehicle facing the opposite direction. The shear and moment diagrams for the resultant axle at 64.5m are provided in Figure A.46. Following the same procedure as that described for LM1, the support reactions below are determined.

$$A_y = -103.365\ \text{kN} \qquad B_y = 849.685\ \text{kN} \qquad C_y = 599.183\ \text{kN}$$

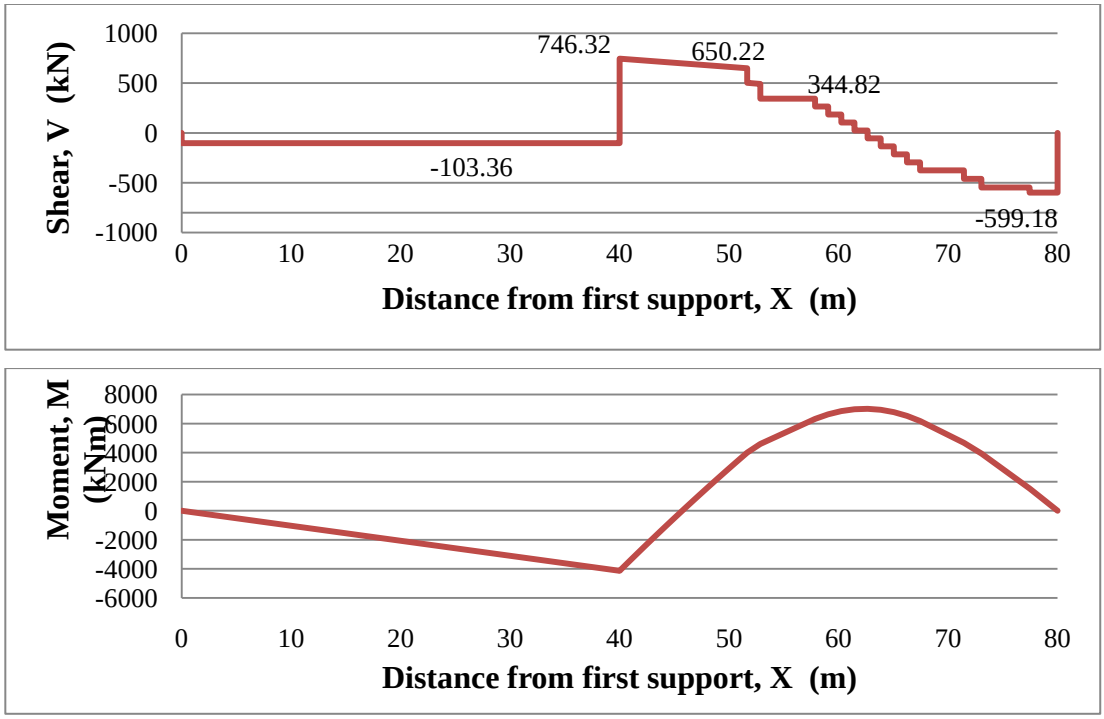

Figure A.46 – Shear and moment diagrams for the overall maximum moment

The maximum moment is calculated based on the area under the shear diagram. The peak in the moment diagram occurs 17.4m from the first support.

For design assume:

$$M_{pgr5} = 7015\ \text{kNm}$$

For the determination of the overall minimum negative moment, a number of factors are considered. First, the tandem system of frequent LM1 is placed at the same location that was determined in Section A.4.1 for negative moment, with the resultant located 56.9m from the first support. Second, after evaluating the negative moments calculated in the determination of the overall maximum moment, shown in Figure A.47, it is discovered that the minimum negative moment occurs when the resultant axle of the special vehicle is placed around 25m.

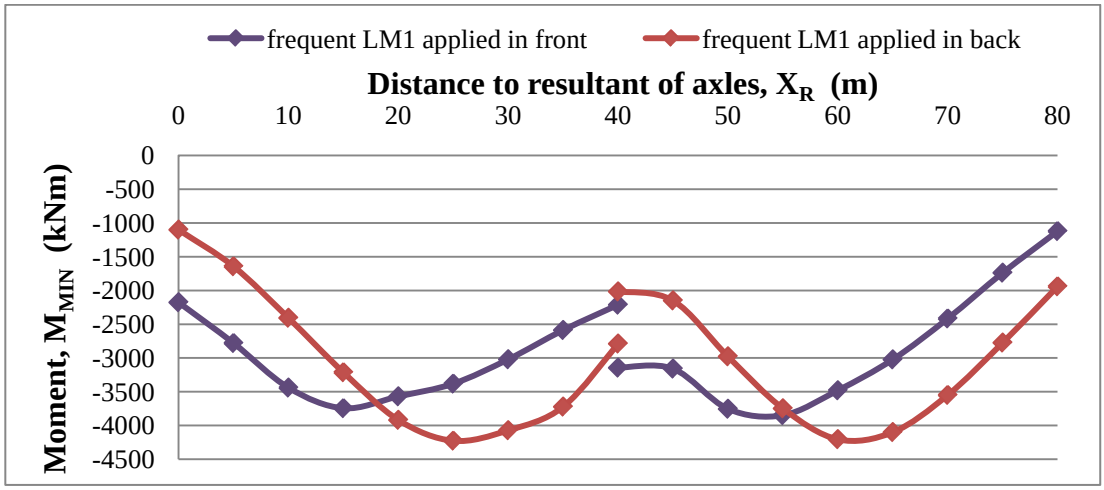

Figure A.47 – Negative moment results from Positive moment calculations for Load Group gr5

Based on these factors, for the determination of the minimum negative moment, the special vehicle is positioned at several points around 25m, along with the frequent UDL from LM1 applied to both spans, and the tandem system applied at 56.9m.

From these calculations, it is confirmed that the overall minimum moment occurs when the resultant for the special vehicle (LM3) is placed at 25m from the first support, and the resultant for the tandem system is placed at 56.9m from the first support, with the UDL applied on both spans, but not within 5.0m of the special vehicle. The shear and moment diagrams for this location are shown in Figure A.49. By once again applying the moment distribution method as illustrated for LM1, the following support reactions are determined.

$$A_y = 274.624 \quad kN \qquad B_y = 1246.018 \ kN \qquad C_y = 134.658 \quad kN$$

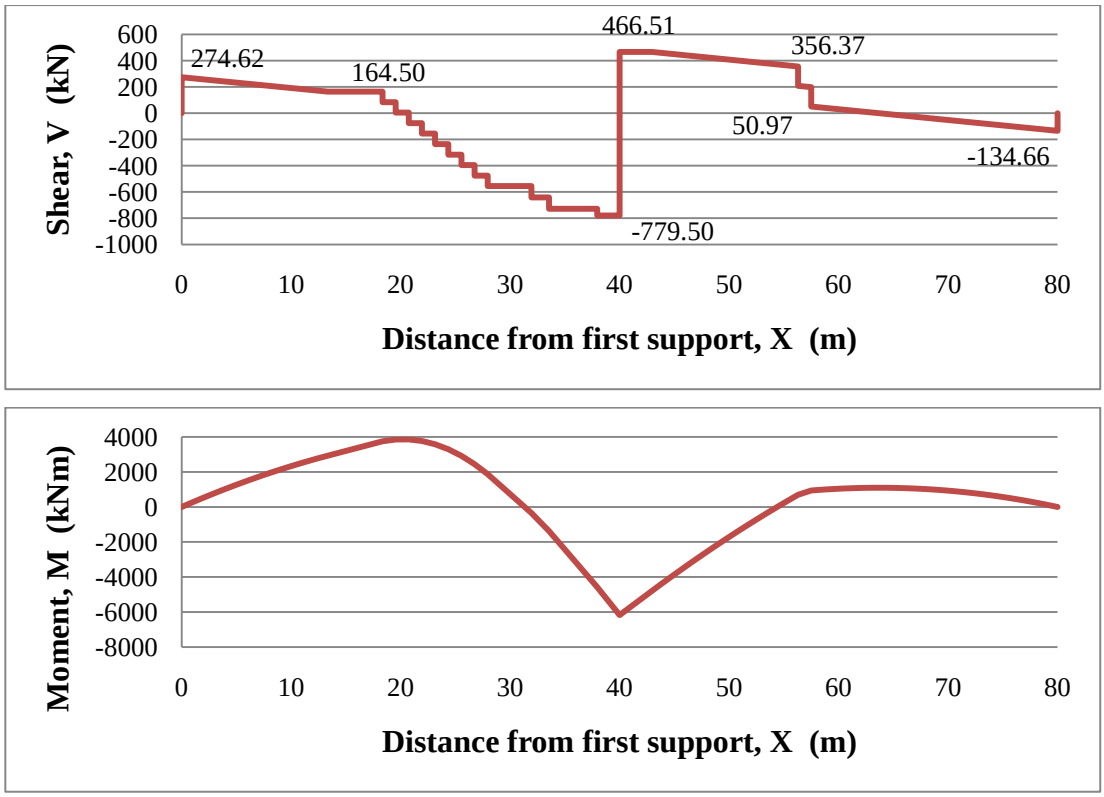

Figure A.48 – Shear and moment diagrams for the overall minimum moment

The maximum moment is calculated based on the area under the shear diagram.

For design assume:

$$M_{ngr5} = -6172 \text{ kNm}$$

The envelope of moments is created to determine the minimum and maximum moments that occur at a number of points along the beam. Figure A.49 presents the envelope of moments for both the minimum and maximum moments and the corresponding trend lines. The results are symmetric around the centre support. Table A.19 presents the moments determined from the envelope and trend line as well as the final moments for design.

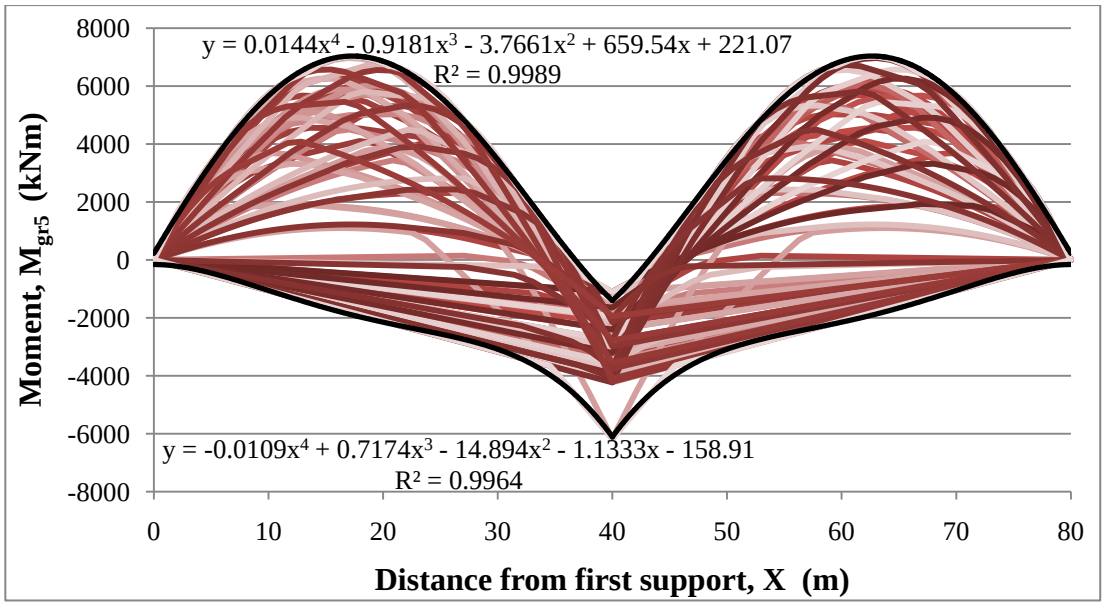

Figure A.49 – Envelope of moments due to Load Group gr5 (LM3+freq. LM1) on the continuous spans

Table A.18 – Summary of M_{pgr5} and M_{ngr5} for the continuous spans

Position (m)	M_{ptrend} (kNm)	M_{MAX} (kNm)	M_{pgr5} (kNm)	M_{ntrend} (kNm)	M_{MIN} (kNm)	M_{ngr5} (kNm)
0	221.07	0	0	-158.91	0	0
5	3318.86	3355.38	3355	-454.064	-528.40	-528
10	5665.76	5708.28	5708	-1051.24	-1056.8	-1057
15	6897.21	6827.28	6897	-1657.65	-1585.19	-1658
20	6864.63	6776.03	6865	-2143.98	-2113.59	-2144
25	5635.45	5723.01	5723	-2544.43	-2641.99	-2642
30	3493.08	3540.94	3541	-3056.71	-3170.39	-3170
35	936.96	756.13	937	-4042.01	-3856.56	-4042
40	-1317.49	-1101.75	-1102	-6025.04	-6171.77	-6172

NOTE: M_{pgr5} represents the maximum positive moment, and M_{ngr5} represents the minimum negative moment. Results are symmetric about the centre support.

A.5 SUMMARY OF RESULTS FOR THE TRAFFIC LOADING

For both design examples, the final moments from each load group are summarized here. These moments will be incorporated into the two design examples presented in Appendices B and C. The following sub-sections present the maximum and minimum moments for each point along the span considered as well.

Table A.19 - Summary of moments due to traffic

Load Group	*Single Span*	*Continuous Spans*	
	Maximum Moment (kNm)	Maximum Moment (kNm)	Minimum Moment (kNm)
gr1a	3205	4841	-3715
gr1b	1513	2008	-932
gr4	782	1532	-2000
gr5	4159	7015	-6172

A.5.1 Maximum Moments for the Single span

Table A.20 – Maximum moments for each load group

Position (m)	Maximum Moments (kNm)			
	gr1a	gr1b	gr4	gr5
0.0	0	0	0	0
2.5	1136	545	281	1535
5.0	2031	968	500	2710
7.5	2672	1271	656	3512
10.0	3071	1452	750	4008
12.5	3205	1513	782	4159
NOTE: Results are symmetric about midspan.				

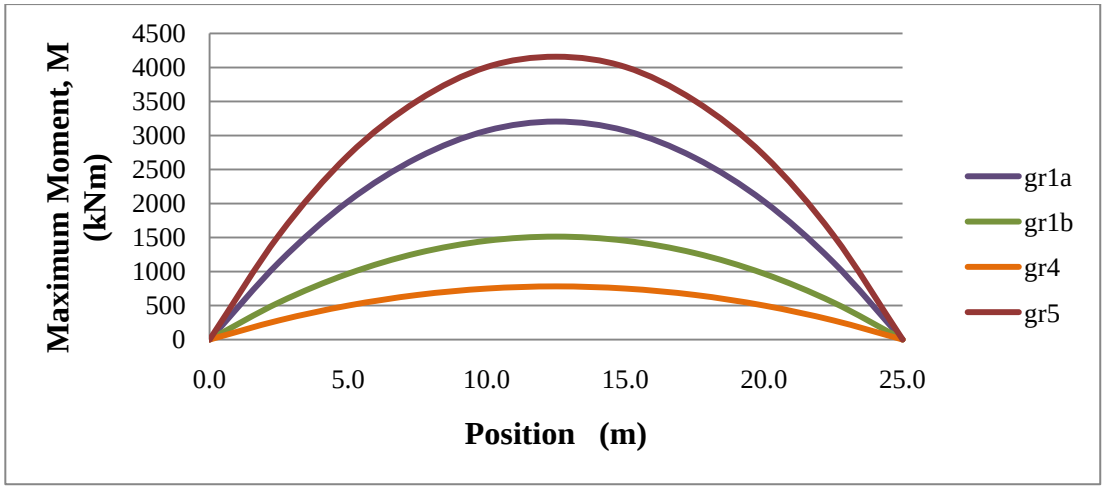

Figure A.50 – Maximum moments for each load group on the single span

From Table A.21 and Figure A.50 it becomes evident that Load Group gr5 has the most adverse effect and will be applied in the design in Appendix B. Also, for frequent loading, for which only two of the load groups are considered, Load Group gr1a will control.

A.5.2 Maximum and Minimum Moments for the Continuous Span

Table A.21 – Maximum positive moments for each load group

Position (m)	Maximum Positive Moments (kNm)				Minimum Negative Moments (kNm)			
	gr1a	gr1b	gr4	gr5	gr1a	gr1b	gr4	gr5
0	0	0	0	0	0	0	0	0
5	2370	1017	750	3355	-325	-116	-125	-528
10	3981	1666	1250	5708	-650	-232	-250	-1057
15	4750	1968	1500	6897	-1017	-348	-375	-1658
20	4734	1958	1500	6865	-1319	-464	-500	-2144
25	4014	1686	1250	5723	-1624	-580	-625	-2642
30	2694	1214	750	3541	-1949	-696	-750	-3170
35	901	622	0	937	-2421	-812	-875	-4042
40	-1130	-297	-1000	-1102	-3715	-928	-2000	-6172
NOTE: Results are symmetric about the centre support.								

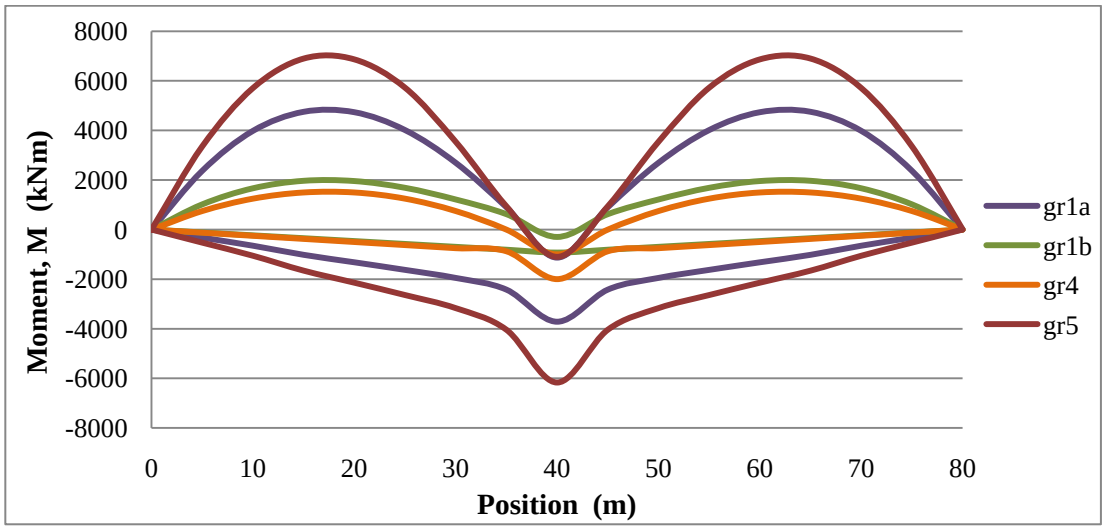

Figure A.51 – Maximum and minimum moments for each load group

From Table A.22 and Figure A.51 it becomes evident that Load Group gr5 has the most adverse effect for the continuous spans as well and will be applied in the design in Appendix C. Also, for frequent loading, Load Group gr1a will control.

APPENDIX B SINGLE SPAN DESIGN

To illustrate the procedure for a prestressed concrete bridge design, a fictional bridge is created with the cross section shown in Figure B.1.

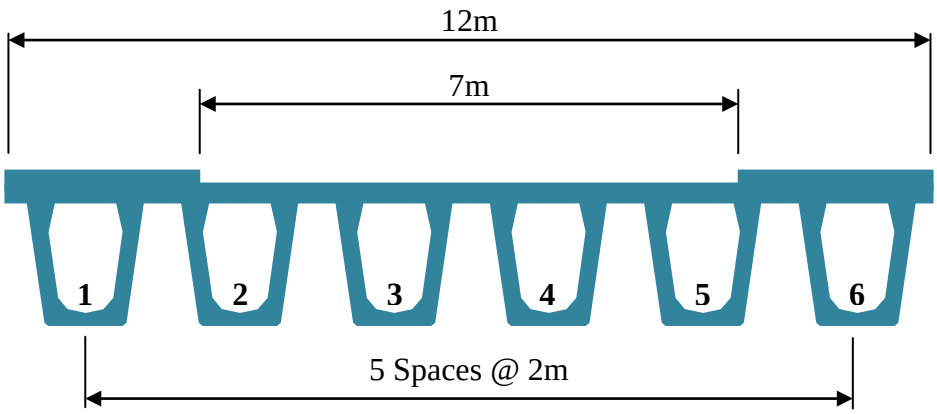

Figure B.1 – Bridge cross section

Design Assumptions:

Span length:	25.0 metres
Beam type:	Pre-tensioned U12 Beams
Beam Spacing:	2.0 metres
Deck width:	12.0 metres
Carriageway width:	7.0 metres
Concrete:	C50/60 for the beams
	C40/50 for the slab

The structure spans a fresh water river.

This design will focus on Beam 3, which is the critical case.

B.1 DESIGN DATA

Bridge width: $b := 12.0 \quad m$ Carriageway width: $b_c := 7.0 \quad m$

Span Length: $L_s := 25.0 \quad m$ Beam spacing: $s_{bm} := 2000 \quad mm$

B.1.1 Material Properties

BS EN 1992-1-1

Beam: C50/60 Concrete

Table 3.1

$f_{ck} := 50 \quad MPa$ $f_{cm} := 58 \quad MPa$

$f_{ckcube} := 60 \quad MPa$ $f_{ctm} := 4.1 \quad MPa$

$E_{cm} := 37 \quad GPa$

Slab: C40/50 Concrete

$f_{sck} := 40 \quad MPa$ $f_{scm} := 48 \quad MPa$

$f_{sckcube} := 50 \quad MPa$ $f_{sctm} := 3.5 \quad MPa$

$E_{scm} := 35 \quad GPa$

CEM 42.5R Cement: $s_c := 0.20$ Cl. 3.1.2(6)

Transfer time: $t := 7 \quad days$

Compressive strength with time t = 7 days for the beams:

$$\beta_{cc} := e^{s_c \cdot \left(1 - \sqrt{\frac{28}{t}}\right)} = 0.819$$ Eq. (3.2)

$f_{cmt} := \beta_{cc} \cdot f_{cm} = 47.486 \quad MPa$ Eq. (3.1)

$f_{ckt} := f_{cmt} - 8 = 39.486 \quad MPa$ Cl. 3.1.2(5)

$$E_{cmt} := E_{cm} \cdot \left(\frac{f_{cmt}}{f_{cm}}\right)^{0.3} = 34.845 \quad GPa$$ Eq. (3.5)

Prestressing strands: (15.2ϕ drawn strand)

Part 3 of prEN 10138

Table 2

$\phi_p := 15.2 \quad mm$ $A_{pstr} := 165 \quad mm^2$

$f_{pk} := 1820 \quad MPa$ $f_{p0.1k} := 0.86 \cdot f_{pk} = 1565.2 \quad MPa$

$P_{ustr} := 300 \quad kN$ $P_{istr} := 219 \quad kN$

$E_s := 195 \quad GPa$

B.2 DURABILITY REQUIREMENTS

B.2.1 Determination of Nominal Cover

BS EN 1992-1-1

Exposure Class: Deck: XC3 (protected by waterproofing) — Table 4.1 (incorp. BS EN 1992-2)

Beams: XC3 (over fresh water)

BS EN 1990

Design Life: Category 5 -- 120 years — Table NA.2.1

BS EN 1992-1-1

Nominal cover: $c_{nom} = c_{min} + \Delta c_{dev}$ — Cl. 4.4.1.1 Eq. (4.1)

Minimum cover: — Cl. 4.4.1.2 Eq. (4.2)

$c_{min} = \max[c_{min,b};\ c_{min,dur} + \Delta c_{dur,\gamma} - \Delta c_{dur,st} - \Delta c_{dur,add};\ 10mm]$

Minimum cover due to bond requirements: — Cl. 4.4.1.2(3)

For pre-tensioned tendons: $c_{minb} := 2.5 \cdot \phi_p = 38$ mm

For reinforcing bars: $c_{minbr} := 25$ mm

Minimum cover due to durability requirements: — Per Cl. 4.4.1.2(5) & Table NA.1

For XC3: $c_{mindur} := 30$ mm — **BS 8500-1** Table A.5

$\Delta c_{dur\gamma} := 0$ mm — **NA to BS EN 1992-1-1** Cl. 4.4.1.2(6), (7), & (8)

$\Delta c_{durst} := 0$ mm

$\Delta c_{duradd} := 0$ mm

$c_{min} := \max\left(c_{minb}, c_{minbr}, c_{mindur} + \Delta c_{dur\gamma} - \Delta c_{durst} - \Delta c_{duradd}, 10\right)$

$c_{min} = 38$ mm

$c_{mind} := \max\left(c_{minbr}, c_{mindur} + \Delta c_{dur\gamma} - \Delta c_{durst} - \Delta c_{duradd}, 10\right)$

$c_{mind} = 30$ mm

Allowance for deviation: $\Delta c_{dev} := 10$ mm — Cl. 4.4.1.3(1)P

Nominal cover for the beams:

$c_{nom} := c_{min} + \Delta c_{dev} = 48$ mm

Nominal cover for the deck:

$c_{nomd} := c_{mind} + \Delta c_{dev} = 40$ mm

B.3 ACTIONS ON THE STRUCTURE

B.3.1 Permanent Actions

BS EN 1991-1-1

Normal weights:

Concrete	$\gamma_{conc} := 24 \quad kN/m^2$	Table A.1
Reinforced/Prestressed Concrete	$\gamma_{rc} := 25 \quad kN/m^2$	
Wet Concrete	$\gamma_{rcwet} := 26 \quad kN/m^2$	
Hot Rolled Asphalt	$\gamma_{pvmt} := 23 \quad kN/m^2$	Table A.6

Self weight of beam and slab (U12 Beam)

Area of beam: $A_b := 745153 \quad mm^2$

Weight of beam: $w_b := A_b \cdot 10^{-6} \cdot \gamma_{rc} = 18.629 \quad kN/m$

$$M_b := \frac{w_b \cdot L_s^2}{8} = 1455.377 \quad kNm$$

Area of slab: $d_s := 200 \quad mm \qquad s_{bm} = 2000 \quad mm$

$$A_s := d_s \cdot s_{bm} = 4 \times 10^5 \quad mm^2$$

Weight of beam and slab:

$$w_{bs} := \left(A_b + A_s\right) \cdot 10^{-6} \cdot \gamma_{rc} = 28.629 \quad kN/m \quad \text{per beam}$$

$$M_{bs} := \frac{w_{bs} \cdot L_s^2}{8} = 2236.627 \quad kNm$$

Super-imposed dead load

Surfacing on carriageway: $d_{sf} := 60 \quad mm$

NA to BS EN 1991-1-1 Cl. 5.2.3(3)

Adjustment factor for variation in thickness: $f_{sf} := 1.55$

$$q_{sf} := d_{sf} \cdot 10^{-3} \cdot f_{sf} \cdot \gamma_{pvmt} = 2.139 \quad kN/m^2$$

$$w_{sf} := q_{sf} \cdot s_{bm} \cdot 10^{-3} = 4.278 \quad kN/m$$

$$M_{sf} := \frac{w_{sf} \cdot L_s^2}{8} = 334.219 \quad kNm$$

(Parapet and footpath loading do not apply to Beam 3)

B.3.2 Variable Actions - Traffic Loads — BS EN 1991-2

(From Appendix A) — Table NA.3 and...

Load Group gr1a - Load Model 1 - Normal Traffic — Cl. 4.3.2

Model consists of a tandem system combined with a UDL

$M_{gr1a} := 3205$ kNm

Load Group gr1b - Load Model 2 - Single Axle Load — Cl. 4.3.3

Model consists of only a single axle.

$M_{gr1b} := 1513$ kNm

Load Group gr4 - Load Model 4 - Crowd Loading — Cl. 4.3.5

Model consists of uniformly distributed load.

$M_{gr4} := 782$ kNm

Load Group gr5 - Load Model 3 - Special Vehicles — Cl. 4.3.4

Model consists of SV196 vehicle combined with frequent values of LM1

$M_{gr5} := 4159$ kNm

B.4 COMBINATION OF ACTIONS — BS EN 1990

B.4.1 Serviceability Limit State — Cl. 6.5.3

Table B.1 – ψ factors for road bridges — Table NA.A2.1

		ψ_0	ψ_1	ψ_2
gr1a	TS	0.75	0.75	0
	UDL	0.75	0.75	0
	Pedestrian loads	0.40	0.40	0
gr3	Pedestrian loads	0	0.40	0
gr5	SV Vehicles	0	0	0

Characteristic combination — Eq. (6.14b)

$$E_d = E\left(\Sigma G_{k,j} + P + Q_{k,1} + \Sigma \psi_{0,i} Q_{k,i}\right)$$

$M_{dchar} := M_{bs} + M_{sf} + M_{gr5} = 6729.8457$ kNm

Only one traffic load group is to be appied in a combination. Since M_{gr5} is the greatest loading, it is applied for the characteristic combination.

BS EN 1990

Frequent combination Eq. (6.15b)

$$E_d = E\left(\Sigma G_{k,j} + P + \psi_{1,1}Q_{k,1} + \Sigma\psi_{2,i}Q_{k,i}\right)$$

$$M_{dfreq} := M_{bs} + M_{sf} + 0.75\cdot M_{gr1a} = 4974.596 \quad \text{kNm}$$

Of the frequent traffic load groups, M_{gr1a} is the greatest, and therefore is applied here.

Quasi-permanent combination Eq. (6.16b)

$$E_d = E\left(\Sigma G_{k,j} + P + \Sigma\psi_{2,i}Q_{k,i}\right)$$

$$M_{dquasi} := M_{bs} + M_{sf} = 2570.846 \quad \text{kNm}$$

The moments calculated here do not include the prestressing force. This will be added later in the design process, after the prestressing is designed.

B.4.2 Ultimate Limit State

Bridge design concerned with STR limit state

Table B.2 – Partial factors for design values of actions

	γ_{sup} (Unfavourable)	γ_{inf} (Favourable)	ψ_0
Self weight	1.35	0.95	-
Super-imposed DL	1.20	0.95	-
Prestress	1.10	0.90	-
Traffic	1.35	0	N/A

**Traffic loading will be the leading action

NA to BS EN 1990 Table NA.A2.4(B)
& NA to BS EN 1992-1-1 Cl. 2.4.2.2

Design to be based on Eq. (6.10) Cl. NA.2.3.7.1

BS EN 1990

$$E_d = E\left(\Sigma\gamma_{G,j}G_{k,j} + \gamma_P P + \gamma_{Q,1}Q_{k,1} + \Sigma\gamma_{Q,i}\psi_{0,i}Q_{k,i}\right)$$ Eq. (6.10)

$$M_{dult} := 1.35\cdot M_{bs} + 1.20\cdot M_{sf} + 1.35\cdot M_{gr5}$$

$$M_{dult} = 9035.1589 \quad \text{kNm}$$

The moments calculated here do not include the prestressing force. This will be added later in the design process.

B.5 INITIAL DESIGN OF THE PRESTRESSED BEAMS

For the initial design of the beams, the moment at transfer due to the self-weight of the beam and the moment at service due to the self-weight of the beam and wet slab are considered.

Self-weight of the beam:

$M_b = 1455.377$ kNm

Self-weight of the composite section:

$M_{bs} = 2236.627$ kNm

B.5.1 Beam Properties and Initial Prestress Loss Assumptions

$\alpha := 1 - 0.12 = 0.88$ $\beta := 1 - 0.20 = 0.8$

$A_b = 745153$ mm^2 $d := 1600$ mm

$y_b := 737.7$ mm $y_t := d - y_b = 862.3$ mm

$Z_{tbm} := 24.116 \times 10^7$ mm^3 $Z_{bbm} := 28.190 \times 10^7$ mm^3

B.5.2 Stress Limits

BS EN 1992-1-1

At transfer

$f_{trmax} := 0.6 \cdot f_{ckt} = 23.692$ MPa — Eq. (5.42)

$f_{trmin} := -1.0$ MPa — UK Practice

At service

$f_{max} := 0.6 \cdot f_{ck} = 30$ MPa — Eq. (5.42)

$f_{min} := 0$ MPa

Cl. 5.10.2.2(5) states that the limit for f_{max} can be raised to 0.7 $f_{ck}(t)$ for pre-tensioned members if it can be justified through tests or experience that longitudinal cracking is prevented. Conservatively, the limit will be kept at 0.6 $f_{ck}(t)$.

B.5.3 Basic Inequalities for Concrete Stresses

From the equations for stress in the top and bottom fibres, the following inequalities are determined.

At transfer

Top fibre: $$\frac{\alpha \cdot P_i}{A_b} - \frac{\alpha \cdot P_i \cdot e_b}{Z_{tbm}} + \frac{M_b}{Z_{tbm}} \geq f_{trmin} \qquad \text{(B.1a)}$$

Bottom fibre: $$\frac{\alpha \cdot P_i}{A_b} + \frac{\alpha \cdot P_i \cdot e_b}{Z_{bbm}} - \frac{M_b}{Z_{bbm}} \leq f_{trmax} \qquad \text{(B.1b)}$$

At service

Top fibre: $$\frac{\beta \cdot P_i}{A_b} - \frac{\beta \cdot P_i \cdot e_b}{Z_{tbm}} + \frac{M_{bs}}{Z_{tbm}} \leq f_{max} \qquad \text{(B.1c)}$$

Bottom fibre: $$\frac{\beta \cdot P_i}{A_b} + \frac{\beta \cdot P_i \cdot e_b}{Z_{bbm}} - \frac{M_{bs}}{Z_{bbm}} \geq f_{min} \qquad \text{(B.1d)}$$

B.5.4 Required Elastic Moduli

By combining the inequalities (B.1a) to (B.1d), the following inequalities for required elastic moduli are determined and verified.

$$Z_{tbm} = 2.412 \times 10^8 \ \text{mm}^3 \geq \frac{\alpha \cdot \left(M_{bs} \cdot 10^6\right) - \beta \cdot \left(M_b \cdot 10^6\right)}{\alpha \cdot f_{max} - \beta \cdot f_{trmin}} = 2.956 \times 10^7 \ \text{mm}^3$$

$$Z_{bbm} = 2.819 \times 10^8 \ \text{mm}^3 \geq \frac{\alpha \cdot \left(M_{bs} \cdot 10^6\right) - \beta \cdot \left(M_b \cdot 10^6\right)}{\beta \cdot f_{trmax} - \alpha \cdot f_{min}} = 4.242 \times 10^7 \ \text{mm}^3$$

Note that these equations do not take into account the prestress force and eccentricity. As a result, larger values for Z_{tbm} and Z_{bbm} should be chosen than those calculated.

B.5.5 Determination of Prestress and Eccentricity

By rearranging the basic inequalities (B.1a) to (B.1d), the permissible zones for initial prestressing force, P_i, and eccentricity, e_b, are defined which make up the Magnel Diagram in Figure B.2.

$$\frac{1}{P_i} \leq \frac{\alpha \cdot \left(\frac{Z_{tbm}}{A_b} - e_b \right)}{Z_{tbm} \cdot f_{trmin} - M_b} \qquad \frac{10^8}{P_i} \geq -16.7872 + 0.0519 e_b \quad 1/N \quad \text{(B.2a)}$$

$$\frac{1}{P_i} \geq \frac{\alpha \cdot \left(\frac{Z_{bbm}}{A_b} + e_b \right)}{Z_{bbm} \cdot f_{trmax} + M_b} \qquad \frac{10^8}{P_i} \geq 4.0928 + 0.0108 e_b \quad 1/N \quad \text{(B.2b)}$$

$$\frac{1}{P_i} \geq \frac{\beta \cdot \left(\frac{Z_{tbm}}{A_b} - e_b \right)}{Z_{tbm} \cdot f_{max} - M_{bs}} \qquad \frac{10^8}{P_i} \geq 5.1801 - 0.0160 e_b \quad 1/N \quad \text{(B.2c)}$$

$$\frac{1}{P_i} \leq \frac{\beta \cdot \left(\frac{Z_{bbm}}{A_b} + e_b \right)}{Z_{bbm} \cdot f_{min} + M_{bs}} \qquad \frac{10^8}{P_i} \leq 13.5315 + 0.0358 e_b \quad 1/N \quad \text{(B.2d)}$$

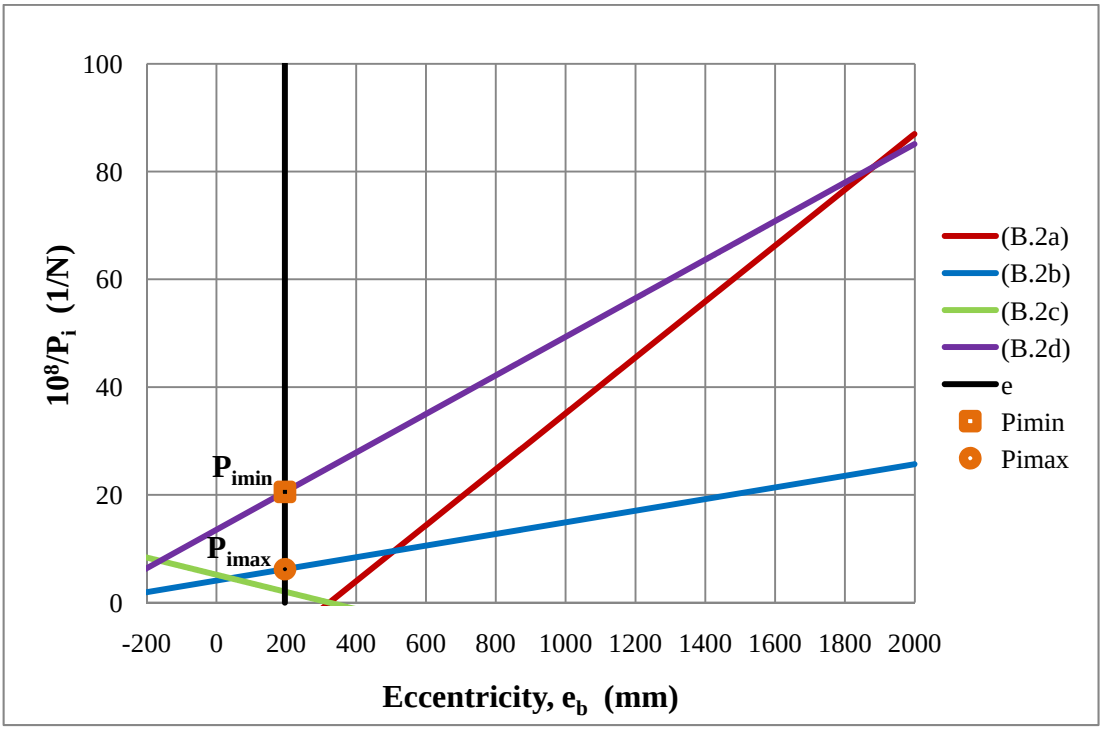

Figure B.2 – Magnel Diagram

From the Magnel Diagram:

Upper limit of eccentricity; let Eq. (B.2a) = Eq. (B.2d):

Try $e_{max} := 1500$ mm

Given $-16.7872 + 0.0519e_{max} = 13.5315 + 0.0358e_{max}$

Find$(e_{max}) = 1883.149$ mm

Lower limit of eccentricity; let Eq. (B.2c) = Eq. (B.2d):

Try $e_{min} := -100$ mm

Given $5.1801 - 0.0160e_{min} = 13.5315 + 0.0358e_{min}$

Find$(e_{min}) = -161.224$

Selection of prestressing strands:

Eccentricity of the strands

Maximum allowable eccentricity based on nominal cover:

$e_{maxallow} := y_b - c_{nom} = 689.7$ mm

Take: $N_{str} := 58$ strands

$c = 541.552$ mm

$e_b := y_b - c = 196.148$ mm

Figure B.3 illustrates the cross section and strand layout of the beam for this eccentricity.

N_{str}	c' (mm)
17	60
11	110
4	160
2	210
2	260
4	800
2	1200
2	1250
4	1300
2	1350
4	1400
4	1500

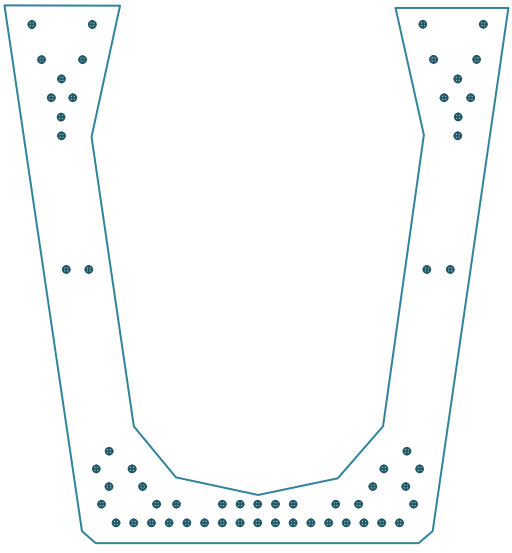

Figure B.3 – Beam cross section for U12 Beam

Limits for initial prestressing force

$$P_{imin} := \frac{10^8}{\left(13.5315 + 0.0358e_b\right)} \cdot 10^{-3} = 4865.326 \quad kN$$

$$P_{imax} := \frac{10^8}{\left(4.0928 + 0.0108e_b\right)} \cdot 10^{-3} = 16099.945 \quad kN$$

Y1820S7G strands with 15.2mm ϕ are chosen

$P_{ustr} = 300$ kN $\quad P_{istr} = 219$ kN

Required prestressing force after allowances for losses:

BS EN 1992-1-1
Cl. 5.10.3(2)

(BS EN 1992-1-1 limits stress of the strands afer allowance for losses to avoid stresses in tendons under serviceability conditions that could lead to inelastic deformation of the tendons)

$$P_{req} := \frac{P_{imin}}{0.75} = 6487.101 \quad kN$$

$$N_{req} := \frac{P_{req}}{P_{ustr}} = 21.624 \quad \text{strands} < N_{str} = 58 \quad \text{strands} \quad \text{OK!}$$

Total prestressing force:

$$P_{pk} := P_{ustr} \cdot N_{str} = 17400 \quad kN > P_{req} = 6487.101 \quad kN \quad \text{OK!}$$

$$A_p := A_{pstr} \cdot N_{str} = 9570 \quad mm^2$$

Actual prestressing force:

$$P_i := P_{istr} \cdot N_{str} = 12702 \quad kN > P_{imin} = 4865.326 \quad kN \quad \text{OK!}$$

$$< P_{imax} = 16099.9449 \quad kN \quad \text{OK!}$$

B.5.6 Summary of Selected Prestress – 15.2mm ϕ Y1820S7G strands

Number of Strands: $N_{str} = 58$

Initial Prestressing Force: $P_i = 12702$ kN

Eccentricity: $e_b = 196.148$ mm (Straight tendon profile)

B.5.7 Verification of the Basic Inequalities

At transfer

$$f_{trtbm} := \frac{\alpha \cdot P_i \cdot 10^3}{A_b} - \frac{\alpha \cdot P_i \cdot 10^3 \cdot e_b}{Z_{tbm}} + \frac{M_b \cdot 10^6}{Z_{tbm}} \qquad \text{(B.1a)}$$

$f_{trtbm} = 11.944$ MPa $\geq$ $f_{trmin} = -1$ MPa OK!

$$f_{trbbm} := \frac{\alpha \cdot P_i \cdot 10^3}{A_b} + \frac{\alpha \cdot P_i \cdot 10^3 \cdot e_b}{Z_{bbm}} - \frac{M_b \cdot 10^6}{Z_{bbm}} \qquad \text{(B.1b)}$$

$f_{trbbm} = 17.615$ MPa $\leq$ $f_{trmax} = 23.692$ MPa OK!

At service

$$f_{tbm} := \frac{\beta \cdot P_i \cdot 10^3}{A_b} - \frac{\beta \cdot P_i \cdot 10^3 \cdot e_b}{Z_{tbm}} + \frac{M_{bs} \cdot 10^6}{Z_{tbm}} \qquad \text{(B.1c)}$$

$f_{tbm} = 14.646$ MPa $\leq$ $f_{max} = 30$ MPa OK!

$$f_{bbm} := \frac{\beta \cdot P_i \cdot 10^3}{A_b} + \frac{\beta \cdot P_i \cdot 10^3 \cdot e_b}{Z_{bbm}} - \frac{M_{bs} \cdot 10^6}{Z_{bbm}} \qquad \text{(B.1d)}$$

$f_{bbm} = 12.773$ MPa $\geq$ $f_{min} = 0$ MPa OK!

B.5.8 Confirmation of Selected Tendon Profile

By rearranging inequalities (B.2a) to (B.2d) the range of allowable eccentricity, i.e. the cable zone, can be determined at multiple sections along the member. The limits correspond to the resultant of tendons.

$$e_b \leq \frac{Z_{tbm}}{A_b} + \frac{1}{\alpha \cdot P_i}\left(M_b - Z_{tbm} \cdot f_{trmin}\right) \qquad \text{(B.3a)}$$

$$e_b \leq \frac{1}{\alpha \cdot P_i} \cdot \left(Z_{bbm} \cdot f_{trmax} + M_b\right) - \frac{Z_{bbm}}{A_b} \qquad \text{(B.3b)}$$

$$e_b \geq \frac{Z_{tbm}}{A_b} + \frac{1}{\beta \cdot P_i} \cdot \left(M_{bs} - Z_{tbm} \cdot f_{max}\right) \qquad \text{(B.3c)}$$

$$e_b \geq \frac{1}{\beta \cdot P_i} \cdot \left(M_{bs} + Z_{bbm} \cdot f_{min}\right) - \frac{Z_{bbm}}{A_b} \qquad \text{(B.3d)}$$

Table B.3 defines M_b and M_{bs} at multiple locations along the beam and the corresponding limits for eccentricity at those locations. These equations ensure that requirements for the concrete stresses are met.

Table B.3 – Limits of eccentricity for the prestressed beam

Position (m)	M_b (kNm)	M_{bs} (kNm)	Eccentricity Limits (mm)			
			e_b (B.3a)	e_b (B.3b)	e_b (B.3c)	e_b (B.3d)
0	0.000	0.000	345.21	**219.19**	-388.34	**-378.31**
2.5	523.935	805.185	392.09	**266.06**	-309.10	**-299.07**
5	931.440	1431.440	428.54	**302.52**	-247.47	**-237.44**
7.5	1222.515	1878.765	454.58	**328.56**	-203.45	**-193.42**
10	1397.160	2147.160	470.21	**344.18**	-177.03	**-167.01**
12.5	1455.375	2236.625	475.42	**349.39**	-168.23	**-158.21**

Symmetric about midspan.

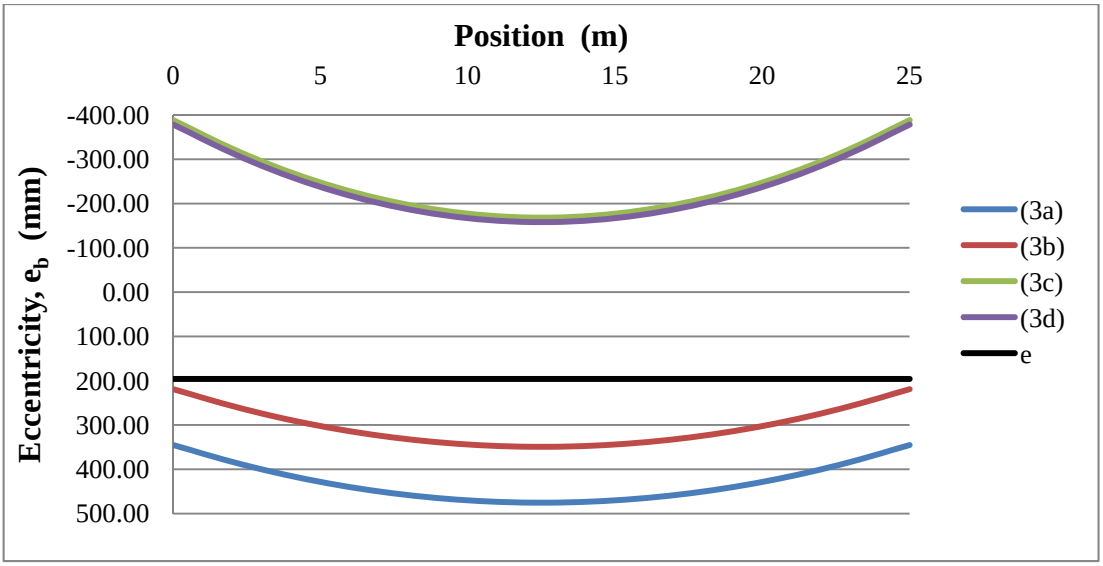

Figure B.4 – Profile of eccentricity limits for the prestressed beam

It can be seen that equations (B.3b) and (B.3d) will control for this stage. Based on the limits, the eccentricity of 196.148 mm determined in B.5.5 is satisfactory.

B.6 DESIGN OF THE COMPOSITE STRUCTURE

Properties of the Composite Section

$A_c := A_b + A_s = 1145153 \quad mm^2$ $\qquad d_c := d + d_s = 1800 \quad mm$

$$y_c := \frac{A_b \cdot y_b + A_s \cdot \left(d_c - 0.5 d_s\right)}{A_b + A_s} = 1073.83 \quad mm$$

$I_b := Z_{bbm} \cdot y_b = 2.08 \times 10^{11} \quad mm^4$ $\qquad I_s := \frac{s_{bm} \cdot d_s^{\,3}}{12} = 1.333 \times 10^{9} \quad mm^4$

$I_c := I_b + A_b \cdot \left(y_c - y_b\right)^2 + I_s + A_s \cdot \left(d_c - 0.5 d_s - y_c\right)^2 = 4.503 \times 10^{11} \quad mm^4$

$y_{tbm} := d - y_c = 526.17 \quad mm$ $\qquad y_{tsb} := d_c - y_c = 726.17 \quad mm$

$y_{bbm} := y_c = 1073.83 \quad mm$ $\qquad y_{bsb} := d - y_c = 526.17 \quad mm$

Imposed loading: $M_{imp} := M_{dchar} - M_{bs} = 4493.219 \quad kNm$

B.6.1 Stress Limits

For composite prestressed beams at service **BS EN 1992-1-1**

$f_{bmax} := 0.6 \cdot f_{ck} = 30 \quad MPa$ Eq (5.42)

$f_{bmin} := -f_{ctm} = -4.1 \quad MPa$

For composite concrete slab at service

$f_{smax} := 0.6 \cdot f_{sck} = 24 \quad MPa$ Eq (5.42)

$f_{smin} := -f_{sctm} = -3.5 \quad MPa$

B.6.2 Verification of the Inequalities for Final Stresses

At this point the characteristic serviceability load is considered in full. (Prestressing force part of f_{tbm} and f_{bbm})

Verification at the critical section:

For the beam

$$f_{ctbm} := f_{tbm} + \frac{M_{imp} \cdot 10^6 \cdot y_{tbm}}{I_c} = 19.896 \quad \text{MPa} \qquad \text{(B.4a)}$$

$f_{ctbm} = 19.896$ MPa $<$ $f_{bmax} = 30$ MPa OK!

$$f_{cbbm} := f_{bbm} - \frac{M_{imp} \cdot 10^6 \cdot y_{bbm}}{I_c} = 2.059 \quad \text{MPa} \qquad \text{(B.4b)}$$

$f_{cbbm} = 2.059$ MPa $>$ $f_{bmin} = -4.1$ MPa OK!

For the slab

$$f_{ctsb} := \frac{M_{imp} \cdot 10^6 \cdot y_{tsb}}{I_c} = 7.2457 \quad \text{MPa} \qquad \text{(B.4c)}$$

$f_{ctsb} = 7.246$ MPa $<$ $f_{smax} = 24$ MPa OK!

$$f_{cbsb} := \frac{M_{imp} \cdot 10^6 \cdot y_{bsb}}{I_c} = 5.25 \quad \text{MPa} \qquad \text{(B.4d)}$$

$f_{cbsb} = 5.25$ MPa $>$ $f_{smin} = -3.5$ MPa OK!

For the slab, the concrete stresses only need checked at midspan since it is always in compression. Therefore, since the requirements at midspan are met and it may be assumed that they are met at all locations.

On the contrary, the stresses in the beam are in both compression and tension. Therefore, the stresses must be checked at each section.

Verification for the beam at all locations

NOTE: Stresses in the beam are verified every 2.5m along the beam.
Values for M_{gr5} are taken from A.4.3 in Appendix A.
All results are symmetric about the centre support.

Table B.4 – Imposed loading every 2.5m

Position (m)	M_{sf} (kNm)	M_{gr5} (kNm)	M_{imp} (kNm)
0	0.000	0.000	0
2.5	120.319	1535.272	1656
5	213.900	2709.682	2924
7.5	280.744	3511.724	3793
10	320.850	4007.999	4329
12.5	334.219	4159.000	4494

Table B.5 – Verification of concrete stresses in the beam

Position (m)	e_b (mm)	M_{imp} (kNm)	f_{tbm} (MPa)	f_{bbm} (MPa)	f_{ctbm} (MPa)	f_{cbbm} (MPa)
0	196.148	0	5.372	20.708	5.372	20.708
2.5	196.148	1656	8.711	17.851	10.646	13.902
5	196.148	2924	11.308	15.630	14.724	8.657
7.5	196.148	3793	13.163	14.043	17.594	4.998
10	196.148	4329	14.275	13.091	19.334	2.768
12.5	196.148	4494	14.646	12.773	**19.897**	**2.057**
Limits			30	0	30	-4.1

Requirements for concrete stresses are met at all locations.

B.7 DEFLECTION CHECKS

BS EN 1992-2 does not provide specific limits for deflection, but specifies that the deformation of the structure should not be such that it adversely affects its proper function or appearance. The limits should be set on a case by case basis.

For the purpose of this design example, it has been decided to apply a limit of L/1000 which is specified in the American AASHTO LFD codes.

Deflections are checked at midspan, where the deflection will be the greatest.

$P_i = 12702$ kN $\qquad e_b = 196.148$ mm

$L_s = 25$ m $\qquad$ Assume limit of: $\dfrac{L_s \cdot 1000}{1000} = 25$ mm

At transfer (non-composite section)

$E_{cmt} = 34.845$ GPa $\qquad I_b = 2.08 \times 10^{11}$ mm^4

$w_b = 18.629$ kN/m

$$\delta_t := \frac{5}{384} \cdot \frac{w_b \cdot \left(L_s \cdot 10^3\right)^4}{E_{cmt} \cdot 10^3 \cdot I_b} - \frac{1}{8} \cdot \frac{P_i \cdot 10^3 \cdot e_b \cdot \left(L_s \cdot 10^3\right)^2}{E_{cmt} \cdot 10^3 \cdot I_b} = -13.786 \text{ mm}$$

At slab placement (non-composite section)

$E_{cm} = 37$ GPa $\qquad I_b = 2.08 \times 10^{11}$ mm^4

$\alpha = 0.88$ $\qquad w_s := w_b + \gamma_{rcwet} \cdot \dfrac{A_s}{10^6} = 29.029$ kN/m

$$\delta_{sl} := \frac{5}{384} \cdot \frac{w_s \cdot \left(L_s \cdot 10^3\right)^4}{E_{cm} \cdot 10^3 \cdot I_b} - \frac{1}{8} \cdot \frac{\alpha \cdot P_i \cdot 10^3 \cdot e_b \cdot \left(L_s \cdot 10^3\right)^2}{E_{cm} \cdot 10^3 \cdot I_b} = -3.072 \text{ mm}$$

At service (composite section, frequent load combination)

$\beta = 0.8$ $\qquad I_c = 4.503 \times 10^{11}$ mm^4

$M_{dfreq} = 4974.596$ kNm $\qquad w_{freq} := \dfrac{M_{dfreq} \cdot 8}{L_s^2} = 63.675$ kN/m

BS EN 1990 Cl. A2.4.2(3)

Conservatively, the modulus of elasticity for the slab (C40/50) is applied.

$E_{scm} = 35$ GPa

Determine effective modulus of elasticity: **BS EN 1992-1-1**

$A_b = 7.452 \times 10^5$ mm^2 $u := 1600 \cdot 2 + 970 = 4170$ mm Figure 3.1

$h_0 := \frac{2 \cdot A_b}{u} = 357.388$ mm

$\varphi := 1.2$ for $t_0 > 100$ days

$E_{ceff} := \frac{E_{scm}}{1 + \varphi} = 15.909$ GPa Eq (7.20)

$$\delta_s := \frac{5}{384} \cdot \frac{w_{freq} \cdot \left(L_s \cdot 10^3\right)^4}{E_{ceff} \cdot 10^3 \cdot I_c} - \frac{1}{8} \cdot \frac{\beta \cdot P_i \cdot 10^3 \cdot e_b \cdot \left(L_s \cdot 10^3\right)^2}{E_{ceff} \cdot 10^3 \cdot I_c} = 23.471 \text{ mm}$$

B.8 ULTIMATE BENDING MOMENT RESISTANCE

Partial factors for the steel and concrete: **BS EN 1992-1-1**

$\gamma_c := 1.50$ for concrete Cl. 2.4.2.4 & Table NA.1

$\gamma_s := 1.15$ for prestressing steel

Strain limit:

$\varepsilon_{ud} := 0.0200$ Cl. 3.3.6(7)

B.8.1 Stress-Strain Relationship for the Prestressing Strands

p1 - at yield point of steel:

$\sigma_{p1} := \frac{f_{p0.1k}}{\gamma_s} = 1361.043$ MPa $\varepsilon_{p1} := \frac{\sigma_{p1}}{E_s \cdot 1000} = 0.0070$

p3 - at failure of steel:

$\sigma_{p3} := \frac{f_{pk}}{\gamma_s} = 1582.609$ MPa $\varepsilon_{p3} := \frac{\varepsilon_{ud}}{0.9} = 0.022$

p2 - at maximum design:

$\varepsilon_{p2} := \varepsilon_{ud} = 0.0200$

$$\sigma_{p2} := \sigma_{p1} + \left(\sigma_{p3} - \sigma_{p1}\right) \cdot \frac{\left(\varepsilon_{p2} - \varepsilon_{p1}\right)}{\left(\varepsilon_{p3} - \varepsilon_{p1}\right)} = 1550.306 \text{ MPa}$$

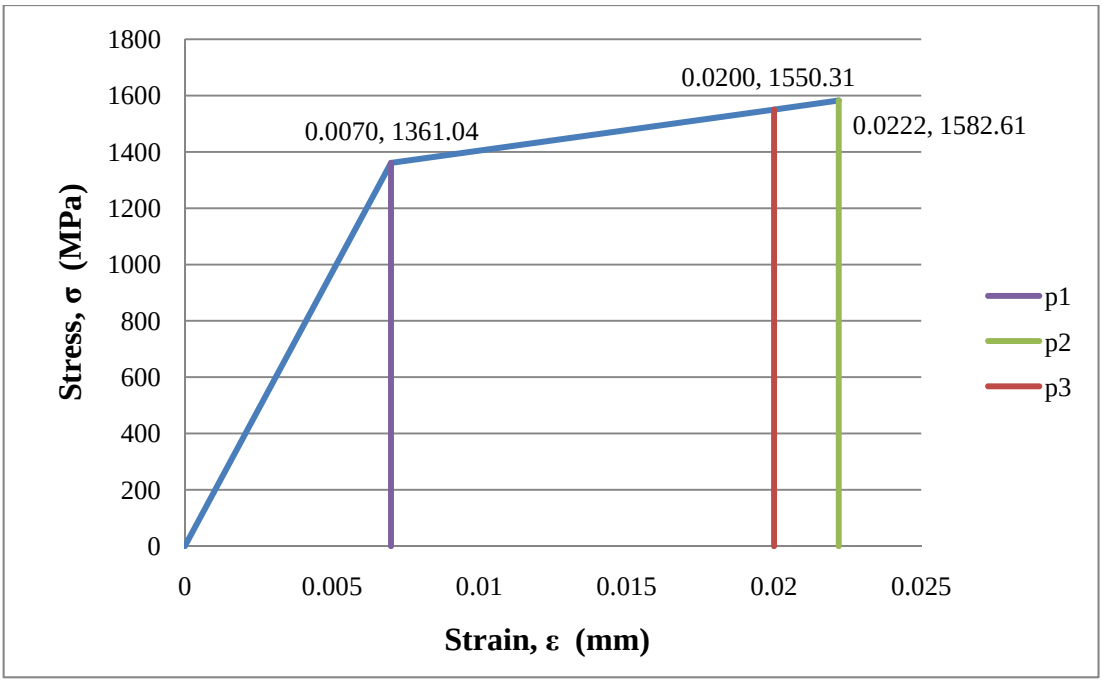

Figure B.5 – Stress-strain relationship for the prestressing steel

B.8.2 Stress and Strain Distribution for the Beam and Slab

Ultimate compressive strain in the concrete, ε_c: **BS EN 1992-1-1**

$\varepsilon_c := 0.0035$ Table 3.1

Strain in the prestressing steel at ULS due to prestress only, ε_{p0}:

Partial factor for prestress: **NA to BS EN 1992-1-1**

$\gamma_{pfav} := 0.9$ Cl. 2.4.2.2(1)

Initial stress in tendons:

$$f_{pi} := \frac{P_{istr} \cdot 10^3}{A_{pstr}} = 1327.273 \quad \text{MPa}$$

$$\varepsilon_{p0} := \frac{f_{pi}}{E_s \cdot 10^3} = 0.00681$$

Total strain at ULS, ε_p:

$\varepsilon_p = \Delta\varepsilon_p + \gamma_{p,fav}\varepsilon_{p0} = \Delta\varepsilon_p + 0.00613$

Defining the compressive zone:

BS EN 1992-1-1
Cl. 3.1.6 &
Cl. 3.1.7(3)

$\lambda := 0.80$ $\quad \lambda x = 0.8x$

$\eta := 1.0$

NA to BS EN 1992-2
Cl. 3.1.6

$\alpha_{cc} := 0.85$

$f_{cd} := \frac{\alpha_{cc} \cdot f_{ck}}{\gamma_c} = 28.333$ MPa $\quad f_{scd} := \frac{\alpha_{cc} \cdot f_{sck}}{\gamma_c} = 22.667$ MPa

$\eta \cdot f_{cd} = 28.333$ MPa $\quad \eta \cdot f_{scd} = 22.667$ MPa

$$\frac{\eta \cdot \alpha_{cc}}{\gamma_c} = 0.567 \quad f_{ck}$$

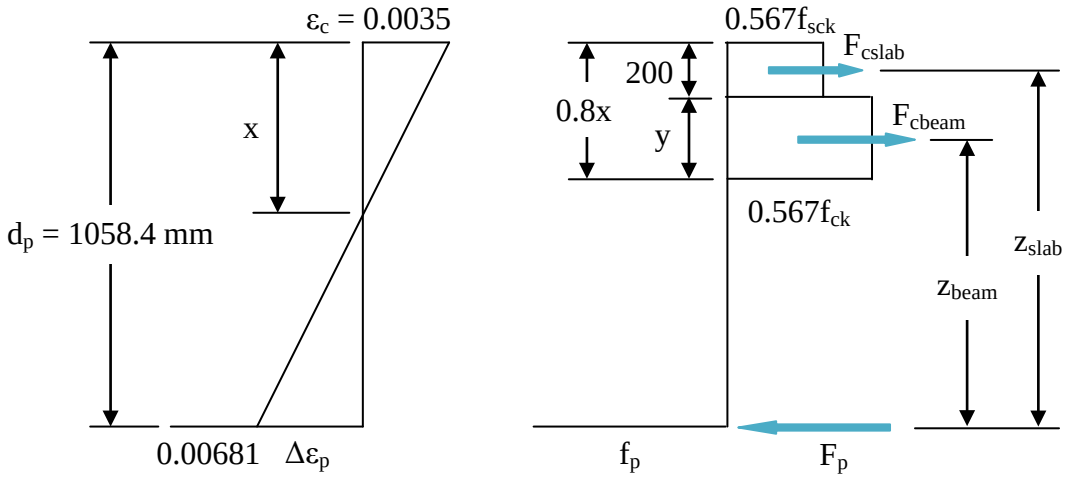

Figure B.6 – Strain and stress diagrams

This check is based on a resultant force from the prestressing strands. For more accurate results, the prestressing force should be considered at each row of strands, since some of the strands fall inside the compressive zone of the concrete. Due to time constraints, this is not done here.

B.8.3 Calculation of the Ultimate Bending Moment Resistance

$\Delta\varepsilon_p$ can be determined from the following ratio:

$$\frac{0.0035}{x} := \frac{\Delta\varepsilon_p}{d_p - x} \quad \text{where} \quad d_p := d - c = 1058.448 \text{ mm}$$

The value of x is determined from $F_p = F_c$

Steel tensile force:

$F_p = f_p A_p = \min(\varepsilon_p E_s , f_{pd}) A_p = \min[(\Delta\varepsilon_p + \gamma_{p,fav}\varepsilon_{p0})E_s , f_{pd}]A_p$

Concrete compressive force:

$F_c = F_{c,slab} + F_{c,beam}$

$F_c = s_{bm} d_s (0.567 f_{sck}) + 2(0.8x - d_s)(254)(0.567 f_{ck})$

At $x := 722.25$ mm ($0.8x = 577.8$ mm), $F_p = F_c$

$$\Delta\varepsilon_p := \frac{0.0035\cdot\left(d_p - x\right)}{x} = 0.002 \qquad f_{pd} := \sigma_{p1}$$

$$F_p := \min\left[\left(\Delta\varepsilon_p + \gamma_{pfav}\cdot\varepsilon_{p0}\right)\cdot E_s , f_{pd}\right]\cdot A_p = 14472.1426 \text{ kN}$$

$y := 0.8x - d_s = 377.8$ mm $\qquad b_{bm} := 0.5(340 + 165) = 252.5$ mm (avg)

$$F_{cslab} := s_{bm}\cdot d_s\cdot\left(\frac{\eta\cdot\alpha_{cc}}{\gamma_c}\cdot f_{sck}\right) = 9.067\times 10^{6} \text{ kN}$$

$$F_{cbeam} := y\cdot 2\cdot b_{bm}\cdot\left(\frac{\eta\cdot\alpha_{cc}}{\gamma_c} f_{ck}\right) = 5.406\times 10^{6} \text{ kN}$$

$$F_c := \left(F_{cslab} + F_{cbeam}\right)\cdot 10^{-3} = 14472.355 \text{ kN}$$

Check strain limits:

$\varepsilon_p := \Delta\varepsilon_p + \gamma_{pfav}\cdot\varepsilon_{p0} = 0.008$ << $\varepsilon_{ud} = 0.0200$ OK!

Determine ultimate bending moment resistance (M_{Rd}):

$z_{slab} := d_p - d_s\cdot 0.5 = 958.448$ mm

$z_{beam} := d_p - d_s - 0.5y = 669.548$ mm

$M_{Rd} := F_{cslab}\cdot z_{slab}\cdot 10^{-6} + F_{cbeam}\cdot z_{beam}\cdot 10^{-6} = 12309.3$ kNm

Maximum bending moment applied to the beam:

$M_{Ed} := M_{dult} = 9035.159 \quad kNm$

$$\frac{M_{Ed}}{M_{Rd}} = 0.734 \quad < \quad 1.00$$

The ultimate limit state requirements for bending moment are met.

B.9 SHEAR DESIGN AT ULTIMATE LIMIT STATE

B.9.1 Shear Forces Acting on the Beam

At the ultimate limit state

At 0m: $V_{bs} := \frac{w_{bs} \cdot L_s}{2} = 357.86 \quad kN$ $V_{sf} := \frac{w_{sf} \cdot L_s}{2} = 53.475 \quad kN$

$V_{gr5} := 652.9 \quad kN$

See Table B.2 for ULS factors

$V_{Ed} := 1.35 \cdot V_{bs} + 1.20 \cdot V_{sf} + 1.35 \cdot V_{gr5} = 1428.696 \quad kNm$

Table B.6 – Summary of shear forces acting on the beam

Position (m)	V_{bs} (kN)	V_{sf} (kN)	V_{gr5} (kN)	V_{Ed} (kN)
0	357.860	53.475	652.909	1429
1.25	322.074	48.128	636.163	1351
2.5	286.288	42.780	544.824	1173
3.75	250.502	37.433	517.170	1081
5	214.716	32.085	441.787	925
6.25	178.930	26.738	407.810	824
7.5	143.144	21.390	323.529	656
8.75	107.358	16.043	299.725	569
10	71.572	10.695	213.735	398
11.25	35.786	5.348	203.423	329
12.5	0.000	0.000	99.701	135

Symmetric about midspan.

V_{Ed} is factored as the example above shows.

For simplicity in design, the shear links are designed based on the maximum shear force at 0m, although in a true design the design should be based on a distance d from the support.

B.9.2 Shear Resistance of the Concrete

BS EN 1992-2
Cl. 6.2.2(101),
Table NA.1

$V_{Rd,c} = [C_{Rd,c}k(100\rho_1 f_{ck})^{1/3} + k_1\sigma_{cp}]b_w d$

with a minimum of $V_{Rd,c} = (\nu_{min} + k_1\sigma_{cp})b_w d$

where $\gamma_c = 1.5$ $\quad C_{Rdc} := \frac{0.18}{\gamma_c} = 0.12$

$k_1 := 0.15$

$f_{ck} = 50$ MPa

$d_p = 1058.448$ mm

$k := 1 + \sqrt{\frac{200}{d_p}} = 1.435 \quad < \quad 2.0$

$b_w := 2 \cdot 165 = 330$ mm $\quad A_p = 9570$ mm^2

$\rho_1 = \frac{A_p}{b_w \cdot d_p} = 0.027 \quad > 0.020$; therefore, $\rho_1 := 0.02$

$\gamma_{pfav} = 0.9$ (from Table B.4)

BS EN 1992-2
Cl. 3.1.6(101)P
& Table NA.1

$\alpha_{scc} := 1.0$

$f_{shcd} := \frac{\alpha_{scc} \cdot f_{ck}}{\gamma_c} = 33.333$ MPa

$\sigma_{cp} := \frac{\gamma_{pfav} \cdot 0.75 \cdot P_i \cdot 10^3}{A_c}$

$\sigma_{cp} = 7.487$ MPa $\quad > \quad 0.2 \cdot f_{shcd} = 6.667$ MPa

$\upsilon_{min} := 0.035k^{1.5} \cdot f_{ck}^{0.5} = 0.425$

$$V_{Rdc} := \left[C_{Rdc} \cdot k \cdot \left(100 \cdot \rho_1 \cdot f_{ck}\right)^{\frac{1}{3}} + k_1 \cdot \sigma_{cp} \right] \cdot b_w \cdot d_p \cdot 10^{-3} = 671.391 \text{ kN}$$

with a minimum of $V_{rdcmin} := \left(\upsilon_{min} + k_1 \cdot \sigma_{cp}\right) \cdot b_w \cdot d_p \cdot 10^{-3} = 540.822$ kN

Based on these results, shear reinforcement will be required. It should be noted that shear reinforcement will not be required in the center of the span, however some shear links may be provided for stability of the beam.

B.9.3 Shear Reinforcement

Assumptions for Shear Reinforcement:

10 mm ϕ strands $\phi_{sh} := 10$ mm

$f_{yk} := 500$ MPa $A_{sh} := 79$ mm^2

4 legged shear links at each location

For members with shear reinforcement, the shear resistance is the smaller of: **BS EN 1992-2** Cl. 6.2.3(103)

$V_{Rd,s} = (A_{sw}/s)\, z\, (0.8 f_{ywd})\, \cot\theta$ Eq (6.8)

and $V_{Rd,max} = \alpha_{cw} b_w z \upsilon_1 f_{cd} / (\cot\theta + \tan\theta)$ Eq (6.9)

First, the crushing strength, $V_{Rd,max}$ of the concrete diagonal strut is checked.

Cl. 6.2.3(103) NOTE 3 and 4

$b_w = 330$ mm $z_{beam} = 669.548$ mm

$f_{shcd} = 33.333$ MPa

$\upsilon_1 := 0.6 \cdot \left(1 - \frac{f_{ck}}{250}\right) = 0.48$

$\alpha_{cw} := 1.25$ for $0.25 f_{shcd} < \sigma_{cp} = 7.487 < 0.5 f_{shcd}$

Start by assuming: $\theta := 22$

$\cot\theta := 2.5$ $\tan\theta := 0.40$

$V_{Rdmax} := \frac{\alpha_{cw} \cdot b_w \cdot z_{beam} \cdot \upsilon_1 \cdot f_{shcd}}{(\cot\theta + \tan\theta) 1000} = 1523.8$ kN > $V_{Edmax} = 1429$ kN OK!

Next, the number of required shear links must be determined with Equation (6.8)

$V_{Rd,s} = (A_{sw}/s)\, z\, (0.8 f_{ywd})\, \cot\theta$ ---> $(A_{sw}/s) = V_{Rd,s}/[z\, (0.8 f_{ywd})\, \cot\theta]$

where $A_{sw} := 4 \cdot A_{sh} = 316$ mm^2 $z_{beam} = 669.548$ mm

$f_{ywd} := f_{yk} = 500$ MPa

$\cot\theta = 2.5$

assume $V_{Rd,s} = V_{Ed}$

From the results for shear resistance of the concrete and the applied shear forces in Table B.6 it is determined that shear reinforcement is required from 0m to 7.5m and 17.5m to 25.0m.

Beginning at 5.0m, with $V_{Ed5} := 925 \quad kN$

$$s_{req1} := \frac{A_{sw} \cdot z_{beam} \cdot 0.8 \cdot f_{ywd} \cdot \cot\theta}{V_{Ed5} \cdot 1000} = 228.732 \quad mm$$

Take $s_1 := 175 \quad mm$

$$V_{Rds1} := \frac{A_{sw} \cdot z_{beam} \cdot 0.8 \cdot f_{ywd} \cdot \cot\theta}{s_1 \cdot 1000} = 1209.013 \quad kN$$

Spacing s_1 satisfies requirements from 2.5m to 7.5m

Then at 1.25m, with $V_{Ed1.25} := 1351 \quad kN$

$$s_{req2} := \frac{A_{sw} \cdot z_{beam} \cdot 0.8 \cdot f_{ywd} \cdot \cot\theta}{V_{Ed1.25} \cdot 1000} = 156.608 \quad mm$$

Take $s_2 := 150 \quad mm$

$$V_{Rds2} := \frac{A_{sw} \cdot z_{beam} \cdot 0.8 \cdot f_{ywd} \cdot \cot\theta}{s_2 \cdot 1000} = 1410.515 \quad kN$$

Spacing s_2 satisfies requirements from 1.25m to 2.5m

Then at 0m, with $V_{Ed0} := 1429 \quad kN$

$$s_{req3} := \frac{A_{sw} \cdot z_{beam} \cdot 0.8 \cdot f_{ywd} \cdot \cot\theta}{V_{Ed0} \cdot 1000} = 148.06 \quad mm$$

Take $s_3 := 125 \quad mm$

$$V_{Rds3} := \frac{A_{sw} \cdot z_{beam} \cdot 0.8 \cdot f_{ywd} \cdot \cot\theta}{s_3 \cdot 1000} = 1692.618 \quad kN$$

Spacing s_3 satisfies requirements from 0m to 1.25m

From the results, assume the following distribution of shear links:

Maximum spacing: $0.75 \cdot d = 1200$ mm

Starting at 0m, 10 spaces at 125mm	$10 \cdot 0.125 = 1.25$	m
Starting at 1.25m, 9 spaces at 150mm	$1.25 + 9 \cdot .150 = 2.6$	m
Starting at 2.6m, take 28 spaces at 175mm	$2.6 + 28 \cdot 0.175 = 7.5$	m

Provide links at 1000mm c/c for the remaining span

All results are symmetric about midspan.

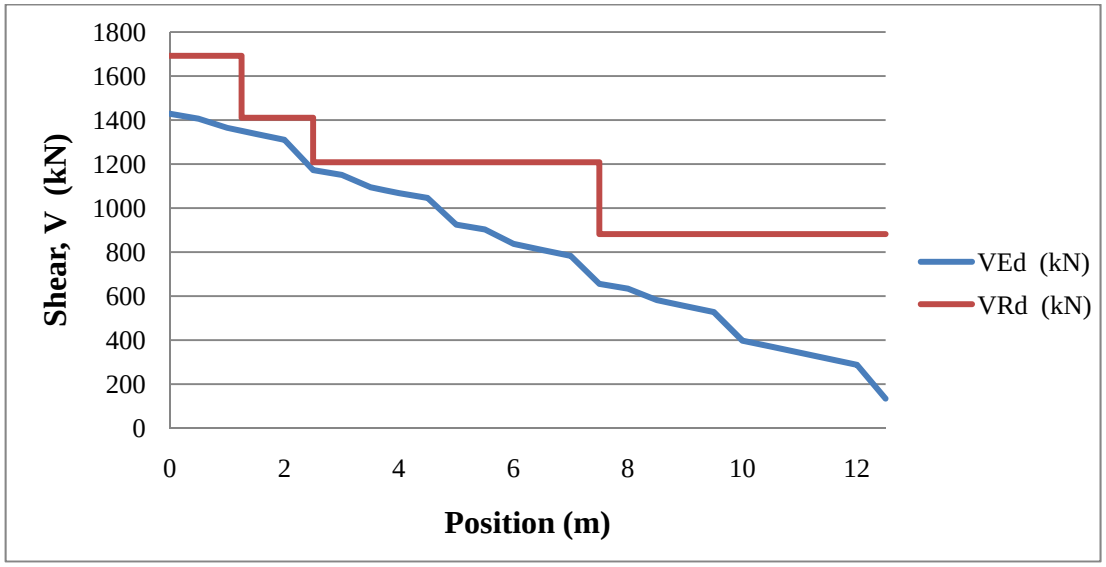

Figure B.7 – Plot of shear forces and shear resistance for the beam

B.10 DESIGN SUMMARY

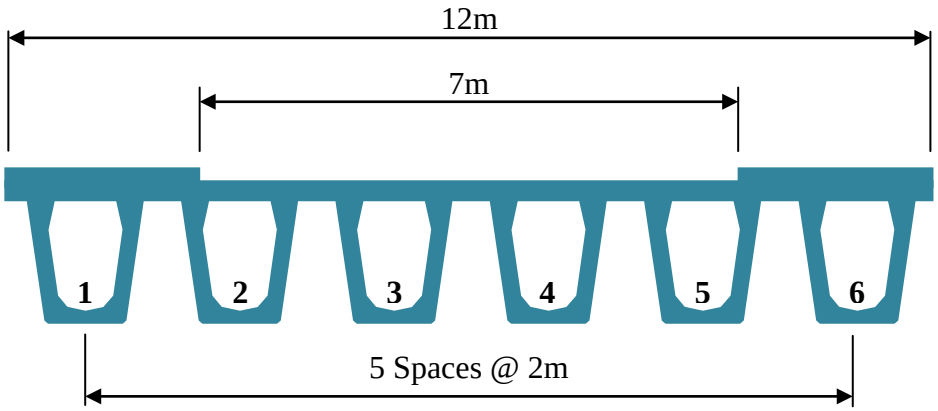

Figure B.8 – Bridge cross section

Span Length	25.0 metres
Beam type	Pre-tensioned U12 Beams
Concrete Properties	Beam: C50/60; Slab: C40/50
Prestressing Strands	Y1820S7G – 15.2mm diameter, 7 wire drawn strands
Nominal cover	48 mm
Number of strands	58
Total initial prestress force	12702 kN
Total prestress force	17400 kN
Eccentricity of CGS	196.148 mm
Shear links	10mm diameter 4 legged shear links
	0m to 1.25m – 125mm spacing
	1.25m to 2.5m – 150mm spacing
	2.5m to 7.5m – 175mm spacing
	7.5m to midspan – 1000mm spacing

APPENDIX C – CONTINUOUS SPAN DESIGN

To illustrate the procedure for a prestressed concrete bridge design, a fictional bridge is created with the cross section shown in Figure C.1.

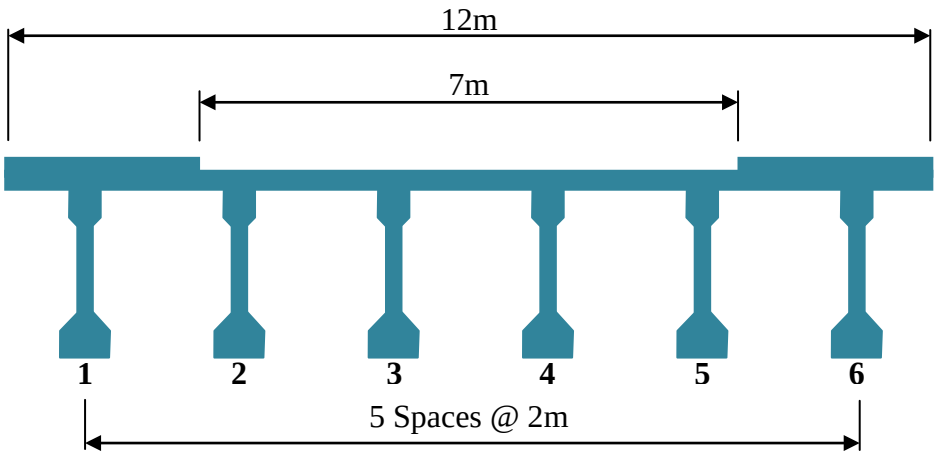

Figure C.1 – Bridge cross section

Design Assumptions:

Span length:	40.0 metres each
Beam type:	Post-tensioned I Beams
Beam Spacing:	2.0 metres
Deck width:	12.0 metres
Carriageway width:	7.0 metres
Concrete:	C50/60 for the beams
	C40/50 for the slab

The structure spans a fresh water river.

This design will focus on Beam 3, which is the critical case.

C.1 DESIGN DATA

Bridge width: $b := 12.0 \quad m$ Carriageway width: $b_c := 7.0 \quad m$

Span Length: $L_c := 40.0 \quad m$ Beam spacing: $s_{bm} := 2000 \quad mm$

C.1.1 Material Properties

BS EN 1992-1-1

Beam: C50/60 Concrete

Table 3.1

$f_{ck} := 50 \quad MPa$ $f_{cm} := 58 \quad MPa$

$f_{ckcube} := 60 \quad MPa$ $f_{ctm} := 4.1 \quad MPa$

$E_{cm} := 37 \quad GPa$

Slab: C40/50 Concrete

$f_{sck} := 40 \quad MPa$ $f_{scm} := 48 \quad MPa$

$f_{sckcube} := 50 \quad MPa$ $f_{sctm} := 3.5 \quad MPa$

$E_{scm} := 35 \quad GPa$

CEM 42.5R Cement: $s_c := 0.20$ Cl. 3.1.2(6)

Transfer time: $t := 7 \quad days$

Compressive strength with time t = 7 days for the beams:

$$\beta_{cc} := e^{s_c \cdot \left(1 - \sqrt{\frac{28}{t}}\right)} = 0.819$$ Eq (3.2)

$f_{cmt} := \beta_{cc} \cdot f_{cm} = 47.486 \quad MPa$ Eq (3.1)

$f_{ckt} := f_{cmt} - 8 = 39.486 \quad MPa$ Cl. 3.1.2(5)

$$E_{cmt} := E_{cm} \cdot \left(\frac{f_{cmt}}{f_{cm}}\right)^{0.3} \quad E_{cmt} = 34.845 \quad GPa$$ Eq (3.5)

Prestressing strands: (12.7ϕ drawn strand)

Part 3 of prEN 10138

Table 2

$\phi_p := 12.7 \quad mm$ $A_{pstr} := 112 \quad mm^2$

$f_{pk} := 1860 \quad MPa$ $f_{p0.1k} := 1610 \quad MPa$

$P_{ustr} := 208.32 \quad kN$ $P_{istr} := 153 \quad kN$

$E_s := 195 \quad GPa$ $P_{jack} := 162 \quad kN$

C.1.2 Beam Properties

Finding a standard beam to accommodate the high loading on this structure has proven to be difficult. Therefore, to allow the example to be completed, it has been decided to adjust the properties of a standard I20 beam.

I20 Beam Properties:

$b_{wI20} := 200 \quad mm$

$A_{I20} := 628475 \quad mm^2$

$d_{I20} := 1980 \quad mm$

$b_{tI20} := 410 \quad mm$

$b_{bI20} := 660 \quad mm$

$y_{bI20} := 862 \quad mm$

$y_{tI20} := d_{I20} - y_{bI20} = 1118 \quad mm$

$I_{I20} := 274650000000 \quad mm^4$

$Z_{tI20} := 24.557 \times 10^7 \quad mm^3$

$Z_{bI20} := 31.873 \times 10^7 \quad mm^3$

The beam is adjusted by increasing the height of the top and bottom flange by 100 mm. The properties of the new portion are denoted by "n".

$d_{nt} := 100 \quad mm$

$d_{nb} := 100 \quad mm$

$b_{nt} := 410 \quad mm$

$b_{nb} := 660 \quad mm$

$A_{nt} := d_{nt} \cdot b_{nt} = 41000 \quad mm^2$

$A_{nb} := d_{nb} \cdot b_{nb} = 66000 \quad mm^2$

$d := d_{nt} + d_{I20} + d_{nb} = 2180 \quad mm$

$A_b := A_{nt} + A_{I20} + A_{nb} = 735475 \quad mm^2$

$$y_b := \frac{A_{I20} \cdot \left(y_{bI20} + d_{nb}\right) + A_{nt} \cdot \left(d - 0.5 d_{nt}\right) + A_{nb} \cdot \left(d_{nb} \cdot 0.5\right)}{A_b} = 945.271 \quad mm$$

$y_t := d - y_b = 1234.729 \quad mm$

$$I_{nt} := \frac{b_{nt} \cdot d_{nt}^3}{12} = 3.417 \times 10^7 \quad mm^4 \qquad I_{nb} := \frac{b_{nb} \cdot d_{nb}^3}{12} = 5.5 \times 10^7 \quad mm^4$$

$I_{b1} := I_{I20} + A_{I20} \cdot \left(y_b - y_{bI20}\right)^2 = 2.79 \times 10^{11} \quad mm^4$

$I_{b2} := I_{nt} + A_{nt} \cdot \left(y_t - 0.5 d_{nt}\right)^2 = 5.758 \times 10^{10} \quad mm^4$

$I_{b3} := I_{nb} + A_{nb} \cdot \left(y_b - 0.5 d_{nb}\right)^2 = 5.295 \times 10^{10} \quad mm^4$

$I_b := I_{b1} + I_{b2} + I_{b3} = 3.895 \times 10^{11} \quad mm^4$

$$Z_{tbm} := \frac{I_b}{y_t} = 3.155 \times 10^8 \quad mm^3 \qquad Z_{bbm} := \frac{I_b}{y_b} = 4.121 \times 10^8 \quad mm^4$$

Adjusted Properties:

$A_b = 735475 \quad mm^2$ $\qquad$ $d = 2180 \quad mm$

$y_b = 945.271 \quad mm$ $\qquad$ $y_t = 1234.729 \quad mm$

$Z_{tbm} = 3.155 \times 10^8 \quad mm^3$ $\qquad$ $Z_{bbm} = 4.121 \times 10^8 \quad mm^3$

$I_b = 3.895 \times 10^{11} \quad mm^3$

C.2 DURABILITY REQUIREMENTS

C.2.1 Determination of Nominal Cover

BS EN 1992-1-1

Exposure Class: Deck: XC3 (protected by waterproofing) — Table 4.1 (incorp. BS EN 1992-2)

Beams: XC3 (over fresh water)

BS EN 1990

Design Life: Category 5 -- 120 years — Table NA.2.1

BS EN 1992-1-1

Nominal cover: $c_{nom} = c_{min} + \Delta c_{dev}$ — Cl. 4.4.1.1 Eq (4.1)

Minimum cover: — Cl. 4.4.1.2 Eq (4.2)

$c_{min} = \max[c_{min,b}; c_{min,dur} + \Delta c_{dur,\gamma} - \Delta c_{dur,st} - \Delta c_{dur,add}; 10mm]$

Minimum cover due to bond requirements: — Cl. 4.4.1.2(3)

For post-tensioned duct: $c_{minb} := 60 \quad mm$

For reinforcing bars: $c_{minbr} := 25 \quad mm$

Minimum cover due to durability requirements: — Per Cl. 4.4.1.2(5) & Table NA.1

For XC3: $c_{mindur} := 30 \quad mm$ — **BS 8500-1** Table A.5

$\Delta c_{dur\gamma} := 0 \quad mm$

$\Delta c_{durst} := 0 \quad mm$

$\Delta c_{duradd} := 0 \quad mm$ — **NA to BS EN 1992-1-1** Cl. 4.4.1.2(6), (7), & (8)

$c_{min} := \max\left(c_{minb}, c_{minbr}, c_{mindur} + \Delta c_{dur\gamma} - \Delta c_{durst} - \Delta c_{duradd}, 10\right)$

$c_{min} = 60 \quad mm$

$c_{mind} := \max\left(c_{minbr}, c_{mindur} + \Delta c_{dur\gamma} - \Delta c_{durst} - \Delta c_{duradd}, 10\right)$

$c_{mind} = 30 \quad mm$

Allowance for deviation: $\Delta c_{dev} := 10 \quad mm$

NA to BS EN 1992-1-1 Cl. 4.4.1.3(1)P

Nominal cover for the beams:

$c_{nom} := c_{min} + \Delta c_{dev} = 70 \quad mm$

Nominal cover for the deck:

$c_{nomd} := c_{mind} + \Delta c_{dev} = 40 \quad mm$

C.3 ACTIONS ON THE STRUCTURE

For all moment calculations, M_p represents positive moments, and M_n represents negative moments.

For the positive moments, the maximum moment due to traffic loading occurs at 17.4m and the maximum moment due to self-weight occurs at 15.0m. Therefore, two moments are calculated for all of the positive moments, to ensure that the maximum loading is considered. For the negative moments, the minimum values all coincide at the centre support.

C.3.1 Permanent Actions

BS EN 1991-1-1

Normal weights:

Concrete	$\gamma_{conc} := 24 \quad kN/m^2$	Table A.1
Reinforced/Prestressed Concrete	$\gamma_{rc} := 25 \quad kN/m^2$	
Wet Concrete	$\gamma_{rcwet} := 26 \quad kN/m^2$	
Hot Rolled Asphalt	$\gamma_{pvmt} := 23 \quad kN/m^2$	Table A.6

Self weight of beam and slab (Initial trial section: U12)

Area of beam: $A_b = 735475 \quad mm^2$

Weight of beam: $w_b := A_b \cdot 10^{-6} \cdot \gamma_{rc} = 18.387 \quad kN/m$

Maximum Moment: $M_{pb} := \frac{9}{128} \cdot w_b \cdot L_c^{\,2} = 2068.523 \quad kNm$

$M_{17pb} := 2015.583 \quad kNm$

Minimum Moment: $M_{nb} := \frac{w_b \cdot L_c^{\,2}}{8} = 3677.375 \quad kNm$

Area of slab: $d_s := 300 \ \text{mm}$ $s_{bm} = 2000 \ \text{mm}$

$A_s := d_s \cdot s_{bm} = 600000 \ \text{mm}^2$

Weight of beam and slab:

$w_{bs} := \left(A_b + A_s\right) \cdot 10^{-6} \cdot \gamma_{rc} = 33.387 \ \text{kN/m per beam}$

Maximum Moment: $M_{pbs} := \frac{9}{128} \cdot w_{bs} \cdot L_c^{\,2} = 3756.023 \ \text{kNm}$

$M_{17pbs} := 3659.883 \ \text{kNm}$

Minimum Moment: $M_{nbs} := \frac{w_{bs} \cdot L_c^{\,2}}{8} = 6677.375 \ \text{kNm}$

Super-imposed dead load

Surfacing on carriageway: $d_{sf} := 60 \ \text{mm}$

NA to BS EN 1991-1-1 Cl. 5.2.3(3)

Adjustment factor for variation in thickness: $f_{sf} := 1.55$

$q_{sf} := d_{sf} \cdot 10^{-3} \cdot f_{sf} \cdot \gamma_{pvmt} = 2.139 \ \text{kN/m}^2$

$w_{sf} := q_{sf} \cdot s_{bm} \cdot 10^{-3} = 4.278 \ \text{kN/m}$

Maximum Moment: $M_{psf} := \frac{9}{128} \cdot w_{sf} \cdot L_c^{\,2} = 481.275 \ \text{kNm}$

$M_{17psf} := 468.95 \ \text{kNm}$

Minimum Moment: $M_{nsf} := \frac{w_{sf} \cdot L_c^{\,2}}{8} = 855.6 \ \text{kNm}$

(Parapet and footpath loading do not apply to Beam 3)

C.3.2 Variable Actions - Traffic Loads

BS EN 1991-2

(From Appendix A)

Table NA.3 and...

The minimum and maximum moments for each load group are listed here. Refer to Table C.10 for moments at each section due to Load Group gr5, which controls.

Load Group gr1a - Load Model 1 - Normal Traffic

Cl. 4.3.2

Model consists of a tandem system combined with a UDL

$M_{17pgr1a} := 4841 \ \text{kNm}$ $M_{15pgr1a} := 4775 \ \text{kNm}$

$M_{ngr1a} := 3715 \ \text{kNm}$

Load Group gr1b - Load Model 2 - Single Axle Load Cl. 4.3.3

Model consists of only a single axle.

$M_{pgr1b} := 2008$ kNm $M_{ngr1b} := 932$ kNm

Load Group gr4 - Load Model 4 - Crowd Loading Cl. 4.3.5

Model consists of uniformly distributed load.

$M_{pgr4} := 1532$ kNm $M_{ngr4} := 2000$ kNm

Load Group gr5 - Load Model 3 - Special Vehicles Cl. 4.3.4

Model consists of SV196 vehicle combined with frequent values of LM1

$M_{17pgr5} := 7015$ kNm $M_{15pgr5} := 6897$ kNm

$M_{ngr5} := 6172$ kNm

C.4 COMBINATIONS OF ACTIONS BS EN 1990

C.4.1 Serviceability Limit State Cl. 6.5.3

Table C.1 – Combination factors (ψ) for traffic loads Table NA.A2.1

		ψ_0	ψ_1	ψ_2
gr1a	TS	0.75	0.75	0
	UDL	0.75	0.75	0
	Pedestrian loads	0.40	0.40	0
gr3	Pedestrian loads	0	0.40	0
gr5	SV Vehicles	0	0	0

For the maximum and minimum moments: BS EN 1990

Characteristic combination Eq (6.14b)

$$E_d = E\left(\Sigma G_{k,j} + P + Q_{k,1} + \Sigma \psi_{0,i} Q_{k,i}\right)$$

$M_{pdchar} := M_{pbs} + M_{psf} + M_{15pgr5} = 11134.2984$ kNm

$M_{17pdchar} := M_{17pbs} + M_{17psf} + M_{17pgr5} = 11143.833$ kNm

$M_{ndchar} := M_{nbs} + M_{nsf} + M_{ngr5} = 13704.975$ kNm

Only one traffic load group is to be appied in a combination. Since M_{gr5} is the greatest loading, it is applied for the characteristic combination.

Frequent combination

BS EN 1990
Eq (6.15b)

$$E_d = E\left(\Sigma G_{k,j} + P + \psi_{1,1}Q_{k,1} + \Sigma\psi_{2,i}Q_{k,i}\right)$$

$M_{pdfreq} := M_{pbs} + M_{psf} + 0.75 \cdot M_{15pgr1a} = 7818.548$ kNm

$M_{17pdfreq} := M_{17pbs} + M_{17psf} + 0.75 \cdot M_{17pgr1a} = 7759.583$ kNm

$M_{ndfreq} := M_{nbs} + M_{nsf} + 0.75 \cdot M_{ngr1a} = 10319.225$ kNm

Of the frequent traffic load groups, M_{gr1a} is the highest, and therefore is applied here.

Quasi-permanent combination

Eq (6.16b)

$$E_d = E\left(\Sigma G_{k,j} + P + \Sigma\psi_{2,i}Q_{k,i}\right)$$

$M_{pdquasi} := M_{pbs} + M_{psf} = 4237.298$ kNm

$M_{ndquasi} := M_{nbs} + M_{nsf} = 7532.975$ kNm

The moments calculated here do not include the prestressing force. This will be added later in the design process, after the prestressing is designed.

For all load combinations, the loading at 15.0m controls.

C.4.2 Ultimate Limit State

Bridge design concerned with STR limit state.

Table C.2 – Partial factors for design values of actions

	γ_{sup} (Unfavourable)	γ_{inf} (Favourable)	ψ_0
Self weight	1.35	0.95	-
Super-imposed DL	1.20	0.95	-
Prestress	1.10	0.90	-
Traffic	1.35	0	N/A**

NA to BS EN 1990
Table NA.A2.4(B)
& NA to BS EN 1992-1-1
Cl. 2.4.2.2

**Traffic loading will be the leading action

For the maximum and minimum moments:

BS EN 1990

Design to be based on Equation (6.10).

Cl. NA.2.3.7.1

$$E_d = E\left(\Sigma\gamma_{G,j}G_{k,j} + \gamma_P P + \gamma_{Q,1}Q_{k,1} + \Sigma\gamma_{Q,i}\psi_{0,i}Q_{k,i}\right)$$

Eq (6.10)

$M_{pdult} := 1.35 \cdot M_{pbs} + 1.20 \cdot M_{psf} + 1.35 \cdot M_{15pgr5} = 14959.112$ kNm

$M_{17pdult} := 1.35 \cdot M_{17pbs} + 1.20 \cdot M_{17psf} + 1.35 \cdot M_{17pgr5} = 14973.832$ kNm

$M_{ndult} := 1.35 \cdot M_{nbs} + 1.20 \cdot M_{nsf} + 1.35 \cdot M_{ngr5} = 18373.376$ kNm

The moments calculated here do not include the prestressing force. This will be added later in the design process.

C.5 INITIAL DESIGN OF THE PRESTRESSED BEAMS

For the initial design of the beams, the moment at transfer due to the self-weight of the beam and the moment at service due to the self-weight of the beam and the wet slab are considered.

Self-weight of the beam:

$M_{pb} = 2068.523$ kNm $\quad$ $M_{nb} = 3677.375$ kNm

Self-weight of the composite section:

$M_{pbs} = 3756.023$ kNm $\quad$ $M_{nbs} = 6677.375$ kNm

C.5.1 Beam Properties and Initial Prestress Loss Assumptions

$\alpha := 1 - 0.12 = 0.88$ $\quad$ $\beta := 1 - 0.2 = 0.8$

$A_b = 735475$ mm^2 $\quad$ $d = 2180$ mm

$y_b = 945.271$ mm $\quad$ $y_t = 1234.729$ mm

$Z_{tbm} = 3.155 \times 10^8$ mm^3 $\quad$ $Z_{bbm} = 4.121 \times 10^8$ mm^3

C.5.2 Stress Limits

BS EN 1992-1-1

At transfer

$f_{trmax} := 0.6 \cdot f_{ckt} = 23.692$ MPa — Eq (5.42)

$f_{trmin} := -1.0$ MPa — UK Practice

At service

$f_{max} := 0.6 \cdot f_{ck} = 30$ MPa — Eq (5.42)

$f_{min} := 0$ MPa

C.5.3 Basic Inequalities for Concrete Stresses

From the equations for stress in the top and bottom fibres, the following inequalities are determined.

For the maximum positive moment...

At transfer

Top fibre: $$\frac{\alpha \cdot P_i}{A_b} - \frac{\alpha \cdot P_i \cdot e_b}{Z_{tbm}} + \frac{M_{pb}}{Z_{tbm}} \geq f_{trmin} \qquad \text{(C.1a)}$$

Bottom fibre: $$\frac{\alpha \cdot P_i}{A_b} + \frac{\alpha \cdot P_i \cdot e_b}{Z_{bbm}} - \frac{M_{pb}}{Z_{bbm}} \leq f_{trmax} \qquad \text{(C.1b)}$$

At service

Top fibre: $$\frac{\beta \cdot P_i}{A_b} - \frac{\beta \cdot P_i \cdot e_b}{Z_{tbm}} + \frac{M_{pbs}}{Z_{tbm}} \leq f_{max} \qquad \text{(C.1c)}$$

Bottom fibre: $$\frac{\beta \cdot P_i}{A_b} + \frac{\beta \cdot P_i \cdot e_b}{Z_{bbm}} - \frac{M_{pbs}}{Z_{bbm}} \geq f_{min} \qquad \text{(C.1d)}$$

For the minimum negative moment...

At transfer

Bottom fibre: $$\frac{\alpha \cdot P_i}{A_b} - \frac{\alpha \cdot P_i \cdot e_b}{Z_{bbm}} + \frac{M_{nb}}{Z_{bbm}} \geq f_{trmin} \qquad \text{(C.2a)}$$

Top fibre: $$\frac{\alpha \cdot P_i}{A_b} + \frac{\alpha \cdot P_i \cdot e_b}{Z_{tbm}} - \frac{M_{nb}}{Z_{tbm}} \leq f_{trmax} \qquad \text{(C.2b)}$$

At service

Bottom fibre: $$\frac{\beta \cdot P_i}{A_b} - \frac{\beta \cdot P_i \cdot e_b}{Z_{bbm}} + \frac{M_{nbs}}{Z_{bbm}} \leq f_{max} \qquad \text{(C.2c)}$$

Top fibre: $$\frac{\beta \cdot P_i}{A_b} + \frac{\beta \cdot P_i \cdot e_b}{Z_{tbm}} - \frac{M_{nbs}}{Z_{tbm}} \geq f_{min} \qquad \text{(C.2d)}$$

C.5.4 Required Elastic Moduli

For the maximum positive moment...

By combining inequalities (C.1a) to (C.1d), the following inequalities for required elastic moduli are determined and verified.

$$Z_{tbm} = 3.155 \times 10^8 \ \text{mm}^3 \geq \frac{\alpha \cdot \left(M_{pbs} \cdot 10^6\right) - \beta \cdot \left(M_{pb} \cdot 10^6\right)}{\alpha \cdot f_{max} - \beta \cdot f_{trmin}} = 6.068 \times 10^7 \ \text{mm}^3$$

$$Z_{bbm} = 4.121 \times 10^8 \ \text{mm}^3 \geq \frac{\alpha \cdot \left(M_{pbs} \cdot 10^6\right) - \beta \cdot \left(M_{pb} \cdot 10^6\right)}{\beta \cdot f_{trmax} - \alpha \cdot f_{min}} = 8.708 \times 10^7 \ \text{mm}^3$$

For the minimum negative moment...

By combining inequalities (C.2a) to (C.2d), the following inequalities for required elastic moduli are determined.

$$Z_{tbm} = 3.155 \times 10^8 \ \text{mm}^3 \geq \frac{\alpha \cdot \left(M_{nbs} \cdot 10^6\right) - \beta \cdot \left(M_{nb} \cdot 10^6\right)}{\beta \cdot f_{trmax} - \alpha \cdot f_{min}} = 1.548 \times 10^8 \ \text{mm}^3$$

$$Z_{bbm} = 4.121 \times 10^8 \ \text{mm}^3 \geq \frac{\alpha \cdot \left(M_{nbs} \cdot 10^6\right) - \beta \cdot \left(M_{nb} \cdot 10^6\right)}{\alpha \cdot f_{max} - \beta \cdot f_{trmin}} = 1.079 \times 10^8 \ \text{mm}^3$$

Note that these equations do not take into account the prestress force and eccentricity. As a result, larger values for Z_{tbm} and Z_{bbm} should be chosen than those calculated.

C.5.5 Initial Determination of Prestress and Eccentricity

To get an approximate value of prestress and eccentricity, the section at the support is designed first.

For the minimum negative moment...

By rearranging the basic inequalities (C.2a) to (C.2d) above, the permissible zones for initial prestressing force, P_i, and eccentricity, $e_{b,}$ are defined which make up the Magnel Diagram in Figure B.2.

$$\frac{1}{P_i} \leq \frac{\alpha \cdot \left(\frac{Z_{bbm}}{A_b} - e_b\right)}{Z_{bbm} \cdot f_{trmin} - M_{nb}} \qquad \frac{10^8}{P_i} \geq -12.0572 + 0.0215 e_b \ \text{1/N} \quad \text{(C.3a)}$$

$$\frac{1}{P_i} \geq \frac{\alpha \cdot \left(\frac{Z_{tbm}}{A_b} + e_b\right)}{Z_{tbm} \cdot f_{trmax} + M_{nb}} \qquad \frac{10^8}{P_i} \geq 3.3849 + 0.0079 e_b \ \text{1/N} \quad \text{(C.3b)}$$

$$\frac{1}{P_i} \leq \frac{\beta \cdot \left(\frac{Z_{bbm}}{A_b} - e_b\right)}{Z_{bbm} \cdot f_{max} - M_{nbs}} \qquad \frac{10^8}{P_i} \geq 7.8841 - 0.0141 e_b \ \text{1/N} \quad \text{(C.3c)}$$

$$\frac{1}{P_i} \geq \frac{\beta \cdot \left(\frac{Z_{tbm}}{A_b} + e_b\right)}{Z_{tbm} \cdot f_{min} + M_{nbs}} \qquad \frac{10^8}{P_i} \leq 5.1393 + 0.0120 e_b \ \text{1/N} \quad \text{(C.3d)}$$

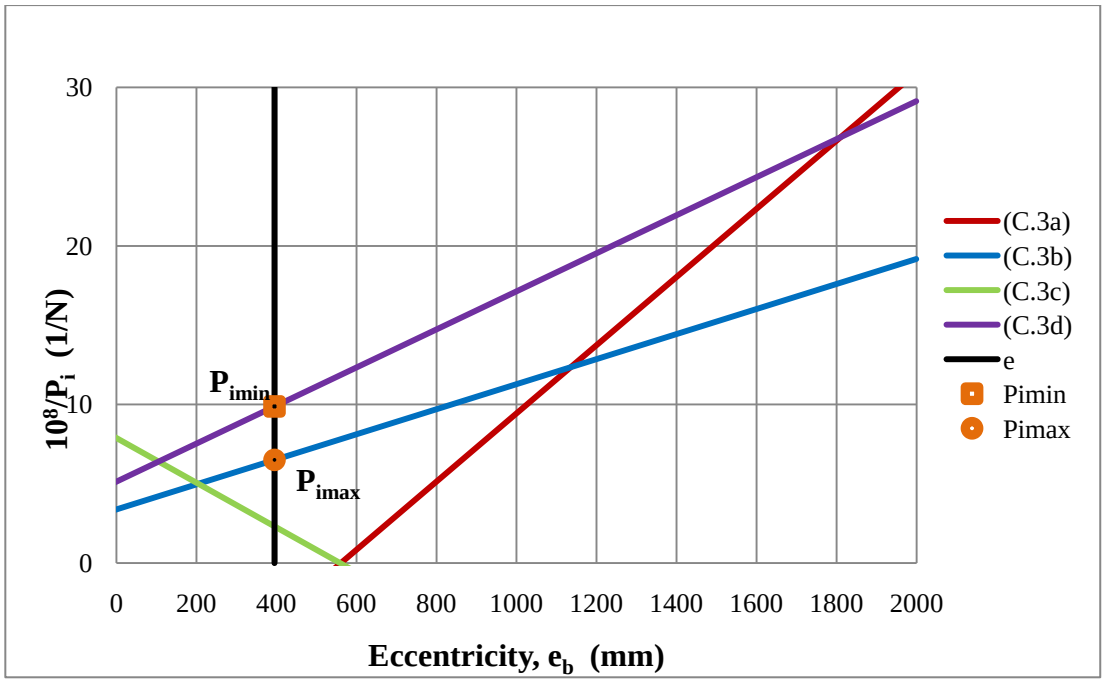

Figure C.2 – Magnel Diagram

From the Magnel Diagram:

Upper limit for eccentricity; let Eq. (C.3a) = Eq. (C.3d)

Try $e_{max} := 1500$ mm

Given $-12.0572 + 0.0215e_{max} = 5.1393 + 0.0120e_{max}$

Find$(e_{max}) = 1810.158$ mm

Lower limit for eccentricity; let Eq. (C.3c) = Eq. (C.3d)

Try $e_{min} := -100$ mm

Given $7.8841 - 0.0141e_{min} = 5.1393 + 0.0120e_{min}$

Find$(e_{min}) = 105.165$ mm

Selection of prestressing strands:

Eccentricity of the strands

Maximum allowable eccentricity based on nominal cover:

$e_{maxallow} := y_t - c_{nom} = 1164.729$ mm

Assume: $N_{str} := 84$ strands

Based on the cover requirements determined in Section C.2 for the web (with a width of 200mm), it is determined that 60mm post-tensioning ducts will be used, with seven 12.7mm ϕ strands in each duct. If a 60mm spacing between each duct is assumed with 12 ducts required, the CGS of the strands will fall 690 mm below the top duct.

$e_{maxallow} - 690 = 474.729 \quad mm$

Take: $e_b := 395 \quad mm$

Limits for initial prestressing force

$$P_{imin} := \frac{10^8}{\left(5.1393 + 0.0120 e_b\right)} \cdot 10^{-3} = 10122.175 \quad kN$$

$$P_{imax} := \frac{10^8}{\left(3.3849 + 0.0079 e_b\right)} \cdot 10^{-3} = 15371.845 \quad kN$$

Y1860S7G strands with 12.7mm ϕ are chosen

$P_{ustr} = 208.32 \quad kN \qquad P_{istr} = 153 \quad kN$

Required prestressing force after allowances for losses

BS EN 1992-1-1
Cl. 5.10.3(2)

(BS EN 1992-1-1 limits stress of the strands afer allowance for losses to avoid stresses in tendons under serviceability conditions that could lead to inelastic deformation of the tendons)

$$P_{req} := \frac{P_{imin}}{0.75} = 13496.233 \quad kN$$

$$N_{req} := \frac{P_{req}}{P_{ustr}} = 64.786 \quad strands < \quad N_{str} = 84 \quad strands \quad OK!$$

Total prestressing force:

$P_{pk} := P_{ustr} \cdot N_{str} = 17498.88 \quad kN > P_{req} = 13496.233 \quad kN \quad OK!$

$A_p := A_{pstr} \cdot N_{str} = 9408 \quad mm^2$

Actual prestressing force:

$P_i := P_{istr} \cdot N_{str} = 12852 \quad kN > P_{imin} = 10122.175 \quad kN \quad OK!$

$< P_{imax} = 15371.845 \quad kN \quad OK!$

C.5.6 Equivalent Loading and Secondary Moments Due to Prestress

Table C.3 - Eccentricities

X (m)	Selected e (mm)
0	0
1	10
2	20
3	40
4	52
5	62
6	70
10	95
15	115
20	116
25	90
30	0
35	-190
36	-295
37	-350
38	-375
39	-390
40	-395
41	-390
42	-375
43	-350
44	-295
45	-190
50	0
55	90
60	116
65	115
70	95
74	70
75	62
76	52
77	40
78	20
79	10
80	0

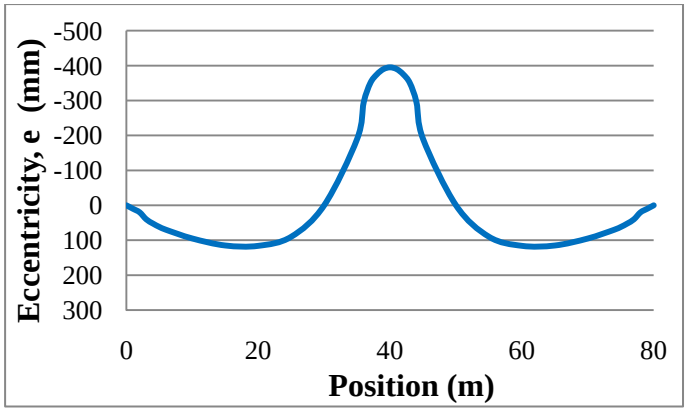

Figure C.3 – Strand Profile

To determine the curvatures and radius of curvature:

Separate each span in to 3 segments

Table C.4 – Segments for curvature calculations

Segment		x_1	e_1	x_2	e_2
Span 1	**1**	0	0	20	116
	2	20	116	36	-295
	3	36	-295	40	-395
Span 2	**1**	40	-395	44	-295
	2	44	-295	60	116
	3	60	116	80	0

Due to symmetry, the results for each span will be equal and opposite. Therefore, the calculations here focus on Span 1.

Segment 1

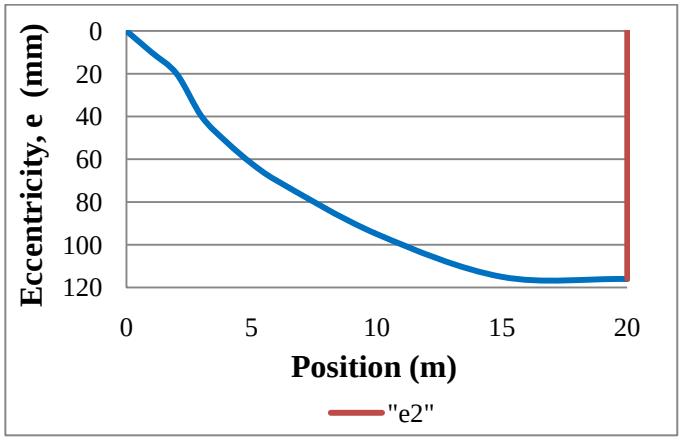

Boundary Conditions:

L =	40	m
x_1 =	0	m
x_2 =	20	m
x =	(1-λ)L	
λ =	0.5	
x =	20	m
e_1 =	0	m
e_2 =	0.116	m

Figure C.4 – Profile of segment 1

Based on the boundary conditions, the following equations can be derived from the equation of the parabola. ($e = Ax^2 + Bx + C$)

$$e = -e_1 - \frac{(e_1 + e_2)}{(1-\lambda)^2} \times \frac{x}{L} \times \left[\frac{x}{L} - 2(1-\lambda)\right]$$

Slope:

$$\frac{de}{dx} = -\frac{(e_1 + e_2)}{(1-\lambda)^2} \times \frac{2}{L} \times \left[\frac{x}{L} - (1-\lambda)\right]$$

Curvature:

$$\frac{d^2e}{dx^2} = -\frac{2}{L^2} \times \frac{(e_1 + e_2)}{(1-\lambda)^2} = -5.80 \times 10^{-4}\, m^{-1}$$

$$\boldsymbol{q_1 = -5.80 \times 10^{-4} \times P}$$

Segment 2

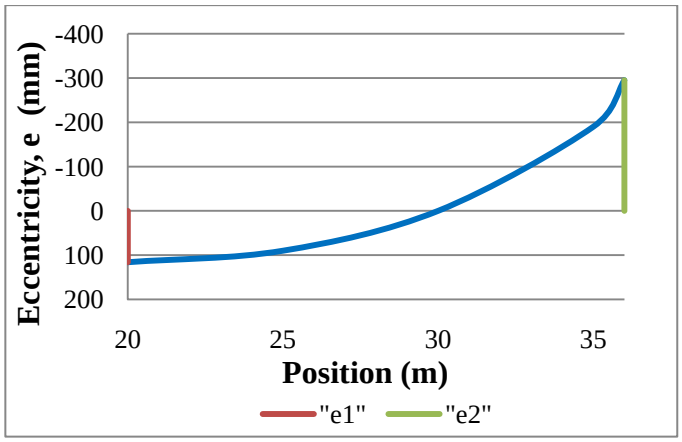

Boundary Conditions:

L =	40	m
x_1 =	20	m
x_2 =	36	m
x =	(λ-β)L	
λ =	0.5	
β =	0.1	
x =	16	m
e_1 =	0.116	m
e_2 =	0.295	m

Figure C.5 – Profile of Segment 2

Based on the boundary conditions, the following equations can be derived from the equation of the parabola. ($e = Ax^2 + Bx + C$)

$$e = e_1 - \frac{(e_1 + e_2)}{(\lambda - \beta)^2} \times \left[\frac{x}{L}\right]^2$$

Slope:

$$\frac{de}{dx} = -\frac{2x}{L^2}\frac{(e_1 + e_2)}{(\lambda - \beta)^2}$$

Curvature:

$$\frac{d^2e}{dx^2} = -\frac{2}{L^2} \times \frac{(e_1 + e_2)}{(\lambda - \beta)^2} = -3.21 \times 10^{-3}\ m^{-1}$$

$$\boldsymbol{q_2 = -3.21 \times 10^{-3} \times P}$$

Segment 3

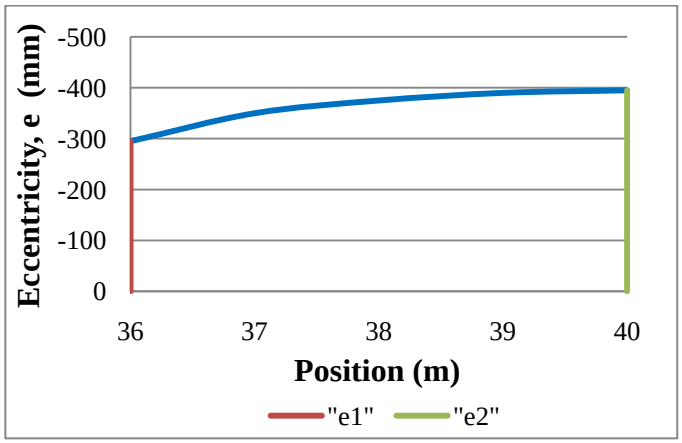

Boundary Conditions:

L =	40	m
x_1 =	36	m
x_2 =	40	m
x =	βL	
λ =	0.5	
β =	0.1	
x =	4	m
e_1 =	0.295	m
e_2 =	0.395	m

Figure C.6 – Profile of Segment 3

Based on the boundary conditions, the following equations can be derived from the equation of the parabola. ($e = Ax^2 + Bx + C$)

$$e = -e_1 + (e_2 - e_1) \times \frac{x}{\beta L} \times \left[\frac{x}{\beta L} - 2\right]$$

Slope:

$$\frac{de}{dx} = (e_2 - e_1) \times \frac{2}{\beta L} \times \left[\frac{x}{\beta L} - 1\right]$$

Curvature:

$$\frac{d^2e}{dx^2} = (e_2 - e_1) \times \frac{2}{(\beta L)^2} = 1.25 \times 10^{-2}\ m^{-1}$$

$$\boldsymbol{q_2 = 1.25 \times 10^{-2} \times P}$$

Fixed End Moments (Bhatt, 2011)

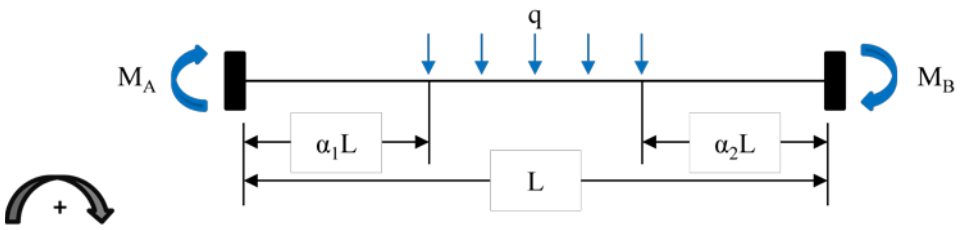

Figure C.7 – Beam with partial loading

$$M_A = -q\frac{L^2}{12}[(1-\alpha_1)^3(1+3\alpha_1) - \alpha_2{}^3(4-3\alpha_2)]$$

$$M_B = q\frac{L^2}{12}[(1-\alpha_2)^3(1+3\alpha_2) - \alpha_1{}^3(4-3\alpha_1)]$$

Table C.5 – Fixed End Moment calculations

Segment	q/P (+ down)	L (m)	α_1L (m)	α_2L (m)	Loaded Length, x	M_A/P	M_B/P
1	-5.80E-04	40	0	20	20	0.053	-0.024
2	-3.21E-03	40	20	4	16	0.132	-0.272
3	1.25E-02	40	36	0	4	-0.006	0.087
				SUM	40	0.179	-0.209

Table C.6 – Moment distribution method

	A	B		C
DF	1	0.5	0.5	1
FEM	0.179	-0.209	0.209	-0.179
Balance	-0.179	0	0	0.179
Carry	0	-0.090	0.090	0
SUM	0	-0.299	0.299	0

Final Moments for each span:

M_{AB} = 0 P M_{BC} = 0.299 P

M_{BA} = -0.299 P M_{CB} = 0 P

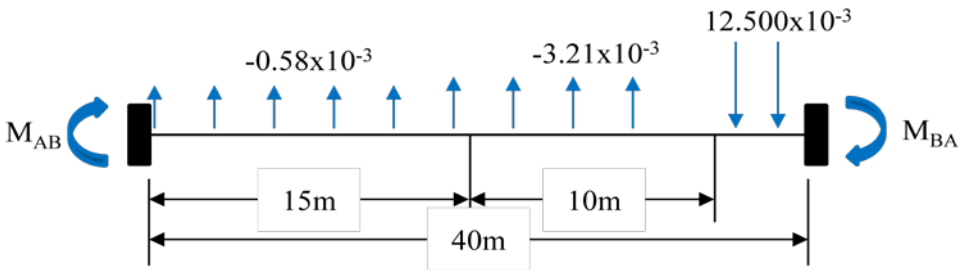

Figure C.8 – Equivalent loads on Span 1 (AB)

Reactions at end of spans:

$$V_A = \frac{-M_{BA}}{L} + \sum \frac{q_i \times x \times (\frac{x}{2} + \alpha_2 L)}{L}$$

$$V_B = \frac{M_{BA}}{L} + \sum \frac{q_i \times x \times (\frac{x}{2} + \alpha_1 L)}{L}$$

Table C.7 – Reactions due to each segment

Segment	q/P (+ down)	L (m)	α_1L (m)	α_2L (m)	Loaded Length, x	L*V_{Ai}/P	L*V_{Bi}/P
1	-5.80E-04	40	0	20	20	-3.48E-01	-1.16E-01
2	-3.21E-03	40	20	4	16	-6.17E-01	-1.44E+00
3	1.25E-02	40	36	0	4	1.00E-01	1.90E+00
				SUM	40	-8.65E-01	3.46E-01

M_{BA} = -0.299 P

V_{1A} = 1.42E-02 P V_{2B} = 1.17E-03 P

V_{1B} = 1.17E-03 P V_{2C} = 1.42E-02 P

Net reactions:

V_A = 1.415E-02 P

V_B = 2.348E-03 P

V_C = 1.415E-02 P

End reactions if intermediate supports are removed:

$$V_A = V_c = \sum \frac{q_i \times x_i}{2}$$

V_{AA} = -1.298E-02 P

V_{BB} = 0 P

V_{CC} = -1.298E-02 P

Reactions due to restraint at support B: (= difference between V_A and V_{AA})

V_A = -1.174E-03 P

V_B = 2.348E-03 P

V_C = -1.174E-03 P

M_B = V_A*L

M_B = -0.047 P *P

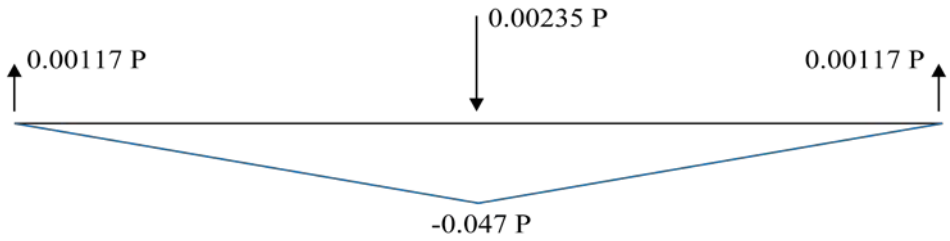

Figure C.9 – Secondary moments induced by reactions

Table C.8 – Effective Eccentricities

X (m)	Selected e (mm)	P_i (kN)	$M_p = P_i e$ (kNm)	$M_s = 0.0198 P_i$ (kNm)	$M_t = M_p + M_s$ (kNm)	$e_{eff} = M_t/P_i$ (mm)
0	0	12852	0	0	0	0
1	10	12852	128.5	-15.086	113.434	8.826
2	20	12852	257.0	-30.172	226.868	17.652
3	40	12852	514.1	-45.258	468.822	36.479
4	52	12852	668.3	-60.343	607.961	47.305
5	62	12852	796.8	-75.429	721.395	56.131
6	70	12852	899.6	-90.515	809.125	62.957
10	95	12852	1220.9	-150.858	1070.082	83.262
15	115	12852	1478.0	-226.288	1251.692	**97.393**
17.4	116	12852	1490.8	-262.494	1228.338	95.576
20	116	12852	1490.8	-301.717	1189.115	92.524
25	90	12852	1156.7	-377.146	779.534	60.655
30	0	12852	0	-452.575	-452.575	-35.214
35	-190	12852	-2441.9	-528.004	-2969.884	-231.083
36	-295	12852	-3791.3	-543.090	-4334.430	-337.257
37	-350	12852	-4498.2	-558.176	-5056.376	-393.431
38	-375	12852	-4819.5	-573.262	-5392.762	-419.605
39	-390	12852	-5012.3	-588.348	-5600.628	-435.779
40	-395	12852	-5076.5	-603.434	-5679.974	**-441.953**
NOTE: Results are symmetric about the centre support.						

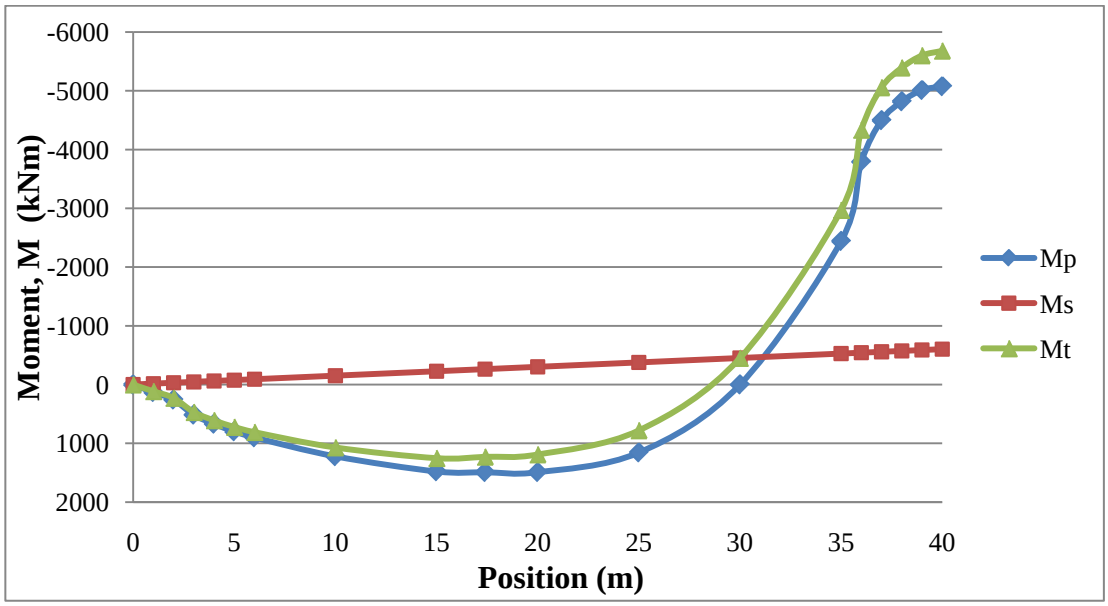

Figure C.10 – Primary, secondary and total moments due to prestress

The following effective eccentricities are determined for the locations of maximum and minimum bending moment:

$$e_{peff} := 97.393 \quad mm \qquad e_{neff} := 441.953 \quad mm$$

C.5.7 Verification of the the Basic Inequalities with Effective Eccentricities

For the maximum positive moment...

At transfer

$$f_{trtbm} := \frac{\alpha \cdot P_i \cdot 10^3}{A_b} - \frac{\alpha \cdot P_i \cdot 10^3 \cdot e_{peff}}{Z_{tbm}} + \frac{M_{pb} \cdot 10^6}{Z_{tbm}} \quad \text{(C.1a)}$$

$f_{trtbm} = 18.443$ MPa $\geq$ $f_{trmin} = -1$ MPa OK!

$$f_{trbbm} := \frac{\alpha \cdot P_i \cdot 10^3}{A_b} + \frac{\alpha \cdot P_i \cdot 10^3 \cdot e_{peff}}{Z_{bbm}} - \frac{M_{pb} \cdot 10^6}{Z_{bbm}} \quad \text{(C.1b)}$$

$f_{trbbm} = 13.031$ MPa $\leq$ $f_{trmax} = 23.692$ MPa OK!

At service

$$f_{tbm} := \frac{\beta \cdot P_i \cdot 10^3}{A_b} - \frac{\beta \cdot P_i \cdot 10^3 \cdot e_{peff}}{Z_{tbm}} + \frac{M_{pbs} \cdot 10^6}{Z_{tbm}} \quad \text{(C.1c)}$$

$f_{tbm} = 22.711$ MPa $\leq$ $f_{max} = 30$ MPa OK!

$$f_{bbm} := \frac{\beta \cdot P_i \cdot 10^3}{A_b} + \frac{\beta \cdot P_i \cdot 10^3 \cdot e_{peff}}{Z_{bbm}} - \frac{M_{pbs} \cdot 10^6}{Z_{bbm}} \quad \text{(C.1d)}$$

$f_{bbm} = 7.295$ MPa $\geq$ $f_{min} = 0$ MPa OK!

For the minimum negative moment...

At transfer

$$f_{ntrtbm} := \frac{\alpha \cdot P_i \cdot 10^3}{A_b} + \frac{\alpha \cdot P_i \cdot 10^3 \cdot e_{neff}}{Z_{tbm}} - \frac{M_{nb} \cdot 10^6}{Z_{tbm}} \quad \text{(C.2a)}$$

$f_{ntrtbm} = 19.565$ MPa $\leq$ $f_{trmax} = 23.692$ MPa OK!

$$f_{ntrbbm} := \frac{\alpha \cdot P_i \cdot 10^3}{A_b} - \frac{\alpha \cdot P_i \cdot 10^3 \cdot e_{neff}}{Z_{bbm}} + \frac{M_{nb} \cdot 10^6}{Z_{bbm}} \quad \text{(C.2b)}$$

$f_{ntrbbm} = 12.172$ MPa $\geq$ $f_{trmin} = -1$ MPa OK!

At service

$$f_{ntbm} := \frac{\beta \cdot P_i \cdot 10^3}{A_b} + \frac{\beta \cdot P_i \cdot 10^3 \cdot e_{neff}}{Z_{tbm}} - \frac{M_{nbs} \cdot 10^6}{Z_{tbm}} \quad \text{(C.2c)}$$

$f_{ntbm} = 7.217$ MPa $\geq$ $f_{min} = 0$ MPa OK!

$$f_{nbbm} := \frac{\beta \cdot P_i \cdot 10^3}{A_b} - \frac{\beta \cdot P_i \cdot 10^3 \cdot e_{neff}}{Z_{bbm}} + \frac{M_{nbs} \cdot 10^6}{Z_{bbm}} \quad \text{(C.2d)}$$

$f_{nbbm} = 19.156$ MPa $\leq$ $f_{max} = 30$ MPa OK!

C.5.8 Confirmation of Selected Tendon Profile

With the selected tendon profile in Section C.5.8, the concrete stresses are checked at a series of points along the beam to verify that all of the stresses fall within the required limits set in Section C.5.1.

Table C.9 – Concrete stresses at transfer and service every 5m

X (m)	e_{eff} (mm)	P_i (kN)	M_b (kNm)	M_{bs} (kNm)	f_{trtbm} (MPa)	f_{trbbm} (MPa)	f_{tbm} (MPa)	f_{bbm} (MPa)
0	0	12852	0	0	**15.377**	**15.377**	13.980	13.980
5	56.131	12852	1149	2087	17.008	14.129	18.764	10.316
10	83.262	12852	1839	3339	18.221	13.201	21.848	7.955
15	97.393	12852	2069	3756	18.443	13.031	**22.711**	**7.295**
17.4	95.576	12852	2016	3660	18.340	13.109	22.465	7.483
20	92.524	12852	1839	3339	17.889	13.455	21.547	8.186
25	60.655	12852	1149	2087	16.846	14.253	18.617	10.429
30	-35.214	12852	0	0	16.640	14.411	15.127	13.101
35	-231.083	12852	-1609	-2921	18.562	12.940	12.251	15.303
40	-441.953	12852	-3677	-6677	**19.564**	**12.172**	**7.218**	**19.156**
Limits for positive eccentricity:					-1	23.692	0	30
Limits for negative eccentricity:					23.692	-1	30	0

All requirements are met for this stage in the design process.

C.6 DESIGN OF THE COMPOSITE SECTION

Properties of the Composite Section

$A_c := A_b + A_s = 1335475 \quad mm^2$ $\qquad d_c := d + d_s = 2480 \quad mm$

$$y_c := \frac{A_b \cdot y_b + A_s \cdot \left(d_c - 0.5 d_s\right)}{A_b + A_s} = 1567.4 \quad mm$$

$I_b = 3.895 \times 10^{11} \quad mm^4$ $\qquad I_s := \frac{s_{bm} \cdot d_s^{\,3}}{12} = 4.5 \times 10^9 \quad mm^4$

$$I_c := I_b + A_b \cdot \left(y_c - y_b\right)^2 + I_s + A_s \cdot \left(d_c - 0.5 d_s - y_c\right)^2 = 1.028 \times 10^{12} \quad mm^4$$

$y_{tbm} := d - y_c = 612.6 \quad mm$ $\qquad y_{tsb} := d_c - y_c = 912.6 \quad mm$

$y_{bbm} := y_c = 1567.4 \quad mm$ $\qquad y_{bsb} := d - y_c = 612.6 \quad mm$

Imposed loading: $M_{pimp} := M_{pdchar} - M_{pbs} = 7378.275 \quad kNm$

$M_{nimp} := M_{ndchar} - M_{nbs} = 7027.6 \quad kNm$

At this point characteristic serviceability load considered in full. (Prestressing force part of f_{tbm} and f_{bbm})

C.6.1 Stress Limits

For composite prestressed beams at service **BS EN 1992-1-1**

$f_{bmax} := 0.6 \cdot f_{ck} = 30$ MPa Eq (5.42)

$f_{bmin} := -f_{ctm} = -4.1$ MPa

For composite concrete slab at service

$f_{smax} := 0.6 \cdot f_{sck} = 24$ MPa Eq (5.42)

$f_{smin} := -f_{sctm} = -3.5$ MPa

C.6.2 Verification of the Inequalities for Final Stresses

For the maximum positive moment...

For the beam

$$f_{ctbm} := f_{tbm} + \frac{M_{pimp} \cdot 10^6 \cdot y_{tbm}}{I_c} = 27.109 \text{ MPa} \quad \text{(C.4a)}$$

$f_{ctbm} = 27.109$ MPa $<$ $f_{bmax} = 30$ MPa OK!

$$f_{cbbm} := f_{bbm} - \frac{M_{pimp} \cdot 10^6 \cdot y_{bbm}}{I_c} = -3.959 \text{ MPa} \quad \text{(C.4b)}$$

$f_{cbbm} = -3.959$ MPa $>$ $f_{bmin} = -4.1$ MPa OK!

For the slab

$$f_{ctsb} := \frac{M_{pimp} \cdot 10^6 \cdot y_{tsb}}{I_c} = 6.5523 \text{ MPa} \quad \text{(C.4c)}$$

$f_{ctsb} = 6.552$ MPa $<$ $f_{smax} = 24$ MPa OK!

$$f_{cbsb} := \frac{M_{pimp} \cdot 10^6 \cdot y_{bsb}}{I_c} = 4.398 \text{ MPa} \quad \text{(C.4d)}$$

$f_{cbsb} = 4.398$ MPa $>$ $f_{smin} = -3.5$ MPa OK!

For the minimum negative moment...

For the beam

$$f_{nctbm} := f_{ntbm} - \frac{M_{nimp} \cdot 10^6 \cdot y_{tbm}}{I_c} = 3.028 \text{ MPa} \quad \text{(C.5a)}$$

$f_{nctbm} = 3.028$ MPa $>$ $f_{bmin} = -4.1$ MPa OK!

$$f_{ncbbm} := f_{nbbm} + \frac{M_{nimp} \cdot 10^6 \cdot y_{bbm}}{I_c} = 29.875 \text{ MPa} \quad \text{(C.5b)}$$

$f_{ncbbm} = 29.875$ MPa $<$ $f_{bmax} = 30$ MPa OK!

For the slab

$$f_{nctsb} := \frac{M_{nimp} \cdot 10^6 \cdot y_{tsb}}{I_c} = 6.2409 \quad MPa \qquad (C.5c)$$

$$f_{nctsb} = 6.241 \quad MPa \quad > \quad f_{smin} = -3.5 \quad MPa \qquad OK!$$

$$f_{ncbsb} := \frac{M_{nimp} \cdot 10^6 \cdot y_{bsb}}{I_c} = 4.189 \quad MPa \qquad (C.5d)$$

$$f_{ncbsb} = 4.189 \quad MPa \quad < \quad f_{smax} = 24 \quad MPa \qquad OK!$$

Since the slab is always in compression, it only needs to be checked at the locations of maximum and minimum moments. It may be assumed that the requirements are met at all locations as long as they are met at the critical locations.

On the contrary, the stresses in the beam are in both compression and tension. Therefore, the stresses must be checked at each section.

Verification for the beam at all locations

NOTE: Stresses in the beam are verified every 5.0m along the beam.
Values for M_{gr5} are taken from A.4.3 in Appendix A.
All results are symmetric about the centre support.

Table C.10 – Imposed loading every 5.0m

X (m)	M_{sf} (kNm)	M_{pgr5} (kNm)	M_{ngr5} (kNm)	M_{pimp} (kNm)	M_{nimp} (kNm)
0	0.000	0.000	0.000	0	0
5	267.375	3355.382	-528.398	3623	-261
10	427.800	5708.276	-1056.795	6136	-629
15	481.275	6897.210	-1657.647	7378	-1176
17.4	468.954	7014.478	-1785.980	7483	-1317
20	427.800	6864.630	-2143.976	7292	-1716
25	267.375	5723.012	-2641.988	5990	-2375
30	0.000	3540.940	-3170.386	3541	-3170
35	-374.325	936.960	-4042.013	563	-4416
40	-855.600	-1101.753	-6171.772	-1957	-7027

Table C.11 – Verification of concrete stresses in the beam

					Due to M_{pimp}		Due to M_{nimp}	
X (m)	e_{eff} (mm)	P_i (kN)	M_{pimp} (kNm)	M_{nimp} (kNm)	f_{ctbm} (MPa)	f_{cbbm} (MPa)	f_{ctbm} (MPa)	f_{cbbm} (MPa)
0	0	12852	0	0	13.980	13.980	13.980	13.980
5	56.131	12852	3623	-261	20.924	4.791	18.609	10.715
10	83.262	12852	6136	-629	25.506	-1.404	21.473	**8.915**
15	97.393	12852	7378	-1176	**27.109**	**-3.959**	**22.009**	9.089
17.4	95.576	12852	7483	-1317	26.008	-3.228	20.761	10.195
20	92.524	12852	7292	-1716	25.894	-2.936	20.524	10.804
25	60.655	12852	5990	-2375	22.188	1.292	17.201	14.051
30	-35.214	12852	3541	-3170	17.238	7.700	13.237	17.937
35	-231.083	12852	563	-4416	12.586	14.445	9.618	22.039
40	-441.953	12852	-1957	-7027	**6.051**	**22.142**	**3.028**	**29.875**
Limits for positive eccentricity:					-4.1	30	-4.1	30
Limits for negative eccentricity:					30	-4.1	30	-4.1

Requirements for concrete stresses are met at all locations.

C.7 DEFLECTION CHECKS

BS EN 1992-2 does not provide specific limits for deflection, but specifies that the deformation of the structure should not be such that it adversely affects its proper function or appearance. The limits should be set on a case by case basis.

For the purpose of this design example, it has been decided to apply a limit of L/1000 which is specified in the American AASHTO LFD codes.

Deflections are checked based on the maximum positive moment and the maximum positive effective eccentricity. Effective span lengths are applied as well to account for the continuous spans.

$P_i = 12852$ kN $\quad e_{peff} = 97.393$ mm

BS EN 1992-1-1

$L_c = 40$ m $\quad L_{eff} := 0.85 \cdot L_c = 34$ m

Figure 5.2

Assume limit of: $\frac{L_c \cdot 10^3}{1000} = 40$ mm

AASHTO LFD

Cl. 8.9.3.1

At transfer (non-composite section)

$E_{cmt} = 34.845$ GPa $I_b = 3.895 \times 10^{11}$ mm^4

$w_b = 18.387$ kN/m

$$\delta_t := \frac{5}{384} \cdot \frac{w_b \cdot \left(L_{eff} \cdot 10^3\right)^4}{E_{cmt} \cdot 10^3 \cdot I_b} - \frac{5}{48} \cdot \frac{P_i \cdot 10^3 \cdot e_{peff} \cdot \left(L_{eff} \cdot 10^3\right)^2}{E_{cmt} \cdot 10^3 \cdot I_b} = 12.466 \text{ mm}$$

At slab placement (non-composite section)

$E_{cm} = 37$ GPa $I_b = 3.895 \times 10^{11}$ mm^4

$\alpha = 0.88$ $w_s := w_b + \gamma_{rcwet} \cdot \frac{A_s}{10^6} = 33.987$ kN/m

$$\delta_{sl} := \frac{5}{384} \cdot \frac{w_s \cdot \left(L_{eff} \cdot 10^3\right)^4}{E_{cm} \cdot 10^3 \cdot I_b} - \frac{5}{48} \cdot \frac{\alpha \cdot P_i \cdot 10^3 \cdot e_{peff} \cdot \left(L_{eff} \cdot 10^3\right)^2}{E_{cm} \cdot 10^3 \cdot I_b} = 31.828 \text{ mm}$$

At service (composite section, frequent load combination)

$\beta = 0.8$ $I_c = 1.028 \times 10^{12}$ mm^4 **BS EN 1990** Cl. A2.4.2(3)

$M_{pdfreq} = 7818.548$ kNm $w_{freq} := \frac{M_{pdfreq} \cdot 8}{L_{eff}^2} = 54.108$ kN/m

Conservatively, the modulus of elasticity for the slab (C40/50) is applied.

$E_{scm} = 35$ GPa

Determine effective modulus of elasticity: **BS EN 1992-1-1**

$A_b = 735475$ mm^2 $u := 5288$ mm Figure 3.1

$h_0 := \frac{2 \cdot A_b}{u} = 278.168$ mm

$\varphi := 1.3$ for $t_0 > 100$ days

$E_{ceff} := \frac{E_{scm}}{1 + \varphi} = 15.217$ GPa Eq (7.20)

$$\delta_s := \frac{5}{384} \cdot \frac{w_{freq} \cdot \left(L_{eff} \cdot 10^3\right)^4}{E_{ceff} \cdot 10^3 \cdot I_c} - \frac{5}{48} \cdot \frac{\beta \cdot P_i \cdot 10^3 \cdot e_b \cdot \left(L_{eff} \cdot 10^3\right)^2}{E_{ceff} \cdot 10^3 \cdot I_c} = 28.932 \text{ mm}$$

C.8 END BLOCK DESIGN

For the anchorage, a 7C15 anchorage is selected from Freyssinett products (Freyssinet, 2010a), with 60mm diameter ducts. This is a conical anchorage, which will hold up to seven strands.

The beams have been designed for 84 strands. Therefore, 12 achorage systems will be required. Due to the geometry of the beam, it is assumed that the anchorages are all stacked on top of each other.

C.8.1 Bearing Stress Under the Anchor

(Bungey, Hulse, & Mosley, 2007)

Actual bearing stress:

BS EN 1992-1-1
Cl. 2.4.2.2(3)

For local effects: $\gamma_{punfav} := 1.2$

Assume a loaded area of 200mm x 150mm

$$A_o := 200 \cdot 150 = 30000 \quad mm^2$$

$$\sigma_c := \frac{\gamma_{punfav} \cdot P_{istr} \cdot 7 \cdot 1000}{A_o} = 42.84 \quad MPa$$

Allowable bearing stress:

Maximum area, based on width of the web and proportional to the loaded area

$$A_{c1} := 267 \cdot 200 = 53400 \quad mm^2$$

$$f_{Rdu} := 0.67 f_{ck} \cdot \sqrt{\frac{A_{c1}}{A_o}} = 44.695 \quad MPa \quad > \quad \sigma_c = 42.84 \quad MPa \quad OK!$$

C.8.2 Required Reinforcement

BS EN 1992-2
Cl. 8.10.3

The design forces are based on the strut and tie model, illustrated in Figure C.10.

For each individual anchor:

From the strut and tie model:

$$T_p := 0.33 \cdot \gamma_{punfav} \cdot \left(P_{istr} \cdot 7 \right) = 424.116 \quad kN$$

Stress limit for the reinforcement:

$$f_{yklimit} := 250 \quad MPa$$

$$A_{sreq} := \frac{T_p \cdot 1000}{f_{yklimit}} = 1696.464 \quad mm^2$$

This may be provided by six 14mm closed links (1848 mm^2) distributed over a length of 200mm, the largest dimension of the loaded area.

Considering all 12 of the anchorages:

From the strut and tie model:

$$T_{pa} := 0.33 \cdot \gamma_{punfav} \cdot P_i = 5089.392 \quad kN$$

Stress limit for the reinforcement:

$$f_{yklimit} = 250 \quad MPa$$

$$A_{sareq} := \frac{T_{pa} \cdot 1000}{f_{yklimit}} = 20357.568 \quad mm^2$$

This may be provided by fifty-one 16mm closed links (20502 mm^2) distributed over a length of 2400mm (=200x12), the largest dimension of the loaded area.

C.8.3 Compressive Stress in the Struts

Actual stress in the strut:

(From the strut and tie model)

$$\sigma_{strut} := \frac{0.6 \cdot \gamma_{punfav} \cdot P_{istr} \cdot 1000 \cdot 7}{200 \cdot 267 \cdot \cos\left(33.7 \cdot \frac{\pi}{180}\right)} = 17.357 \quad MPa$$

Allowable compressive stress: (Hurst, 1998)

$$\sigma_{allow} := 0.4 \cdot f_{ck} = 20 \quad MPa \quad > \quad \sigma_{strut} = 17.357 \quad MPa \quad OK!$$

C.9 ULTIMATE BENDING MOMENT RESISTANCE

Partial factors for the steel and concrete: **BS EN 1992-1-1**

$\gamma_c := 1.50$ for concrete — Cl. 2.4.2.4 & Table NA.1

$\gamma_s := 1.15$ for prestressing steel

Strain limit:

$\varepsilon_{ud} := 0.0200$ — Cl. 3.3.6(7)

C.9.1 Stress-Strain Relationship for the Prestressing Strands

p1 - at yield point of steel:

$$\sigma_{p1} := \frac{f_{p0.1k}}{\gamma_s} = 1400 \quad \text{MPa} \qquad \varepsilon_{p1} := \frac{\sigma_{p1}}{E_s \cdot 1000} = 0.0072$$

p3 - at failure of steel:

$$\sigma_{p3} := \frac{f_{pk}}{\gamma_s} = 1617.391 \quad \text{MPa} \qquad \varepsilon_{p3} := \frac{\varepsilon_{ud}}{0.9} = 0.022$$

p2 - at maximum design:

$$\varepsilon_{p2} := \varepsilon_{ud} = 0.0200$$

$$\sigma_{p2} := \sigma_{p1} + \left(\sigma_{p3} - \sigma_{p1}\right) \cdot \frac{\left(\varepsilon_{p2} - \varepsilon_{p1}\right)}{\left(\varepsilon_{p3} - \varepsilon_{p1}\right)} = 1585.277 \quad \text{MPa}$$

C.9.2 Stress and Strain Distribution for the Beam and Slab

Ultimate compressive strain in the concrete, ε_c:

BS EN 1992-1-1

$\varepsilon_c := 0.0035$

Table 3.1

Strain in the prestressing steel at ULS due to prestress only, ε_{p0}:

Partial factor for prestress:

NA to BS EN 1992-1-1

$\gamma_{pfav} := 0.9$

Cl. 2.4.2.2(1)

Initial stress and strain in tendons:

$$f_{pi} := \frac{P_{istr} \cdot 10^3}{A_{pstr}} = 1366.071 \quad MPa \qquad \varepsilon_{p0} := \frac{f_{pi}}{E_s \cdot 10^3} = 0.00701$$

Total strain at ULS, ε_p:

$$\varepsilon_p = \Delta\varepsilon_p + \gamma_{p,fav}\varepsilon_{p0} = \Delta\varepsilon_p + 0.00701$$

Defining the compressive zone:

BS EN 1992-1-1
Cl. 3.1.6 &
Cl. 3.1.7(3)

$\lambda := 0.80 \qquad \lambda x = 0.8x$

$\eta := 1.0$

NA to BS EN 1992-2
Cl. 3.1.6

$\alpha_{cc} := 0.85$

$$f_{cd} := \frac{\alpha_{cc} \cdot f_{ck}}{\gamma_c} = 28.333 \quad MPa \qquad f_{scd} := \frac{\alpha_{cc} \cdot f_{sck}}{\gamma_c} = 22.667 \quad MPa$$

$\eta \cdot f_{cd} = 28.333 \quad MPa \qquad \eta \cdot f_{scd} = 22.667 \quad MPa$

$$\frac{\eta \cdot \alpha_{cc}}{\gamma_c} = 0.567 \quad f_{ck}$$

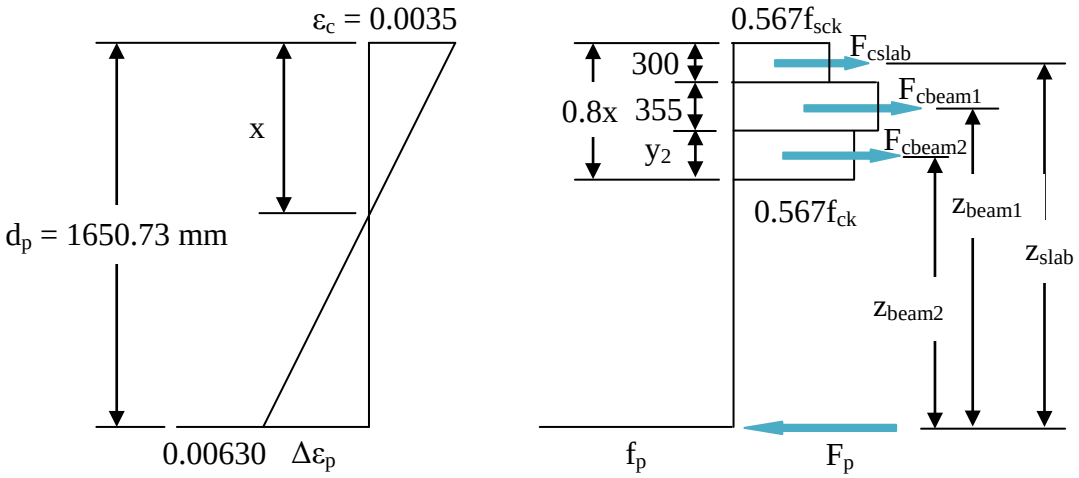

Figure C.12 – Strain and stress diagrams

This check is based on a resultant force from the prestressing strands. For more accurate results, the prestressing force should be considered at each row of strands, since some of the strands fall inside the compressive zone of the concrete. Due to time constraints, this is not done here.

C.9.3 Calculation of the Ultimate Bending Moment Resistance

For the maximum positive moment...

$e_{pb} := 116 \quad mm$

$\Delta\varepsilon_p$ can be determined from the following ratio: $c_p := y_b - e_{pb}$

$\frac{0.0035}{x} := \frac{\Delta\varepsilon_p}{d_p - x}$ where $d_p := d_c - c_p = 1650.729 \quad mm$

The value of x is determined from $F_p = F_c$

Steel tensile force:

$F_p = f_p A_p = \min(\varepsilon_p E_s , f_{pd}) A_p = \min[(\Delta\varepsilon_p + \gamma_{p,fav}\varepsilon_{p0})E_s , f_{pd}]A_p$

Concrete compressive force:

$F_c = F_{c,slab} + F_{c,beam}$

$F_c = s_{bm} d_s (0.567 f_{sck}) + (0.8x - d_s)(410)(0.567 f_{ck})$

At $x := 840.4 \quad mm \quad (\ 0.8x = 672.32 \ mm \ ), \quad F_p = F_c$

$\Delta\varepsilon_p := \frac{0.0035 \cdot (d_p - x)}{x} = 0.003 \qquad f_{pd} := \sigma_{p1}$

$F_p := \min\left[\left(\Delta\varepsilon_p + \gamma_{pfav} \cdot \varepsilon_{p0}\right) \cdot E_s , f_{pd}\right] \cdot A_p = 17758.009 \quad kN$

$y_1 := 355 \quad mm \qquad b_{bm1} := 410 \quad mm$

$y_2 := 0.8x - d_s - 355 = 17.32 \quad mm$

$x_2 := y_2 \cdot \frac{210}{105} \qquad b_{bm2} := \frac{\left[410 + (410 - x_2)\right]}{2} = 392.68 \quad mm$

$F_{cslab} := s_{bm} \cdot d_s \cdot \left(\frac{\eta \cdot \alpha_{cc}}{\gamma_c} \cdot f_{sck}\right) = 1.36 \times 10^7 \quad kN$

$F_{cbeam1} := y_1 \cdot b_{bm1} \cdot \left(\frac{\eta \cdot \alpha_{cc}}{\gamma_c} f_{ck}\right) = 4.124 \times 10^6 \quad kN$

$F_{cbeam2} := y_2 \cdot b_{bm2} \cdot \left(\frac{\eta \cdot \alpha_{cc}}{\gamma_c} f_{ck}\right) = 1.927 \times 10^5 \quad kN$

$F_c := \left(F_{cslab} + F_{cbeam1} + F_{cbeam2}\right) \cdot 10^{-3} = 17916.618 \quad kN$

Check strain limits:

$\varepsilon_p := \Delta\varepsilon_p + \gamma_{pfav}\cdot\varepsilon_{p0} = 0.01$ << $\varepsilon_{ud} = 0.0200$ OK!

Determine ultimate bending moment resistance (M_{Rd}):

$z_{slab} := d_p - d_s\cdot 0.5 = 1500.729$ mm

$z_{beam1} := d_p - d_s - 0.5y_1 = 1173.229$ mm

$z_{beam2} := d_p - d_s - y_1 - 0.5y_2 = 987.069$ mm

$M_{Rd} := F_{cslab}\cdot z_{slab}\cdot 10^{-6} + F_{cbeam1}\cdot z_{beam1}\cdot 10^{-6} + F_{cbeam2}\cdot z_{beam2}\cdot 10^{-6}$

$M_{Rd} = 25438.428$ kNm

Maximum bending moment applied to the beam:

Secondary Moment: $M_s := -301.717$ kNm

$M_{Ed} := M_{pdult} + M_s = 14657.395$ kNm

$\frac{M_{Ed}}{M_{Rd}} = 0.576$ < 1.00 OK!

For the minimum negative moment at the support...

Following the same procedure:

$e_{nb} := 395$ mm

$\Delta\varepsilon_p$ can be determined from the following ratio:

$c_{np} := \left(y_{tbm} - e_{nb}\right) = 217.6$ mm

$\frac{0.0035}{x} := \frac{\Delta\varepsilon_p}{d_p - x}$ where $d_{np} := d - c_{np} = 1962.4$ mm

The value of x is determined from $F_p = F_c$

Steel tensile force:

$F_p = f_pA_p = \min(\varepsilon_pE_s\,,\, f_{pd})A_p = \min[(\Delta\varepsilon_p + \gamma_{p,fav}\varepsilon_{p0})E_s\,,\, f_{pd}]A_p$

Concrete compressive force:

$F_c = F_{c,beam}$

$F_c = (0.8x)(b)(0.567f_{ck})$

At $x_n := 1684 \quad mm \quad (\ 0.8x_n = 1347.2 \quad mm\ ), \quad F_p = F_c$

$$\Delta\varepsilon_{np} := \frac{0.0035\cdot\left(d_{np} - x_n\right)}{x} = 0.001$$

$$F_{np} := \min\left[\left(\Delta\varepsilon_{np} + \gamma_{pfav}\cdot\varepsilon_{p0}\right)\cdot E_s, f_{pd}\right]\cdot A_p = 13693.873 \quad kN$$

$b_{nbm1} := 660 \ mm$ $\qquad$ $y_{n1} := 350 \ mm$

$b_{nbm2} := \frac{660 + 200}{2} = 430 \quad mm$ $\qquad$ $y_{n2} := 230 \quad mm$

$b_{nbm3} := 200 \quad mm$ $\qquad$ $y_{n3} := 0.8x_n - y_{n1} - y_{n2} = 767.2 \quad mm$

$$F_{ncbeam1} := y_{n1}\cdot b_{nbm1}\cdot\left(\frac{\eta\cdot\alpha_{cc}}{\gamma_c}f_{ck}\right) = 6545000 \quad kN$$

$$F_{ncbeam2} := y_{n2}\cdot b_{nbm2}\cdot\left(\frac{\eta\cdot\alpha_{cc}}{\gamma_c}f_{ck}\right) = 2802166.667 \quad kN$$

$$F_{ncbeam3} := y_{n3}\cdot b_{nbm3}\cdot\left(\frac{\eta\cdot\alpha_{cc}}{\gamma_c}f_{ck}\right) = 4347466.667 \quad kN$$

$$F_{nc} := \left(F_{ncbeam1} + F_{ncbeam2} + F_{ncbeam3}\right)\cdot 10^{-3} = 13694.633 \ kN$$

Check strain limits:

$\varepsilon_{np} := \Delta\varepsilon_{np} + \gamma_{pfav}\cdot\varepsilon_{p0} = 0.007 \quad << \quad \varepsilon_{ud} = 0.0200$ $\qquad$ OK!

Determine ultimate bending moment resistance (M_{Rd}):

$z_{nbeam1} := d_{np} - 0.5y_{n1} = 1787.4 \quad mm$

$z_{nbeam2} := d_{np} - y_{n1} - 0.5y_{n2} = 1497.4 \quad mm$

$z_{nbeam3} := d_{np} - y_{n1} - y_{n2} - 0.5y_{n3} = 998.8 \quad mm$

$M_{nRd} := F_{ncbeam1}\cdot z_{nbeam1}\cdot 10^{-6} + F_{ncbeam2}\cdot z_{nbeam2}\cdot 10^{-6} + F_{ncbeam3}\cdot z_{nbeam3}\cdot 10^{-6}$

$M_{nRd} = 20236.741 \ kNm$

Maximum bending moment applied to the beam:

Secondary Moment: $M_{ns} := -603.434 \text{ kNm}$

$M_{nEd} := M_{ndult} + M_s = 18071.659 \text{ kNm}$

$\frac{M_{nEd}}{M_{nRd}} = 0.893 \quad < 1.00 \quad \text{OK!}$

The ultimate limit state requirements for bending moment are met.

Due to time constraints, the shear design is not included in this design example. It is recommended that future investigations complete this portion of the design, following the same procedure as that applied in Appendix B.

C.10 DESIGN SUMMARY

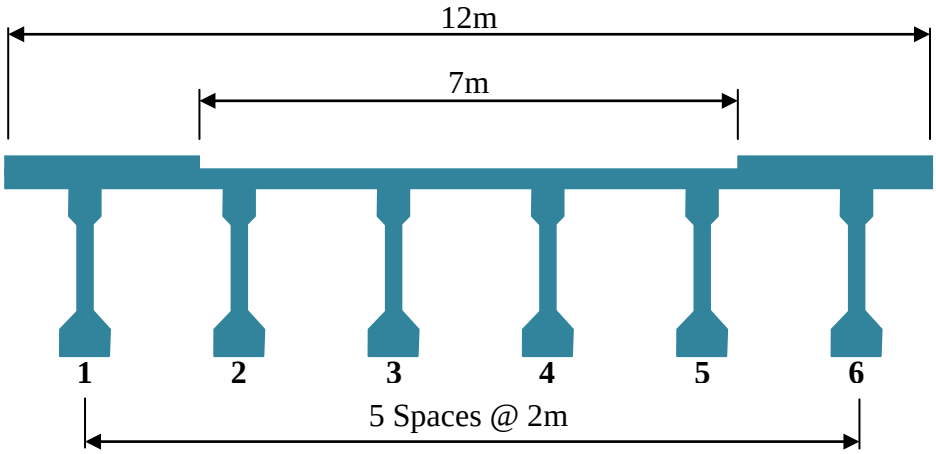

Figure C.13 – Bridge cross section

Span Lengths	40.0 metres each
Beam type	Post-tensioned I Beams (adjusted)
Concrete Properties	Beam: C50/60; Slab: C40/50
Prestressing Strands	Y1860S7G – 12.7mm diameter, 7 wire drawn strands
Nominal cover	70 mm
Number of strands	84
Total initial prestress force	12852 kN
Total prestress force	17500 kN
Eccentricity at support	-395mm
Eccentricity at midspan	116mm
Ducts	60mm diameter, 7 strands in each
End Block Reinforcement	Individual anchorages – six 14mm closed links, distributed over 200mm All anchorages – fifty-one 16mm closed links, distributed over 2400mm